

EVALUATION OF EFFECT OF SULFATE ON CLASS C FLY ASH AND LIME  
STABILIZED EXPANSIVE SOIL

A THESIS SUBMITTED TO  
THE GRADUATE SCHOOL OF NATURAL AND APPLIED SCIENCES  
OF  
MIDDLE EAST TECHNICAL UNIVERSITY

BY

MEHMET AS

IN PARTIAL FULFILLMENT OF THE REQUIREMENTS  
FOR  
THE DEGREE OF DOCTOR OF PHILOSOPHY  
IN  
CIVIL ENGINEERING

DECEMBER 2019



Approval of the thesis:

**EVALUATION OF EFFECT OF SULFATE ON CLASS C FLY ASH AND  
LIME STABILIZED EXPANSIVE SOIL**

submitted by **MEHMET AS** in partial fulfillment of the requirements for the degree  
of **Doctor of Philosophy in Civil Engineering Department, Middle East Technical  
University** by,

Prof. Dr. Halil Kalıpçılar  
Dean, Graduate School of **Natural and Applied Sciences**

\_\_\_\_\_

Prof. Dr. Ahmet Türer  
Head of Department, **Civil Engineering**

\_\_\_\_\_

Prof. Dr. Erdal Çokça  
Supervisor, **Civil Engineering, METU**

\_\_\_\_\_

**Examining Committee Members:**

Prof. Dr. Nihat Sinan Işık  
Civil Engineering, Gazi University Faculty of Technology

\_\_\_\_\_

Prof. Dr. Erdal Çokça  
Civil Engineering, METU

\_\_\_\_\_

Assoc. Prof. Dr. Nejan Huvaj Sarihan  
Civil Engineering, METU

\_\_\_\_\_

Assoc. Prof. Dr. Mustafa Kerem Koçkar  
Civil Engineering, Hacettepe University

\_\_\_\_\_

Assist. Prof. Dr. Onur Pekcan  
Civil Engineering, METU

\_\_\_\_\_

Date: 24.12.2019

**I hereby declare that all information in this document has been obtained and presented in accordance with academic rules and ethical conduct. I also declare that, as required by these rules and conduct, I have fully cited and referenced all material and results that are not original to this work.**

Name, Surname: Mehmet As

Signature:

## ABSTRACT

### EVALUATION OF EFFECT OF SULFATE ON CLASS C FLY ASH AND LIME STABILIZED EXPANSIVE SOIL

As, Mehmet  
Doctor of Philosophy, Civil Engineering  
Supervisor: Prof. Dr. Erdal Çokça

December 2019, 282 pages

In this study, effect of sulfate on expansive soil treated with Class C Fly Ash was investigated. Also, lime was used for comparison purposes. The swelling soil was prepared at laboratory environment by mixing kaolinite and bentonite. Class C Fly Ashes obtained from Soma and Sivas-Kangal Thermal Power Plants were used as main additives for stabilization.  $\text{Na}_2\text{SO}_4$  and  $\text{CaSO}_4 \cdot 2\text{H}_2\text{O}$  were used as sulfate sources with different concentrations (3000ppm to 40000ppm). Optimum fly ash content was chosen as 15% and 10% for Soma (SFA) and Sivas-Kangal Fly Ash (KFA) respectively.

Index tests, swelling and unconfined compressive strength tests were performed to understand the effect of fly ash on sulfate bearing soils. XRD analysis, zeta potential tests and scanning electron microscope were also used to see the effect of treatment on chemical structure and microstructure.

Sulfate addition affected the swell potential of each treated specimen differently. Swell potential of 15% SFA treated specimen was positively affected from sulfate addition. Although not dramatic, general increase was observed in the swell potential of 4% lime treated specimen after sulfate addition. Swell potential of 10% KFA treated specimen was not affected much from the sulfate addition, especially for

$\text{CaSO}_4 \cdot 2\text{H}_2\text{O}$ . The strength of fly ash and lime treated specimens was generally affected negatively from  $\text{Na}_2\text{SO}_4$  addition however,  $\text{CaSO}_4 \cdot 2\text{H}_2\text{O}$  addition had no significant effect. A dramatic decrease was observed in strength of 40000ppm  $\text{Na}_2\text{SO}_4$  added fly ash treated specimens that were cured at  $10^\circ\text{C}$  as a result of the probable salination and ettringite formation.

**Keywords:** Expansive Soils, Class C Fly Ash, Sulfate, Ettringite, Salt Heave

## ÖZ

### SÜLFATIN C SINIFI UÇUCU KÜL VE KİREÇ İLE STABİLİZE EDİLEN ŞİŞEN ZEMİNE ETKİSİNİN DEĞERLENDİRİLMESİ

As, Mehmet  
Doktora, İnşaat Mühendisliği  
Tez Danışmanı: Prof. Dr. Erdal Çokça

Aralık 2019, 282 sayfa

Bu araştırmada sülfatın ( $\text{Na}_2\text{SO}_4$  ve  $\text{CaSO}_4 \cdot 2\text{H}_2\text{O}$ ) C sınıfı uçucu kül ile stabilizasyonu sağlanan şişen zemin üzerindeki etkisi incelenmiştir. Aynı zamanda karşılaştırma amaçlı olarak kireç kullanılmıştır. Şişen zemin laboratuvar ortamında kaolin ve bentonit kullanılarak elde edilmiştir. Soma ve Sivas-Kangal Termik santrallerinden temin edilen C sınıfı uçucu küller ana katkı malzemeleri olarak kullanılmıştır. Sülfat kaynağı olarak değişik oranlarda (3000ppm ila 40000ppm)  $\text{Na}_2\text{SO}_4$  ve  $\text{CaSO}_4 \cdot 2\text{H}_2\text{O}$  kullanılmıştır. Optimum uçucu kül oranı Soma (SFA) ve Sivas-Kangal (KFA) uçucu külleri için sırasıyla %15 ve %10 olarak seçilmiştir.

Uçucu külün sülfat içeren zeminler üzerindeki etkisinin belirlenmesi amacı ile tanımlama, şişme ve tek eksenli basınç dayanımı deneyleri yapılmıştır. Aynı zamanda iyileştirmenin kimyasal ve mikroyapı üzerindeki etkisinin belirlenmesi amacı ile XRD analizleri, zeta potansiyel testleri ve taramalı elektron mikroskobu görüntüleri kullanılmıştır.

Sülfat eklemek, stabilize edilen zeminlerin şişme potansiyellerini değişik şekillerde etkilemiştir. %15 SFA ile iyileştirilen numunenin şişme potansiyeli sülfat eklenmesinden pozitif olarak etkilenmiştir. Ciddi oranda olmasa da sülfat eklemek %4 oranında kireç ile stabilize edilen numunenin şişme potansiyelinde genelde bir artışa

neden olmuştur. %10 KFA ile iyileştirilen numunenin şişme potansiyeli özellikle  $\text{CaSO}_4 \cdot 2\text{H}_2\text{O}$ 'dan olmak üzere sülfat eklenmesinden pek fazla etkilenmemiştir.  $\text{Na}_2\text{SO}_4$  eklemek uçucu kül ve kireç ile iyileştirilen numunelerin dayanımlarını genelde olumsuz etkilemiş ancak  $\text{CaSO}_4 \cdot 2\text{H}_2\text{O}$  eklemenin dayanıma önemli bir etkisi olmamıştır. Tuzlanma (salination) ve etrenjit oluşumu nedeniyle  $10^\circ\text{C}$ 'de kürlenmiş 40000ppm  $\text{Na}_2\text{SO}_4$  eklenmiş uçucu kül ile iyileştirilen numunelerde ciddi dayanım kayıpları gözlenmiştir.

**Anahtar Kelimeler:** Şişen Zeminler, C Sınıfı Uçucu Kül, Sülfat, Etrenjit, Tuz Kaynaklı Kabarma

To My Mom

## ACKNOWLEDGEMENTS

I would like to express sincere appreciation to my supervisor, Prof. Dr. Erdal Çokça for his guidance, continuous understanding, invaluable patience and support throughout this research.

I also wish to express my special thanks to my thesis monitoring committee members Prof. Dr. Nihat Sinan Işık and Assoc. Prof. Dr. Nejan Huvaj Sarıhan for their valuable advices and guidance from the beginning of this research.

Special thanks go to the staff of Toker Drilling and Construction Engineering Consulting Co., especially Mustafa Toker and Soil and Rock Mechanics Laboratory department for their support and great encouragements during my studies.

I would like to thank to my friend Dr. Ceren Atila Dinçer for her valuable contributions about chemical tests.

My thankfulness goes to Mr. Kamber Bilgen for his support and friendly approach throughout the laboratory works.

I would like to acknowledge my friend Civil Engineer M.Sc. Ertaç Tuç for his helpful suggestions, encouragements and help during this study.

Finally, I express sincere thanks to my aunt Sibel Ören and to my mother Ayşe As for their endless supports throughout my life.

## TABLE OF CONTENTS

ABSTRACT .....	v
ÖZ .....	vii
ACKNOWLEDGEMENTS .....	x
TABLE OF CONTENTS .....	xi
LIST OF TABLES .....	xvii
LIST OF FIGURES .....	xx
LIST OF ABBREVIATIONS .....	xxxı
LIST OF SYMBOLS .....	xxxiii
CHAPTERS	
1. INTRODUCTION .....	1
1.1. General .....	1
1.2. Aim of the Study .....	3
1.3. Scope of the Study .....	3
1.4. Outline of the Study .....	4
2. LITERATURE REVIEW .....	5
2.1. Expansive Soils .....	5
2.2. Mechanism of Swelling .....	6
2.3. Factors Influencing Swelling .....	7
2.4. Clay Mineralogy .....	8
2.4.1. Kaolinite .....	9
2.4.2. Illite .....	10
2.4.3. Montmorillonite .....	10

2.5. Methods for Treatment of Expansive Soils.....	11
2.5.1. Chemical Stabilization .....	11
2.5.1.1. Soil- Lime Reactions .....	12
2.5.1.2. Lime Treatment .....	15
2.5.1.3. Fly Ash Treatment .....	17
3. EFFECT OF SULFATE ON CHEMICALLY STABILIZED SOILS.....	23
3.1. Effect of Sulfate on Lime Stabilized Soils.....	23
3.1.1. Soil- Lime- Sulfate Reactions .....	25
3.2. Mechanism of Heaving or Disruption During Ettringite Formation.....	27
3.3. Factors Affecting Sulfate Attack.....	28
3.3.1. pH .....	28
3.3.2. Moisture Availability .....	28
3.3.3. Temperature.....	28
3.3.4. Clay Content and Mineralogy .....	29
3.3.5. Sulfate Level.....	29
3.4. Sources of Sulfate .....	30
3.5. Determination of Sulfate Content of Soil and Groundwater.....	31
3.6. Techniques for Treating Sulfate-Rich Soils.....	32
3.6.1. Mellowing .....	33
3.6.2. Progressive (Double) Application of Lime .....	34
3.6.3. Use of Additives .....	34
3.7. Misconceptions about Heave Problems .....	35
3.8. Case Studies .....	35
3.9. Previous Studies on Ettringite Induced Heave Problems.....	38

4. EXPERIMENTAL WORKS .....	59
4.1. Purpose .....	59
4.2. Materials .....	59
4.3. Scope of the Experimental Study .....	62
4.4. Sample Preparation.....	66
4.4.1. Swell and UCS Tests .....	67
4.5. Methodology of the Tests .....	70
4.5.1. Swell Tests .....	70
4.5.1.1. Molds .....	70
4.5.1.2. Compaction .....	73
4.5.1.3. Procedure.....	75
4.5.1.4. Cured Specimens.....	77
4.5.2. UCS Tests .....	78
4.5.2.1. Degree of Saturation .....	78
4.5.2.2. Compaction .....	80
4.5.2.3. Procedure.....	82
4.5.2.4. Curing.....	83
4.5.3. Shear Wave Velocity ( $V_s$ ) Tests .....	84
4.5.4. SEM .....	86
4.5.5. XRD .....	88
4.5.6. Zeta Potential .....	90
4.5.7. Optimum Lime Content .....	93
4.5.8. Index Tests .....	95
5. TEST RESULTS.....	99

5.1. Determination of Optimum Additive Content .....	99
5.1.1. Lime.....	99
5.1.2. Fly Ash .....	100
5.2. Physical Properties .....	101
5.2.1. Specific Gravity Tests .....	102
5.2.2. LL, PL & PI.....	104
5.2.2.1. 4% L and sulfate added samples.....	104
5.2.2.2. 15% SFA and sulfate added samples.....	106
5.2.2.3. 10% KFA and sulfate added samples .....	108
5.2.3. Shrinkage Limit.....	110
5.2.4. Grain Size Distribution.....	112
5.2.5. Soil Classification.....	116
5.3. Swell Tests .....	120
5.3.1. Swell Tests at 25°C .....	120
5.3.2. Swell Tests at 10°C and 40°C .....	122
5.3.3. Swell Tests at 7 days and 28 days Cured Specimens .....	125
5.4. UCS Tests .....	127
5.4.1. UCS Tests at 25°C.....	127
5.4.2. UCS Tests for 7 days and 28 days cured specimens at 10, 25 and 40°C.....	129
5.4.2.1. 15% SFA treated specimens .....	129
5.4.2.2. 10% KFA treated specimens .....	134
5.5. Shear Wave Velocity ( $V_s$ ) Tests .....	139
5.6. Zeta Potential Tests.....	140
5.7. SEM .....	142

5.8. XRD.....	153
6. DISCUSSION ON TEST RESULTS .....	157
6.1. Effect of Additives on Specific Gravity (G <sub>s</sub> ) .....	157
6.2. Effect of Additives on LL, PL and PI.....	162
6.3. Effect of Additives on Shrinkage Limit (SL).....	170
6.4. Effect of Additives on Grain Size Distribution .....	173
6.5. Effect of Additives on Swell Percentage.....	176
6.5.1. Effect of Additives on Swell Percentage of Specimen A .....	176
6.5.2. Effect of Sulfate on Swell Potential of Chemically Treated Soils.....	178
6.5.3. Swell Tests at 10°C and 40°C.....	182
6.5.4. Swell Tests for 7 days and 28 days Cured Specimens.....	187
6.6. Effect of Additives on Strength.....	192
6.6.1. Effect of Additives on Strength of Specimen A .....	192
6.6.2. Effect of Sulfate on Strength of Chemically Treated Soils .....	197
6.6.3. Effect of Curing Time and Temperature on Strength of Sulfate Added Fly Ash Treated Specimens .....	200
6.6.3.1. Sulfate Added 15% SFA Treated Specimens.....	200
6.6.3.2. Sulfate Added 10% KFA Treated Specimens.....	208
6.7. Effect of Additives on Shear Wave Velocity .....	230
6.8. Effect of Additives on Zeta Potential .....	235
6.9. SEM.....	239
6.10. XRD.....	243
7. CONCLUSIONS .....	249
REFERENCES.....	253

## APPENDICES

A. CHEMICAL ANALYSES REPORTS.....	265
B. XRD RESULTS .....	270
C. SWELL VERSUS TIME GRAPHS.....	271
CURRICULUM VITAE.....	281

## LIST OF TABLES

### TABLES

Table 2.1. Overview of previous studies on lime (Jawad et al., 2014) .....	16
Table 2.2. The chemical composition and classification of fly ashes in Turkey (Turker et al., 2009).....	20
Table 2.3. Total ash production in Turkey (Ozmen, 2011).....	21
Table 3.1. Degree of risk relative to the sulfate level in lime treated soils (Little and Graves, 1995) .....	29
Table 3.2. Summary of cases related to ettringite induced heave problems (Puppala and Vempati, 2005).....	38
Table 3.3. Main properties of the clay used in the studies of McCarthy (2009).....	42
Table 3.4. Properties of soils (Gaily, 2012) .....	48
Table 3.5. UCS and volumetric swelling test results (Gaily, 2012).....	49
Table 3.6. Reactive alumina and silica (ppm) in present soils (Puppala et al.,2013) .....	51
Table 4.1. Chemical composition of sample A, fly ashes and lime .....	61
Table 4.2. Composition of samples.....	67
Table 4.3. Required water content for S=81.7%.....	79
Table 4.4. Typical peaks for ettringite and thaumasite in XRD (“x-ray diffraction table” (n.d)) .....	89
Table 4.5. Index tests for physical properties and related standards.....	96
Table 5.1. Classification of samples according to USCS .....	119
Table 5.2. Samples chosen for SEM analyses.....	142
Table 6.1. Measured and calculated $G_s$ values for chemically stabilized soil .....	157
Table 6.2. $G_s$ values obtained in Yesilbas (2004), Baytar (2005), and As (2012) studies .....	158
Table 6.3. The measured and calculated (by mass basis) $G_s$ values for sulfate added 4% L treated sample.....	159

Table 6.4. The measured and calculated (by mass basis) $G_s$ values for sulfate added 15% SFA treated sample .....	160
Table 6.5. The measured and calculated (by mass basis) $G_s$ values for sulfate added 10% KFA treated sample.....	161
Table 6.6. LL, PL, PI of Sample A, 15% SFA, 10% KFA and 4% L treated samples .....	162
Table 6.7. LL, PL, PI of the 4% L and sulfate added samples .....	164
Table 6.8. LL, PL, PI of the 15% SFA and sulfate added samples .....	165
Table 6.9. LL, PL, PI of the 10% KFA and sulfate added samples.....	166
Table 6.10. SL of sulfate added 4% L treated samples .....	171
Table 6.11. SL of sulfate added 15% SFA treated samples.....	171
Table 6.12. SL of sulfate added 10% KFA treated samples .....	172
Table 6.13. Grain size distribution for Sample A, 4% L treated, and sulfate added samples .....	173
Table 6.14. Grain size distribution for Sample A, 15% SFA treated and sulfate added samples .....	174
Table 6.15. Grain size distribution for Sample A, 10% KFA treated and sulfate added samples .....	175
Table 6.16. Swell percent for fly ash and lime treated expansive soil .....	177
Table 6.17. Swell percent for sulfate added 4% L treated specimens .....	179
Table 6.18. Swell percent for sulfate added 15% SFA treated specimens .....	180
Table 6.19. Swell percent for sulfate added 10% KFA treated specimens.....	181
Table 6.20. Swell percent for sulfate added 15% SFA treated specimens at 10°C, 25°C and 40°C .....	183
Table 6.21. Change in $q_u$ according to curing conditions (Beeghly, 2003).....	185
Table 6.22. Swell percent for sulfate added 10% KFA treated specimens at 10°C, 25°C and 40°C .....	186
Table 6.23. Swell percent for sulfate added 15% SFA treated specimens cured at 25°C for 7 and 28 days.....	188

Table 6.24. Swell percent for sulfate added 10% KFA treated specimens cured at 25°C for 7 and 28 days .....	190
Table 6.25. $q_u$ for Specimen A, fly ash and lime treated soils.....	193
Table 6.26. $q_u$ for sieved and non-sieved specimens .....	196
Table 6.27. $q_u$ for sulfate added 4% L treated specimens .....	198
Table 6.28. $q_u$ for sulfate added 15% SFA treated specimens .....	198
Table 6.29. $q_u$ for sulfate added 10% KFA treated specimens.....	199
Table 6.30. Average $q_u$ for sulfate added 15% SFA treated specimens after 7days curing at 10, 25 and 40°C.....	201
Table 6.31. Average $q_u$ for sulfate added 15% SFA treated specimens after 28 days curing at 10, 25 and 40°C.....	204
Table 6.32. Average $q_u$ for sulfate added 15% SFA treated specimens after 7 and 28 days curing at 10, 25 and 40°C .....	207
Table 6.33. Average $q_u$ for sulfate added 10% KFA treated specimens after 7 days curing at 10, 25 and 40°C.....	209
Table 6.34. Average $q_u$ for sulfate added 10% KFA treated specimens after 28 days curing at 10, 25 and 40°C.....	212
Table 6.35. Average $q_u$ for sulfate added 10% KFA treated specimens after 7 and 28 days curing at 10, 25 and 40°C .....	216
Table 6.36. Correlations between $c_u$ and $V_s$ .....	230
Table 6.37. Measured and calculated $V_s$ values.....	232
Table 6.38. Results of pH and zeta potential tests for Sample A and fly ash treated samples.....	236
Table 6.39. Results of pH and zeta potential tests for sulfate added fly ash treated samples.....	236
Table A.1. Chemical Analyses results for lime (BASTAS Cement Factory).....	269

## LIST OF FIGURES

### FIGURES

Figure 2.1. Expansive soil related problems. a- longitudinal cracks in road (Wang, 2016), b- heave in road and pavements (Colorado Geological Survey, n.d.).....	5
Figure 2.2. Schematic representation of soil expansion (Stavredakis, 2006).....	6
Figure 2.3. Factors affecting swell potential of expansive soils (Nelson and Miller, 1992).....	7
Figure 2.4. Basic units of clay minerals and main clay minerals (Knappett and Craig, 2012).....	9
Figure 2.5. Schematic representation of cation exchange (Prusinski and Bhattacharja, 1999).....	13
Figure 2.6. Schematic representation of flocculation (Prusinski and Bhattacharja, 1999).....	13
Figure 2.7. Schematic representation of pozzolonic reactions (Prusinski and Bhattacharja, 1999).....	14
Figure 2.8. Schematic representation of the lime treatment process (Britpave, 2007).....	15
Figure 2.9. Schematic representation of fly ash production (FHWA, 2008).....	17
Figure 2.10. Percent distribution of the fly ash class in Turkey .....	22
Figure 3.1. Vertical heave problem in roads due to the ettringite formation (Puppala et al., 2019).....	24
Figure 3.2. Evidence of accumulation of considerable lateral strain resulting in shear failure in lime- treated high sulfate soil layer (Little and Nair, 2009).....	24
Figure 3.3. Chemical structure of ettringite columns (Puppala et al., 2019).....	27
Figure 3.4. Gypsum crystals monitored below lime treated heaved layers and optical microscopy image of the soil containing gypsum (Little et al., 2010) .....	30

Figure 3.5. Guideline for the stabilization of sulfate soils (Texas Department of transportation, 2005) .....	33
Figure 3.6. Pavement surface failure (Mitchell, 1986) .....	36
Figure 3.7. Linear expansion vs. soaking time graphs for kaolinite, 6% lime treated kaolinite and gypsum added 6% lime treated kaolinite specimens (Abdi and Wild, 1993) .....	39
Figure 3.8. Swell potential of soils after cement treatment (Puppala et al., 2004) ....	40
Figure 3.9. Strength of soils after cement treatment (Puppala et al., 2004).....	41
Figure 3.10. Typical appearance of ettringite-induced swelling and the effect of fly ash (McCarthy, 2009).....	42
Figure 3.11. Effect of mellowing period and fly ash content in swelling of test specimens (McCarthy, 2009) .....	43
Figure 3.12. Effect of lime content and fly ash content on swelling properties of test specimens (McCarthy, 2009) .....	44
Figure 3.13. SEM images of the raw clay and test mixes at 40 °C water (McCarthy, 2009).....	45
Figure 3.14. Effect of fly ash content on swelling of lime treated clays (McCarthy et al., 2012a).....	46
Figure 3.15. Effect of temperature on swell potential of fly ash added 3% lime treated clays (McCarthy et al., 2012b).....	47
Figure 3.16. Volumetric swell, a- Childress soil, b- Sherman soil .....	51
Figure 3.17. Comparison of the swell percentages of the untreated soil (CS), lime treated soil (CS+5L) and lime treated soil (CS+5L) with different concentration of sulfates (Celik, 2014) .....	53
Figure 3.18. XRD of lime treated soils with 10000ppm sulfate concentration (Celik, 2014) .....	54
Figure 3.19. SEM views, a- natural soil, b- lime treated soil with 10000ppm sulfate concentration (Celik, 2014).....	54
Figure 3.20. Swell potential of soils with 6% GBFS and different sulfate concentrations (Celik, 2014) .....	55

Figure 3.21. Swell vs. time graphs for (a) natural soil, (b) lime treated soil, (c) fly ash treated soil (Mohammed and Vipulandan, 2015) .....	57
Figure 4.1. Materials (a-kaolinite, b-bentonite, c-soma fly ash, d-sivas-kangal fly ash, e-lime).....	61
Figure 4.2. Annual temperature variation at different depth of soil located at Maslak / Istanbul in 2013 (Aydin et al., 2015).....	63
Figure 4.3. Test plan for index tests .....	64
Figure 4.4. Test plan for swell and UCS tests .....	65
Figure 4.5. Test Plan for SEM, XRD, zeta potential and shear wave velocity tests .	66
Figure 4.6. Proctor Test Results for Specimen A .....	68
Figure 4.7. Addition of water to the dry mixture and mixing.....	69
Figure 4.8. Crushing particles that sticked to each other with wooden blocks and sieving.....	69
Figure 4.9. Final condition of the sample and putting sample to plastic bag .....	70
Figure 4.10. Swelling apparatus type-1 .....	71
Figure 4.11. Swelling apparatus type-2 .....	72
Figure 4.12. Schematic representation of oedometer (modified from Knappett and Craig, 2012).....	72
Figure 4.13. View from compaction.....	74
Figure 4.14. Time- swell curve (ASTM D4546-14).....	75
Figure 4.15. View from water bath.....	76
Figure 4.16. Curing for swelling tests .....	77
Figure 4.17. Water bath for 10°C tests .....	78
Figure 4.18. Distribution of water content required for S=81.7%.....	80
Figure 4.19. Apparatus for specimen compaction for unconfined compressive strength test.....	81
Figure 4.20. View from specimen compaction.....	81
Figure 4.21. UCS Device.....	82
Figure 4.22. Views from UCS tests (Specimen A).....	83
Figure 4.23. Curing for UCS test.....	84

Figure 4.24. Measurement of $V_s$ with V-meter Mark IV .....	85
Figure 4.25. SEM view of ettringite (Weir et al., 2014) .....	86
Figure 4.26. SEM view of purified thaumasite (Mittermayr et al., 2012) .....	87
Figure 4.27. Scanning electron microscope and vacuum device .....	88
Figure 4.28. XRD Patterns of thaumasite and ettringite (Collepari, 1999) .....	89
Figure 4.29. Rigaku Ultimate-IV brand X-ray diffractometer .....	90
Figure 4.30. The electrical double layer and zeta potential (modified from Malvern Instruments Ltd, 2004) .....	91
Figure 4.31. Variation in aggregation/ dispersion level depending on the average zeta potential value (Yong et al., 2012) .....	92
Figure 4.32. Views from zeta potential tests .....	93
Figure 4.33. pH test photos .....	95
Figure 4.34. $G_s$ samples in water tank .....	96
Figure 4.35. View form hydrometer tests .....	97
Figure 5.1. pH vs. lime content .....	99
Figure 5.2. Swell percent for lime treated specimens .....	100
Figure 5.3. Swell percent for fly ash treated specimens .....	101
Figure 5.4. $G_s$ values of NS and CS added 4% L treated samples .....	102
Figure 5.5. $G_s$ values of NS and CS added 15% SFA treated samples .....	103
Figure 5.6. $G_s$ values of NS and CS added 10% KFA treated samples .....	103
Figure 5.7. LL of NS and CS added 4% L treated samples .....	104
Figure 5.8. PL of NS and CS added 4% L treated samples .....	105
Figure 5.9. PI of NS and CS added 4% L treated samples .....	105
Figure 5.10. LL of NS and CS added 15% SFA treated samples .....	106
Figure 5.11. PL of NS and CS added 15% SFA treated samples .....	107
Figure 5.12. PI of NS and CS added 15% SFA treated samples .....	107
Figure 5.13. LL of NS and CS added 10% KFA treated samples .....	108
Figure 5.14. PL of NS and CS added 10% KFA treated samples .....	109
Figure 5.15. PI of NS and CS added 10% KFA treated samples .....	109
Figure 5.16. SL of NS and CS added 4% L treated samples .....	110

Figure 5.17. SL of NS and CS added 15% SFA treated samples .....	111
Figure 5.18. SL of NS and CS added 10% KFA treated samples .....	111
Figure 5.19. Grain size distribution of NS added 4% L treated samples.....	112
Figure 5.20. Grain size distribution of CS added 4% L treated samples.....	113
Figure 5.21. Grain size distribution of NS added 15% SFA treated samples.....	113
Figure 5.22. Grain size distribution of CS added 15% SFA treated samples .....	114
Figure 5.23. Grain size distribution of NS added 10% KFA treated samples .....	114
Figure 5.24. Grain size distribution of CS added 10% KFA treated samples .....	115
Figure 5.25. Hydrometer test for KFA .....	116
Figure 5.26. Plasticity chart for 4% L treated samples.....	117
Figure 5.27. Plasticity chart for 15% SFA treated samples.....	117
Figure 5.28. Plasticity chart for 10% KFA treated samples .....	118
Figure 5.29. Swell percent for sulfate added 4% L treated specimens.....	120
Figure 5.30. Swell percent for sulfate added 15% SFA treated specimens.....	121
Figure 5.31. Swell percent for sulfate added 10% KFA treated specimens .....	121
Figure 5.32. Swell vs. time graph for 40000ppm NS and CS added 15% SFA and 10% KFA treated specimens.....	122
Figure 5.33. Swell percent for NS added 15% SFA treated specimens at 10, 25 and 40°C .....	123
Figure 5.34. Swell percent for CS added 15% SFA treated specimens at 10, 25 and 40°C .....	123
Figure 5.35. Swell percent for NS added 10% KFA treated specimens at 10, 25 and 40°C .....	124
Figure 5.36. Swell percent for CS added 10% KFA treated specimens at 10, 25 and 40°C .....	124
Figure 5.37. Swell percent for NS added 15% SFA treated specimens cured 7 and 28 days at 25°C.....	125
Figure 5.38. Swell percent for CS added 15% SFA treated specimens cured 7 and 28 days at 25°C.....	126

Figure 5.39. Swell percent for NS added 10% KFA treated specimens cured 7 and 28 days at 25°C .....	126
Figure 5.40. Swell percent for CS added 10% KFA treated specimens cured 7 and 28 days at 25°C .....	127
Figure 5.41. UCS of sulfate added 4% L treated specimens.....	128
Figure 5.42. UCS of sulfate added 15% SFA treated specimens.....	128
Figure 5.43. UCS of sulfate added 10% KFA treated specimens .....	129
Figure 5.44. Swell percent of NS added 15% SFA treated specimens cured 7 days at 10, 25 and 40°C.....	130
Figure 5.45. Swell percent of CS added 15% SFA treated specimens cured 7 days at 10, 25 and 40°C.....	131
Figure 5.46. Swell percent of NS added 15% SFA treated specimens cured 28 days at 10, 25 and 40°C.....	132
Figure 5.47. Swell percent of CS added 15% SFA treated specimens cured 28 days at 10, 25 and 40°C.....	133
Figure 5.48. Swell percent of NS added 10% KFA treated specimens cured 7 days at 10, 25 and 40°C.....	135
Figure 5.49. Swell percent of CS added 10% KFA treated specimens cured 7 days at 10, 25 and 40°C.....	136
Figure 5.50. Swell percent of NS added 10% KFA treated specimens cured 28 days at 10, 25 and 40°C.....	137
Figure 5.51. Swell percent of CS added 10% KFA treated specimens cured 28 days at 10, 25 and 40°C.....	138
Figure 5.52. $V_s$ of sulfate added 15% SFA treated specimens.....	139
Figure 5.53. $V_s$ of sulfate added 10% KFA treated specimens .....	140
Figure 5.54. Zeta Potential of the samples .....	141
Figure 5.55. pH of the samples .....	141
Figure 5.56. Crystal formed within the 40000ppm NS added 15% SFA treated sample cured for 6 months at 10°C .....	143

Figure 5.57. SEM images of (a)- Sample A, (b)-15% SFA treated sample (magnification factor=20000).....	143
Figure 5.58. SEM images of (a)- 10% KFA treated sample, (b)- 40000ppm NS added 10% KFA treated sample (magnification factor=20000) .....	144
Figure 5.59. SEM images of 15% SFA treated sample with (a)-40000ppm NS (b)-40000ppm CS (magnification factor=20000).....	144
Figure 5.60. SEM images of 28 days cured 40000ppm NS added 15% SFA treated sample at 10°C (magnification factor=20000 and 5000).....	145
Figure 5.61. SEM images of 28 days cured 40000ppm NS added 15% SFA treated sample at 25°C (magnification factor=2500 and 20000).....	145
Figure 5.62. SEM images of 28 days cured 40000ppm NS added 10% KFA treated samples (a)-10°C (b)- 25°C (magnification factor=20000 and 10000).....	146
Figure 5.63. SEM images of 28 days cured 40000ppm CS added (a)-15% SFA (b)-10% KFA treated sample at 10°C (magnification factor= 10000) .....	146
Figure 5.64. SEM images of 6 months cured 40000ppm NS added 15% SFA treated sample at 10°C (magnification factor= 8000 and 12000).....	147
Figure 5.65. SEM images of crystals observed in 6 months cured 40000ppm NS added 15% SFA treated sample at 10°C (magnification factor= 800 and 12000).....	147
Figure 5.66. EDX diagram of Sample A .....	148
Figure 5.67. EDX diagram of 15% SFA treated sample .....	149
Figure 5.68. EDX diagram of 10% KFA treated sample.....	150
Figure 5.69. EDX diagram of 40000ppm NS added 15% SFA treated sample.....	151
Figure 5.70. EDX diagram of 40000ppm NS added 15% SFA treated sample cured at 10°C for 6 months.....	152
Figure 5.71. 40000ppm NS added 15% SFA treated specimens cured at 10°C for a,b - 28 days, c,d-6 months .....	153
Figure 5.72. XRD of 15% SFA treated sample .....	154
Figure 5.73. XRD of 40000ppm NS added 15% SFA treated sample cured at 10°C for 28 days.....	155

Figure 5.74. XRD of 40000ppm NS added 15% SFA treated sample cured at 10°C for 6 months.....	156
Figure 6.1. Atterberg limits vs. sulfate content for 6% lime treated soil with different metal sulfate addition (Kinuthia et al., 1999).....	167
Figure 6.2. Variation of LL and PI with gypsum content (Yılmaz and Civelekoglu, 2009) .....	168
Figure 6.3. Hydrometer view of 40000ppm CS added 4% L treated sample .....	174
Figure 6.4. Photos of specimens a- Specimen A (sieved), b- Specimen A (non-sieved), c- 10% KFA treated soil (sieved), d-10% KFA treated soil (non-sieved) .....	194
Figure 6.5. $q_u$ test results for Specimen A.....	195
Figure 6.6. $q_u$ test results for 15% SFA treated specimen.....	195
Figure 6.7. $q_u$ test results for 10% KFA treated specimen.....	196
Figure 6.8. 40000ppm NS added 15% SFA treated specimen after 28 days curing at 10°C .....	205
Figure 6.9. 40000ppm NS added 10% KFA treated specimen after 28 days curing at 10°C .....	213
Figure 6.10. 40000ppm NS added 15% SFA treated specimen cured at 10°C for a- 28 days, b- 6 months .....	217
Figure 6.11. 40000ppm NS added 10% KFA treated specimen cured at 10°C for a- 28 days, b- 3 months, c- 9 months .....	218
Figure 6.12. 40000ppm NS added 4% L treated specimen cured at 10°C for a- 4 months, b- 9 months.....	219
Figure 6.13. 40000ppm NS added a-10% KFA, b-4% L, c-15% SFA treated specimen cured at 40°C for 6 months .....	220
Figure 6.14. Crystal morphology of sodium sulfate (Xusheng et al., 2017).....	222
Figure 6.15. Views form powdered of NS, a- study of Xusheng et al., 2017, b- this study (dry form of 40000ppm NS Added 10% KFA treated specimen cured at 40°C for 28 days.) .....	223
Figure 6.16. UCS against curing time for soil-lime cylinders of various compositions cured in a moist environment at 25°C (Wild et al., 1986) .....	224

Figure 6.17. UCS against curing time for soil-lime cylinders of various compositions cured in a moist environment at 75°C (Wild et al., 1986).....	224
Figure 6.18. $q_u$ vs. gypsum content for kaolinite- lime- GBFS mixtures moist cured at 30°C and 100% relative humidity at a- 7 days, b- 28 days (Wild, 1998).....	226
Figure 6.19. Variation of UCS with gypsum content (Yılmaz and Civelekoglu, 2009) .....	228
Figure 6.20. Measured and calculated $V_s$ values for sulfate added 15% SFA treated specimens.....	233
Figure 6.21. Measured and calculated $V_s$ values for sulfate added 10% KFA treated specimens.....	234
Figure 6.22. The variation in aggregation/ dispersion level of the samples according to zeta potential values (Yong et al. 2012) .....	237
Figure 6.23. SEM micrograph of ettringite needles demonstrating porous volume (Cardenas et al., 2011).....	240
Figure 6.24. SEM views of thenardite a- this study, b- study performed by Rodriques-Navarro et al. (2000).....	242
Figure 6.25. XRD pattern of different phases of thenardite (phases III and V) (Rodriquez- Navarro et al., 2000).....	244
Figure 6.26. XRD analyses of 40000ppm NS added 15% SFA treated sample after 28 days curing at 10°C.....	245
Figure 6.27. XRD analyses of 40000ppm NS added 15% SFA treated sample after 6 months curing at 10°C .....	246
Figure 6.28. XRD analyses of uncured 15% SFA treated and 40000ppm NS added 15% SFA treated samples cured at 10°C for 28 days and 6 months and cured at 25°C for 28 days .....	247
Figure A.1. Chemical analyses report of Sample A (Central Laboratory of METU, Report No. 16544) .....	265
Figure A.2. Chemical analyses report of SFA (Central Laboratory of METU, Report No. 16916).....	266

Figure A.3. Chemical analyses report of KFA (Central Laboratory of METU, Report No. 16916) .....	267
Figure A.4. Chemical analyses report of lime (BASTAS Cement Factory) .....	268
Figure B.1. XRD for 40000ppm NS added 15% SFA cured 28 days at 10°C and 25°C .....	270
Figure C.1. Swell vs. time graphs for specimen A and lime treated specimens .....	271
Figure C.2. Swell vs. time graphs for specimen A and SFA treated specimens .....	272
Figure C.3. Swell vs. time graphs for specimen A and KFA treated specimens .....	272
Figure C.4. Swell vs. time graphs for NS added 4% L treated specimens .....	273
Figure C.5. Swell vs. time graphs for CS added 4% L treated specimens .....	273
Figure C.6. Swell vs. time graphs for NS added 15% SFA treated specimens .....	274
Figure C.7. Swell vs. time graphs for CS added 15% SFA treated specimens .....	274
Figure C.8. Swell vs. time graphs for NS added 10% KFA treated specimens .....	275
Figure C.9. Swell vs. time graphs for CS added 10% KFA treated specimens .....	275
Figure C.10. Swell vs. time graphs for NS added 15% SFA treated specimens at 10°C and 40°C .....	276
Figure C.11. Swell vs. time graphs for CS added 15% SFA treated specimens at 10°C and 40°C .....	276
Figure C.12. Swell vs. time graphs for NS added 10% KFA treated specimens at 10°C and 40°C .....	277
Figure C.13. Swell vs. time graphs for CS added 10% KFA treated specimens at 10°C and 40°C .....	277
Figure C.14. Swell vs. time graphs for NS added 15% SFA treated specimens cured for 7 and 28 days .....	278
Figure C.15. Swell vs. time graphs for CS added 15% SFA treated specimens cured for 7 and 28 days .....	278
Figure C.16. Swell vs. time graphs for NS added 10% KFA treated specimens cured for 7 and 28 days .....	279

Figure C.17. Swell vs. time graphs for CS added 10% KFA treated specimens cured for 7 and 28 days..... 279

## LIST OF ABBREVIATIONS

### ABBREVIATIONS

ASTM	American Society for Testing and Materials
BS	British Standard
CAH	Calcium Aluminate Hydrate
CBR	California Bearing Ratio
CEC	Cation Exchange Capacity
CS	Calcium Sulfate Dihydrate
CSH	Calcium Silicate Hydrate
EDX	Energy Dispersive X-Ray Analysis
FHWA	Federal Highway Administration
GBFS	Granulated Blast Furnace Slag
KFA	Sivas-Kangal Fly Ash
KISAD	Turkey Lime Industrialists Association
LOI	Loss on Ignition
METU	Middle East Technical University
NS	Sodium Sulfate
ppm	Parts per million
SEM	Scanning Electron Microscope
SFA	Soma Fly Ash
SSA	Specific Surface Area

TEM	Transmission Electron Microscopy
TS	Turkish Standard
TUIK	Turkish Statistical Institute
UCS	Unconfined Compressive Strength
USCS	Unified Soil Classification System
XRD	X-Ray Diffraction

## LIST OF SYMBOLS

### SYMBOLS

CH	Inorganic Clay with High Plasticity
CL	Inorganic Clay with Low Plasticity
CaSO <sub>4</sub> .2H <sub>2</sub> O	Calcium Sulfate Dihydrate
C <sub>u</sub>	Undrained Shear Strength
e	Void Ratio
G <sub>s</sub>	Specific Gravity
LL	Liquid Limit
ML	Inorganic Silt with Low Plasticity
MH	Inorganic Silt with High Plasticity
mV	Millivolts
Na <sub>2</sub> SO <sub>4</sub>	Sodium Sulfate
P <sub>a</sub>	Atmospheric Pressure
PI	Plasticity Index
PL	Plastic Limit
q <sub>u</sub>	Unconfined Compressive Strength
S	Degree of Saturation
SL	Shrinkage Limit
SO <sub>4</sub>	Sulfate
SO <sub>3</sub>	Sulfite

$V_s$	Shear Wave Velocity
$w$	Water Content
$\gamma_b$	Bulk Unit Weight of Soil
$\gamma_d$	Dry Unit Weight of Soil
$\gamma_w$	Unit Weight of Water
$\sigma$	Standard Deviation

## CHAPTER 1

### INTRODUCTION

#### 1.1. General

The number of constructed houses, apartments, hospitals, industrial buildings, social facilities increases rapidly with the rise in population, however areas with available soil conditions decreases and treatment techniques gain importance. One of the challenging soil types is expansive soil that causes many problems in lightweight civil engineering structures due to the cyclic swell-shrink behavior of this type of soils as a result of the fluctuation of moisture content with the seasonal conditions. Swelling and shrinking of expansive soils cause an estimated annual cost of several millions of euros (Chindris et al., 2017). Several methods are applied for the improvement of this type of soils such as; soil replacement, moisture control, chemical stabilization, prewetting, etc. One of the most widely used methods among these is chemical stabilization. Lime, cement and class C fly ash are generally used as calcium-based stabilizers for this method. Lime stabilization is widely used to improve the strength and plastic properties of high clay content cohesive soils.

There are many studies in the literature that proves the beneficiary effect of calcium-based stabilizers on the treatment of expansive soils. However, sulfate, existing in clays can also react with lime which results in the formation of ettringite (McCarthy, 2009). Ettringite that is a weak sulfate mineral will undergo significant heaving when exposed to hydration and this heave which is named sulfate-induced heave in literature caused also many problems in highways, runway, parking lots, residential and industrial buildings, etc. Repairing and reconstruction of the failed structures cost millions of dollars (Puppala et al., 2004).

The studies performed on sulfate bearing soils have been focused on understanding the behavior of lime treated soils, however, all the calcium-based stabilizers have the potential to cause sulfate-induced heave problems.

Little and Nair (2009) stated that cases have been reported where soils stabilized with portland cement and/or fly ash has heaved. The effect of different cement types and the influence of various compositions of fly ash on ettringite/thaumasite formation are not completely understood and further investigation in this area is needed.

There are some recommendations in the literature to classify the level of risk associated with lime stabilization in sulfate-bearing clays according to sulfate content (Little and Graves, 1995, etc.). However, there are not any recommendations in the literature about fly ash stabilization and any data even the classifications for lime based on the sulfate concentration of soil is applicable for fly ash or not. This gap in the literature is continuing.

Turkey is a country with a rich sulfate reserve. Sodium sulfate is used in detergent, paper, glass, and textile industry and in the production of many chemicals. One of the biggest sodium sulfate reserve of Turkey exists in Çayırhan, Ankara with a 192.5 million tons reserve capacity. Şereflikoçhisar, Beypazarı, and Nallıhan are rich in gypsum which is a potential source of sulfate. The total gypsum reserve in these areas is estimated to be 150 million tons (General Directorate of Mineral Research and Exploration, 2010).

General Directorate of Highways made a protocol with Lime Industrialists Association (KİSAD) to conduct studies for examining performance of lime stabilization in some parts of the real roads (Kavak et al., 2008). The aim of these studies is to extend the use of lime stabilization and reduce the cost of constructions spent on the treatment of soils.

The most prevailing technical specification about the lime even the only one in Turkey has been prepared by the General Directorate of Highways (2013). The limit presented

in the technical specification related to sulfate ( $\text{SO}_4$ ) content of soil for lime treatment is as follows;

“The reaction of sulfate with lime can cause additional lime consumption and volume increase in the mix. The ratio of the total  $\text{SO}_3$  (sulfite) content to dry soil weight should be smaller than 3% for the soil sieved from No.10 sieve (2.0mm).”

3%  $\text{SO}_3$  is equal to 3.6%  $\text{SO}_4$  (36000 ppm) and this value is far more higher than the 10000ppm (1%) which is classified as the unacceptable risk in the literature. Therefore, study related to chemical treatment of sulfate bearing clays gains extra importance in Turkey.

### **1.2. Aim of the Study**

There are lots of studies concerning the effect of class C fly ash on the engineering properties of expansive clays. Although, there are studies about the effect of lime stabilization on sulfate bearing soils, there are insufficient number of studies about the fly ash treatment of these type of soils.

Also, Turkey is rich in fly ash production with a high sulfate level which cannot be used in concrete production. The aim of this study is to investigate the behavior of class C fly ashes beside lime that is used with sulfate bearing soils, attract attention to ettringite induced heave problems in Turkey and also investigate the suitability of usage of high sulfate class C fly ashes in stabilization of non-sulfate bearing soils.

### **1.3. Scope of the Study**

In the scope of the study, two different fly ashes with different CaO and sulfate content; Soma fly ash (SFA) and Sivas- Kangal fly ash (KFA) were used. Lime was also used for comparison purposes.

Initially swelling tests were performed to determine the optimum additive content. Besides swelling tests, pH tests were also performed according to ASTM D6276 standard derived from the method proposed by Eades and Grim (1983) to obtain the optimum lime content. Optimum additive content for SFA, KFA and lime was selected

as 15%, 10% and 4% respectively. Two different sulfates namely;  $\text{Na}_2\text{SO}_4$  (NS) and  $\text{CaSO}_4 \cdot 2\text{H}_2\text{O}$  (CS) were added to fly ash treated samples with 3000ppm, 5000ppm, 10000ppm, 20000ppm, and 40000ppm concentrations. Tests on lime were performed on samples with 5000ppm, 10000ppm, and 40000ppm sulfate concentrations.

Firstly, tests were performed to understand the effect of calcium-based stabilizers and sulfate on index properties (grain size, Atterberg limits, specific gravity, etc.). Swell and unconfined compressive strength tests were performed to understand the effect of sulfate on physical and mechanical properties of soils treated with calcium-based stabilizers. Swell tests were performed at three different temperatures; 10°C, 25°C, and 40°C and 7 days and 28 days cured specimens at 25°C. Unconfined compressive strength tests were performed on both uncured specimens prepared at 25°C and 7 days and 28 days cured specimens at 10°C, 25°C, and 40°C.

Scanning electron microscope views, XRD and zeta potential analysis were used to see the effect of treatment in chemical structure and microstructure. Shear Wave Velocity ( $V_s$ ) tests were also performed for comparison purposes since  $V_s$  is a valuable parameter that frequently used for determination of other soil parameters by using correlations recommended in the literature. These tests were performed only on representative sulfate added fly ash treated samples.

#### **1.4. Outline of the Study**

In the scope of this thesis, a literature review on expansive soil, chemical stabilization, and fly ashes are given in Chapter 2. In Chapter 3, a literature review on sulfate-induced heave problem including case studies and previous studies is given. In Chapters 4, 5, 6 and 7 the methodology of experimental works, test results, discussions of the test results and conclusions are presented respectively.

## CHAPTER 2

### LITERATURE REVIEW

#### 2.1. Expansive Soils

Expansive soils show considerable volume changes as a result of the variation of water content. This type of soils exists worldwide and in charge of serious economic losses by causing many damages to buildings and infrastructures (Seco et. al., 2011).

United States, Canada, China, Israel, Australia, Egypt are the countries that are frequently faced with expansive soils related problems (Murthy, 2002). Turkey is also one of the countries that reported expansive soil-related problems (Cokca, 2001; Fredlund et al., 2012). The annual cost of the damages due to the expansive soils are expected to vary between one to thirteen billion dollars in the USA (Puppala and Cerato, 2009; Firoozi et al., 2017). Representative expansive soil related problems in roads and pavements are presented in Figure 2.1.

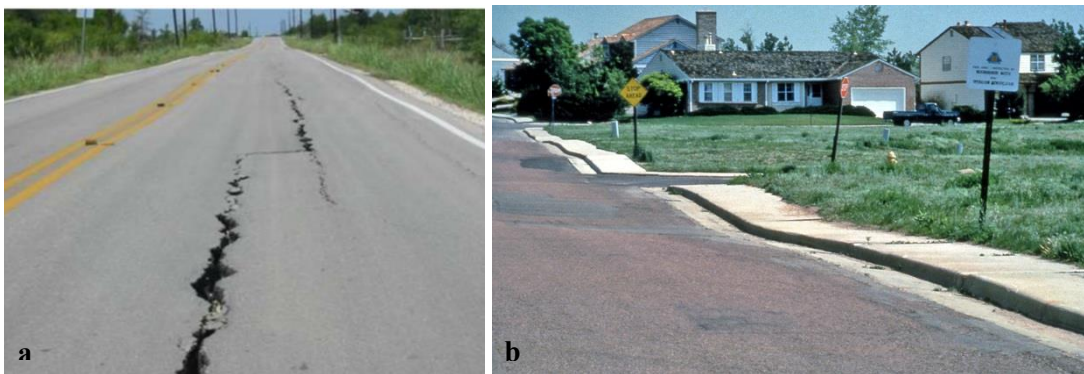


*Figure 2.1.* Expansive soil related problems. a- longitudinal cracks in road (Wang, 2016), b- heave in road and pavements (Colorado Geological Survey, n.d.)

## 2.2. Mechanism of Swelling

The zone in the ground where the seasonal change in water content observed is called the active zone. The depth of this zone can vary between 0.3 – 6.0m depending on the local conditions. The active zone is exposed to significant volume changes as a result of the fluctuations in water content. Depth of this zone could be determined by plotting depth versus liquidity index of the soil profile during a couple of seasons (Kalantari, 2012).

Clay particles have a negative surface charge which causes attraction of H<sub>2</sub>O molecules. This phenomenon provides the orientation of H<sub>2</sub>O molecules on the surface of the clay. The water molecules are separated in layers dependent on electronic forces with the increase in distance from the clay surface (Stavredakis, 2006). Soil expansion mechanism is presented in Figure 2.2.

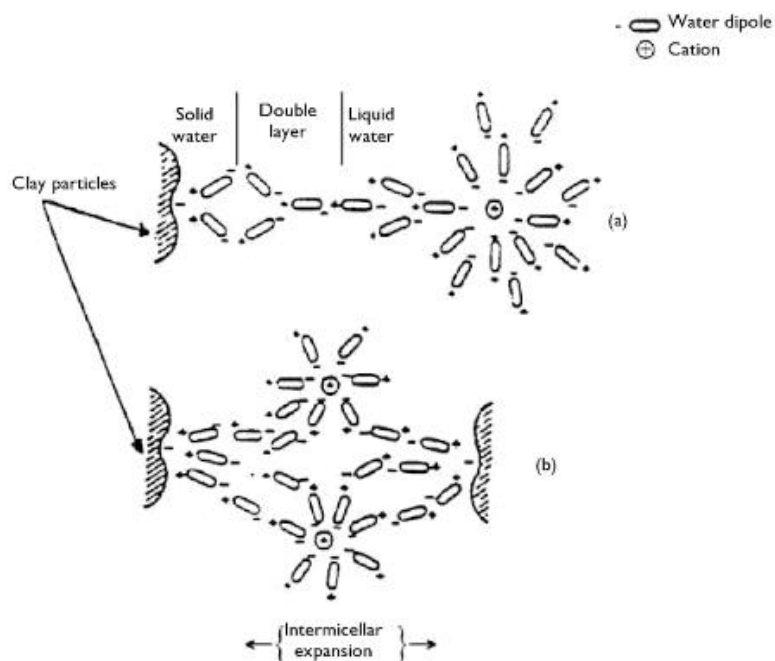


Figure 2.2. Schematic representation of soil expansion (Stavredakis, 2006)

### 2.3. Factors Influencing Swelling

Soil properties, environmental factors, and stress conditions are the main factors that affect the swelling properties of expansive soils (Jayalath et. al., 2016). The sub-factors for each previously mentioned main factor are presented in Figure 2.3 (Nelson and Miller, 1992).

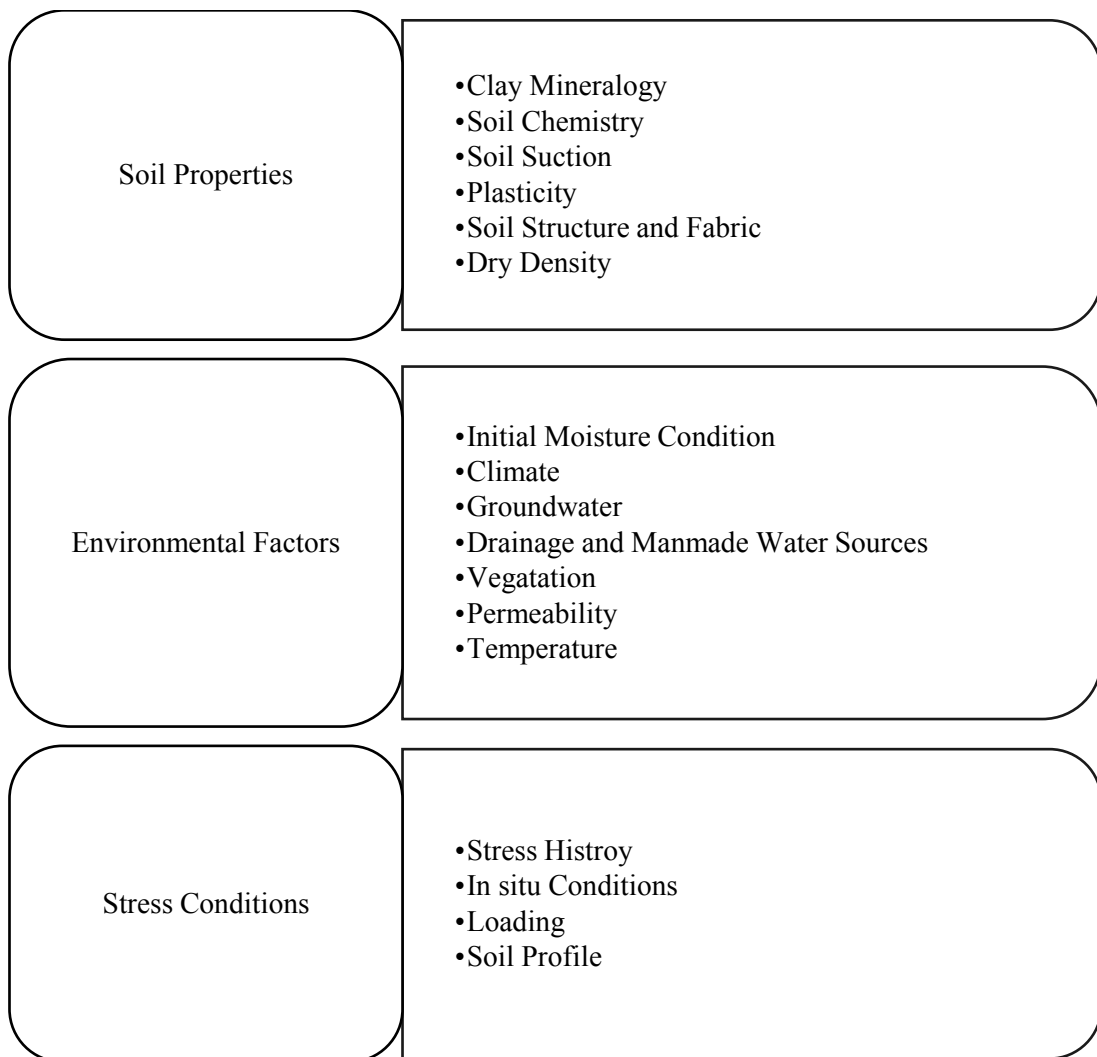


Figure 2.3. Factors affecting swell potential of expansive soils (Nelson and Miller, 1992)

## 2.4. Clay Mineralogy

Although clay hydration is related to the swelling phenomenon, being in contact with water does not result swell for all clays (Foster, 1954). Chemical stabilization of soils depends on pH, specific surface area, cation exchange capacity, zeta potential and origin of soils, etc. (Cherian and Arnepalli, 2015). Since all these factors depend on clay mineralogy, this phenomenon is an important factor both for swelling properties and effectiveness of treatment.

Kaolinite, illite, and montmorillonite are the main clay minerals (Verruijt, 2001). The chemical properties, physical properties, and type of clay minerals directly related to the arrangement of sheets within the aluminosilicate layers (Barton and Karathanasis, 2002). Tetrahedral and octahedral sheets are the two main units that form the clay minerals' atomic structure (Murray, 2007).

The tetrahedron occurs by the connection of four oxygen atoms from the centers that surround the silicon atom. Cations are located at the center and the hydroxyls at the corners for the formation of octahedron. Magnesium, iron, and aluminum are the main cations that form the octahedron (Al-Ani and Sarapaa, 2008).

Silica sheet is formed as a result of the combination of tetrahedral units by means of sharing oxygen atoms. Combination of octahedrons from the shared hydroxyl ions results in the formation of octahedral sheets (Knappett and Craig, 2012). The octahedral sheet is called as gibbsite, if the aluminum is the only existing cation. Brucite is the octahedral sheet that contains magnesium as a cation (Oweis and Khera, 1998). Although the gibbsite sheet is neutral, the silica sheet carries a negative charge (Knappett and Craig, 2012).

Schematic representation of basic units and structures of main clay minerals are presented in Figure 2.4.

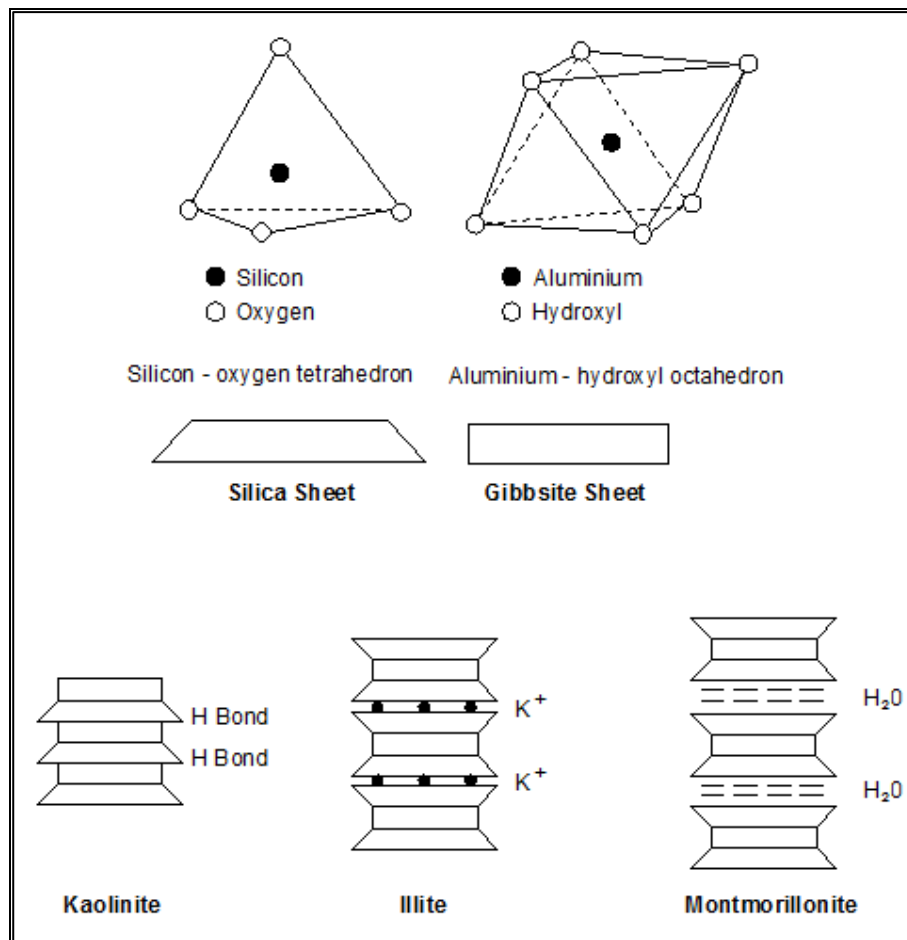


Figure 2.4. Basic units of clay minerals and main clay minerals (Knappett and Craig, 2012)

The properties of kaolinite, illite, and montmorillonite are given below.

### 2.4.1. Kaolinite

Kaolinite is a 1:1 mineral (Barton and Karathanasis, 2002). Crystals of kaolinite consist of repetitive layers which connect each other by hydrogen bonding. Silica sheet and alumina sheet that shares an oxygen atom layer form each layer. A hydrogen bond occurs between the hydroxyls and oxygens of the alumina sheet and silica sheet respectively taking parts in opposite faces. Forces caused by hydrogen bonding is strong and prevent the entering of water between the layers (Yong and Warkentin, 1975).

SSA of kaolinite varies between 8-20 m<sup>2</sup>/g according to Das (2008), Murray (2007) and Yong et al. (2012). CEC of kaolinite varies between 1-15 meq/100g (Das, 2008; Al-Ani and Sarapaa, 2008 and Yong et. al., 2012). Kaolinite is a low activity clay mineral that is not showing a considerable swell potential (Oweis and Khera, 1998).

#### **2.4.2. Illite**

Illite is a 2:1 mineral (Al-Ani and Sarapaa, 2008). Each layer of illite occurs by the combination of two silica sheets that contain an alumina sheet between. The layers of illite are connected to each other by potassium ions (Yong and Warkentin, 1975).

SSA of illite varies between 80-120 m<sup>2</sup>/g according to Das (2008), Murray (2007) and Yong et. al. (2012). CEC of illite varies between 10-40 meq/100g (Das, 2008; Al-Ani and Sarapaa, 2008; Yong et al., 2012).

Illite is more active compared to kaolinite and shows a medium swell potential (Oweis and Khera, 1998).

#### **2.4.3. Montmorillonite**

The basic structure of montmorillonite is same as the illite (Yong and Warkentin, 1975). Instead of potassium, water molecules exist in the space located between the combined sheets which resulted in a weak bond (Knappett and Craig, 2012). Substitution of aluminum with magnesium and iron is observed within the alumina sheet. Different substitution is observed for variant montmorillonite minerals (Yong and Warkentin, 1975).

SSA of montmorillonite varies between 700-800 m<sup>2</sup>/g according to Das (2008) and Yong et. al. (2012). CEC of montmorillonite varies between 80-120 meq/100g (Das, 2008; Al-Ani and Sarapaa, 2008; Yong et al., 2012). Montmorillonite is a high active clay with great swell potential (Yong and Warkentin, 1975). Calcium montmorillonite is the most widespread mineral within this group (Murray, 2007). Sodium montmorillonite has a more water adsorption capacity and a less hydraulic conductivity than calcium montmorillonite (Grim, 1942).

One of the important reserves of bentonite clay which is included in this group exists in Turkey. 11.8 million tons of bentonite was produced worldwide in 2007. Turkey is the third country after USA and Greece with an annual production of 1.0 million tons (Al-Ani and Sarapaa, 2008).

XRD, SEM, and TEM are the main methods that are used for the identification of different clay minerals (Barton and Karathanasis, 2002 and Al-Ani and Sarapaa, 2008).

## **2.5. Methods for Treatment of Expansive Soils**

Investigation and elimination methods of expansive soils gain importance as a result of high repairing cost of damaged structures (Al-Mhaidib and Al-Shamrani, 1996). Ardani (1992) listed the methods for the treatment of expansive soils as presented below;

- Sub-excavation and removal of expansive soil and replacement with non-expansive soil
- Application of heavy applied load to balance the swelling pressure
- Preventing access of water to the soil by encapsulation
- Stabilization by means of chemical admixtures
- Mechanical stabilization
- Pre-wetting the soil
- Avoiding the expansive soil

### **2.5.1. Chemical Stabilization**

Chemical treatment is a commonly used method in many of the geotechnical related civil engineering projects such as embankments, roads, highways, etc. for soil improvement purposes (Tran et al., 2014). Stabilizers are divided into three main groups namely; traditional (lime, fly ash, cement, etc.), non-traditional (enzymes, potassium compounds, polymers, ammonium chloride, etc.) and by-product (cement

kiln dust, lime kiln dust, etc.). Lime is the most widely used stabilizer among previously mentioned stabilizers (Little and Nair, 2009).

### **2.5.1.1. Soil- Lime Reactions**

Cation exchange, flocculation and pozzolanic reactions are the leading mechanisms that results improvement of engineering properties of soils when clayey soils are mixed with lime in an aqueous medium. Carbonation is the other chemical reaction that occurs when the soil is mixed with lime (Little, 1995; West and Carder, 1997; Al-Rawas, 2005). Properties of each mechanism are presented below.

#### **2.5.1.1.1. Cation Exchange and Flocculation**

Cation exchange and flocculation are the rapid reactions that occur immediately with the mixing of soil and lime (Mallela et. al., 2004). Lyotropic series give the replaceability of cations as follows;  $\text{Th}^{4+} > \text{Fe}^{3+} > \text{Al}^{3+} > \text{Cu}^{2+} > \text{Ba}^{2+}=\text{Sr}^{2+} > \text{Ca}^{2+} > \text{Mg}^{2+} > \text{Cs}^+ > \text{Rb}^+ > \text{K}^+=\text{NH}_4^+ > \text{Li}^+ > \text{Na}^+$  (Cherian and Arnepalli, 2015).  $\text{Ca}^{2+}$  ions, released from lime replace with  $\text{Na}^+$ ,  $\text{K}^+$  and  $\text{H}^+$  ions that exist in the soil. Replacement of univalent ions with calcium ions results in an increase in the attraction between soil particles (Mallela et. al., 2004). Floccs are formed when the soil particles come closer to each other as a result of the attraction and cation exchange. This phenomenon is called flocculation (Al-Rawas, 2005). Cation exchange and flocculation result in a more granular structure with a lower swell potential, plasticity and higher permeability coefficient (Seco et al., 2011). Schematic representations of cation exchange and flocculation reactions are presented in Figure 2.5 and 2.6 respectively.

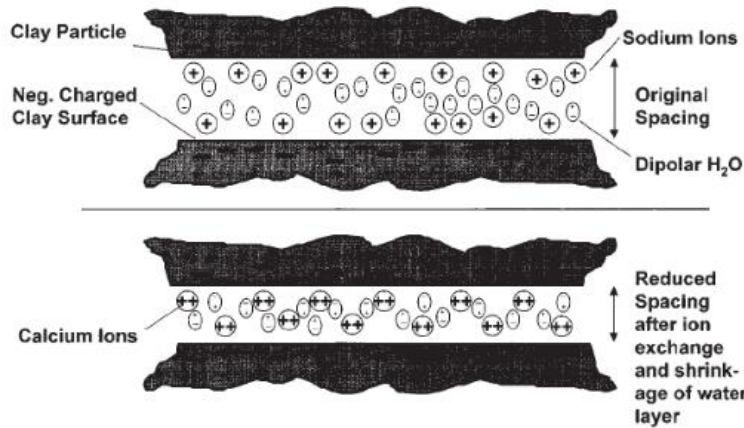


Figure 2.5. Schematic representation of cation exchange (Prusinski and Bhattacharja, 1999)

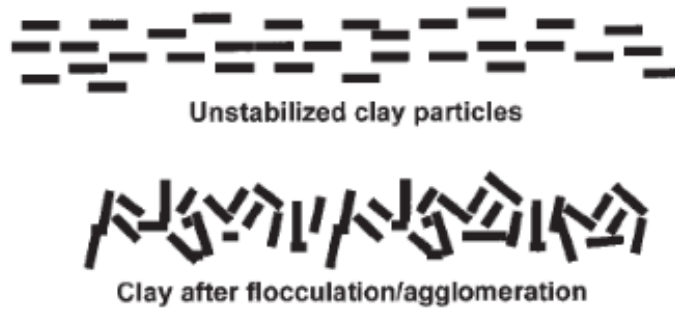
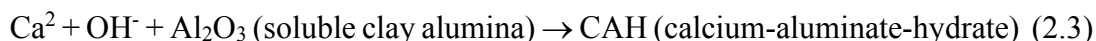
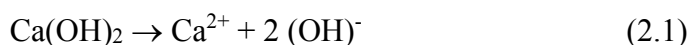


Figure 2.6. Schematic representation of flocculation (Prusinski and Bhattacharja, 1999)

### 2.5.1.1.2. Pozzolonic Reactions

Addition of enough quantity of lime results an increase of soil's pH approximately to 12.4 that cause the dissolution of silica and alumina from the clay (Seco et al., 2011). The reaction between the Ca from the lime and silica or alumina from the soils is called pozzolanic reactions. Especially calcium silicate and calcium aluminate hydrates are formed as cementing agents at the end of the pozzolanic reactions (ASTM, 1970).

Some basic soil-lime pozzolonic reactions are presented below (Mallela et. al., 2004);



The cementing compounds cause an improvement in the mechanical properties (such as strength) and a reduction in swelling properties (Seco et al., 2011).

Organic content, mineralogy, weathering degree, presence of carbonates and natural drainage are the main soil properties that affect the release of alumina and silica. Besides soil properties, pozzolanic reactions are also affected from curing temperature, curing time and lime percentage (ASTM, 1970). The schematic representation of the pozzolanic reactions is presented in Figure 2.7.

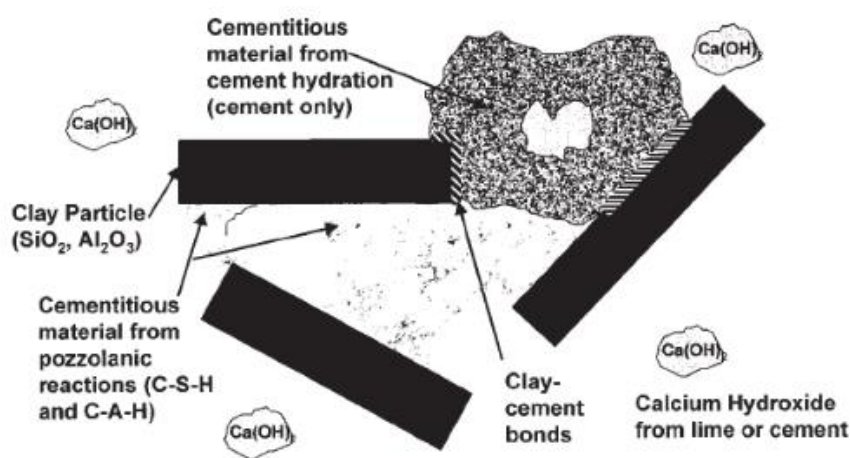


Figure 2.7. Schematic representation of pozzolonic reactions (Prusinski and Bhattacharja, 1999)

### 2.5.1.1.3. Carbonation

This reaction occurs between lime and CO<sub>2</sub>. CaCO<sub>3</sub> is formed as a result of the carbonation reaction instead of CSH and CAH (Mallela et al., 2004). It is an unwanted

reaction since carbonation consumes some part of the lime which will be used for other reactions (West and Carder, 1997) and  $\text{CaCO}_3$  is a plastic material causing an increase in the plasticity of soil (Fang, 1991).

### 2.5.1.2. Lime Treatment

Main construction steps of lime treatment given by the National Lime Association (2004) are presented below;

- scarifying or pulverization of the soil
- lime spreading
- water addition and mixing
- compaction
- curing before the placement of the next layer

Schematic representation of the lime treatment process is given in Figure 2.8.

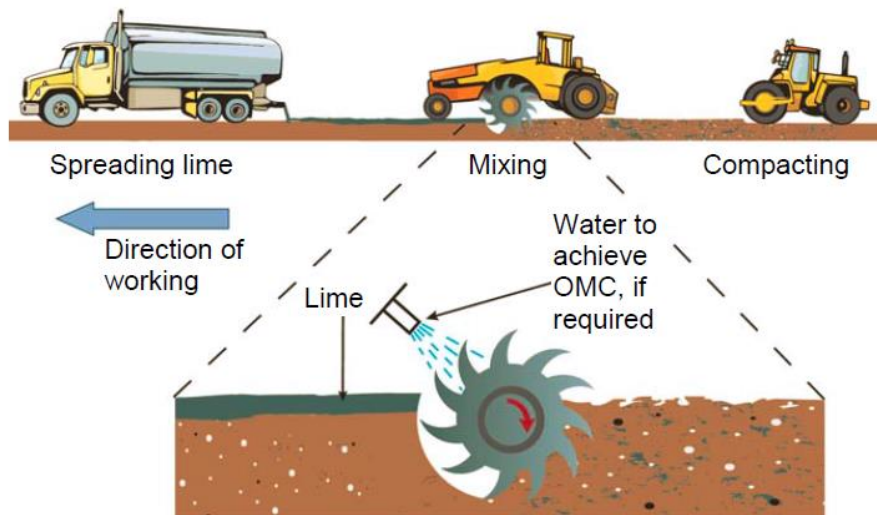


Figure 2.8. Schematic representation of the lime treatment process (Britpave, 2007)

Many researchers (Dempsey and Thompson, 1968; Al-Mhaidib and Al-Shamrani, 1995; Güney et al., 2007; Baglari and Dash, 2013; Bhuvaneshwari et al., 2014; Tran et al., 2014; Belchior et al., 2017; etc.) studied the effect of lime stabilization on soils. Jawad et al. (2014) summarized the outcomes of some of the previous studies and the effect of lime treatment in different soil properties with the reasons as given in Table 2.1.

Table 2.1. *Overview of previous studies on lime (Jawad et al., 2014)*

<b>Property</b>	<b>Effect</b>	<b>Reason</b>
Water- Content - Density Relationship	<ul style="list-style-type: none"> <li>- Increase in void ratio</li> <li>- Decrease in maximum dry density</li> <li>- Increase in optimum moisture content</li> </ul>	<ul style="list-style-type: none"> <li>- Flocculation- agglomeration</li> </ul>
Plasticity Index	<ul style="list-style-type: none"> <li>- Increase or decrease in liquid limit and plastic limit depending on the treated soil properties</li> <li>- Decrease in plasticity index</li> </ul>	<ul style="list-style-type: none"> <li>- Flocculation- agglomeration</li> </ul>
Soil Strength	<ul style="list-style-type: none"> <li>- Significant increase in soil cohesion</li> <li>- Slight improvement in internal friction angle</li> </ul>	<ul style="list-style-type: none"> <li>- Decrease in plasticity</li> <li>- Improvement in compaction features</li> <li>- Pozzolanic reactions</li> </ul>
Swell Potential and Volume Change	<ul style="list-style-type: none"> <li>- Decrease in swell potential and swell pressure</li> </ul>	<ul style="list-style-type: none"> <li>- Decrease in plasticity</li> <li>- Decrease in the thickness of diffuse double layer</li> </ul>
Permeability	<ul style="list-style-type: none"> <li>- Decrease or increase in soil permeability</li> </ul>	<ul style="list-style-type: none"> <li>- Increase is explained with flocculation and agglomeration</li> <li>- Decrease is explained by the formation of bonds between the soil particles and formation of cementitious products that results contraction of pore spaces</li> </ul>
Compressibility	<ul style="list-style-type: none"> <li>- Increase in pre-consolidation pressure (<math>P_c</math>)</li> <li>- Decrease in compression index</li> <li>- Decrease in coefficient of volume compressibility</li> <li>- Increase in coefficient of consolidation (<math>C_v</math>)</li> </ul>	<ul style="list-style-type: none"> <li>- Bond formation between the soil particles</li> </ul>

### 2.5.1.3. Fly Ash Treatment

Fly ash is a by-product that is generated in coal-fired thermal power plants (Ji-ru and Xing, 2002). It is produced during the burning of powdered coal in the boiler. Electrostatic precipitators, flue gas desulphurization, and baghouses are used to remove the fly ash from the flue gases (Hartuti et al., 2018).

The schematic representation of fly ash production is given in Figure 2.9.

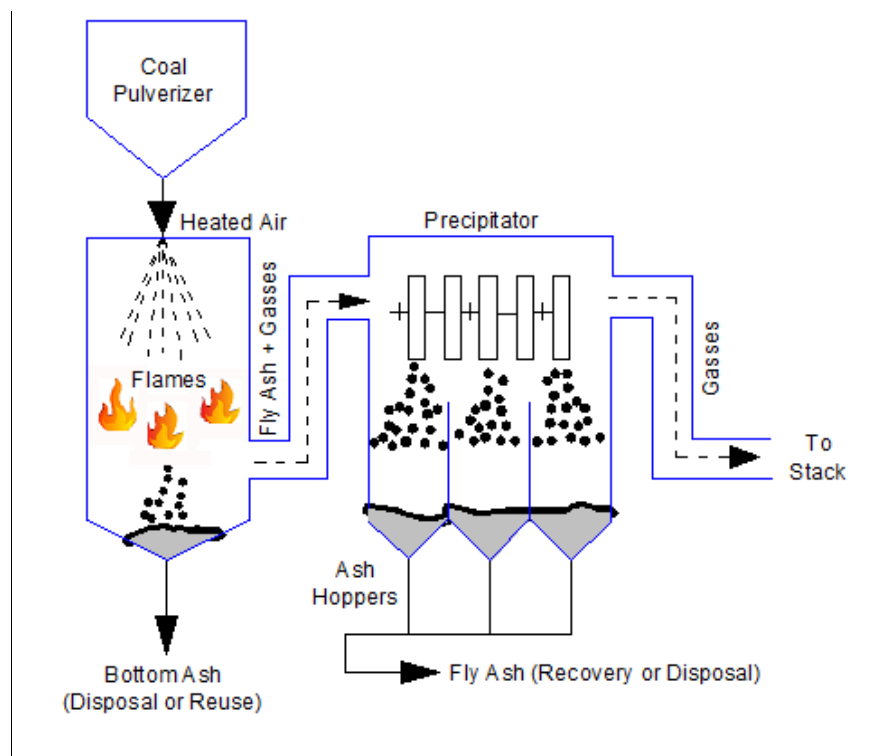


Figure 2.9. Schematic representation of fly ash production (FHWA, 2008)

Fly ash is originated from the silt-sized particles that are spherical in general. The primary oxides that form the fly ash are silicon, aluminum, iron, and calcium. Sodium, sulfur, potassium, magnesium, and titanium are also observed within fly ash as secondary oxides (American Coal Ash Association, 2003).

Fly Ashes are divided into two main groups namely; Class C and Class F according to ASTM C-618. Class C fly ashes have both pozzolanic and cementitious properties whereas the Class F fly ashes have only pozzolanic properties.  $\text{SiO}_2 + \text{Al}_2\text{O}_3 + \text{Fe}_2\text{O}_3$  content is greater than 70% and 50% for Class F and Class C Fly ashes respectively. CaO concentration of Class F fly ash is smaller than 10%, however, Class C fly ash has a CaO content greater than 10%. Also, for both type of fly ashes,  $\text{SO}_3$  content should be lower than 5%.

The main factors that affect the fly ash properties are boiler and emission control design and coal source. The coal type determines the content of fly ash. Ash produced from bituminous and lignite coals have not self-cementing properties whereas burning of sub-bituminous coal lead to the production of fly ashes with self-cementing properties and higher calcium content. Boiler and emission control design has a major effect on the crystalline structure which specifies the hydration properties of fly ash (Mackiewicz and Ferguson, 2005).

Development in industry and population growth results in an increase in electrical energy demand. One of the leading energy sources are the thermal power plants. The increase in fly ash production become unavoidable with the going of new thermal power plants into operation (Mir and Shidharan, 2019).

Concrete and brick production, soil stabilization, embankment construction, etc. are the areas where fly ash is used in civil engineering applications (Dwivedi and Jain, 2014).

There exist many studies in the literature that show the beneficiary effect of fly ash in soil stabilization (Cokca, 2001; Koliyas et al., 2005; Al-Dahlaki, 2007; Zha et al., 2008; Deb and Pal, 2014; Ige and Ajamu, 2015; Nath et al., 2017, Mir and Shidharan, 2019).

ASTM C-618 “Standard Specification for Coal Fly Ash and Raw or Calcined Natural Pozzolan for Use in Concrete” limits the maximum allowable  $\text{SO}_3$  content of fly ash as 5% to be used in concrete. However, there are no criteria about the  $\text{SO}_3$  content of

fly ash for soil stabilization in ASTM D5239 “Standard Practice for Characterizing Fly Ash for Use in Soil”.

#### **2.5.1.3.1. Fly Ash Production in Turkey**

The energy demand of Turkey is increasing day-by-day with industrial development. 22% of the used energy is produced in thermal power plants by using coal (Uyanik and Topeli, 2012).

24.2 million tons of waste material, 98.5% of which consisted of mineral wastes (ash, gypsum, fly ash, slag, etc), were produced in 2014 at thermal power plants with a capacity greater than 100 mW. 70% of the waste material was deposited at ash dams and disposal areas, 15% of it was sold or sent to recycling firms and remaining 15% were disposed by other ways (sent to mine and quarries, thrown away to the municipal rubbish tip, etc.) (TUIK, 2014).

Turker et al. (2009) performed chemical tests on fly ashes taken from 11 different thermal power plants namely; Afşin-Elbistan, Çatalağzı, Çayırhan, Kangal, Kemerköy, Orhaneli, Seyitömer, Soma, Tunçbilek, Yatağan, and Yeniköy. The chemical composition of fly ashes is given in Table 2.2.

Table 2.2. The chemical composition and classification of fly ashes in Turkey (Turker et al., 2009)

Thermal Power Plant	SiO <sub>2</sub> +Al <sub>2</sub> O <sub>3</sub> +Fe <sub>2</sub> O <sub>3</sub> (%)	CaO (%)	SO <sub>3</sub> (%)	Class
Afşin-Elbistan	16.6 - 30.6	53.9 - 54.4	11.2 - 24.2	Satisfies the CaO criteria for Class C however SiO <sub>2</sub> + Al <sub>2</sub> O <sub>3</sub> + Fe <sub>2</sub> O <sub>3</sub> and SO <sub>3</sub> criteria could not be satisfied
Çayırhan	73.8	11.8	3.9	C
Çatalağzı	89.8	1.5	0.1	F
Kemerköy	43.8	38.5	13.8	Satisfies the CaO criteria for Class C however SiO <sub>2</sub> + Al <sub>2</sub> O <sub>3</sub> + Fe <sub>2</sub> O <sub>3</sub> and SO <sub>3</sub> criteria could not be satisfied
Orhaneli	80.7	9.5	2.5	F
Seyitömer	84.3	4.3	0.5	F
Sivas-Kangal	51.3 - 55.3	30.0 - 34.9	6.2 - 7.6	C with high SO <sub>3</sub>
Soma	68.2 - 73.9	17.2 - 23.5	1.5 - 4.1	C
Tunçbilek	88.8	1.7	0.6	F
Yatağan	80.7	10.5	1.3	C
Yeniköy	30.4 - 33.7	39.3 - 39.5	22.2 - 25.7	Satisfies the CaO criteria for Class C however SiO <sub>2</sub> + Al <sub>2</sub> O <sub>3</sub> + Fe <sub>2</sub> O <sub>3</sub> and SO <sub>3</sub> criteria could not be satisfied

Özmen (2011) listed the total ash production in previously mentioned 11 thermal power plants in Turkey as given in Table 2.3.

Table 2.3. Total ash production in Turkey (Ozmen, 2011)

Thermal Power Plant	Ash Production (ton/year)	Fly Ash Class	Total Ash Production (ton/year)
Çatalağzı	803.703	Class F	3.741.948
Orhaneli	357.391		
Seyitömer	1.989.000		
Tunçbilek	591.854		
Soma	2.373.439	Class C	5.601.921
Yatağan	1.320.570		
Çayırhan	1.907.912		
Kangal	1.322.832	Class C with high sulfate level	9.763.011
Kemerköy	1.585.195	Class C according to CaO $\geq$ 10% criteria. Has a high sulfate level	
Yeniköy	713.847		
Afşin-Elbistan	6.141.137		

Özmen (2011) stated that “75-80% of the total produced ash is fly ash and the remaining part is bottom ash”. Therefore, the maximum produced type of fly ash is Class C Fly Ash with high sulfate content (Figure 2.10) in Turkey. As these materials could not satisfy the criteria to be used in the concrete industry, investigation of the suitability of these materials to be used in soil stabilization gains extra importance due to deposition problems of these waste materials and related environmental concerns.

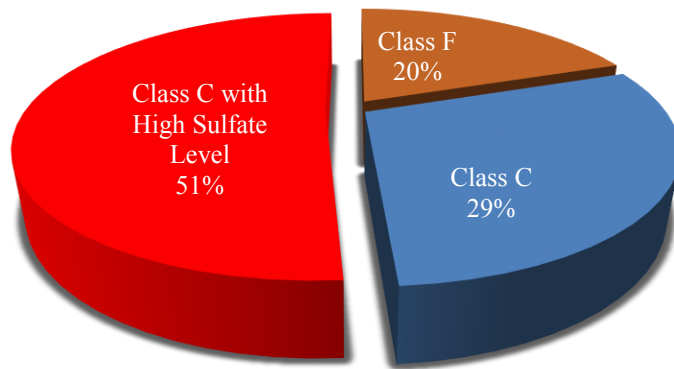


*Figure 2.10.* Percent distribution of the fly ash class in Turkey

## CHAPTER 3

### EFFECT OF SULFATE ON CHEMICALLY STABILIZED SOILS

#### 3.1. Effect of Sulfate on Lime Stabilized Soils

Treatment of soils with calcium-based stabilizers may cause heave dependent problems as a result of the sulfate included chemical reactions (Harris et al.,2006).

During construction, when the calcium-based stabilizers are mixed with water, a high pH environment is developed. Presence of lime and high pH create a favorable environment to the formation of two expansive minerals, ettringite and thaumasite when sulfate exists in soil (Little and Nair, 2009).

When subjected to hydration, ettringite which is a weak sulfate mineral shows significant heaving, this heave is named as sulfate-induced heave in literature and causes severe damages in highways, parking lots, runways, residential and industrial buildings, etc. (Puppala et al., 2004). As the repairing or reconstruction works causes closure of highway lanes and delays in traffic, sulfate-induced heave attracts great attention especially in the transportation division of civil engineering (Puppala et al., 2019).

Examples of heave problems caused by ettringite formation are given in Figure 3.1 and 3.2.



*Figure 3.1.* Vertical heave problem in roads due to the ettringite formation (Puppala et al., 2019)

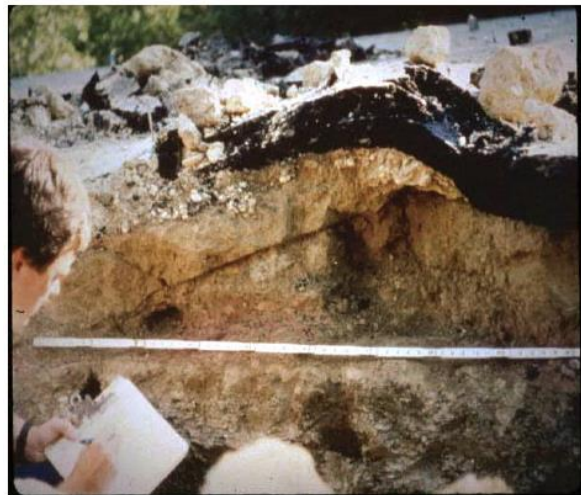


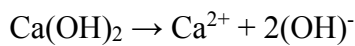
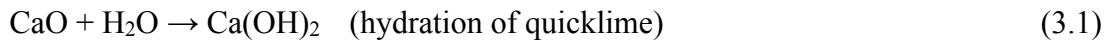
*Figure 3.2.* Evidence of accumulation of considerable lateral strain resulting in shear failure in lime-treated high sulfate soil layer (Little and Nair, 2009)

The rate of sulfate related reactions depends on the water amount and sulfate crystals' size. Reactions could occur within one day as a result of rainfall or may take several years (Texas Department of Transportation, 2005).

Unforeseen failure of lightweight civil engineering structures resulted in questions regarding the efficiency of calcium base stabilizers in soil stabilization (Puppala et al., 2013).

### 3.1.1. Soil- Lime- Sulfate Reactions

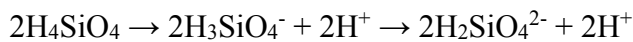
Hunter (1988) summarizes the geochemical reactions for lime-induced heave as follows;



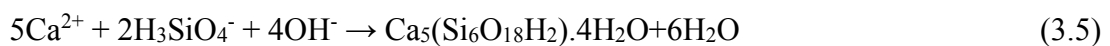
(ionization of calcium hydroxide; pH rises to 12.3) (3.2)



(dissolution of clay mineral, at pH>10.5) (3.3)



(dissociation of silicic acid) (3.4)

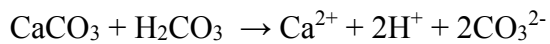


(dissolution of sulfate minerals; x=1, y=2 or x=2, y=1) (3.6)

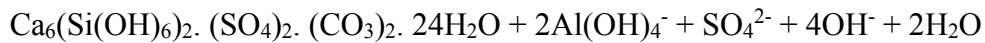
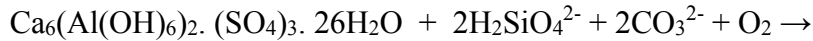


$\text{Ca}_6(\text{Al(OH)}_6)_2 \cdot (\text{SO}_4)_3 \cdot 26\text{H}_2\text{O}$  (formation of ettringite) (3.7)





(dissolution of calcite in carbonic acid) (3.9)



(formation of thaumasite) (3.10)

Hunter (1988) explains the reactions as follows;

- Equations 3.1-3.4 are pozzolanic reactions that cause the siliceous cementation of lime – treated soils (Equation 3.3 is given for montmorillonite),
- The rate of the reaction given in equation 3.5 approaches to zero in the presence of excessive sulfate,
- Sulfate coming from Equation 3.6 reacts with alumina (coming from Equation 3.3 which is the dissolution of any clay mineral) to form ettringite (Equation 3.7).
- Once ettringite forms, it proceeds growing as far as the temperature decreases below 15°C and when the temperature decreases below 15°C, ettringite is transformed to thaumasite (Equation 3.10).

Ettringite crystals have a prism structure which is hexagonal as shown in Figure 3.3.

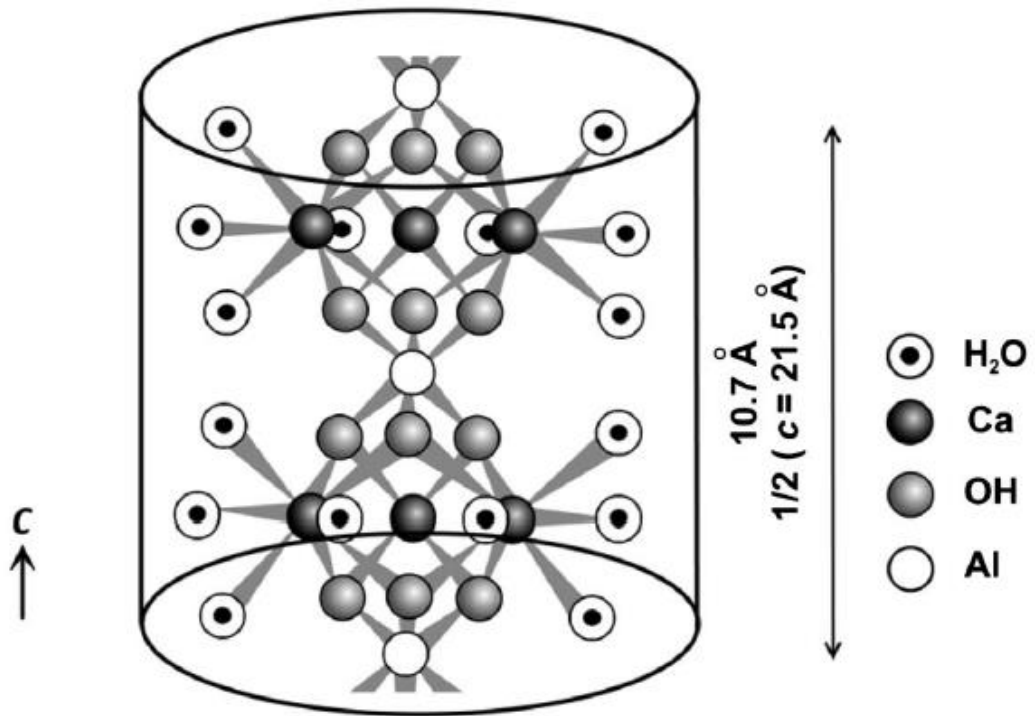


Figure 3.3. Chemical structure of ettringite columns (Puppala et al., 2019)

### 3.2. Mechanism of Heaving or Disruption During Ettringite Formation

Two theories exist in the literature related to the cause of expansion during the formation of ettringite namely;

1. topochemical formation and aelotropic growth of the ettringite crystals
2. expansion resulted from the water absorption of ettringite crystals

The chemical potential of adsorbed water could be lowered due to the negative surface charge of ettringite crystals. A considerable amount of water could be attracted due to the high surface area and the negative charge. Interparticle repulsion that occurs due to the water can result in matrix expansion since inter-crystalline chemical bonding does not exist between the ettringite crystals. The mechanism is parallel with the swelling that is observed when clays electrostatically attract bipolar molecules. Previous studies show that absorption of water enhances the ettringite induced

expansion. In both theories, external water could be accepted as one of the leading activators of the detrimental reactions in treated soil (Little et al., 2010).

### **3.3. Factors Affecting Sulfate Attack**

pH, moisture availability, temperature, sulfate level, and clay mineralogy are the factors that affect the sulfate attack of stabilized materials (Rollings et al., 1999).

#### **3.3.1. pH**

The pH of soil raises above 12 after the use of calcium-based stabilizers. The solubility of alumina and silica increases exponentially when the pH exceeds 9. This phenomenon is also very important for the release of materials from the clay particles to take part in pozzolanic reactions that cause strength gain in chemical treatment. Released active alumina is also one of the main factors that participate in the formation of ettringite. pH value significantly decreases with the ettringite formation (Rollings et al., 1999).

#### **3.3.2. Moisture Availability**

Water is one of the main factors that participate in ettringite reactions. Ettringite formation is strengthened with the existence of moisture and results cracks or joints in pavements. The reactions of ettringite are affected positively from rainfall originated water coming from the joints/ cracks or movement of water vapor. The previous studies show that the deposition of water as a result of the insufficient drainage or ponding causes considerable swelling in sulfate bearing soils that are chemically treated with lime (Rajasekaran, 2005).

#### **3.3.3. Temperature**

The occurrence of sulfoalumina hydrates depends on temperature (Rollings et al., 1999). Temperature is one of the leading reasons of swelling in clayey soils exist in sulfate environments. The formation of ettringite and swelling occur with a higher rate in summer compared to other seasons (Rajasekaran, 2005).

### 3.3.4. Clay Content and Mineralogy

The amount of clay existing in soil system has a critical role in sulfate activated heave, observed in lime treated soils (Rajasekaran, 2005). There is a direct relationship between the extent of strength loss and clay percent. Increase in clay content results in a decrease in strength. Alumina is one of the principal components that take parts in ettringite formation and clay minerals that have a high potential of releasing alumina like kaolin are more vulnerable to sulfate attack compared to the ones with lower potential like montmorillonite (Rollings et al., 1999).

### 3.3.5. Sulfate Level

Damage caused by sulfate-induced heave is also based on the sulfate within the soil or environment. Parts per million (ppm) and mg/kg are the general expressions used to describe sulfate concentrations. 10000ppm is equal to 10000 mg/kg and 1% by dry weight (Little and Nair, 2009).

Degree of risk relative to the sulfate level in lime treated soils is summarized in Table 3.1.

Table 3.1. Degree of risk relative to the sulfate level in lime treated soils (Little and Graves, 1995)

Degree of Risk	Soluble Sulfate Concentration	
	ppm	Percent Dry Weight (%)
Low Risk	< 3000	< 0.3
Moderate Risk	3000 ≤ - ≤ 5000	0.3 ≤ - ≤ 0.5
Moderate to High Risk	5000 < - ≤ 8000	0.5 < - ≤ 0.8
High to Unacceptable Risk	> 8000	> 0.8
Unacceptable Risk	> 10000	> 1.0

The sulfate content of the soils, in which sulfate-induced heave problems occurred, found to vary between 320 – 43500ppm in many of the cases (Puppala et al., 2013).

Little et al. (2005) listed the factors that affect the amount of ettringite induced heave;

- Thermodynamic suitability of ettringite formation in soils
- Quantity of restraining reactants determining the quantity of ettringite
- Amount of water, sulfate and other ions that play main roles in ettringite formation
- The resistance of the cementitious matrix
- Spatial placement of the crystals of ettringite in the matrix of soil

### 3.4. Sources of Sulfate

The source of sulfate responsible for the heave of soils is divided into two groups as primary and secondary. The primary source includes the native sulfate existing in natural soils. Sulfate coming from the construction wastes, spilled chemicals and industrial wastes form the secondary source (Rao and Shivananda, 2005).

Gypsum mineral observed in soils is the main source of calcium sulfate. Water resulted from the rainfall and flow of groundwater cause perpetual disintegration of gypsum and this phenomenon supplies sulfate needed for ettringite formation (Little and Nair, 2009). Representative photo of gypsum related heave in lime treated soil is presented in Figure 3.4.

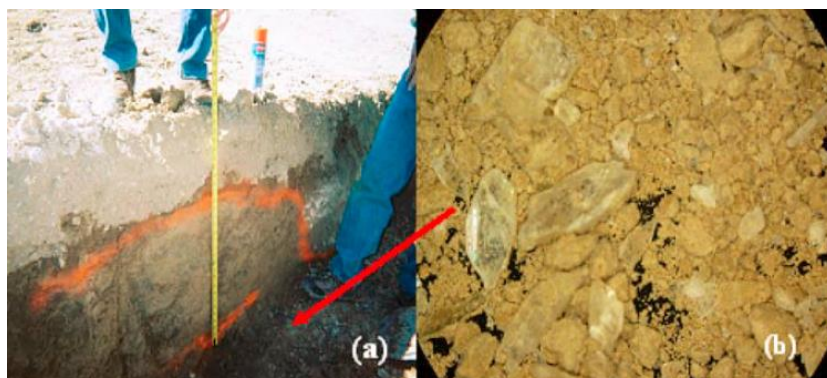


*Figure 3.4.* Gypsum crystals monitored below lime treated heaved layers and optical microscopy image of the soil containing gypsum (Little et al., 2010)

One of the major sources of sulfur is also surface bedrocks that are located all over the world (Little and Nair, 2009). There are also minerals other than gypsum that are possible source of sulfate/sulfide. Texas Department of Transportation (2005) listed the previously mentioned minerals that generally exist within rocks as follows; Alunite, Bassinite, Kainite, Kierserite, Mirabilite, Thenardite, Arcanite, Pyritic, Marcasite, Gypsiferous, Selenite, Selenitic, Marcasitic, Pyrite, Jarosite, Barite, Antlerite, Anglesite, Alabaster, Anhydrite and Anhydritic.

Another main source of sulfate is water since sulfate ions exist in many water supplies and additionally in wastewater (Onitsuka et al., 2001).

The solubility of gypsum ( $\text{CaSO}_4 \cdot 2\text{H}_2\text{O}$ ),  $\text{Na}_2\text{SO}_4$ , and  $\text{MgSO}_4$  in water are 2.5, 408 and 260 g/L respectively (Puppala et al., 2019). Considering its low solubility, the water that is required in mixing and compacting procedures of chemically stabilized soil is very low for the dissolution of all favorable sulfates in gypsum (Little and Nair, 2009).

### **3.5. Determination of Sulfate Content of Soil and Groundwater**

Sulfate content of soil and groundwater is usually determined by using the methodology given in BS 1377-3:1990. This test gives the sulfate content at the time of sampling. Tests could be applied to acid extract soil samples which are prepared by using hydrochloric acid, water extract soil samples, and groundwater samples.

There are two methods suggested in the standard namely;

- a. Gravimetric Method
- b. Ion-exchange Method

Summary of the methods given in BS 1377-3:1990 are presented below;

A solution of barium chloride is used in the gravimetric method. The solution is included to the sample and collected barium sulfate precipitate is dried and weighed. The initial mass of the sample and mass of precipitated barium sulfate is used to

determine the sulfate content. Acid extract, water extract soil samples, and groundwater samples could be tested by this method.

In the ion-exchange method, the sample is passed through an ion-exchange resin column and quantity of present anions is determined by titration against a sodium hydroxide standardized solution. This method is applicable for samples that do not contain other strong acid anions like nitrates, chlorides, and phosphates. Only water extracted soil samples and groundwater samples could be tested by this method.

Technical guideline prepared by Britpave (2005) explained the deficiencies related to sample preparation methods as follows;

#### Water Soluble Sulfate (2:1 Water Soil Extract)

As the calcium sulfate has low solubility, this test method has a constricted use for the evaluation of gypsum content of samples. If the soil has a gypsum content that results more than 0.3% SO<sub>4</sub>, the quantity exceeding 0.3% SO<sub>4</sub> could not be measured.

#### Acid Soluble Sulfate (Total Sulfate)

All sulfate existing in soil including the portion that does not dissolve in water is probably measured by acid extracts method. Sulfide (S<sup>-2</sup>) that has the potential to convert to sulfate and causing expansion will not be detected by this method.

### **3.6. Techniques for Treating Sulfate-Rich Soils**

Four main materials that play a major role in ettringite formation are aluminum, water, calcium, and sulfates. The mitigation of ettringite induced heave which may reach up to 250% in some cases, could be probable by preventing the source of at least one of the main components (National Lime Association, 2000).

Texas Department of Transportation (2005) provides a guideline for stabilization of sulfate-rich soils (Figure 3.5).

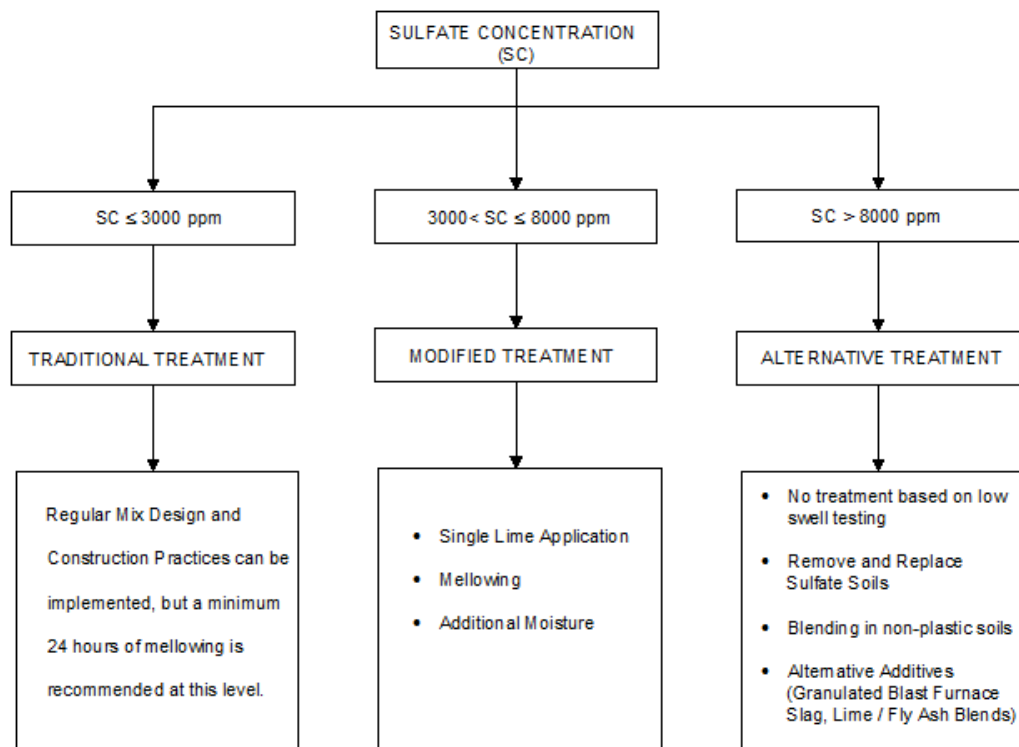


Figure 3.5. Guideline for the stabilization of sulfate soils (Texas Department of transportation, 2005)

### 3.6.1. Mellowing

Forcing the formation of the harmful minerals before compaction is the optimal approach while dealing with stabilization of clay that includes a significant amount of soluble sulfate by using lime (The National Lime Association, 2000).

Mellowing is defined as the process of letting lime stabilized soil to stay in uncompacted state for a length of time for the occurrence of reactions of lime with clay and sulfate (Texas Department of Transportation, 2005). The formation of ettringite will be rapid if a release of alumina from the clays occurs and there exists soluble sulfate and required amount of water in the environment (The National Lime Association, 2000).

The required reaction time for decreasing of sulfate content to a tolerable level increases with the increase in sulfate level (Texas Department of Transportation, 2005).

Sufficient time for mellowing may vary between 24 hours and 7 days according to the level of soluble sulfates in the soil. A satisfactory amount of water is 3 to 5% higher than the optimum moisture content (The National Lime Association, 2000). Additional moisture can help to decrease the mellowing time by means of increasing the reaction rate (Texas Department of Transportation, 2005).

### **3.6.2. Progressive (Double) Application of Lime**

Double application is another concept used in treating sulfate-rich soils. In double mixing method, half of the lime is used firstly. The soil, lime, and excess water are mixed and mellowed for a period of 3 to 7 days to give time for the occurrence of expansive reactions prior to compaction. After mellowing, remaining half of lime is applied to the soil and finally, the mixture is compacted (The National Lime Association, 2000).

The first half of the lime is used for ettringite formation and the second half of the lime application provides actual stabilization (Rollings et al., 1999). Rollings et al. (1999) also define the mellowing period after mixing clay with the first half of the lime as one month.

### **3.6.3. Use of Additives**

Researchers are continuing to identify the efficiency of using additives such as soluble silica (normally in the form of fly ash/lime blends or GBFS) in decreasing the risks related to the ettringite formation. The effectiveness of using additives should be considered carefully for specific soil before site applications because these additives are foreigner for the soils system (Little and Nair, 2009).

Combinations of barium chloride, fly ash, GBFS, lime, amorphous silica and portland cement are used to mitigate the ettringite induced heave problem. Obtaining GBFS

becomes harder due to its high usage in the concrete industry for the mitigation of alkali-silica reactivity of aggregates that take part in concrete production (Harris et al., 2014). Therefore, detailed studies on other materials gain extra importance.

### **3.7. Misconceptions about Heave Problems**

National Lime Association (2000) listed the three main misconceptions about the ettringite induced heave problems as given below;

1) The problem could be faced only on lime stabilized soil

Any of the calcium-based stabilizers has a potential of causing heave problems since they are all sources of calcium which is one of the four main components for ettringite formation.

2) Sulfate induced heave problem is not a problem for the soils stabilized with sulfate resistant portland cement

The aim of using sulfate resistant portland cement in concrete is the elimination of ettringite formation by reducing the aluminum content. However, this phenomenon is not applicable to soil stabilization since the aluminum source is soil.

3) Heave could be minimized by using class F fly ash

Using solely of class F fly ash is not effective in soil stabilization, it requires an additional lime source. Therefore, although class F fly ash may not cause ettringite induced heave problems, it is not an effective stabilizer.

### **3.8. Case Studies**

Mitchell (1986) presented a case study in the Twentieth Terzaghi Lecture which attracted attention to the issue of sulfate-induced heave problems.

The subbase of 5 km section of major arterial street in Las Vegas, Nevada was constructed by using lime treated expansive silty clay. Lime treatment for base stabilization was used in another street section and a parking lot of a school before this

application, and their performance was sufficient, and no problems had been observed one or two years after the construction.

The street was constructed in 1975 with approximately 27.0m width. The street's initial performance was excellent and there was no problem. However, surface heaves and cracks (Figure 3.6) suddenly developed more than two years after the initial construction, in some parts of the street and in remaining parts the pavement was in very good condition and appearance.



*Figure 3.6. Pavement surface failure (Mitchell, 1986)*

After heaves and cracks, tests were performed to investigate the soil composition, chemistry, and the reaction products and the following information were obtained.

- The soil at the project site contained soluble sodium up to 15000ppm and expansive clay minerals were present in the soil.
- The soil comprised significant amount of gypsum, calcite and some dolomite.
- Lime was observed both in failed and intact zones.

- Calcium Silicate Hydrates (CSH) which is a cementing material and a product of a successful lime-clay minerals reaction was not observed in the soils taken from the failed and intact zones due to low pH environment.
- Considerable amount of ettringite and thaumasite was observed in lime-treated soils taken from the heaved zones.
- Negligible amounts of ettringite and thaumasite were found in treated samples taken from zones where failures had not occurred

The author explained the heaving and cracking problems with the formation of ettringite and thaumasite which are recognized as very expansive and responsible for the damages in concrete, originated from sulfate attack.

In other case study, bumps were observed on 3.5 km long section of a Bush Road in Georgia within six months following the construction period. Rollings et al. (1999) performed field and laboratory studies to understand the mechanism behind the occurrence of these unforeseen bumps. Laboratory tests were performed on the representative samples taken from both problematic and unproblematic parts of the road. The test results showed that the reason behind the observed mechanism was the sulfate attack on cement-treated sand that was used as a base course in pavement construction. The sand had a low clay content varying between 6-13% and it was stabilized with 5-6% cement. The XRD analyses showed that the clay within the sand mostly formed of halloysite mineral which was rich in alumina. At the end of the study, it was found out by the investigators that cement and clay were the sources of alumina and the well water that was used in the cement and soil mixing procedure was the potential source of sulfate and sulfate was not observed within cement or soil.

Puppala et al. (2005) summarized the details of the other important cases where ettringite related heave problems occurred as presented in Table 3.2.

Table 3.2. Summary of cases related to ettringite induced heave problems  
(Puppala and Vempati, 2005)

Researcher	Location	Soil	Type and % of additive	Sulfate content (ppm)	Occurrence of heave after construction
Hunter (1988)	Stewart Avenue, Las Vegas, Nevada	Silty Clay	4% Lime	43500	6 months
Perrin (1992)	Lloyd Park, Joe Pool Lake, Dallas, Texas	Overconsolidated Clay	4.5% Lime	2000-9000	Immediately
Perrin (1992)	Auxiliary Runway, Laughlin AFB, Spofford, Texas	Clay	5% Lime	14000-25000	2 months
Perrin (1992)	Cedar Hill State Park, Joe Pool Lake, Dallas, Texas	Highly Plastic Residual Clays	6 -9 % Lime	21200	2 months
McCallister and Tidwell (1994)	Denver International Airport, Denver, Colorado	Expansive Clays	Not Available Lime	2775	Not Available
Kota et al. (1996)	SH-118, Alpine and SH-161, Dallas, Texas	Clayey Subgrades	4% Cement 6-7% Lime	>12000	6 -18 months
Burkarter et al. (1999)	Localities in Dallas–Fort Worth Region, Texas	Clay	6-9% Lime	233-18000	Variable
Puppala (1999)	Dallas–Fort Worth International Airport, Irving, Texas	Clay	5% Lime	320-13000	3 months

### 3.9. Previous Studies on Ettringite Induced Heave Problems

Abdi and Wild (1993) studied the effect of the addition of gypsum on lime treated kaolinite. During the study; 2, 4, 6 and 8% gypsum was added to the 6% and 14% lime treated kaolinite. Tests were performed on compacted specimens cured at 30<sup>0</sup>C and 100% humidity environment. It was found out that the addition of low rates of gypsum

had a positive effect on reducing swell potential however increase in sulfate rate affected the swell potential adversely. A representative swell percent graph from their study is presented in Figure 3.7.

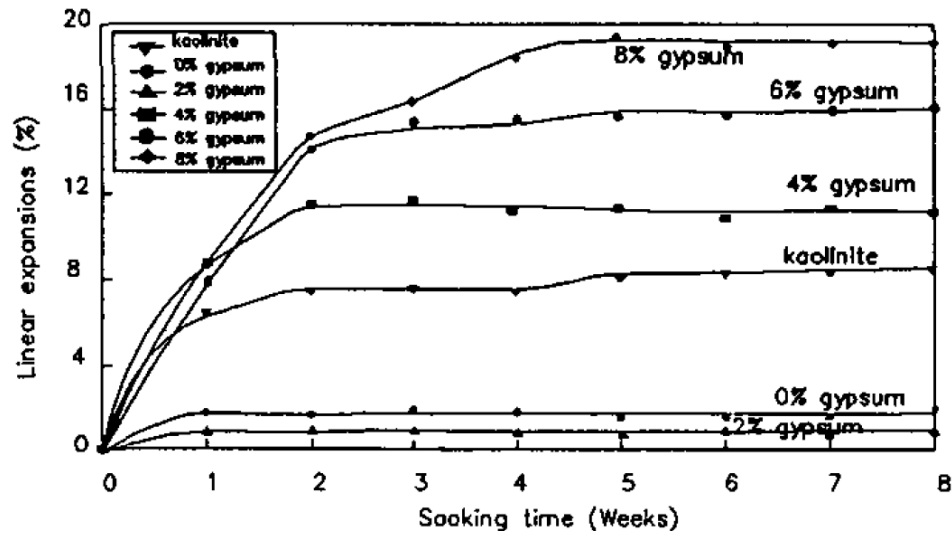


Figure 3.7. Linear expansion vs. soaking time graphs for kaolinite, 6% lime treated kaolinite and gypsum added 6% lime treated kaolinite specimens (Abdi and Wild, 1993)

Puppala et al. (2004) studied the treatment of sulfate bearing soils with sulfate resistant cement. 4 different natural soils which were classified as CH according to USCS with variable sulfate concentrations (287, 1490, 5688, 32122ppm) were used in the studies with Types I/II and V cement. The authors explained the reason for the selection of Type I/II and Type V cements by the usage of these cement types in the preparation of concrete in low-moderate and high sulfate soil environments respectively. At the end of the studies, it was found that both cement types were successful at improving both physical and engineering properties of all four sulfate-rich soils. The decrease in plasticity index and swelling potential and increase in strength properties were observed after the addition of cement.

The authors explained the beneficial effect of sulfate resistant cement treatment by the mitigation of ettringite formation, occurrence of pozzolanic compounds such as tobermorite that were determined according to the XRD analyses. Flocculation of particles due to the ion exchanges was the other contributing effect on improvement. Variation of the swell potential of cement-treated soils for different cement types and concentrations are presented in Figure 3.8.

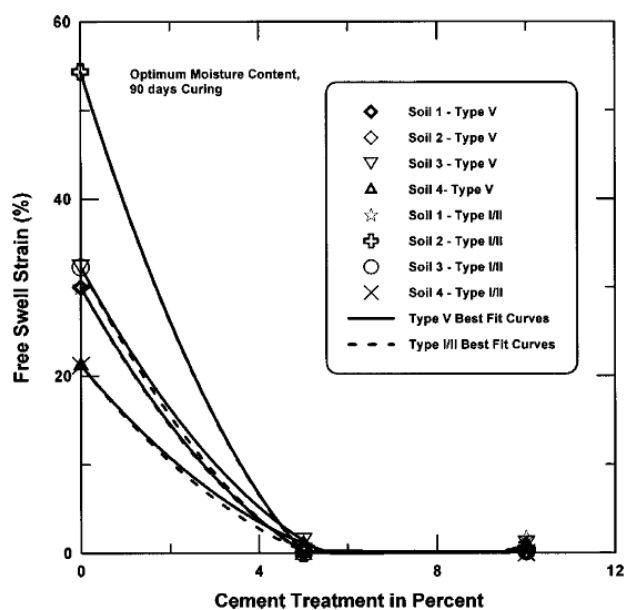


Figure 3.8. Swell potential of soils after cement treatment (Puppala et al., 2004)

Also unconfined compressive strength of the cement added 14 days cured specimens are presented in Figure 3.9.

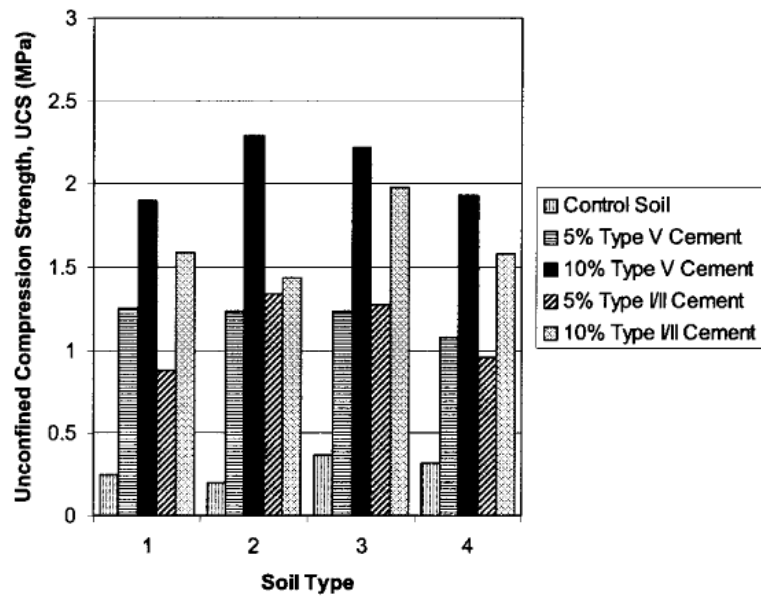


Figure 3.9. Strength of soils after cement treatment (Puppala et al., 2004)

Higgins (2005) investigated on many studies in the literature related to the effect of GBFS on the suppression of sulfate-induced heave problems observed in lime treated soils. The typical outcomes of his study are as follows; the GBFS content had no significant effect on initial lime consumption and physical properties (Atterberg limits, compaction properties, etc.) of treated soil, these properties were dominated by lime. An increase in resistance against expansion was observed with the increase in the ratio of GBFS to lime. Although 1:1 ratio resulted in a considerable resistance, an increase of GBFS:lime ratio to more than 5:1 caused the greatest benefit.

As fly ash is a material that suppresses sulfate attack in concrete, McCarthy (2009) performed studies to determine whether fly ash keeps its beneficiary effect in sulfate-induced heave problems. McCarthy (2009) performed studies on soil with a known risk of ettringite-induced swelling called Kimmeridge Clay. The properties of the test clay are given in Table 3.3.

Table 3.3. *Main properties of the clay used in the studies of McCarthy (2009)*

Natural Moisture Content, %	30
Optimum Moisture Content (OMC), %	24.5
Total Potential Sulfate, %	0.96
Maximum Dry Density, Mg/m <sup>3</sup>	1.54
Particle Density, Mg/m <sup>3</sup>	2.70

Four Class F fly ashes with varying fineness, loss-on-ignition values and different storage history were used. Test samples were prepared by using different percent of quick lime (3, 4 and 6%) and fly ash (6, 12, 18 and 24%) contents. Also, different mellowing periods (0, 1 and 3 days) before remixing with fly ash was applied.

Typical outcomes after 7 days exposure of control 3% lime and 3% lime + 24% FA specimen to water at 40 °C is given in Figure 3.10.

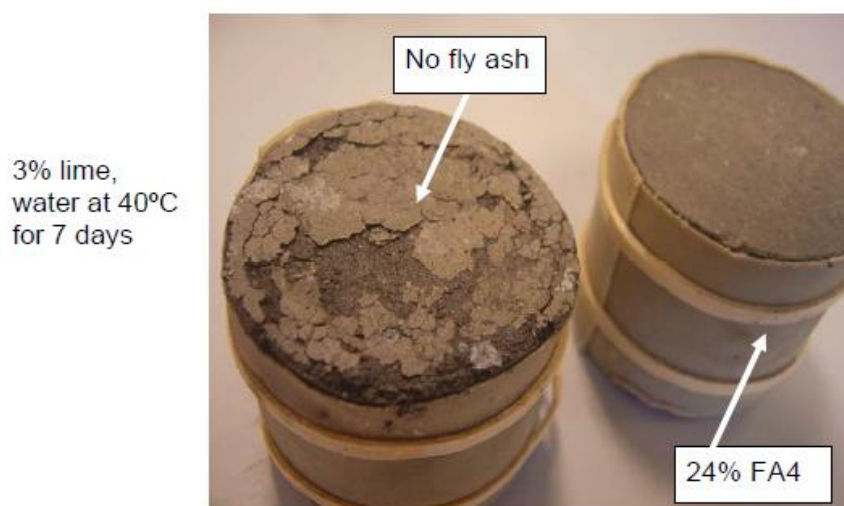


Figure 3.10. *Typical appearance of ettringite-induced swelling and the effect of fly ash (McCarthy, 2009)*

Effect of mellowing period on the volumetric swelling of the lime stabilized soil with varying fly ash content could be seen in Figure 3.11.

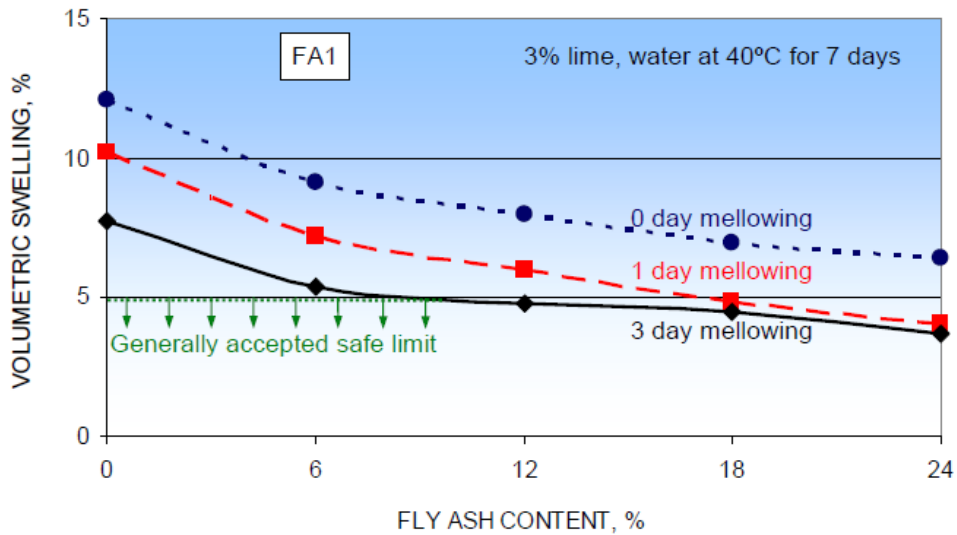


Figure 3.11. *Effect of mellowing period and fly ash content in swelling of test specimens (McCarthy, 2009)*

As can be seen from Figure 3.11, the decrease in swelling increased with the rise in fly ash content and mellowing period.

Different lime contents were examined during the study and although swelling potential reduced with the increasing fly ash content, only a minor difference was observed for the specimens treated with different percentage of lime. The results of the tests are shown in Figure 3.12.

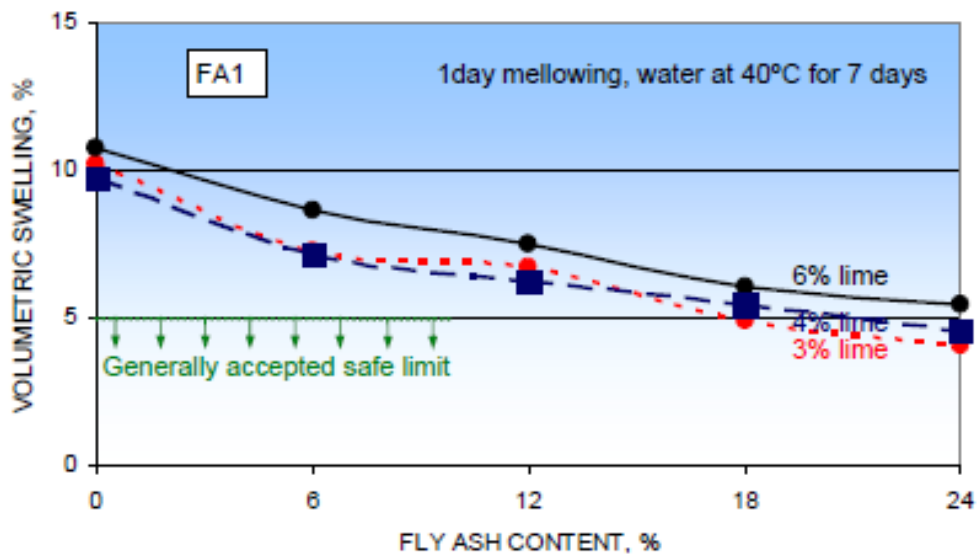


Figure 3.12. *Effect of lime content and fly ash content on swelling properties of test specimens (McCarthy, 2009)*

Also, SEM views of the raw clay sample, 4% lime treated soil and 4% lime + 24% FA treated sample is given in Figure 3.13. The ettringite formation can be seen in the images.

According to the results of the tests following outcomes were obtained by the author;

- A similar amount of ettringite was observed in lime stabilized and lime + fly ash stabilized soils.
- Coarser fly ashes with greater loss-on-ignition were found to be more effective than finer ones due to providing of a more porous structure.
- Although swelling decreased with increasing fly ash and decreasing lime content, higher lime and fly ash content increased strength.
- Mellowing period was an important aspect that mitigated swelling.

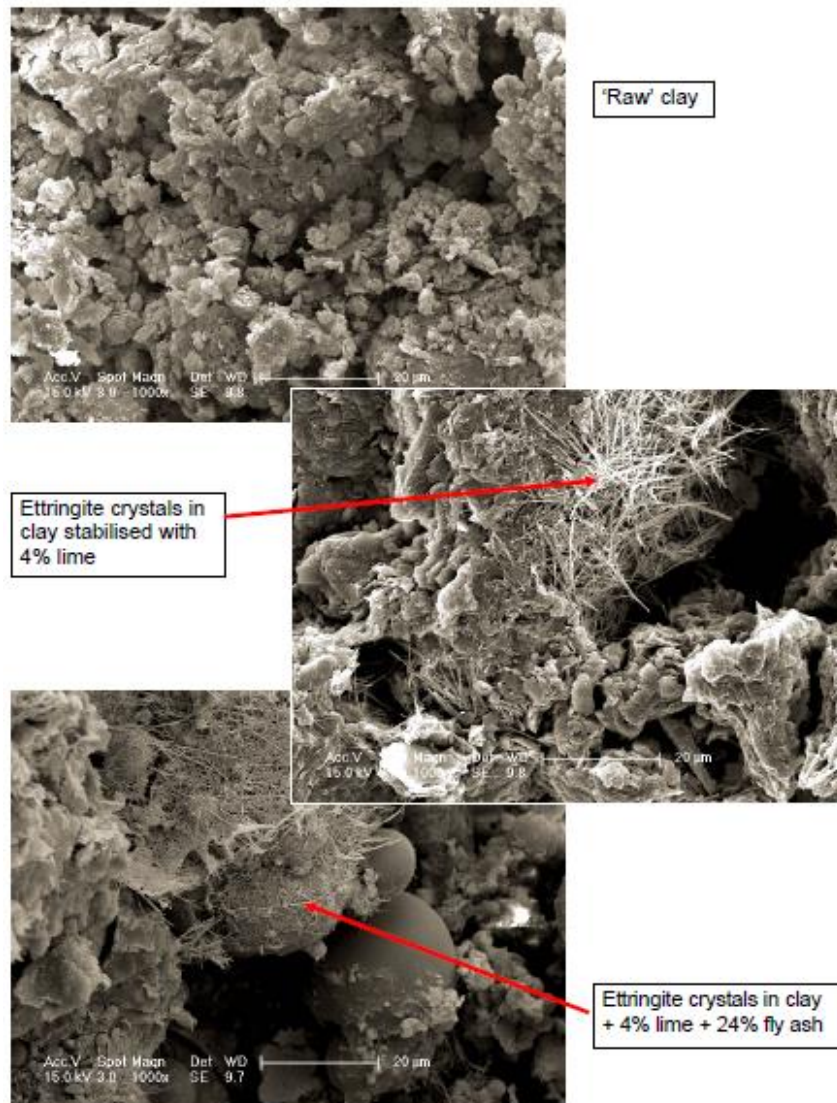


Figure 3.13. SEM images of the raw clay and test mixes at 40°C water  
(McCarthy, 2009)

McCarthy et al. (2012a) studied on the effect of fly ash on reducing the sulfate-induced heave problems of lime treated soils. Three natural soils namely; Oxford, Lias, and Kimmeridge with different sulfite concentrations (1.8%, 1.5%, 1.0%  $\text{SO}_3$  respectively), quicklime and seven different fly ashes generally taken from different sources were used in the study. Fly ashes had variable fineness, LOI and storage

history. Six out of seven fly ashes had a CaO content lower than 5.0%, these fly ashes had also considerably low sulfate concentration that was varying between 0.3-1.1%. The last fly ash (FA-5) had CaO and SO<sub>3</sub> content of 12.0% and 4.1% respectively. Tests were performed on fly ash added 3% lime treated soils. The following conclusions were obtained from their study.

Wet stored fly ashes with high coarseness and LOI had a significant effect on enhancing the compaction properties of lime treated soils while a little effect was observed for dry fly ashes with low LOI.

Addition of fly ashes up to 24% were effective in decreasing the swelling of lime treated soil with a sulfate content smaller or equal to 1.5%. As for the compaction properties, wet stored fly ashes with high coarseness and LOI were more successful. None of the fly ashes achieved to reduce the swelling potential of Oxford soil with sulfate content of 1.8% to the desired level (<5%).

Fly ashes with high sulfate level caused less reduction in swell potential compared to the ones with less sulfate content. The results of the tests that show the effect of sulfate concentration is presented in Figure 3.14.

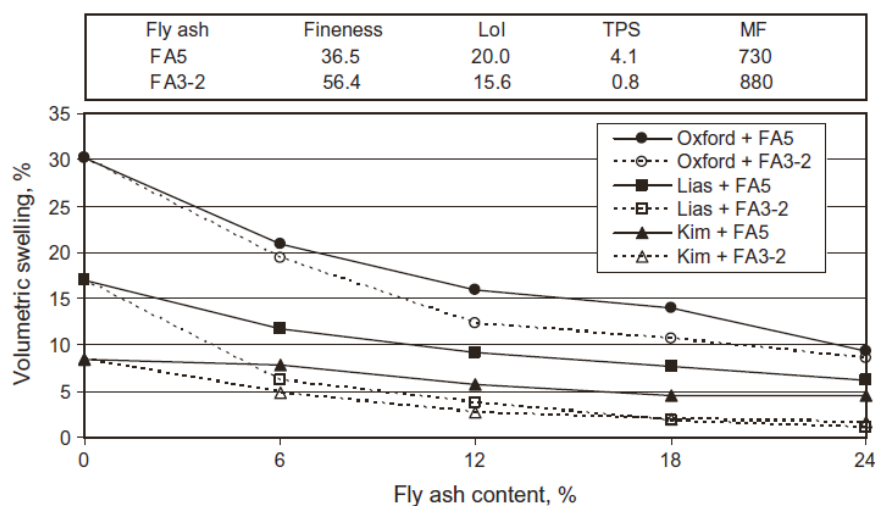


Figure 3.14. Effect of fly ash content on swelling of lime treated clays (McCarthy et al., 2012a)

The beneficial effect of the addition of wet stored, coarse fly ashes with high LOI was explained by causing coarser structure with compaction. Contribution of the addition of dry fine fly ashes with low LOI to the lime stabilized soils was explained with strength increase that withstood the ettringite formation related pressures.

McCarthy et al. (2012b) also performed extra tests for the determination of the effect of temperature variation on fly ash added lime treated sulfate-containing soil. Lias clay with 1.5% SO<sub>3</sub> content and class F fly ash with 3.6% CaO content were used during the studies. Swelling tests were performed at three different temperature (8, 20 and 40°C) on 6%, 12%, 18% and 24% fly ash added 3% lime treated Lias clay. Before the swelling tests, specimens were exposed to 1 day mellowing and 3 days curing. Test results are given in Figure 3.15.

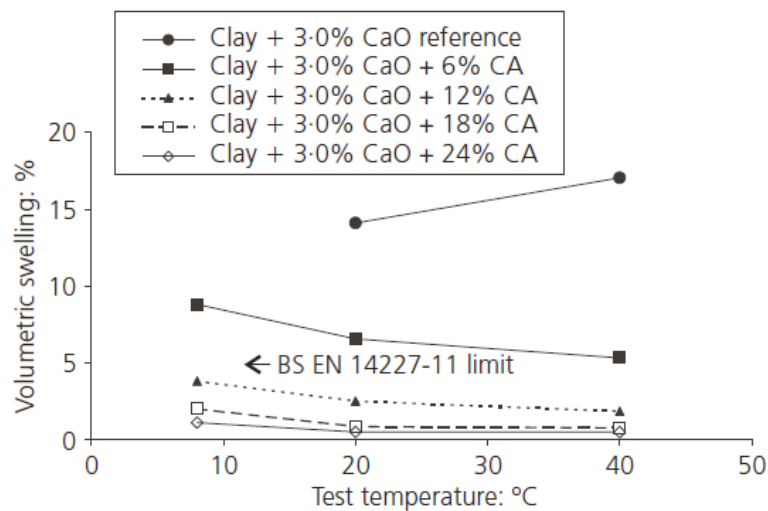


Figure 3.15. Effect of temperature on swell potential of fly ash added 3% lime treated clays (McCarthy et al., 2012b)

An increase in swelling potential of lime treated soil was observed with the increase of temperature from 20 to 40°C. Authors explained this condition by the increase of the rate of ettringite favorable reactions. Opposite behavior was observed for fly ash

added specimens. This time increase in swell potential was obtained with the reducing temperature. The variation on the swelling potential between 8 and 20<sup>0</sup>C was greater than that of 20 and 40<sup>0</sup>C. Effect of temperature on fly ash added specimens showed a decreasing trend with the increase in fly ash concentrations.

Puppala et al. (2003) studied on the effect of class F fly ash, sulfate resistant cement, GBFS and lime (mixed with fibers) on the sulfate bearing soils. Four different natural soils with sulfate concentration higher than 4000ppm were selected as test soils. Two different levels of dosages were used during treatment. Additive percentage by dry weight of soil were as follows; 5% and 10% for cement, 10% and 20% for fly ash and GBFS. Also 8% lime was mixed with 0.15% and 0.30% fiber. Atterberg limits, strength, and swelling tests were performed on 3, 7 and 14 days cured specimens. Sulfate resistant cement and lime- fiber mixtures showed the maximum beneficiary effect and moderate improvement was achieved with fly ash and GBFS.

Gaily (2012) studied the behavior of high sulfate soils treated with lime. Six natural soils with high sulfate content taken from the different regions of Texas were used in the study. Properties of the selected soils are presented in Table 3.4.

Table 3.4. *Properties of soils (Gaily, 2012)*

<b>Soil Name</b>	<b>LL (%)</b>	<b>PI (%)</b>	<b>Classification (USCS)</b>	<b>Sulfate Content (ppm)</b>
Austin	76	51	CH	36000
Childress	71	36	MH	44000
Dallas	80	45	CH	12000
FM1417	72	42	CH	24000
Riverside	35	24	CL	20000
US-82	75	50	CH	12000

6% lime was selected as optimum lime content. The tests were performed both on natural and lime added samples. Also, 3 days mellowing period was applied to see the effect of ettringite formation and mellowing. The results of the swelling and unconfined compressive strength tests performed on specimens compacted at their optimum moisture contents are presented in Table 3.5.

Table 3.5. UCS and volumetric swelling test results (Gaily, 2012)

Soil Name	UCS (kPa)			Volumetric Swelling (%)		
	Untreated	6% Lime Treated		Untreated	6% Lime Treated	
		without mellowing	3 days mellowing		without mellowing	3 days mellowing
Austin	193	607	379	16.6	8.8	11.7
Childress	159	745	310	7.5	14.6	8.5
Dallas	110	634	228	11.0	24.4	10.4
FM1417	228	558	483	16.2	22.0	10.2
Riverside	207	434	324	10.0	16.0	8.4
US-82	214	503	359	18.1	24.4	11.3

The UCS of the lime treated specimens were higher than the untreated specimens. Also, an adverse effect of mellowing on UCS was observed for treated specimens. The decrease in UCS after 3 days mellowing period was explained by using extra water for the preparation of mellowing specimens.

The swell potential of all soils except for Austin increased after addition of lime. This behavior was explained by the ettringite induced heave. Also, after 3 days mellowing period, swell potential of four lime treated specimens decreased below the untreated ones. The common property of these four specimens was the fact that their sulfate content was lower than 30000ppm.

Higgins et al. (2013) studied on the effect of lime, cement, and GBFS on soils containing sulfates and sulfides. Three different high plastic soils with zero sulfate, medium sulfate, and low sulfate + high sulfide were used in the study. CBR, volumetric swelling and strength tests were performed on soils without additives, 2% lime, 2% lime + 2% cement and 2% lime + 2 % GBFS treated specimens. It was found out from the study that the sulfate related problems observed for the clayey soil with medium sulfate concentration and the maximum beneficiary effect was observed with the addition of 2% lime + 2% GBFS.

Puppala et al. (2013) studied on the heaving mechanism in lime treated high sulfate soils. The researchers studied on 2 different soils called Sherman and Childress that belonged to different classification and geological formation. Sherman and Childress soils were classified as CH and MH respectively according to the Unified Soil Classification System. Soluble Sulfate Content was 44000ppm and 24000ppm for Childress soil and Sherman soil respectively. Therefore, both soils were classified as high sulfate soils.

Optimum lime content was found as 6% for both soils. The dominant mineral in Sherman and Childress Soils were montmorillonite and kaolinite respectively and both soils showed swell potential.

In the scope of the study, tests were performed to evaluate the swell and strength characteristics of lime treated soils. As silica and alumina take part in ettringite and thaumasite reactions, reactive silica and alumina that participated in sulfate reactions were measured as a part of the mineralogical tests.

During testing, lime treated soils were mellowed for periods of 0, 3 and 7 days in a moisture-controlled environment to see the effect of mellowing.

Each specimen was compacted at the optimum moisture content (OMC) and wet of optimum moisture content (WOMC) corresponding to 95% of maximum dry density.

Results of the swell tests are presented in Figure 3.16.

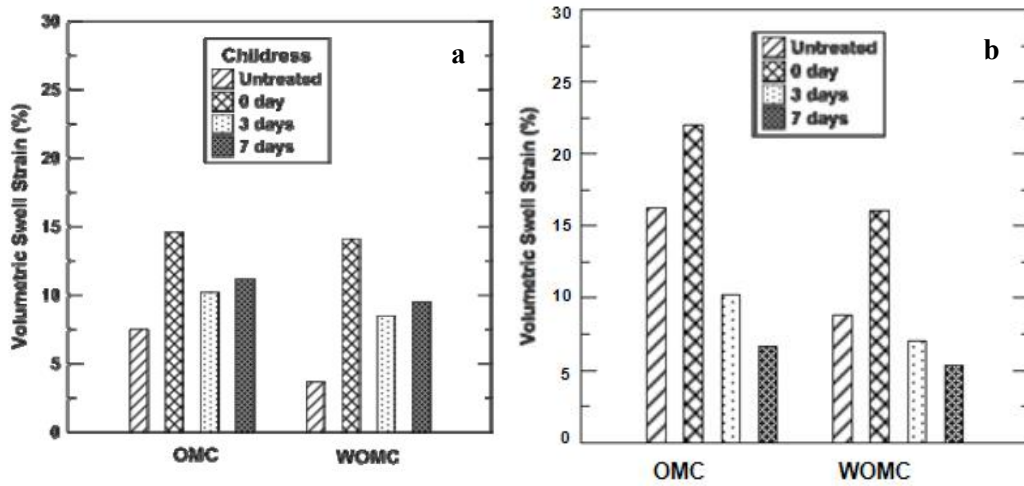


Figure 3.16. Volumetric swell, a- Childress soil, b- Sherman soil

Initial reactive silica and alumina contents of the natural soils and % loss for treated specimens for different mellowing periods are presented in Table 3.6.

Table 3.6. Reactive alumina and silica (ppm) in present soils (Puppala et al.,2013)

Soil	Untreated (Natural)		6%L, 0-day mellowing		6%L, 3-day mellowing	
	Al (ppm)	Si (ppm)	% loss		% loss	
			Al	Si	Al	Si
Sherman at OMC	279	137	58	66	53	64
Sherman at WOMC	279	137	57	64	52	63
Childress at OMC	76	13	63	54	61	46
Childress at WOMC	76	13	62	62	58	54

As it can be seen in Figure 3.16, an increase in swell potential was observed for both soils after treatment and 0 days mellowing period. Authors explained this condition by the fact that sulfate reactions were more dominant than the stabilization reactions. After 3 days mellowing period, a lower swell potential was obtained for lime treated soil compared to the untreated case for Sherman Soil and 7 days mellowing provided additional decrease in swell potential.

A decrease in the swell potential of lime treated Childress soil that exposed to 3 days mellowing period was observed with respect to 0 days mellowing, it was still high compared to the untreated case, and 7 days mellowing caused an increase in the swell potential with respect to 3 days mellowing. It could be stated that mellowing was not beneficial in reducing the swell potential of lime treated Childress soil.

The authors explained the low heaving in Sherman Soil as follows;

Sherman soil had a higher initial reactive alumina and silica content compared to the Childress soil. Ettringite formation depended on the amount of reactive alumina present in the system. Low alumina contents favored the ettringite formation and high alumina contents resulted in both ettringite and pozzolanic reactions. Attractive forces due to the pozzolanic formation resisted the devastating forces caused by hydration reactions of ettringite for Sherman Soil. Combination of low initial reactive alumina content and large sulfate contents for Childress Soil caused large heaving and mellowing was ineffective primarily due to the low alumina content in the soil.

Celik (2014) studied on the swelling behavior of natural and lime treated expansive soils in the lack and presence of sulfate.

Soil with a low sulfate level of 640ppm taken from the Değirmenlik Village of North Cyprus was used as natural soil. The soil composed of 40% silt and 60% clay and had a LL of 56% and a PL of 25%.

Three different sodium sulfate concentrations namely; 2000ppm, 5000ppm and 10000ppm NS were added to the soil with the aim of increasing sulfate level. Also 5% hydrated lime was used during the studies.

Results of the swelling tests are given in Figure 3.17.

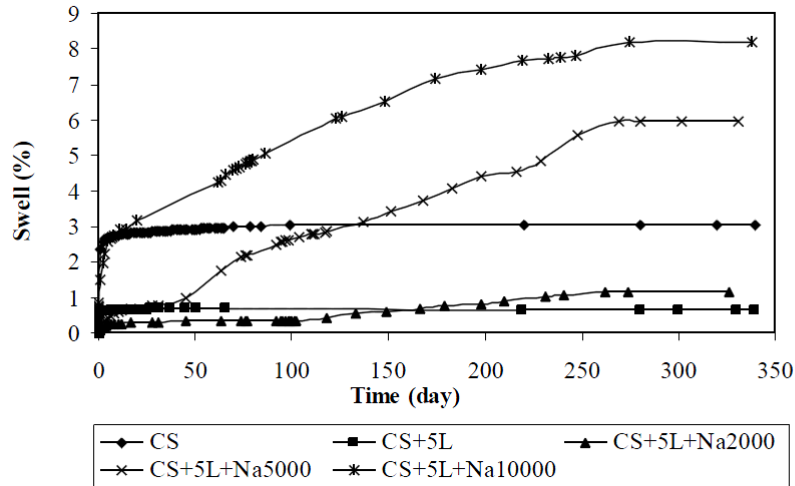


Figure 3.17. Comparison of the swell percentages of the untreated soil (CS), lime treated soil (CS+5L) and lime treated soil (CS+5L) with different concentration of sulfates (Celik, 2014)

According to test results, lime was effective in stabilization of the control soil. However, the swell potential of the 5% lime stabilized soil specimens that were subjected to the 5000ppm and 10000ppm concentration of sulfate increased with the lime treatment. The swell potential for the 5% lime stabilized soil with 2000ppm sulfate concentration remained below the swelling potential of control soil which was a sign that 2000ppm sulfate concentration was not adequate for lime ettringite minerals formation.

XRD were performed and SEM views were taken for control soil and 5% lime stabilized soil sample with 10000ppm sulfate concentration to identify the chemical and microstructural changes. XRD of the lime treated soil with 10000ppm sulfate was

given in Figure 3.18 and SEM views for control soil and lime treated soil with 10000ppm sulfate was given in Figure 3.19.

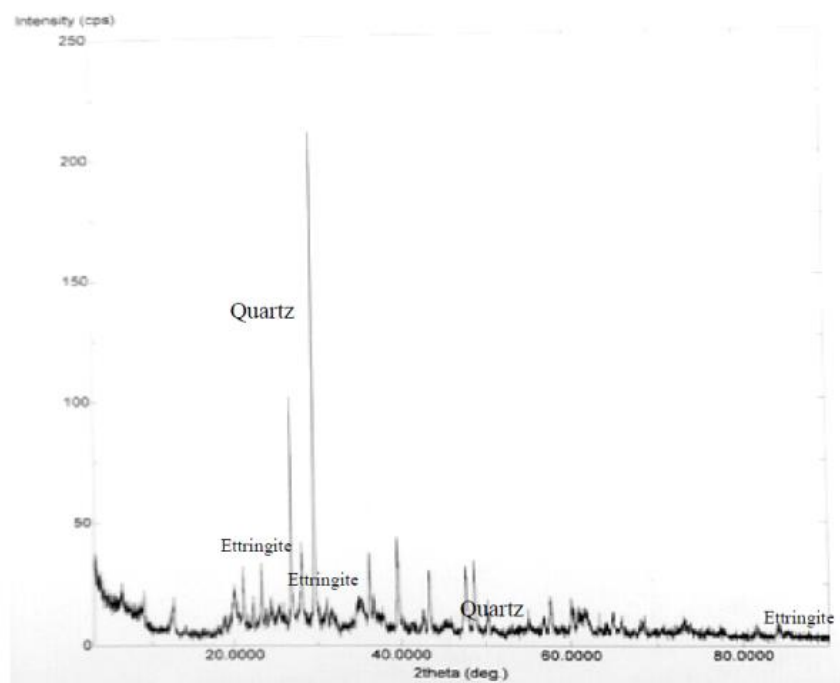


Figure 3.18. XRD of lime treated soils with 10000ppm sulfate concentration (Celik, 2014)

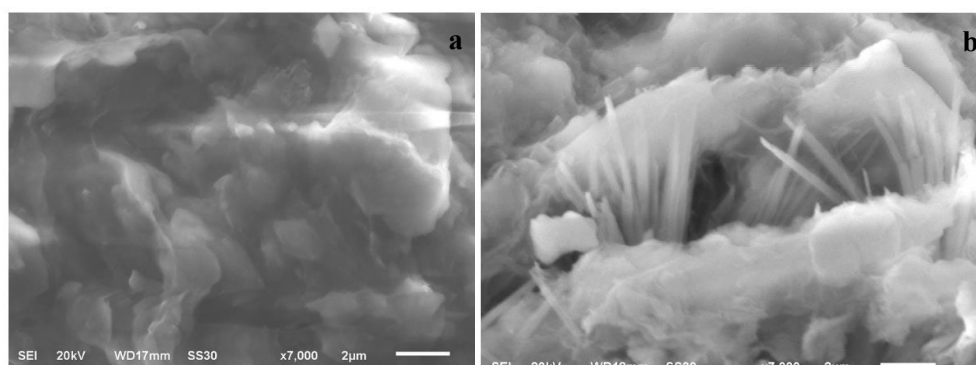


Figure 3.19. SEM views, a- natural soil, b- lime treated soil with 10000ppm sulfate concentration (Celik, 2014)

Both XRD results and SEM views showed the ettringite formation in the sample subjected to 10000ppm sulfate which was thought to be responsible for the increase in swell potential.

Also, GBFS was used in this research to determine whether the addition of this material would be beneficial in reducing the swell potential increase due to the ettringite formation or not. 6% slag was added to the lime treated specimens with different sulfate concentrations. The results of the tests are summarized in Figure 3.20.

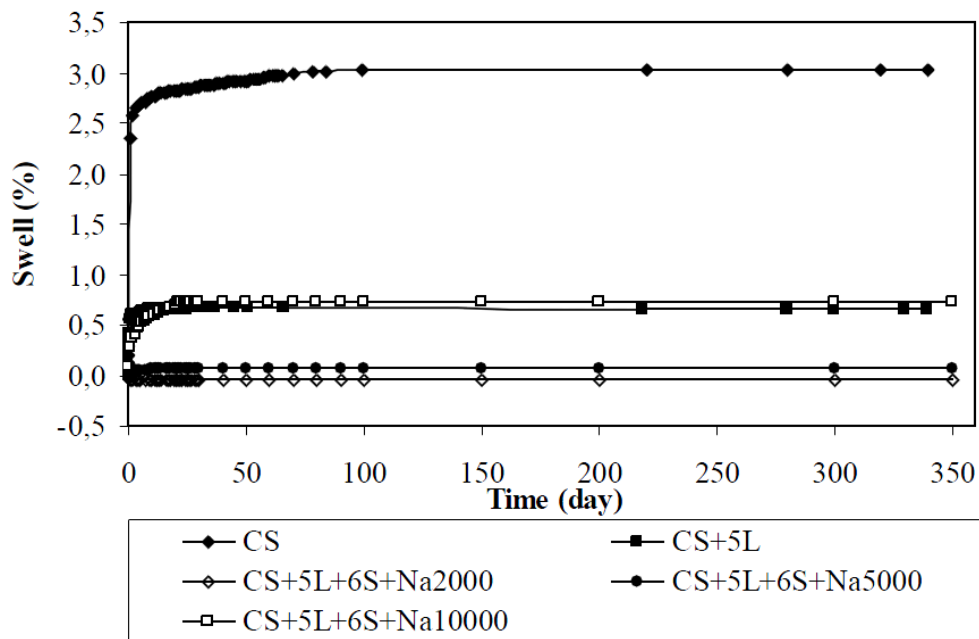


Figure 3.20. Swell potential of soils with 6% GBFS and different sulfate concentrations (Celik, 2014)

As can be seen in Figure 3.20, the undesired effect of sulfate on lime treated soil was eliminated with the use of slag and the swelling of lime-treated soil was prevented.

Harris et al. (2014) studied on the effect of chemicals on preventing the occurrence of ettringite formation. Clay minerals, gypsum, hydrated lime, and water were used to obtain ettringite in the laboratory environment. Smectite rich natural soils and

kaolinite were selected as clay minerals. The occurrence of ettringite was observed with XRD method. Diatomaceous earth, volcanic glass (amorphous silica), and calcium phosphate monobasic monohydrate were selected as main chemicals for preventing the creation of ettringite. Although the addition of calcium phosphate monobasic monohydrate inhibited the formation of ettringite in some soils, any beneficial effect had not been observed with the addition of volcanic glass and diatomaceous earth.

Mohammed and Vipulandan (2015) studied on the effect of calcium sulfate addition on physical and mechanical properties of CL type soil. Also, additional tests were performed on lime and class C fly ash added calcium sulfate contaminated samples to see the effect of calcium-based stabilizers. Different percentages of calcium sulfate (up to 4%), 10% fly ash and 6% lime were chosen as the representative additive concentrations. Tests were performed on 7 days cured specimens at 25°C and 100% humidity environment. Following outcomes were obtained from the study;

LL of the soil increased after 4% calcium sulfate addition. Addition of 6% lime and 10% fly ash resulted a decrease in LL of the 4% sulfate added soil. The reduction was higher for fly ash added sample.

PI of the soil increased after 4% calcium sulfate addition. Addition of 6% lime and 10% fly ash resulted a decrease in PI of the 4% sulfate added soil. The reduction was higher for the lime added sample.

Compaction properties of sulfate added samples improved with the addition of lime and fly ash. The swell percent of the soil increased from 7% to 19% with the addition of 4% sulfate. Adding 6% lime and 10% fly ash decreased the swell percent of 4% sulfate treated specimen to 9 and 10% respectively.

UCS of the soil decreased after 4% calcium sulfate addition. Addition of 6% lime and 10% fly ash resulted an increase in strength of the 4% sulfate added soil. The increase was higher for the lime added specimen.

The changes in Atterberg limits and swelling properties attributed to the alteration in clay mineralogy and the strength increase with the addition of lime and fly ash was explained by the cementing compounds. The results of the free swelling tests are presented in Figure 3.21.

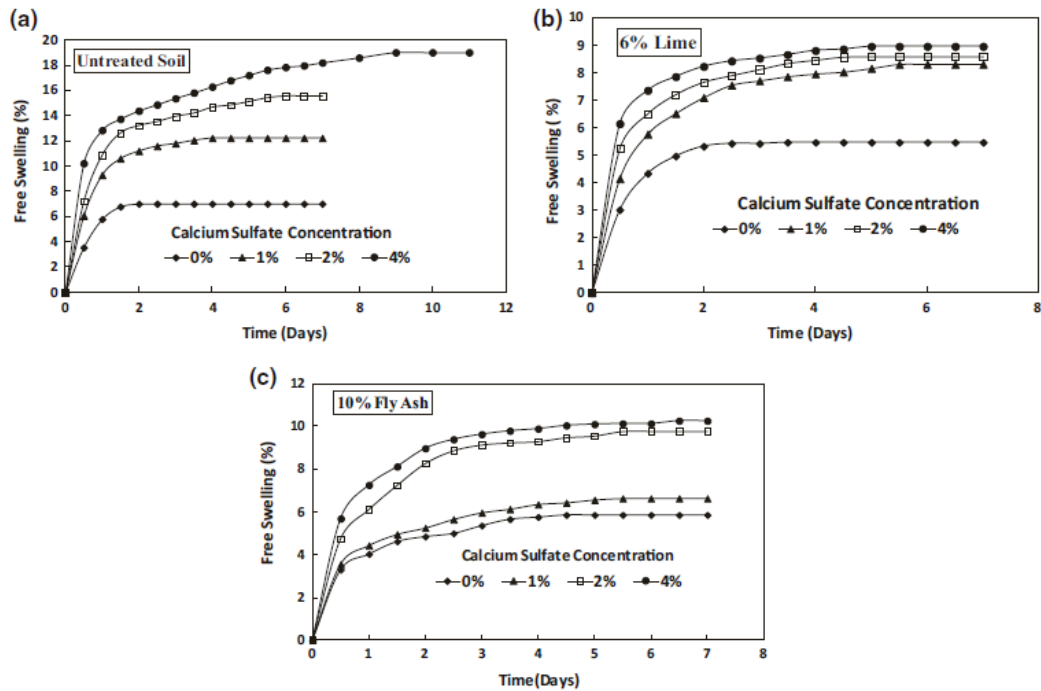


Figure 3.21. Swell vs. time graphs for (a) natural soil, (b) lime treated soil, (c) fly ash treated soil (Mohammed and Vipulandan, 2015)

Mohn (2015) performed a study on the effect of sulfate-containing water on lime and cement treated high sulfate bearing soil ( $\text{SO}_4=9395\text{ppm}$ ). At the end of the study, it was observed that both cement and lime caused ettringite induced heave problems. An increase in swell values was also observed when water containing  $\text{SO}_4$  used instead of distilled water.

Puppala et al. (2019) made an overview of the previous investigations about the sulfate-induced heave problems and problematic cases documented in the USA. As a result of the study, the following outcomes were obtained;

- Sulfate induced heave is directly related to the consumption of reactive alumina and sulfates.
- GBFS and class F fly ash with low calcium content could be used for the treatment of soils with a sulfate content less than 8000ppm.
- Combination of fly ash – lime could be used for high sulfate soils with the application of extended mellowing periods.
- Additional studies with field validation are required for determination of different methods for treatment of high sulfate soils.

## CHAPTER 4

### EXPERIMENTAL WORKS

#### 4.1. Purpose

The aim of this study is to investigate the effects of sulfate addition on physical, chemical and mechanical properties of class C fly ash treated expansive soil.

#### 4.2. Materials

Bentonite, kaolinite, class C fly ash, lime,  $\text{Na}_2\text{SO}_4$  (NS) and  $\text{CaSO}_4 \cdot 2\text{H}_2\text{O}$  (CS) were used in this study. The main stabilizer is the class C fly ash, lime is used for only comparison purposes.

**Kaolinite:** As alumina ( $\text{Al}_2\text{O}_3$ ) content is an important factor in ettringite formation, a grinded kaolinite consisting of a high amount of alumina was obtained from ESAN to be used in studies (Figure 4.1).

**Bentonite:** Na-Bentonite was taken from the Karakaya Bentonite Factory located in Ankara. The producer informed about the fact that the deposit of the bentonite changes within a year. Therefore, not to make the experiments affected by the change in bentonite properties, two times the required amount of bentonite has been obtained (Figure 4.1).

**Fly Ash:** Two different fly ashes were used during the study. They were obtained from Soma and Sivas-Kangal Thermal Power Plants. Both fly ashes have a CaO content greater than 10% and are classified as class C fly Ash. The aim of choosing these fly ashes is that they have different properties and represent different conditions. Soma fly ash (SFA) has low sulfate content and considerably lower CaO content however, Sivas Kangal fly ash (KFA) has a higher CaO and sulfate level. They were both sieved through #40 sieve before usage (Figure 4.1).

Mineralogical composition of fly ashes was determined by using X-Ray Florence Spectrometer. Analyses were performed in Central Laboratory of METU (Appendix-A). Chemical compositions of the fly ashes are presented in Table 4.1. The LOI value could not be determined in Central laboratory, therefore tests were performed at Chemical Engineering Department of Ankara University according to method A presented in ASTM D7348 in which samples are heated up to 750<sup>0</sup>C during the tests. LOI values of SFA and KFA are found as 2.3% and 4.7% respectively.

**Lime:** TS EN 459-1 CL 70-S type hydrated lime was taken from Bastas Cement Trade Inc. This material passed through #40 sieve before usage (Figure 4.1). The chemical composition of lime that was obtained from the supplier is presented in Table 4.1.

**Sulfate:** Pure sodium sulfate (NS) and calcium sulfate dihydrate (CS) with a Merck brand were used as a sulfate source during the study.

Artificial swelling soil (Sample A) that was prepared in the laboratory environment by mixing 85% kaolinite and 15% bentonite by dry weight of the sample was used in the study. The aim of using artificial soil was to know the absolute composition and eliminate the probable effects caused by the variation in soil composition.

Chemical composition of Sample A was determined by XRF method in Central Laboratory of METU (Appendix-A) and is presented in Table 4.1.



Figure 4.1. Materials (a-kaolinite, b-bentonite, c-soma fly ash, d-sivas-kangal fly ash, e-lime)

Table 4.1. Chemical composition of sample A, fly ashes and lime

Chemical Composition	Sample A (%)	Soma Fly Ash (SFA) (%)	Sivas- Kungal Fly Ash (KFA) (%)	Lime (L) (%)
SiO <sub>2</sub>	51.6	45.8	25.3	*
Al <sub>2</sub> O <sub>3</sub>	<b>41.3</b>	26.6	11.9	*
Fe <sub>2</sub> O <sub>3</sub>	1.22	4.38	5.87	*
CaO	0.51	<b>11.6</b>	<b>29.5</b>	<b>83.68</b>
SO <sub>3</sub> (SO <sub>4</sub> )	-	<b>1.79 (2.15)</b>	<b>14.6 (17.5)</b>	<b>0.66 (0.79)</b>
CO <sub>2</sub>	3.46	5.14	7.35	9.23
K <sub>2</sub> O	0.5	1.54	0.97	*
Na <sub>2</sub> O	0.17	0.45	0.31	*
MgO	0.15	1.2	2.77	2.75
P <sub>2</sub> O <sub>5</sub>	0.06	0.3	0.29	*
SrO	0.02	0.06	0.16	*
ZrO <sub>2</sub>	0.02	-	0.02	*

### 4.3. Scope of the Experimental Study

In the scope of the study,

- Two different class C fly ashes with different CaO and sulfate concentrations were used as main calcium-based stabilizers. Hydrated lime was also used for comparison purposes.
- Firstly, tests were performed to determine the optimum additive content.
- Two different sulfates namely;  $\text{Na}_2\text{SO}_4$  (NS) and  $\text{CaSO}_4 \cdot 2\text{H}_2\text{O}$  (CS) were used to better understand the effect of different sulfate sources on treated soils.
- Different sulfate concentrations were used during the study namely; 3000ppm, 5000ppm, 10000ppm, 20000ppm, and 40000 ppm.
- Tests were performed to understand the effect of calcium-based stabilizers and sulfate on index properties (grain size, Atterberg limits, specific gravity, etc.).
- Swell and unconfined compressive strength tests were performed to understand the effect of sulfate on physical and mechanical properties of soils treated with calcium-based stabilizers.
- Daily fluctuation of air temperature does not affect the soil temperature significantly below 1.0m depth however, the annual change in air temperature affects the soil temperature to a depth of 10m. Variations in short-term temperature generally highly effective up to 0.5m depth (Florides and Kalogirou, 2005). The representative graph that shows the annual temperature variation in 2013 at different depths of soil located at Maslak/Istanbul is presented in Figure 4.2 (Aydin et al., 2015).

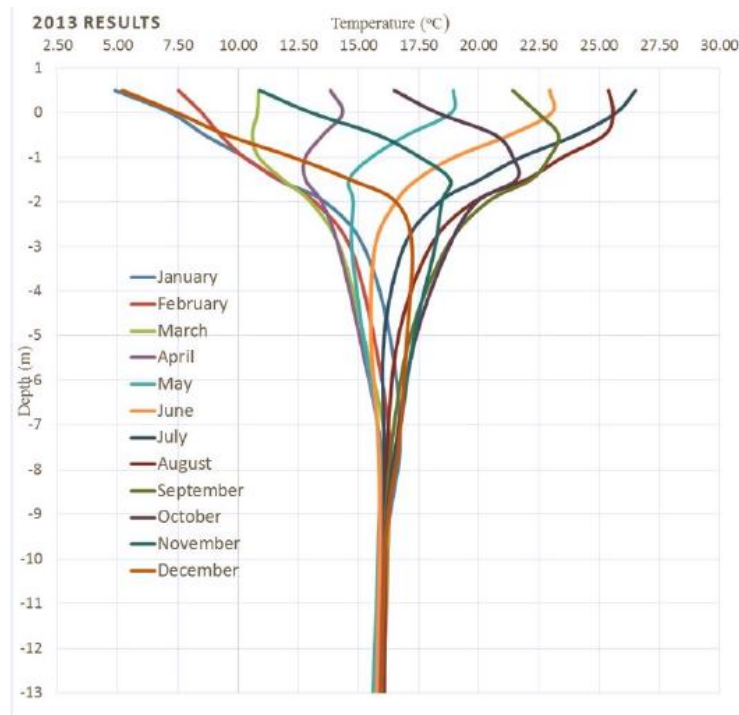


Figure 4.2. Annual temperature variation at different depth of soil located at Maslak / Istanbul in 2013 (Aydin et al., 2015)

- As the temperature at the upper levels of the soil layer is not constant during a year at real site conditions, swell and unconfined compressive strength tests were performed at three different temperatures; 10°C, 25°C, and 40°C. The main working temperature was 25°C, others were selected to reflect different conditions. One of the leading factors that affect the formation of sulfoaluminates is temperature. Ettringite turns into thaumasite when the temperature falls below 15°C (Hunter, 1988). In literature, the studies are mainly focused on the behavior of ettringite so working at low temperatures is beneficial to understand the effect of thaumasite. 40°C was chosen to see the effect of high temperatures and simulate the long-term field conditions by increasing the rate of reactions. ASTM D5102 indicates the 40°C as the most appropriate temperature for the acceleration of the chemical reactions by resulting similar pozzolanic products that occur during curing at field

conditions. Further increase in temperature may result in significantly different products that do not represent real site conditions.

- Scanning electron microscope views, XRD and zeta potential analysis were used to see the effect of treatment in chemical structure and microstructure.
- Shear Wave Velocity ( $V_s$ ) tests were also performed for comparison purposes since  $V_s$  is a valuable parameter that frequently used for determination of other soil parameters by using correlations recommended in the literature.

Test plans are presented in Figure 4.3, 4.4 and 4.5.

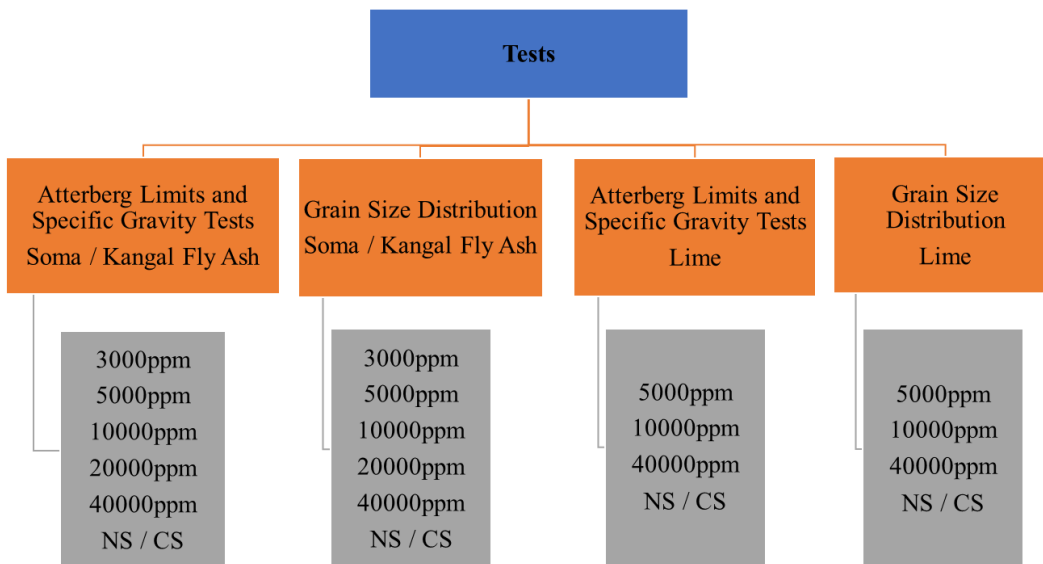


Figure 4.3. Test plan for index tests

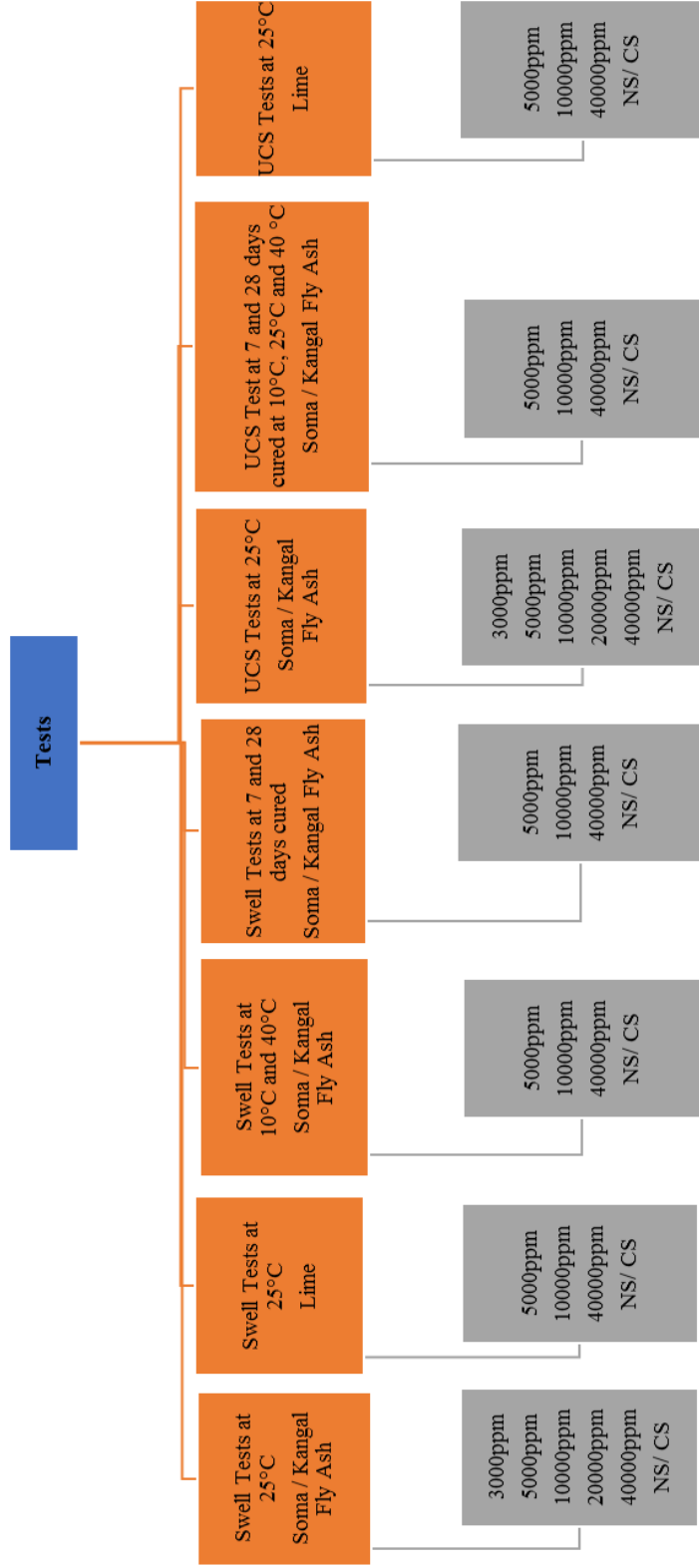


Figure 4.4. Test plan for swell and UCS tests

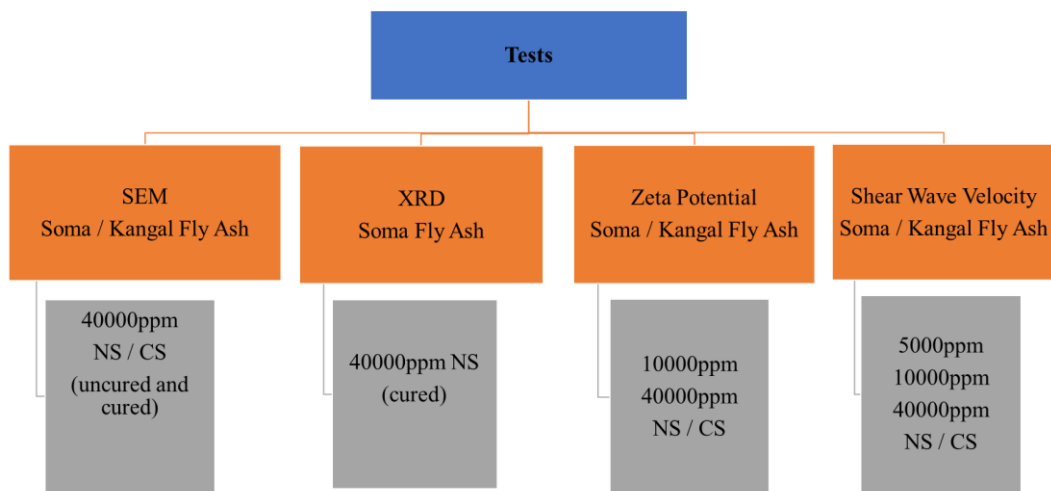


Figure 4.5. Test Plan for SEM, XRD, zeta potential and shear wave velocity tests

#### 4.4. Sample Preparation

All the materials except for sulfates are oven-dried at 60°C and sieved through #40 sieve before mixing. Then the predetermined amount of each material was put into a bowl and mixed with a plastic spoon. After mixing, materials were sieved through #30 sieve two times to obtain a well-mixed, homogenous sample. Class C fly ashes are added to 5, 10, 15 and 20 % by dry weight of Sample A and lime as 2, 3, 4 and 5%. The optimum additive percent for SFA, KFA and L was selected as 15%, 10%, and 4% respectively. Tests conducted to see the sulfate effect were performed on samples treated with optimum additive percentages.

3000ppm, 5000ppm, 10000ppm, 20000ppm and 40000ppm NS and CS were added to fly ash treated samples by dry weight of swelling soil. 5000ppm, 10000ppm and 40000ppm sulfate concentrations were chosen for lime treated samples. The composition of each sample is presented in Table 4.2.

Table 4.2. *Composition of samples*

Sample	Weight of Expansive Soil (M <sub>e</sub> )		Weight of Fly Ash / Lime	Weight of Sulfate (NS or CS)
	Kaolinite	Bentonite		
A	0.85 M <sub>e</sub>	0.15 M <sub>e</sub>	-	-
5% FA			0.05 M <sub>e</sub>	-
10% FA			0.10 M <sub>e</sub>	-
15% FA			0.15 M <sub>e</sub>	-
20% FA			0.20 M <sub>e</sub>	-
2% L			0.02 M <sub>e</sub>	-
3% L			0.03 M <sub>e</sub>	-
4% L			0.04 M <sub>e</sub>	-
5% L			0.05 M <sub>e</sub>	-
15% SFA + 3000ppm NS/CS			0.15 M <sub>e</sub>	0.003 M <sub>e</sub>
15% SFA + 5000ppm NS/CS				0.005 M <sub>e</sub>
15% SFA + 10000ppm NS/CS				0.01 M <sub>e</sub>
15% SFA + 20000ppm NS/CS				0.02 M <sub>e</sub>
15% SFA + 40000ppm NS/CS				0.04 M <sub>e</sub>
10% KFA + 3000ppm NS/CS			0.10 M <sub>e</sub>	0.003 M <sub>e</sub>
10% KFA + 5000ppm NS/CS				0.005 M <sub>e</sub>
10% KFA + 10000ppm NS/CS				0.01 M <sub>e</sub>
10% KFA + 20000ppm NS/CS				0.02 M <sub>e</sub>
10% KFA + 40000ppm NS/CS				0.04 M <sub>e</sub>
4% L + 5000ppm NS/CS			0.04 M <sub>e</sub>	0.005 M <sub>e</sub>
4% L + 10000ppm NS/CS				0.01 M <sub>e</sub>
4% L + 40000ppm NS/CS				0.04 M <sub>e</sub>

#### 4.4.1. Swell and UCS Tests

130g dry Kaoline+Bentonite mixture was used for swell and UCS tests and other materials were added by considering the rates given in Table 4.2. The optimum water content for Specimen A was determined as  $w_{opt.} = 32\%$  from the proctor test however,

the specimens were prepared at a water content of 24.5% due to the workability issues (Figure 4.6).

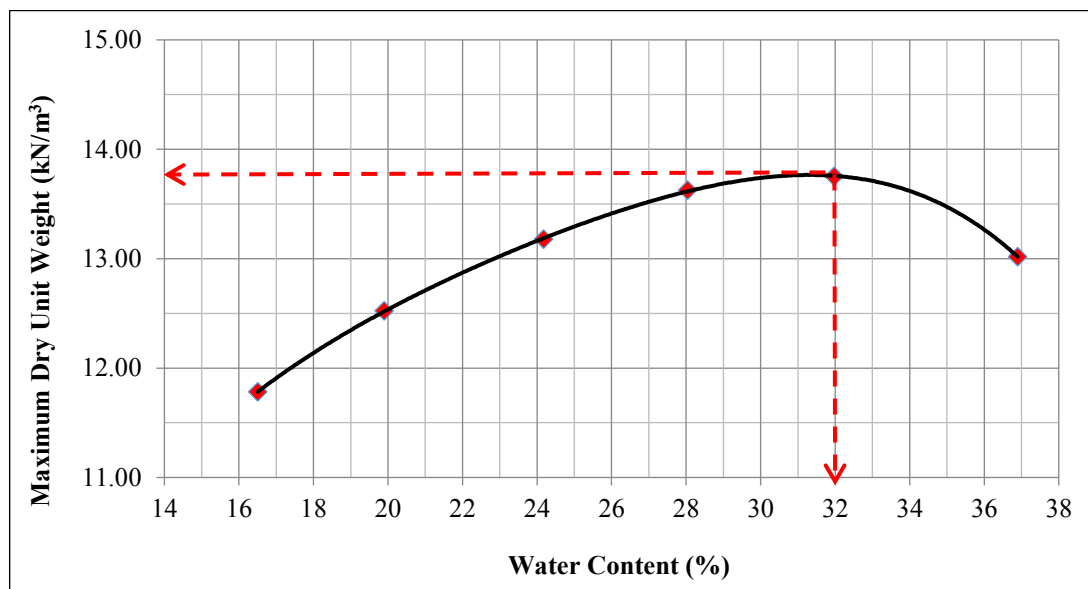


Figure 4.6. Proctor Test Results for Specimen A

Although specimens were prepared with a water content of 24.5%, each time nearly 29% water was added to sample since during the mixing process, some of the water evaporated. After mixing with water, materials that stuck to each other were separated by crushing with hand and wooden block and sieved through #30 and #16 sieve until all the materials passed. The sieved part of the materials was put in a container and top of the container covered with a wet towel not to lose water and crushing process was continued for the remaining part.

Finally, the sample was put into a plastic bag and allowed to wait at least one hour in a desiccator to have homogeneous water distribution.

CS was added to the mixture in a powder form before the sieving process as it was not dissolved in water, however when NS contacted with water it became solid and turned into a crystalline form, therefore it was not directly added to the mixture in a powder form and put into the water that was added to the dry mixture before compacting the

specimen. After addition of water, NS crystals were broken by the help of a stainless-steel rod and mix until all NS was dissolved in water.

The sample preparation process is shown in Figure 4.7, 4.8 and 4.9.



*Figure 4.7.* Addition of water to the dry mixture and mixing



*Figure 4.8.* Crushing particles that stuck to each other with wooden blocks and sieving



*Figure 4.9.* Final condition of the sample and putting sample to plastic bag

## **4.5. Methodology of the Tests**

### **4.5.1. Swell Tests**

Free swell tests were performed by taking the ASTM D4546-14 as reference.

#### **4.5.1.1. Molds**

Two different types of molds were used during the study.

1. The first type of molds had a diameter of 5.0cm and allows to measure very high swell potential (Figure 4.10). These molds had a height of approximately 8.0cm and were used to measure the swell potential of Specimen A. The specimens for this mold were prepared with 2.0cm height.

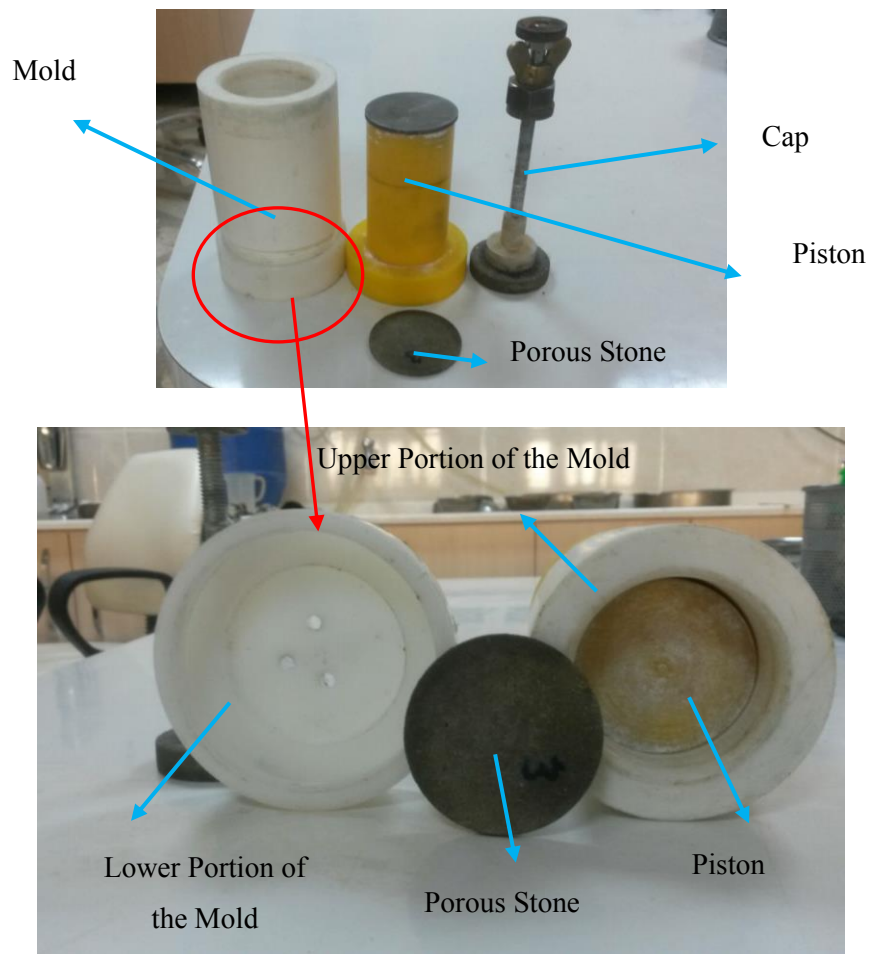


Figure 4.10. Swelling apparatus type-1

2. The second type of molds were actually rings with approximately 7.1cm diameter and 2.1cm height (Figure 4.11). They were used with oedometers for chemically stabilized soils.



Figure 4.11. Swelling apparatus type-2

The schematical representation of the test apparatus is presented in Figure 4.12 (Knappett and Craig, 2012).

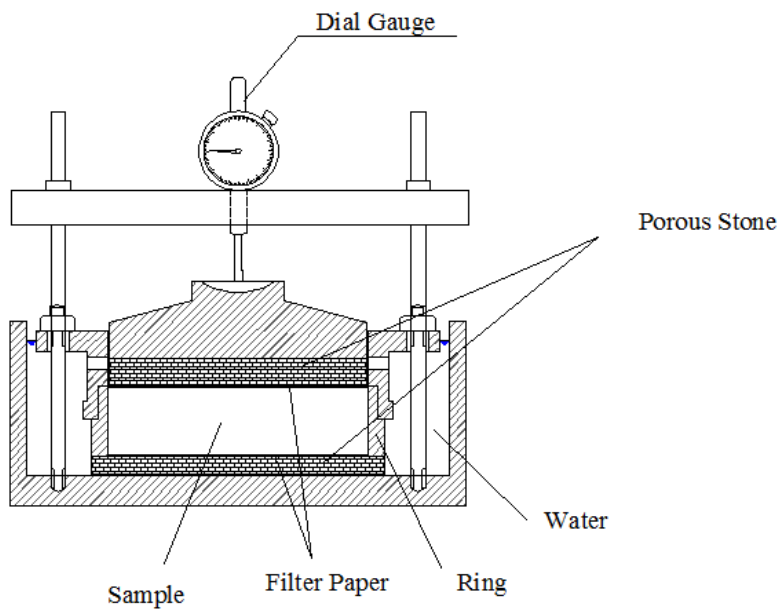


Figure 4.12. Schematic representation of oedometer (modified from Knappett and Craig, 2012)

#### **4.5.1.2. Compaction**

Specimens were compacted directly into consolidation rings /molds statically with a bulk density of  $1.80 \text{ g/cm}^3$  by the help of a Uniaxial Compression / Tension Test Press for Rocks. Before compaction, vaseline was applied to the inner surface of the ring to prevent sticking of particles.

Static compaction was performed in one step, as the height of the specimen was very low and compaction of specimens in layers may result in stratification (poor connections) between layers even if threaded surface formed at the end of the static compaction step of each layer.

At the end of the static compaction, specimens with 2.0cm height and 5.0cm diameter were obtained for the first type of mold and 2.1cm height and 7.1cm diameter for the second type of molds. After compaction, bottom and top of the specimens were trimmed by means of a steel ruler to open the pores. Photos from the compaction process are presented in Figures 4.13.

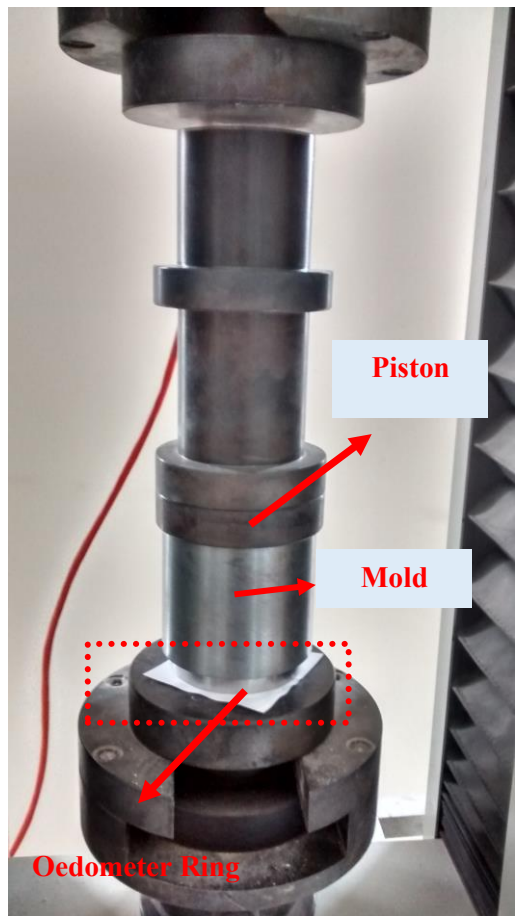


Figure 4.13. View from compaction

### 4.5.1.3. Procedure

3 different methods are recommended in the standard; Method A, B, and C. Procedure, described for Method A except for applying different stress levels to identical specimens are used during testing. Typical time-swelling curve that shows the primary and secondary swelling concepts is given in Figure 4.14.

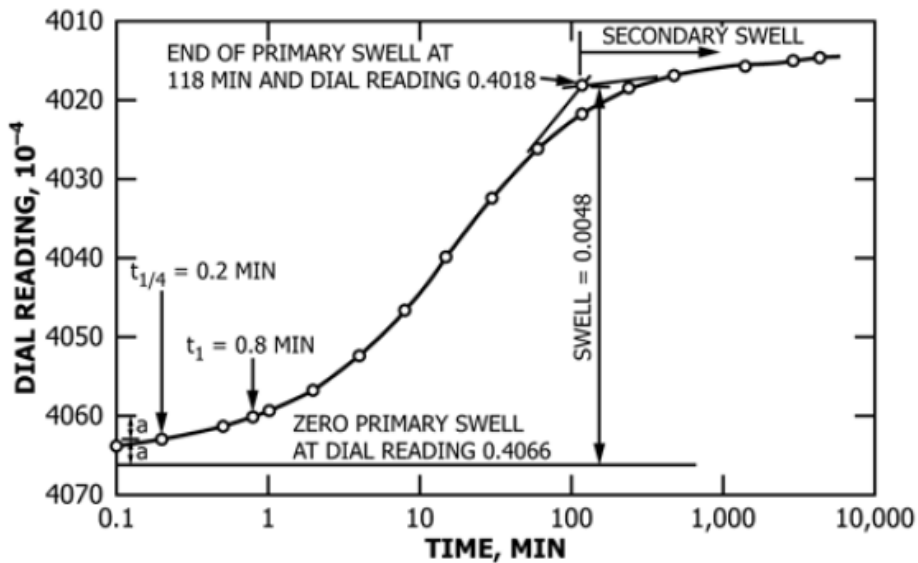


Figure 4.14. Time- swelling curve (ASTM D4546-14)

The methodology of the swell test is summarized below.

- Porous stone, filter paper, consolidation ring (specimen), filter paper and a porous stone was placed on the oedometer cell in given sequence (the first type of mold was also used as oedometer and specimen was directly compacted in it only filter papers and porous stones were placed on top and bottom of the specimen).
- The test was performed under a seating pressure of approximately 1.0 kPa resulted from the mass of the top porous stone and cap of the oedometer.

- The oedometer was put inside the plastic containers that were placed on a water bath (the first type of mold was put into beaker instead of a plastic container).
- The reading of dial gauge was taken and recorded as initial reading.
- The specimen was inundated by filling the cell and plastic containers/beakers with water.
- Deflection values were recorded until taking the same reading at least three successive days (completion of both primary and secondary swell).

Tests were performed by using distilled water for the elimination of ion effects. Swell tests were performed at different temperatures namely; 10°C, 25°C, 40°C.

Distilled water was waited in a water bath before usage not to allow any temperature difference. Also, each oedometer was put into a separate container/beaker in water bath since the specimens were prepared with different sulfate concentrations and probable seepage of water from one oedometer to another may affect the results of the tests. Also, a motor pump was put into the water bath to circulate the water and made the water temperature evenly distributed. View from the water bath is presented in Figure 4.15.



*Figure 4.15.* View from water bath

#### 4.5.1.4. Cured Specimens

Swelling tests were also performed on specimens that were cured for 7 and 28 days at 25°C. Specimens were covered with plastic wrap after compaction procedure and put into plastic bags. Then the specimens were placed in a plastic container which the bottom of it was filled with water. Finally, plastic containers were placed to the water bath, the temperature of which was arranged to 25°C (Figure 4.16).



*Figure 4.16.* Curing for swelling tests

The water bath was also used for the tests performed on 10°C. The water bath can only heat the water but not cool. Therefore, the water bath was put on the basement at winter where the temperature was lower than 10°C and the temperature of the water could easily be kept at 10°C. Photos of the water bath are presented in Figure 4.17.



Figure 4.17. Water bath for 10°C tests

#### 4.5.2. UCS Tests

Unconfined Compressive Strength tests were performed according to ASTM D2166, “Standard Test Method for Unconfined Compressive Strength of Cohesive Soil”.

##### 4.5.2.1. Degree of Saturation

Degree of saturation could be calculated by the equations given below;

$$S = \frac{w \cdot G_s}{e} \quad (4.1)$$

$$e = \frac{G_s \cdot \gamma_w}{\gamma_d} - 1 \quad (4.2)$$

where;

S: Degree of saturation

w: Water content

G<sub>s</sub>: Specific gravity

e: Void ratio

γ<sub>w</sub>: Unit weight of water

$\gamma_d$ : Dry unit weight of soil

By using the equation 4.1 and 4.2, degree of saturation of Specimen A is calculated as 81.7% for the selected specimen preparation water content 24.5%. As degree of saturation is an important item for unconfined compressive strength tests, for other treated specimens required water content to make the degree of saturation as 81.7% was calculated by keeping the dry density constant. Required water contents are tabulated in Table 4.3.

Table 4.3. Required water content for  $S=81.7\%$

Sample	$G_s$	$\gamma_d$	w (%)	e	S	$\gamma_b$ , kN/m <sup>3</sup>
				$G_s \cdot \gamma_w / \gamma_d - 1$	w · $G_s$ / e	
A	2.641	14.46	24.50	0.79	81.7	18.0
%4 L	2.714	14.46	25.32	0.84	81.7	18.1
%4 L+ 5000ppm NS	2.702	14.46	25.19	0.83	81.7	18.1
%4 L + 10000ppm NS	2.717	14.46	25.36	0.84	81.7	18.1
%4 L + 40000ppm NS	2.808	14.46	26.33	0.91	81.7	18.3
%4 L + 5000ppm CS	2.699	14.46	25.16	0.83	81.7	18.1
%4 L + 10000ppm CS	2.701	14.46	25.18	0.83	81.7	18.1
%4 L+ 40000ppm CS	2.724	14.46	25.43	0.85	81.7	18.1
%15 SFA	2.579	14.46	23.75	0.75	81.7	17.9
%15 SFA + 3000ppm NS	2.611	14.46	24.14	0.77	81.7	18.0
%15 SFA + 5000ppm NS	2.646	14.46	24.55	0.79	81.7	18.0
%15 SFA + 10000ppm NS	2.654	14.46	24.64	0.80	81.7	18.0
%15 SFA + 20000ppm NS	2.623	14.46	24.27	0.78	81.7	18.0
%15 SFA + 40000ppm NS	2.695	14.46	25.11	0.83	81.7	18.1
%15 SFA + 3000ppm CS	2.621	14.46	24.25	0.78	81.7	18.0
%15 SFA + 5000ppm CS	2.610	14.46	24.12	0.77	81.7	17.9
%15 SFA + 10000ppm CS	2.580	14.46	23.76	0.75	81.7	17.9
%15 SFA + 20000ppm CS	2.620	14.46	24.25	0.78	81.7	18.0
%15 SFA + 40000ppm CS	2.595	14.46	23.94	0.76	81.7	17.9
%10 KFA	2.699	14.46	25.15	0.83	81.7	18.1
%10 KFA + 3000ppm NS	2.711	14.46	25.29	0.84	81.7	18.1
%10 KFA + 5000ppm NS	2.683	14.46	24.98	0.82	81.7	18.1
%10 KFA + 10000ppm NS	2.724	14.46	25.43	0.85	81.7	18.1
%10 KFA + 20000ppm NS	2.718	14.46	25.36	0.84	81.7	18.1
%10 KFA+ 40000ppm NS	2.781	14.46	26.05	0.89	81.7	18.2
%10 KFA+ 3000ppm CS	2.709	14.46	25.26	0.84	81.7	18.1
%10 KFA + 5000ppm CS	2.697	14.46	25.13	0.83	81.7	18.1
%10 KFA + 10000ppm CS	2.687	14.46	25.02	0.82	81.7	18.1
%10 KFA + 20000ppm CS	2.711	14.46	25.29	0.84	81.7	18.1
%10 KFA + 40000ppm CS	2.670	14.46	24.82	0.81	81.7	18.0

The required water content for S=81.7% varies between 23.75- 26.33%. The distribution of water content, mean ( $\mu$ ) and  $\mu \pm 1\sigma$  and  $\mu \pm 2\sigma$  are presented in Figure 4.18.

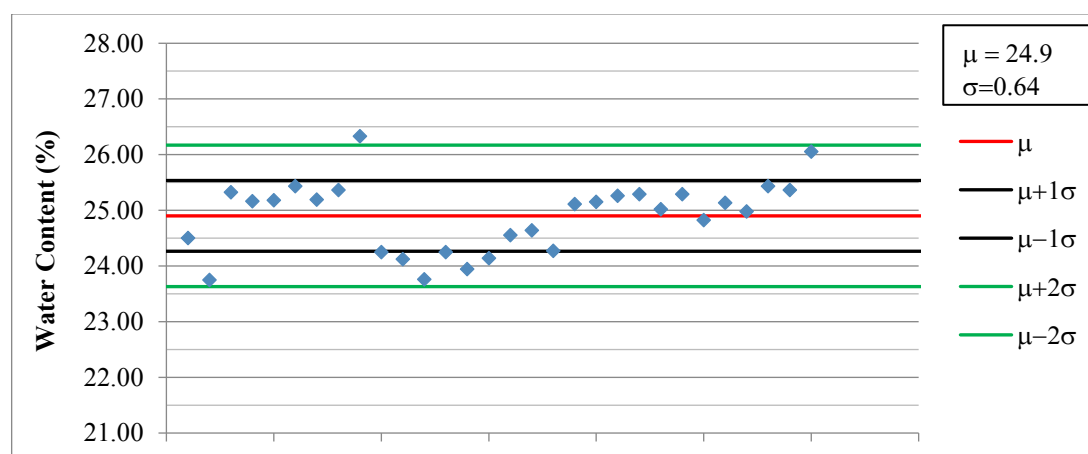


Figure 4.18. Distribution of water content required for S=81.7%

The water content are generally in  $\mu \pm 1\sigma$  range and occasionally  $\mu \pm 2\sigma$ . Required water content for S=81.7% did not alter much for samples, therefore they were decided to be prepared in the same water content which was the same as swelling tests,  $w=24.5\%$ .

#### 4.5.2.2. Compaction

In the compaction stage, specimens were compacted in 3 layers. The apparatus that were used in the compaction procedure is presented in Figure 4.19.

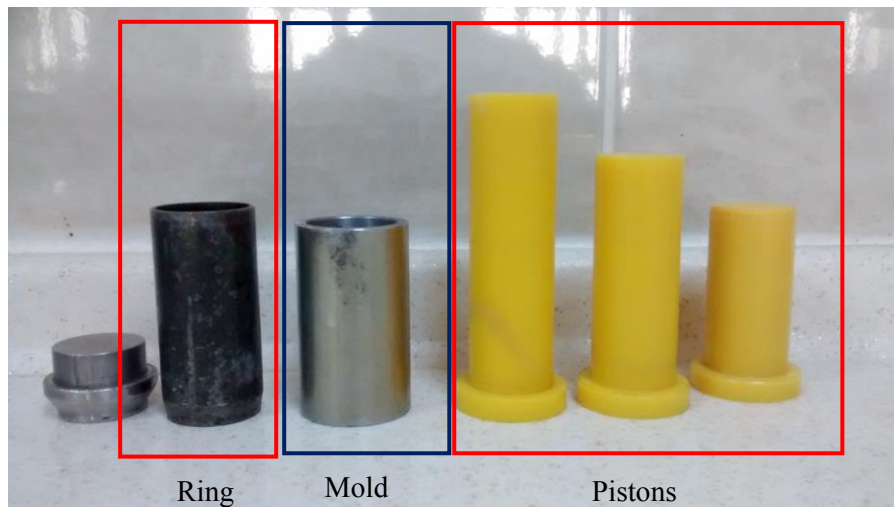


Figure 4.19. Apparatus for specimen compaction for unconfined compressive strength test

At the end of the static compaction specimens with 3.8cm diameter and 7.6cm height were obtained after trimming. Therefore, the height to diameter ratio was  $h/d=2.0$ . This  $h/d$  ratio was within the limit 2.0-2.5 which is given in the specified standard. Also, the diameter of the specimen was in the allowable limit ( $d \geq 30\text{mm}$ ). Photos from the compaction process are presented in Figures 4.20.



Figure 4.20. View from specimen compaction

### 4.5.2.3. Procedure

The test was performed by using Control's brand UCS device (Figure 4.21).



*Figure 4.21. UCS Device*

The test procedure was as follows;

- The specimen was placed in the device and the upper platen of the device was adjusted to contact with the specimen without applying load.
- The dial gauge used for the deformation measurement was adjusted to zero or the initial reading was recorded.
- The load was applied, load readings were taken at predetermined strain intervals.
- The loading was continued until failure or 15% strain was reached.

During the testing procedure, the load was applied as to produce an axial strain rate of 0.716mm /min. The same loading rate was applied for all specimens since it is one of the main factors that affect the strength value. Representative test photo for Specimen A is presented in Figure 4.22.

In ASTM 2166, the acceptable range of two results is suggested as  $1.96\sqrt{2} * 1\sigma$  where  $\sigma$  is the standard deviation. The acceptable range of two results for a rigid polyurethane foam that has an average strength of 989 kPa, is presented as 120 kPa for the single operator tests where  $\sigma$  is found as 42 kPa. The acceptable range of two results was assumed as 50 kPa during the study and if the strength values obtained from two identical specimens differed from 50 kPa, tests were performed on the third specimen. Tests were repeated at least 2 times and average values were taken.



*Figure 4.22. Views from UCS tests (Specimen A)*

#### **4.5.2.4. Curing**

Tests were also performed on specimens that were cured for 7 and 28 days at 10°C, 25°C and 40°C.

For curing, compacted specimens were covered with plastic wrap. Then the specimens were placed in plastic or glass containers which the bottom of it was filled with water. Finally, containers were placed to water bath the temperature of which was arranged to the required temperature (Figure 4.23).

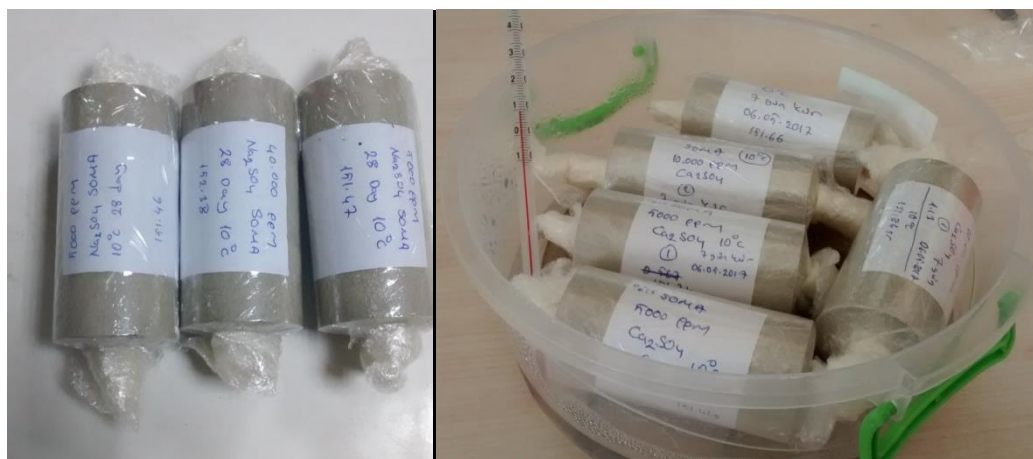


Figure 4.23. Curing for UCS test

#### 4.5.3. Shear Wave Velocity ( $V_s$ ) Tests

The James Instruments brand V-meter Mark IV was used to measure the shear wave velocity ( $V_s$ ) of the specimens (Figure 4.24).

The James Instruments V-meter Mark IV is an ultrasonic pulse velocity instrument designed to determine the quality of concrete, wood and other coarse-grained materials; both in the field or in laboratory specimens.

The specimens with a diameter of 3.8cm and height of 7.6cm were prepared for tests like unconfined compressive strength tests. High vacuum grease was used to improve the transmission of energy between the transducers and specimen during the measurement.



Figure 4.24. Measurement of  $V_s$  with V-meter Mark IV

Although the device automatically measures  $V_s$  after calibration of the transducers and entering the length of the specimen, the general procedure for the test presented in ASTM D2845 is summarized below;

- The length and diameter of the specimen are measured.
- The specimen is placed between the transducers of the device.
- The voltage output of the pulse generator, the gain of the amplifier and the sensitivity of the oscilloscope is increased and countered to an optimum level.
- Travel time is measured by using the delaying circuits jointed to an oscilloscope. The oscilloscope is used with the time-delay circuit to display both the direct pulse, the first arrival of the transmitted pulse, and to measure the travel time.
- Correction to the measured travel times is implemented by determining the zero time of the circuit including both transducers and the travel-time measuring device. Transducers are placed in direct contact to determine the

zero time by directly measuring the delay time or travel time measurement on uniform material such as steel.

#### 4.5.4. SEM

The scanning electron microscope (SEM) is a multipurpose instrument that is used in the characterization of chemical composition and microstructure texture (Zhou et al., 2006).

A focused beam of electrons is utilized to gather information. Random electrons are taken and focused onto a sample. Several detectors that produce the compositional, textural, topographical information related to the surface of the solid sample, analyze the electrons. The method is very valuable for many industrial and science applications (Choudhary and Choudhary, 2017). Magnifications up to 300000 times could be achieved by using SEM (Sharma et al., 2018). Chemical composition of the sample could be determined at a selected point by EDX method. SEM analyses were performed to determine the probable ettringite formation.

Ettringite has a needle-like structure and typical SEM view of ettringite and thaumasite is presented in Figure 4.25 and 4.26 respectively.

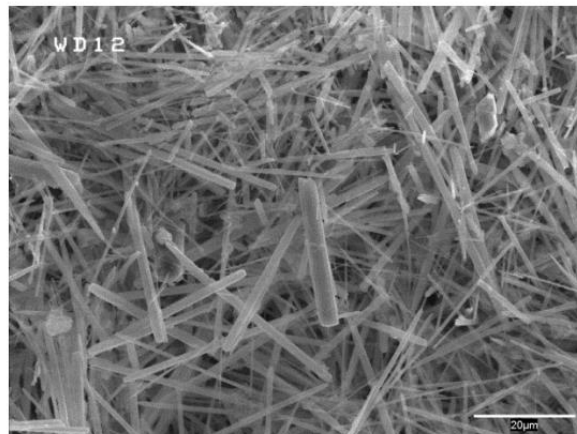


*Figure 4.25. SEM view of ettringite (Weir et al., 2014)*

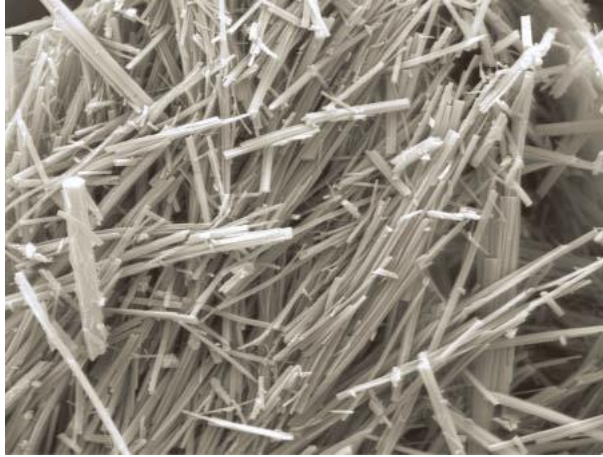


*Figure 4.26.* SEM view of purified thaumasite (Mittermayr et al., 2012)

SEM analysis was performed at Central Laboratory of METU by using QUANTA 400F Field Emission Scanning Microscope that has a 1.2cm resolution.

SEM analysis gives valuable information about the microstructure of soils and change in microstructure for chemically treated soils. The used voltage and magnification factor varied between 20kV and 800-20000 respectively during the analysis. The selected samples were dried at 60°C before the analysis since water vapor has a detrimental effect on the equipment. Soil samples are insulant, therefore, they were vacuumed and covered with palladium and gold right before the analysis. The photos of the Scanning Electron Microscope and vacuum device are given in Figure 4.27.



*Figure 4.27.* Scanning electron microscope and vacuum device

#### **4.5.5. XRD**

X-ray diffraction is one of the nondestructive techniques that is used for the characterization of crystalline materials. Information related to phases, structures and texture, etc. could be obtained from this method. XRD pattern could be assumed as the fingerprint of atomic arrangements within a material (Bunaciu et al., 2015). The concentration of different types of structures that exist within a mixture is directly proportional to the intensity of various diffraction peaks. In XRD, the sample is mounted and then X-radiation is performed. Finally, quantitative and qualitative interpretation is performed (Jackson, 2005).

The advantages of XRD are listed by Sharma et al. (2012) as follows; rapid and powerful technique, minimum sample preparation is required, exact phase determination and straightforward data interpretation procedure.

XRD analyses were performed to determine the probable occurrence of ettringite and thaumasite. Typical peaks of the ettringite and thaumasite that are used to identify these minerals are presented in Table 4.4. XRD patterns of ettringite and thaumasite are presented in Figure 4.28.

Table 4.4. Typical peaks for ettringite and thaumasite in XRD (“x-ray diffraction table” (n.d))

	Ettringite			Thaumasite		
<b>d (Å)</b>	9.65	5.58	3.21	9.56	5.51	3.41
<b>2 θ (Cu Kα )</b>	9.16	15.87	27.77	9.24	16.07	26.11

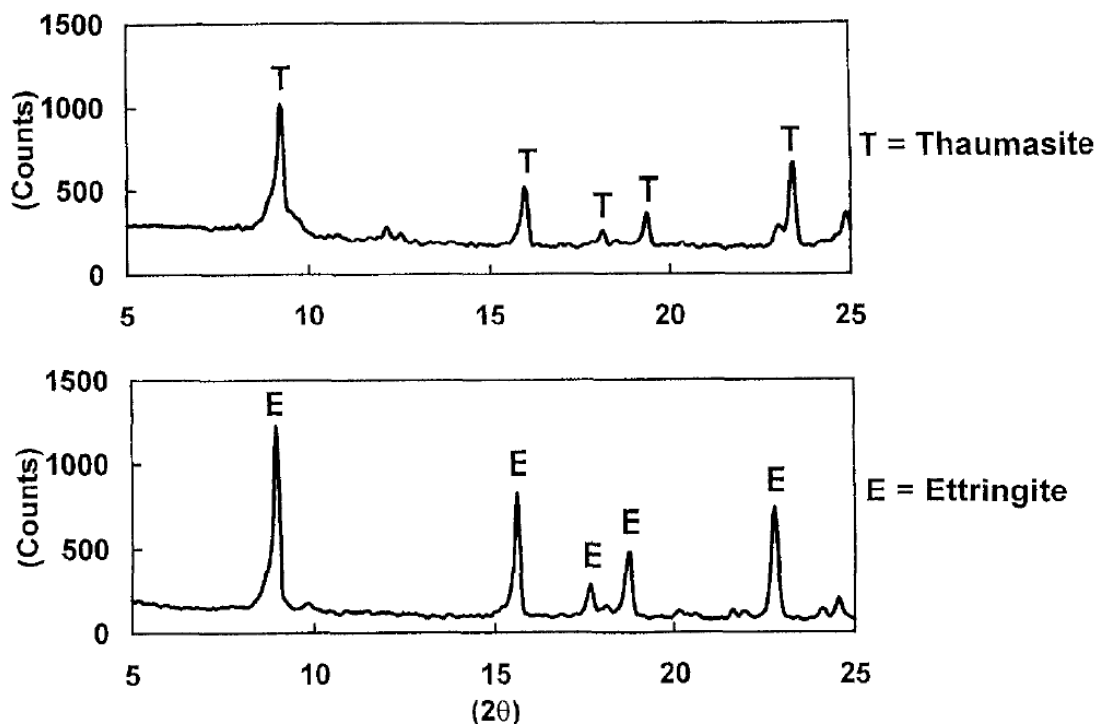


Figure 4.28. XRD Patterns of thaumasite and ettringite (Collepari, 1999)

The XRD analyses were performed at METU Central Laboratory by using the Rigaku Ultima-IV brand X-Ray Diffractometer (Figure 4.29).

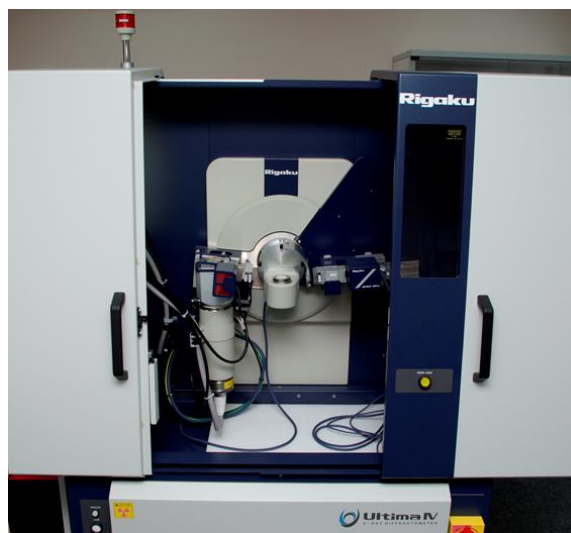


Figure 4.29. Rigaku Ultima-IV brand X-ray diffractometer

#### 4.5.6. Zeta Potential

Electrical double layer takes part around each clay particle. Liquid layer that surrounds the particles are composed of two regions; ions are firmly bounded in the Stern layer whereas they are not highly associated at the diffuse region. There exists an imaginary boundary called the slipping plane within the diffuse layer where the particles move as a single body (Misra et al., 2004). The electric potential existing at the slipping plane is accepted as Zeta potential ( $\zeta$ ) (Moayedi et al., 2011).

Representation of zeta potential on a charged particle is presented in Figure 4.30.

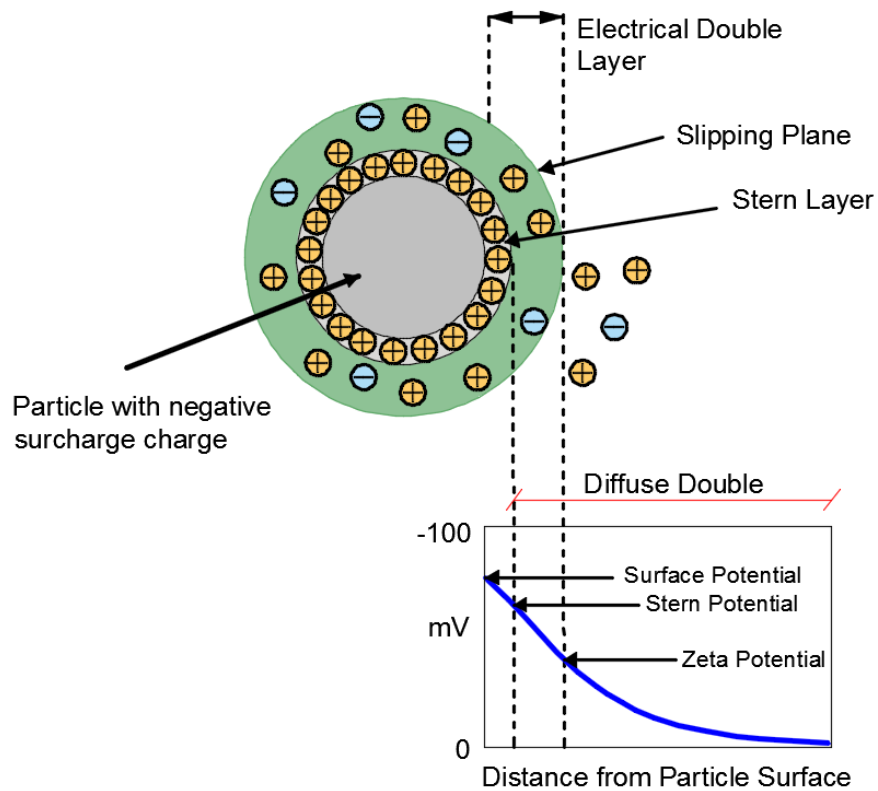


Figure 4.30. The electrical double layer and zeta potential (modified from Malvern Instruments Ltd, 2004)

Stability of colloidal dispersions and zeta potential has a relation that makes zeta potential significant. Zeta potential is an indicator of the repulsion degree between the particles that have similar charges in a dispersion. Attraction surpasses repulsion for low zeta potential which results in flocculation however exactly opposite behavior is observed for high zeta potential. Therefore, a tendency to flocculation or coagulation is observed for colloids with low zeta potential (positive or negative) whereas the colloids that have high zeta potential are stabilized (Kumar and Kumbhat, 2016).

Yong et al. (2012) present a figure that shows the variation in the aggregation/dispersion level depending on the average zeta potential value (Figure 4.31).

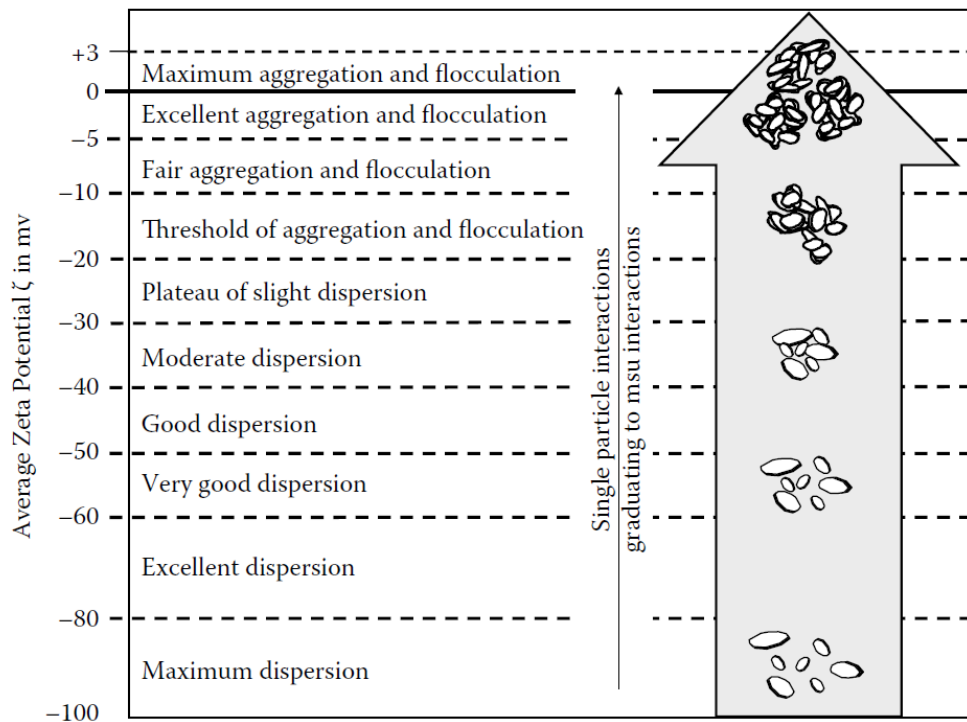


Figure 4.31. Variation in aggregation/ dispersion level depending on the average zeta potential value (Yong et al., 2012)

Zeta potential is one of the most important factors that affect the swelling potential of soils. Also, if chemical stabilization results cation exchange reaction in soils, electrokinetic properties including zeta potential may change (Arasan and Akbulut, 2010). Clays have generally negative zeta potential value (Kaya and Yukselen, 2005).

Zeta potential tests were performed to understand the mechanism behind the variation in soil properties with the addition of class C fly ash and sulfate.

Tests were performed at Central Laboratory of Middle East Technical University by using Malvern brand Zetasizer Nano ZS90 model which is capable of measuring particle size, molecular size, and zeta potential.

The device was calibrated before the start of the tests using a material with a known zeta potential value. Polystyrene latex ( $-42\text{mV} \pm 4.2\text{mV}$ ) was used for the calibration.

Aliquots taken from the sample- water mixtures were put into cuvettes and exposed to testing. The device determines the electrophoretic mobility and calculates the zeta potential by using the Henry equation automatically. Views from zeta potential tests are presented in Figure 4.32.

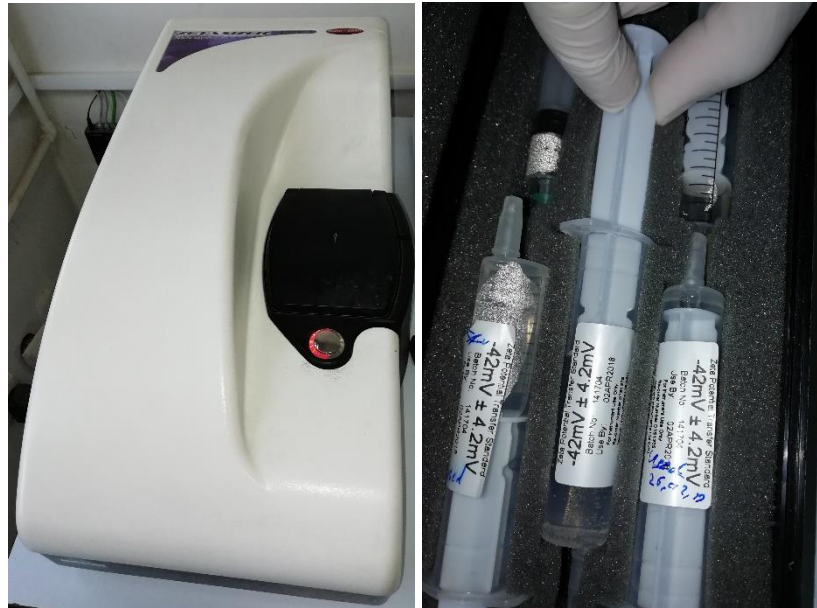


Figure 4.32. Views from zeta potential tests

pH is the primary factor affecting the Zeta Potential and it is senseless without a corresponding pH value (Moayedi et al., 2011). Therefore, pH of the samples was also measured.

#### 4.5.7. Optimum Lime Content

Optimum lime content was determined according to ASTM D6276 standard derived from the method proposed by Eades and Grim (1983). This test is performed to identify the optimal proportion of soil-lime that provides a pH environment required for the occurrence of reactions for the soil stabilization. The minimum lime percentage that resulted a pH of 12.4 is stated as optimum lime content (ASTM D6276).

Oven-dried soil at a temperature of  $\leq 60^{\circ}\text{C}$  that was sieved through No.40 sieve and HI 8314 brand pH meter were used during the tests. The procedure of the test was as follows;

- pH meter was calibrated with buffer solutions.
- Five samples each with 25g were prepared.
- Each sample was put into a plastic bottle and capped tightly.
- Lime equal to 1, 2, 3, 4 and 5 % of soil mass was weighed.
- Different concentrations of lime were added to each sample that was previously put into plastic bottles and mixture was stirred thoroughly by shaking.
- 100 mL of distilled water was added to each soil-lime mixture.
- The bottles were capped and all the soil-lime-water mixtures were shaken for the 30s until the specimens were thoroughly mixed.
- The specimens were shaken for the 30s every 10 min for 1 hour.
- Measurement was performed within 15 minutes after the end of the 1 hour shaking period. The temperature of the mixture was controlled if it was  $25 \pm 1^{\circ}\text{C}$  at the time of measurement.
- The pH value of each soil-lime-water mixture was recorded.
- The minimum lime percentage that resulted in a pH of 12.4 was chosen as the approximate optimum lime content.

Representative test photos are presented in Figure 4.33.



Figure 4.33. pH test photos

#### 4.5.8. Index Tests

Grain size distribution, Atterberg limits, shrinkage limit, and specific gravity tests were also performed to determine the effect of the addition of chemical additives and sulfate on physical properties of expansive soil. The standard of each test is presented in Table 4.5.

Table 4.5. Index tests for physical properties and related standards

Test	Standard
Grain Size Analysis (Sieve Analysis and Hydrometer)	ASTM D422, Standard Test Method for Particle-Size Analysis of Soil
Atterberg Limits	ASTM D4318, Standard Test Methods for Liquid Limit, Plastic Limit, and Plasticity Index of Soils
Shrinkage Limit	ASTM D427, Test Method for Shrinkage Factors of Soils by the Mercury Method
Specific Gravity	ASTM D854, Standard Test Methods for Specific Gravity of Soil Solids by Water Pycnometer

500 ml flasks and 50g of dry samples were used for the specific gravity tests. After putting the soil to flask and addition of water, the mixture was waited in the water tank with a temperature of water inside 20 °C for 1 day to make the bentonite and kaolinite absorb water well (Figure 4.34). Specific Gravity of the fly ashes and lime were performed just after the addition of water to keep the chemical reactions effect smaller.

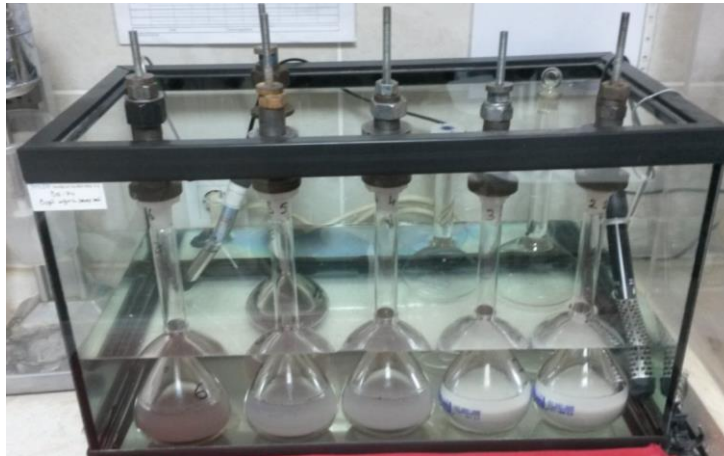


Figure 4.34.  $G_s$  samples in water tank

As fly ashes react with water, specific gravity tests could be performed according to TS EN 196-2 (2013) where kerosene used instead of water to prevent chemical reactions. However, performing specific gravity with kerosene would not show the exact properties, since samples were prepared by addition of water for swelling and unconfined compressive strength tests and chemical reactions start just after the addition of water.

Hydrometer tests were performed by ASTM D422 method but with a slight modification. In related standard, it is recommended to mix the tests sample with 125 mL of sodium hexametaphosphate solution (40 g/L) and allow to soak for at least 16 hours. This procedure was applied for Sample A. However, for fly ash and lime treated samples, only bentonite and kaolinite were soaked for at least 16 hours and chemical stabilizers were added in dispersing procedure in stirring apparatus. Also, sulfate was added to samples at the same time with fly ash and lime. As the NS change into crystalline form when reacts with water, it was mixed with distilled water before adding to the mixture and crushed. However, CS was added to the sample in a dry powder form. View from the hydrometer test is given in Figure 4.35.



*Figure 4.35. View form hydrometer tests*



## CHAPTER 5

### TEST RESULTS

#### 5.1. Determination of Optimum Additive Content

##### 5.1.1. Lime

pH tests were performed according to ASTM D6276 standard derived from the method proposed by Eades and Grim (1983) to obtain the optimum lime content. The results of the tests are presented in Figure 5.1.

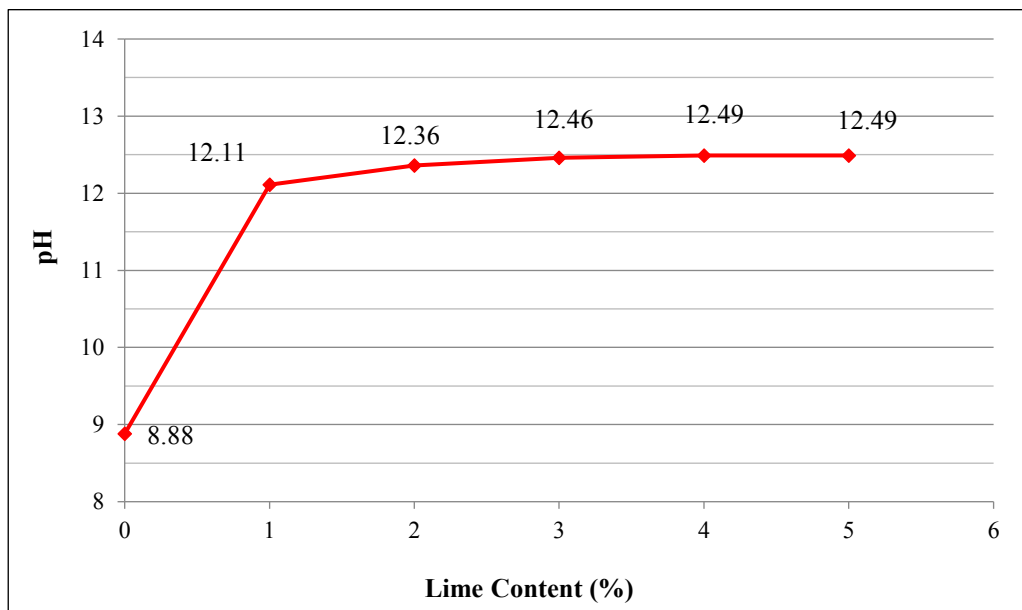


Figure 5.1. pH vs. lime content

In the aforementioned method, the lowest percentage of lime that results in a soil-lime pH of 12.4 is stated as optimum lime content. The tests were performed on 1%, 2%,

3%, 4% and 5% lime treated samples. The obtained pH value for 3% lime added even 2% lime added sample was very close to this value. Therefore, swelling tests were also performed to determine the optimum lime content (Figure 5.2).

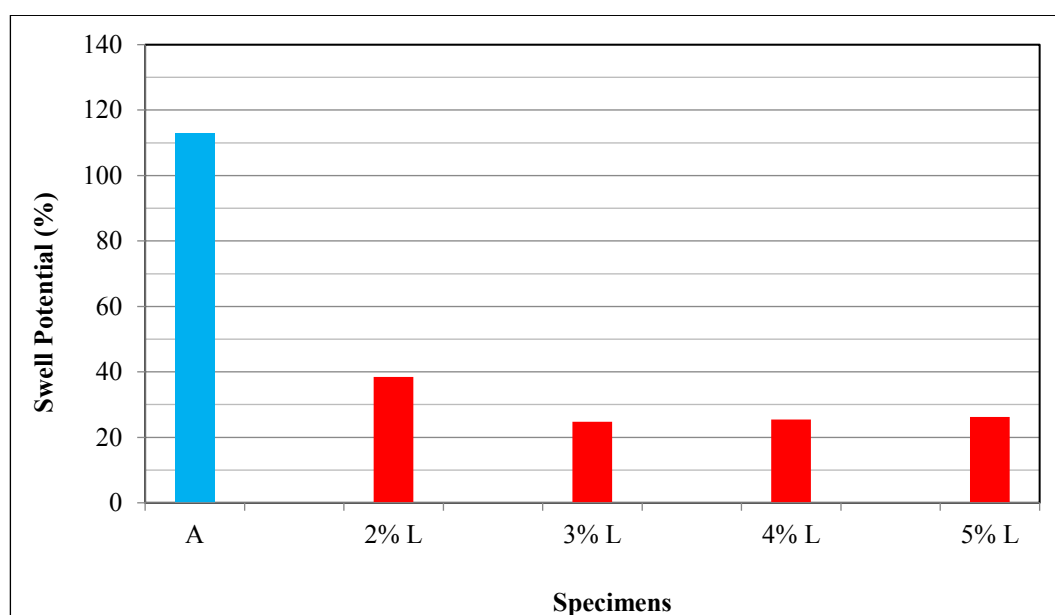


Figure 5.2. Swell percent for lime treated specimens

Swell potential of 3%, 4% and 5% lime treated specimens were very close to each other. Although 3% lime could be chosen as optimum lime content, to make the CaO content higher and to be able to see the ettringite effect better 4% lime was chosen as optimum lime content.

### 5.1.2. Fly Ash

Swell tests were performed on fly ash treated specimens to determine the optimum content for each fly ash. Chemically treated specimens were prepared by mixing 5%, 10%, 15% and 20% fly ashes by dry weight of swelling soil. Test results for SFA (Soma Fly Ash) and KFA (Kangal Fly Ash) treated specimens are presented in Figure 5.3.

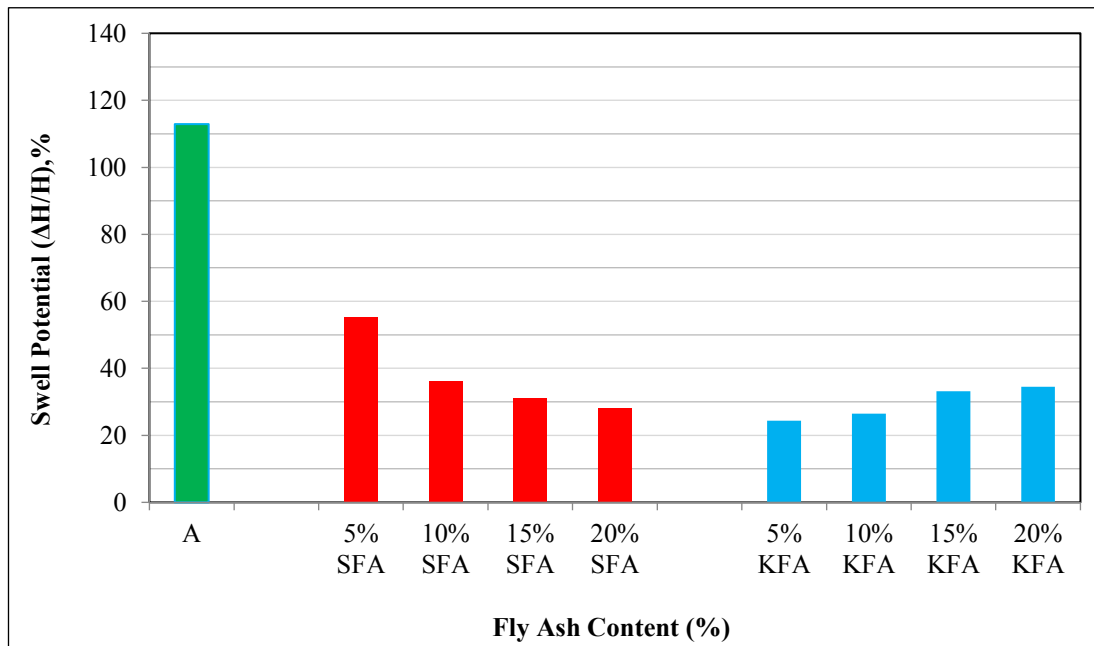


Figure 5.3. Swell percent for fly ash treated specimens

The optimum content for SFA and KFA were selected as 15% and 10% respectively by considering both test results and triggering factors of ettringite formation. Detailed discussion on optimum additive content selection is presented in Section 6.5.1

## 5.2. Physical Properties

Specific gravity, Atterberg limits (LL, PL, PI, SL) and hydrometer (including sieve analyses) tests were performed on samples to determine the effect of chemical additives and sulfates on physical properties of soil. Tests were performed on Sample A, 4% L, 15% SFA, 10% KFA treated samples and sulfate added chemically treated samples. 3000ppm, 5000ppm, 10000ppm, 20000ppm and 40000ppm NS (sodium sulfate) and CS (calcium sulfate dihydrate) were added to fly ash treated samples whereas 5000ppm, 10000ppm and 40000ppm sulfate (NS and CS) concentrations were used for 4% L treated sample.

### 5.2.1. Specific Gravity Tests

$G_s$  values were determined according to ASTM D854. Test results for 4% L, 15% SFA and 10% KFA treated soils are presented in Figure 5.4, 5.5 and 5.6 respectively. Test result for Sample A is also presented in the same graphs for comparison purposes.

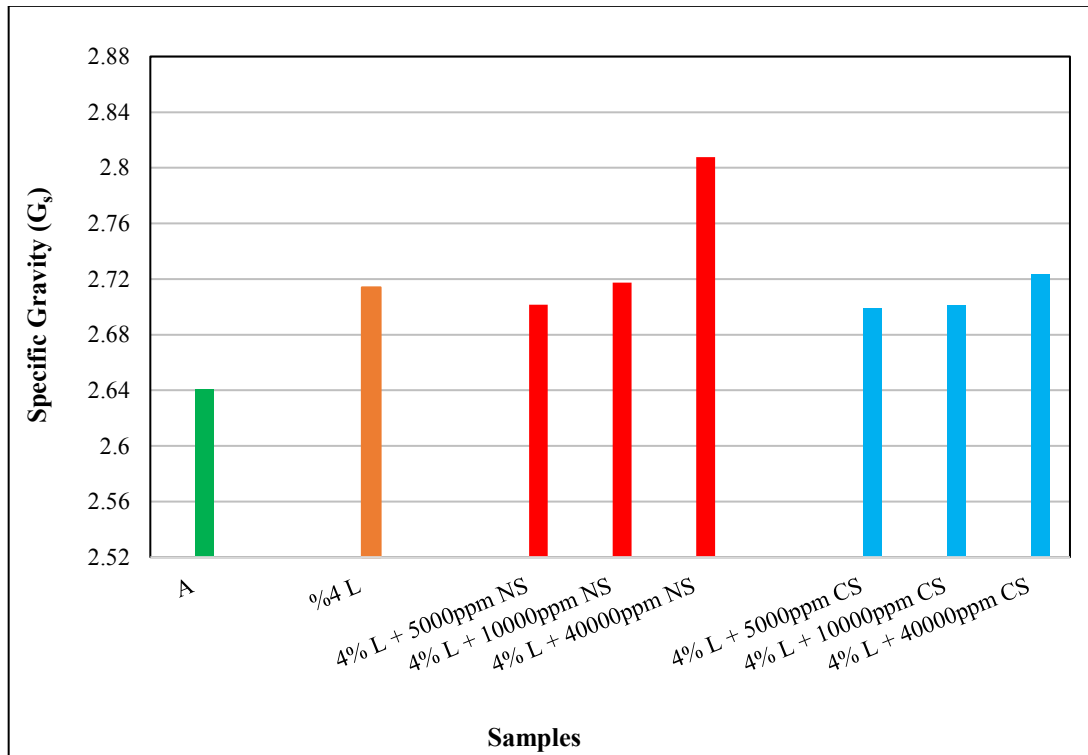


Figure 5.4.  $G_s$  values of NS and CS added 4% L treated samples

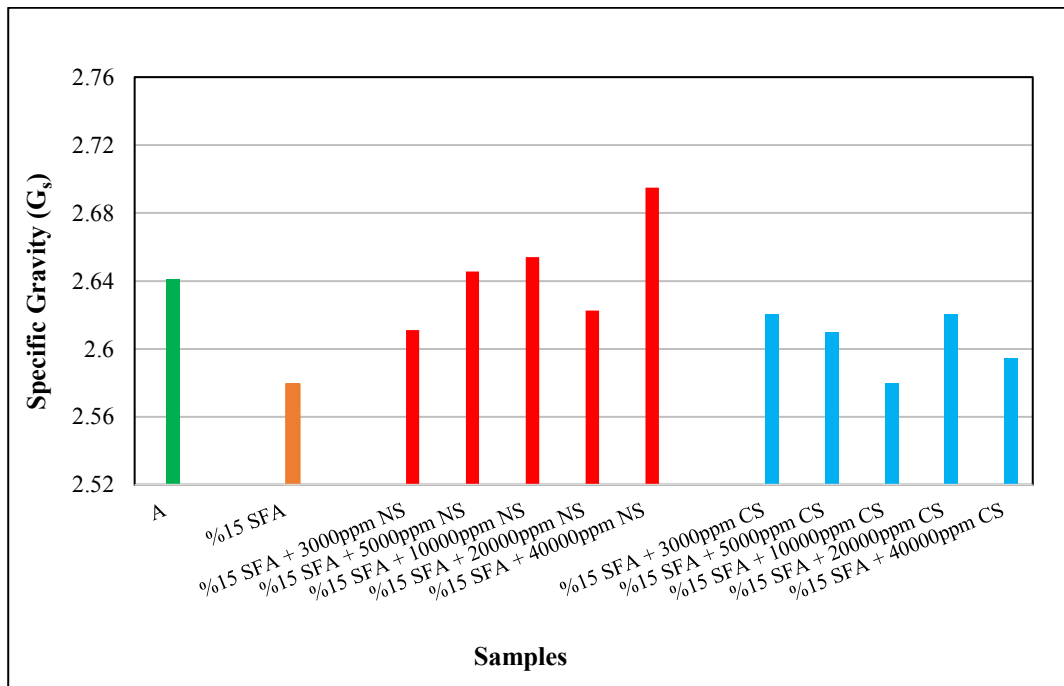


Figure 5.5.  $G_s$  values of NS and CS added 15% SFA treated samples

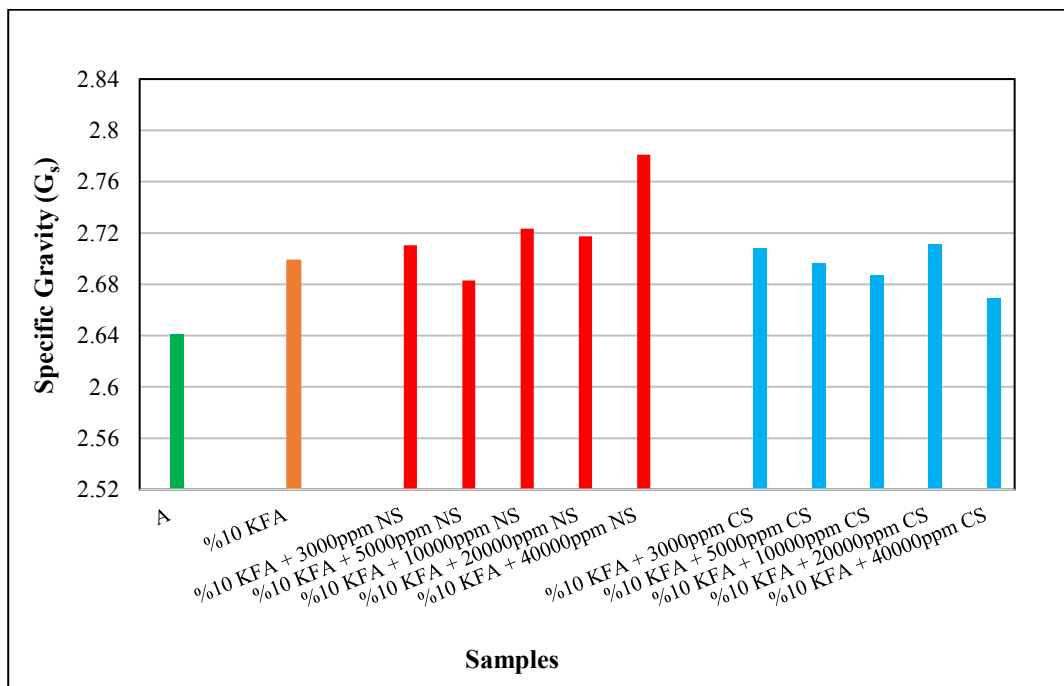


Figure 5.6.  $G_s$  values of NS and CS added 10% KFA treated samples

### 5.2.2. LL, PL & PI

LL, PL and PI were determined according to ASTM D4318.

#### 5.2.2.1. 4% L and sulfate added samples

LL, PL and PI test results for 4% L treated sample and 5000ppm, 10000ppm and 40000ppm NS and CS added 4% L treated sample are presented in Figure 5.7, 5.8 and 5.9 respectively. Test results for Sample A are also presented in the same graphs for comparison purposes.

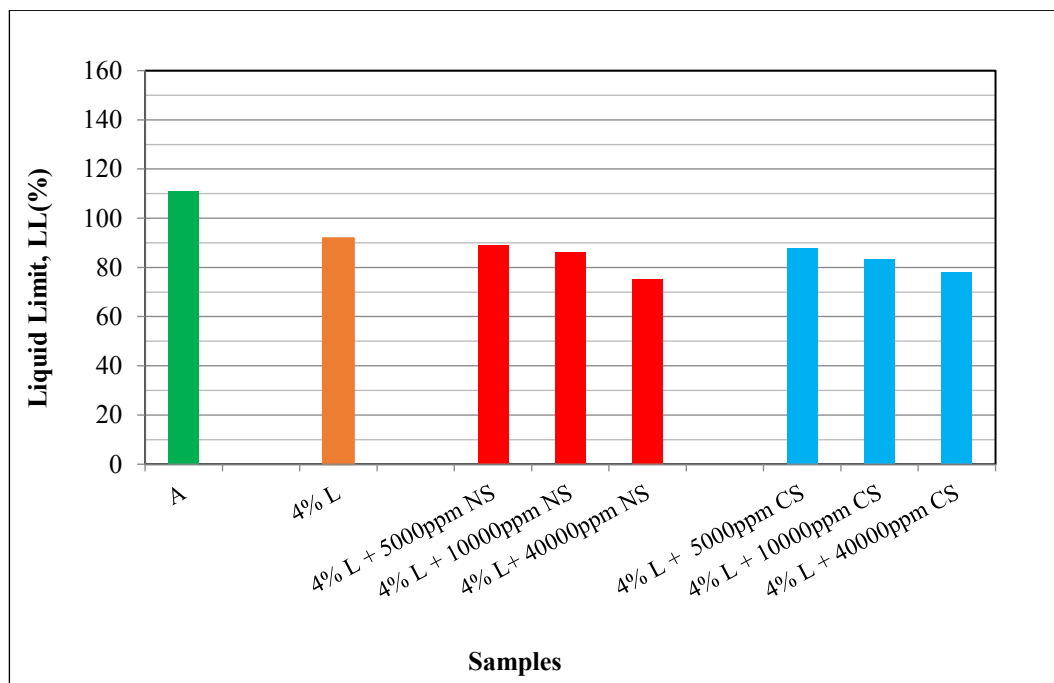


Figure 5.7. LL of NS and CS added 4% L treated samples

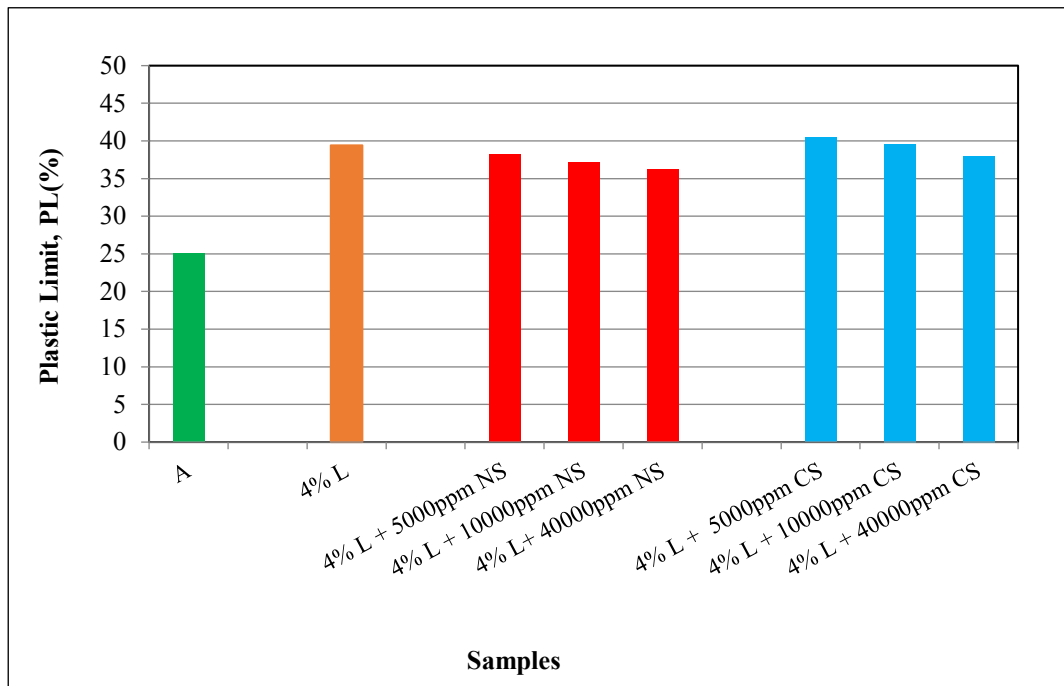


Figure 5.8. PL of NS and CS added 4% L treated samples

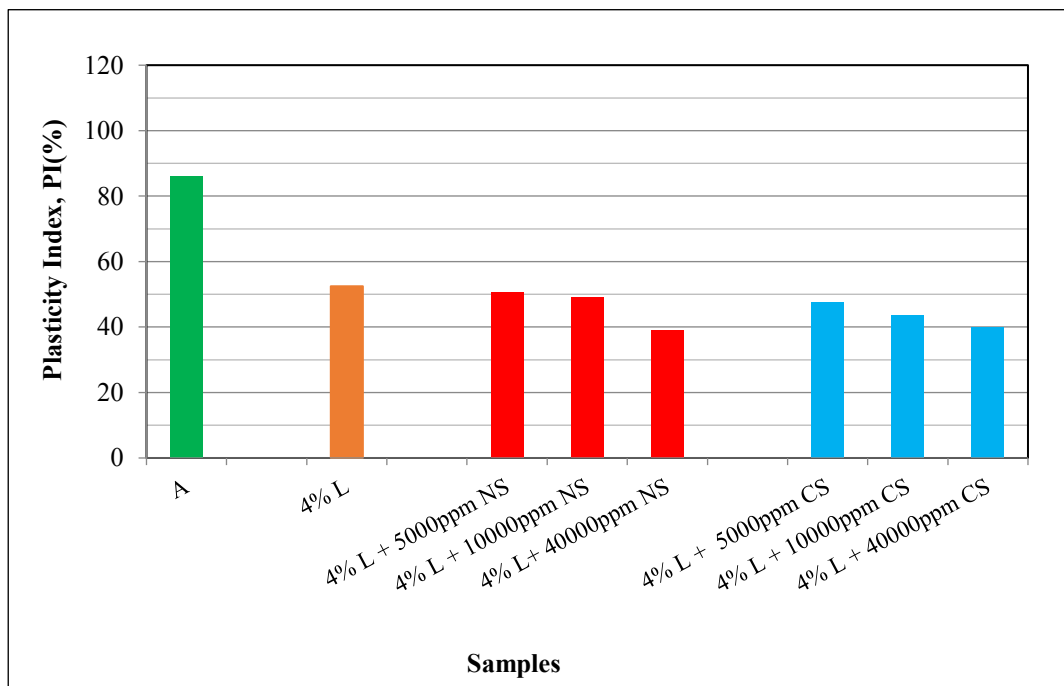


Figure 5.9. PI of NS and CS added 4% L treated samples

### 5.2.2.2. 15% SFA and sulfate added samples

LL, PL and PI test results for 15% SFA treated sample and 3000ppm, 5000ppm, 10000ppm, 20000ppm and 40000ppm NS and CS added 15% SFA treated sample are presented in Figure 5.10, 5.11 and 5.12 respectively. Test results for Sample A are also presented in the same graphs for comparison purposes.

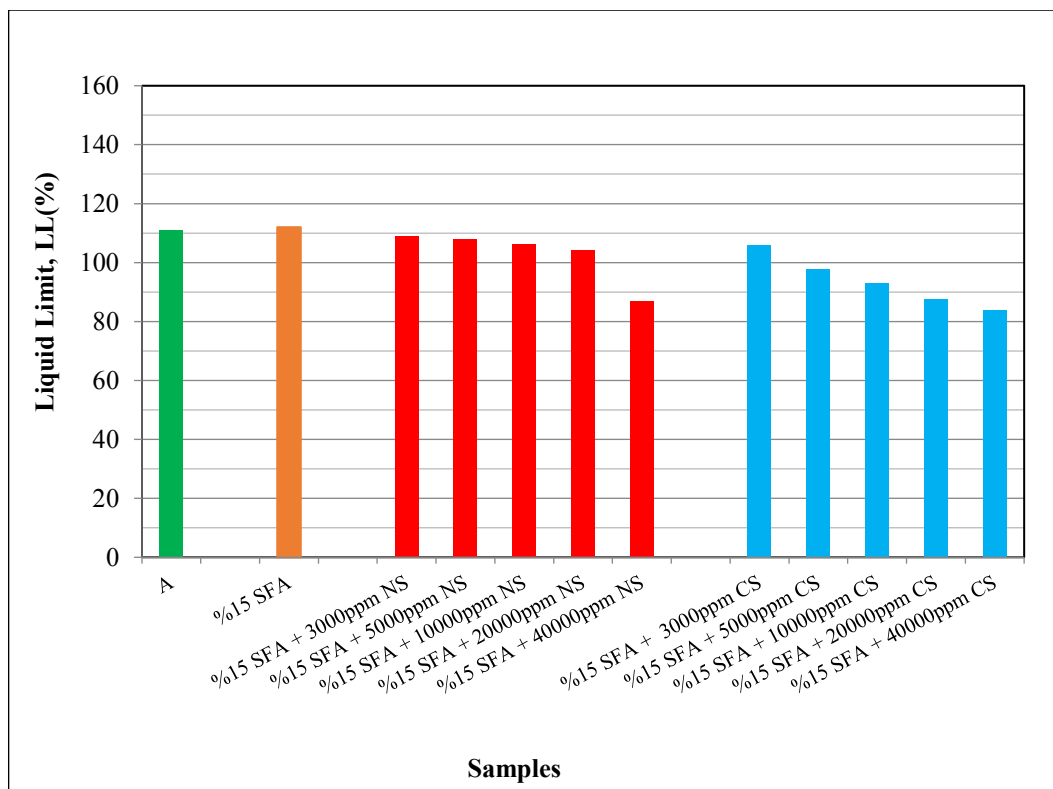


Figure 5.10. LL of NS and CS added 15% SFA treated samples

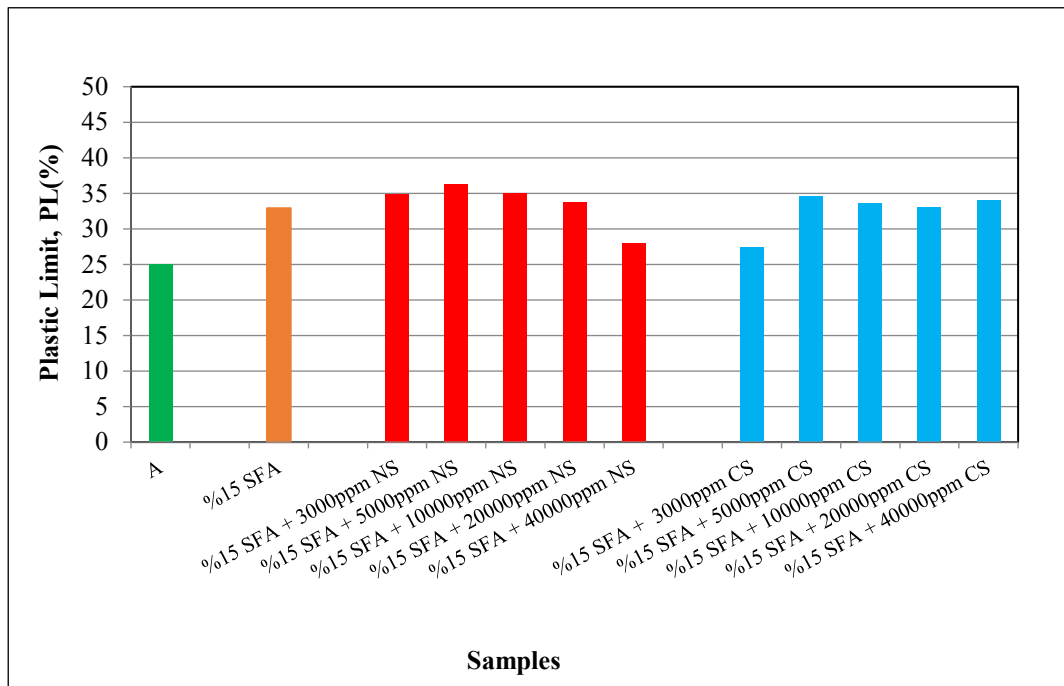


Figure 5.11. PL of NS and CS added 15% SFA treated samples

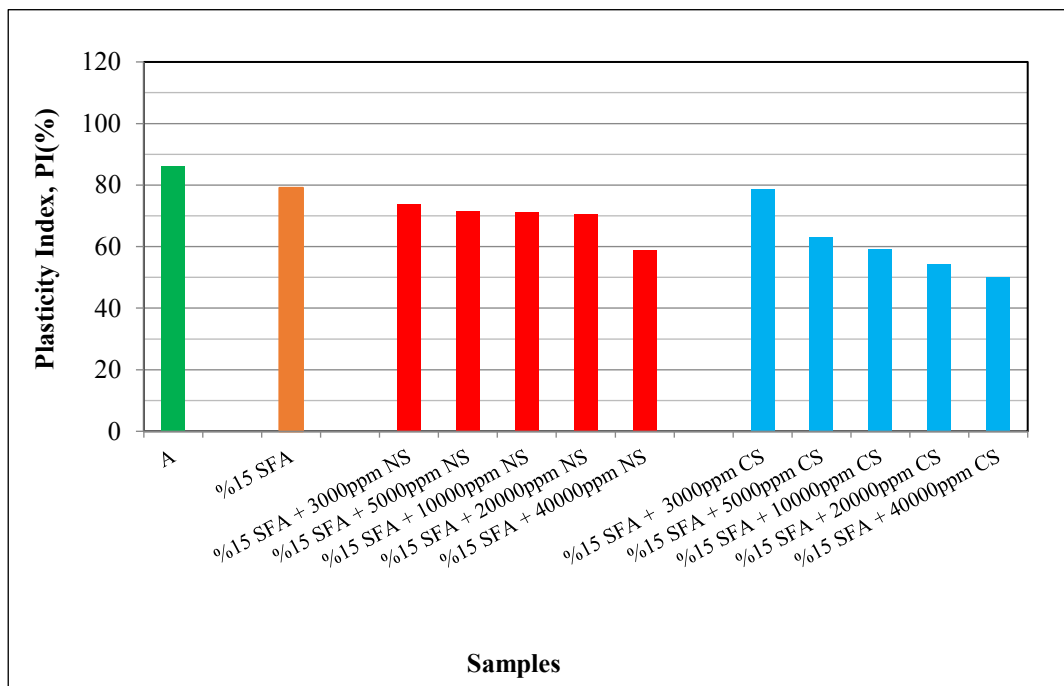


Figure 5.12. PI of NS and CS added 15% SFA treated samples

### 5.2.2.3. 10% KFA and sulfate added samples

LL, PL and PI test results for 10% KFA treated sample and 3000ppm, 5000ppm, 10000ppm, 20000ppm and 40000ppm NS and CS added 10% KFA treated sample are presented in Figure 5.13, 5.14 and 5.15 respectively. Test results for Sample A are also presented in the same graphs for comparison purposes.

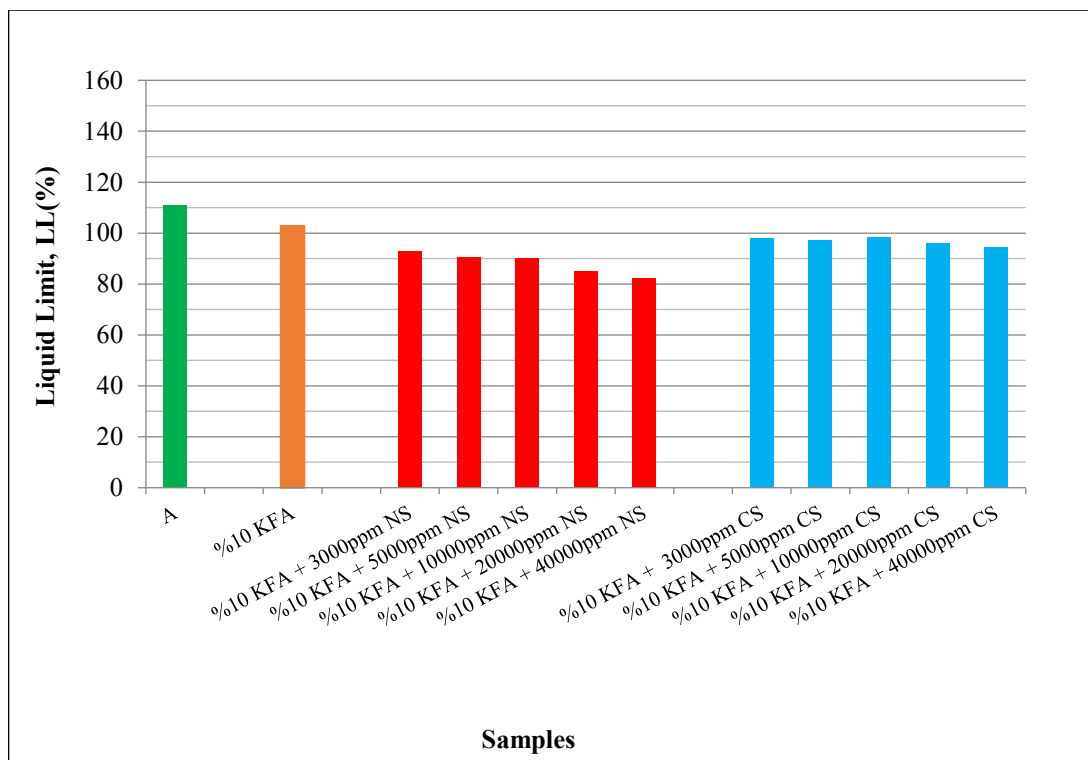


Figure 5.13. LL of NS and CS added 10% KFA treated samples

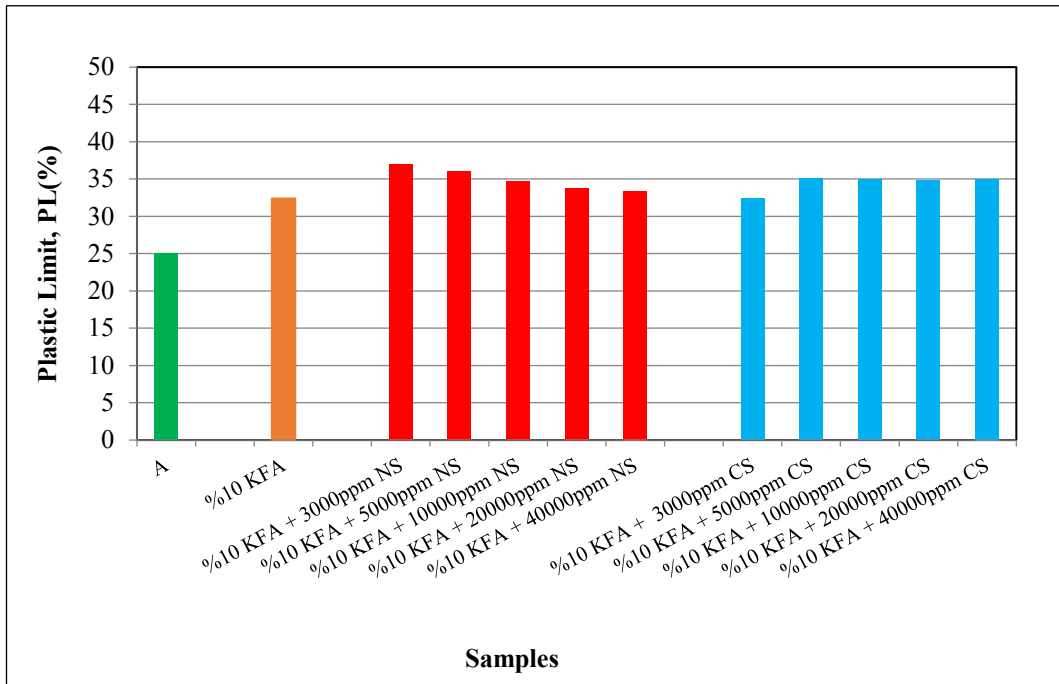


Figure 5.14. PL of NS and CS added 10% KFA treated samples

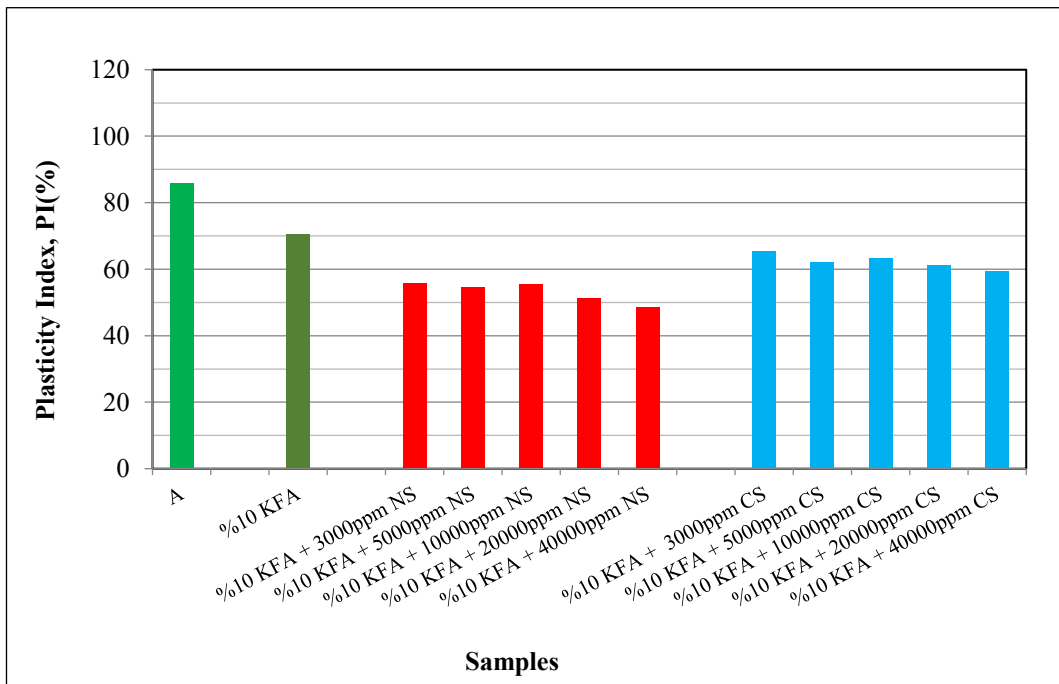


Figure 5.15. PI of NS and CS added 10% KFA treated samples

### 5.2.3. Shrinkage Limit

SL values were determined according to ASTM D427. Tests were performed on Sample A, 4% L, 15% SFA, 10% KFA treated samples and sulfate added chemically treated samples. 3000ppm, 5000ppm, 10000ppm, 20000ppm and 40000ppm NS and CS were added to fly ash treated samples whereas 5000ppm, 10000ppm and 40000ppm sulfate concentrations were used for 4% L treated sample. Test results for 4% L, 15% SFA and 10% KFA treated soils are presented in Figure 5.16, 5.17 and 5.18 respectively. Test result for Sample A is also presented in the same graphs for comparison purposes.

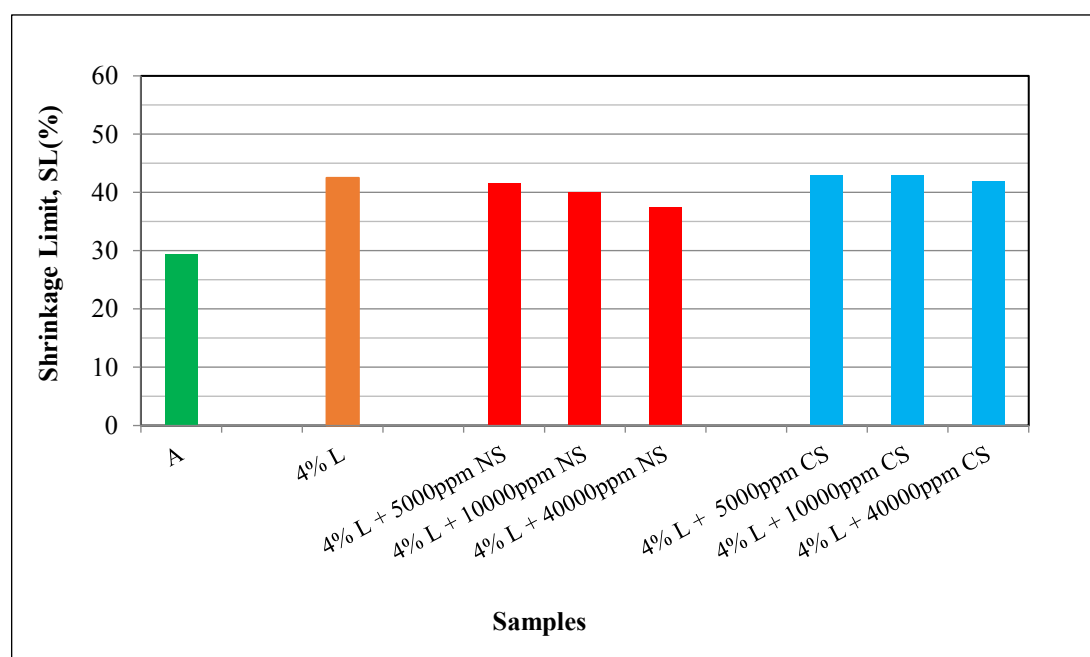


Figure 5.16. SL of NS and CS added 4% L treated samples

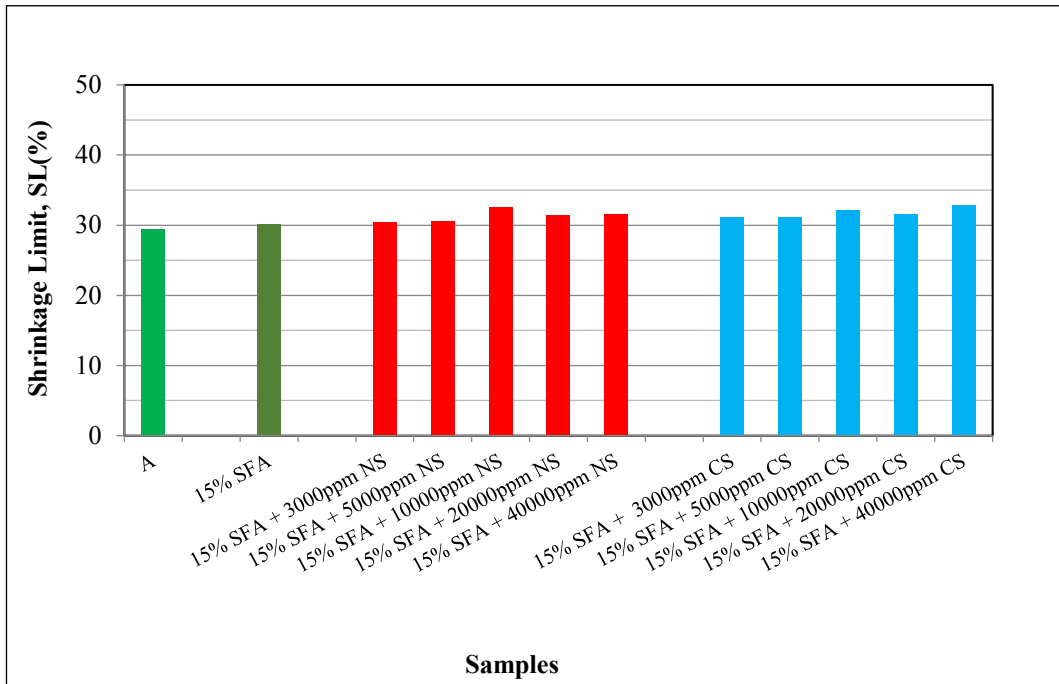


Figure 5.17. SL of NS and CS added 15% SFA treated samples

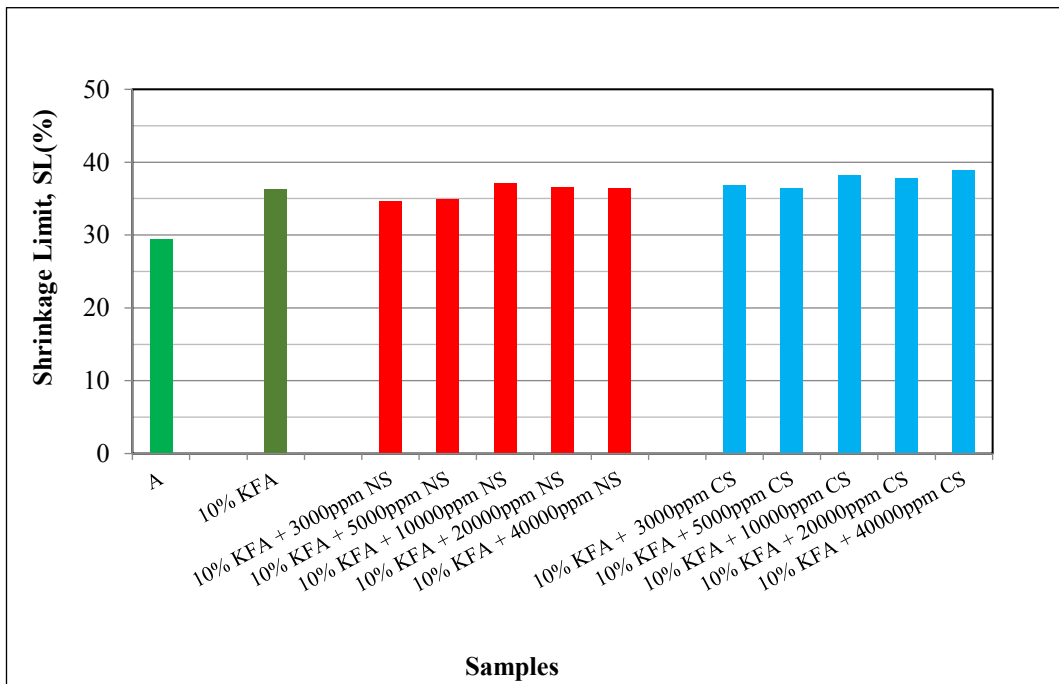


Figure 5.18. SL of NS and CS added 10% KFA treated samples

### 5.2.4. Grain Size Distribution

Grain size distribution of the samples were determined by using the test method recommended in ASTM D422. Grain size distribution curves are presented in Figures 5.19 and 5.20 for 4% L, Figures 5.21 and 5.22 for 15% SFA and Figures 5.23 and 5.24 for 10% KFA treated samples.

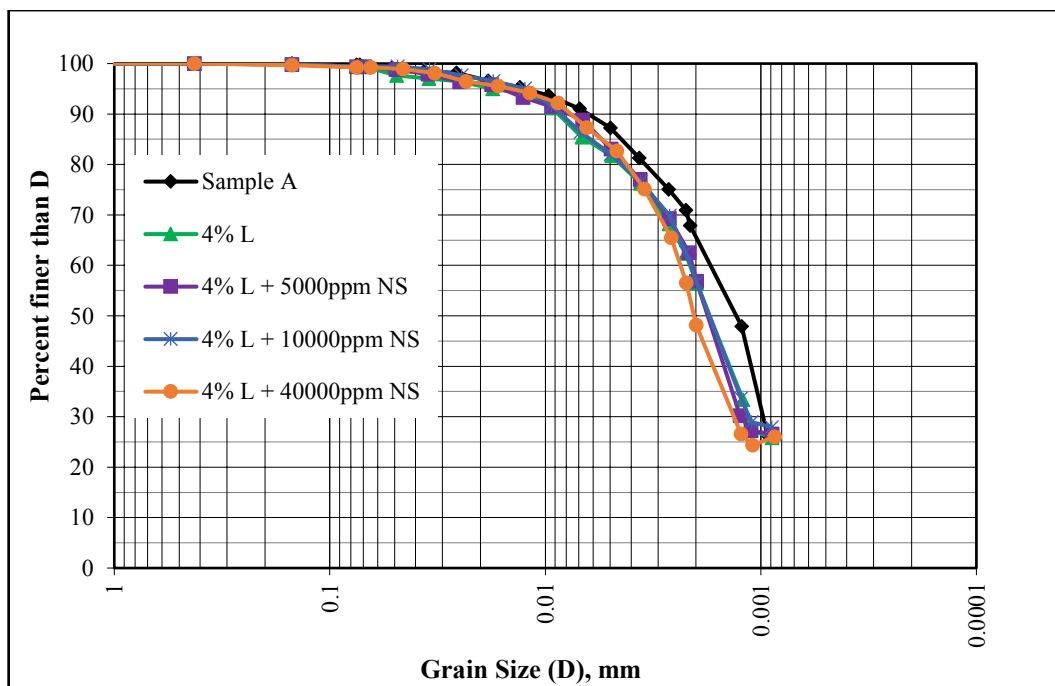


Figure 5.19. Grain size distribution of NS added 4% L treated samples

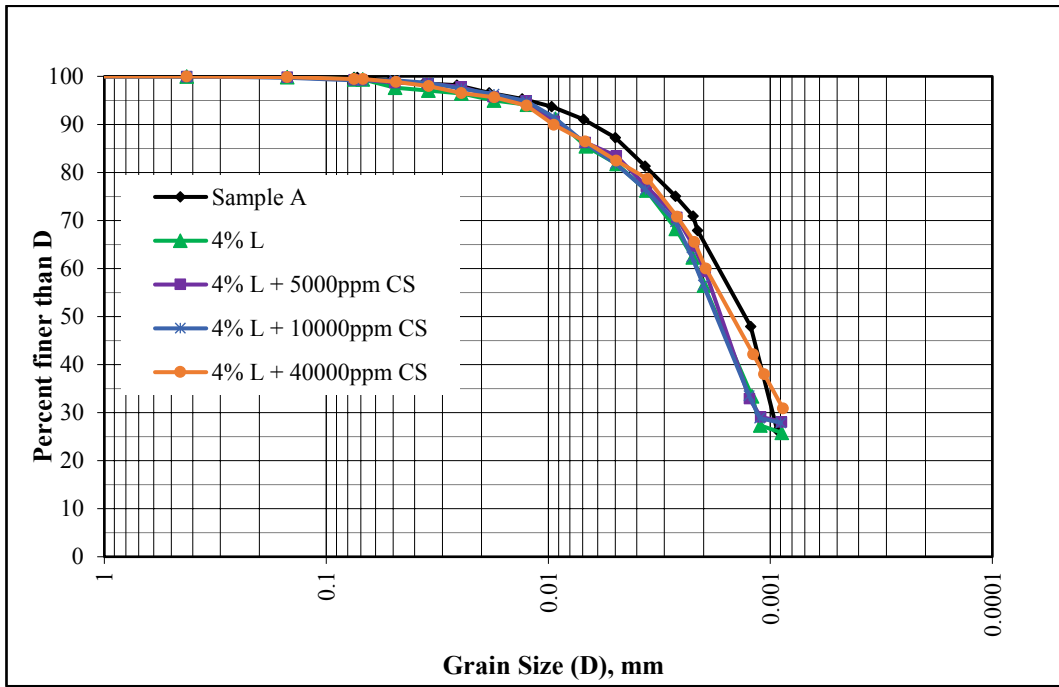


Figure 5.20. Grain size distribution of CS added 4% L treated samples

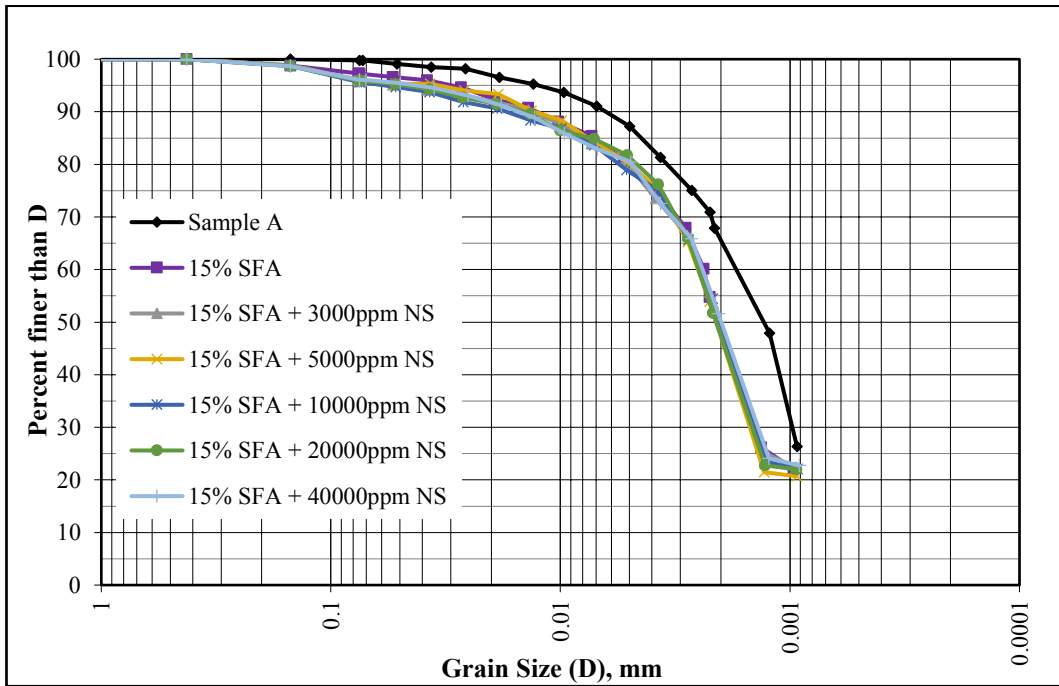


Figure 5.21. Grain size distribution of NS added 15% SFA treated samples

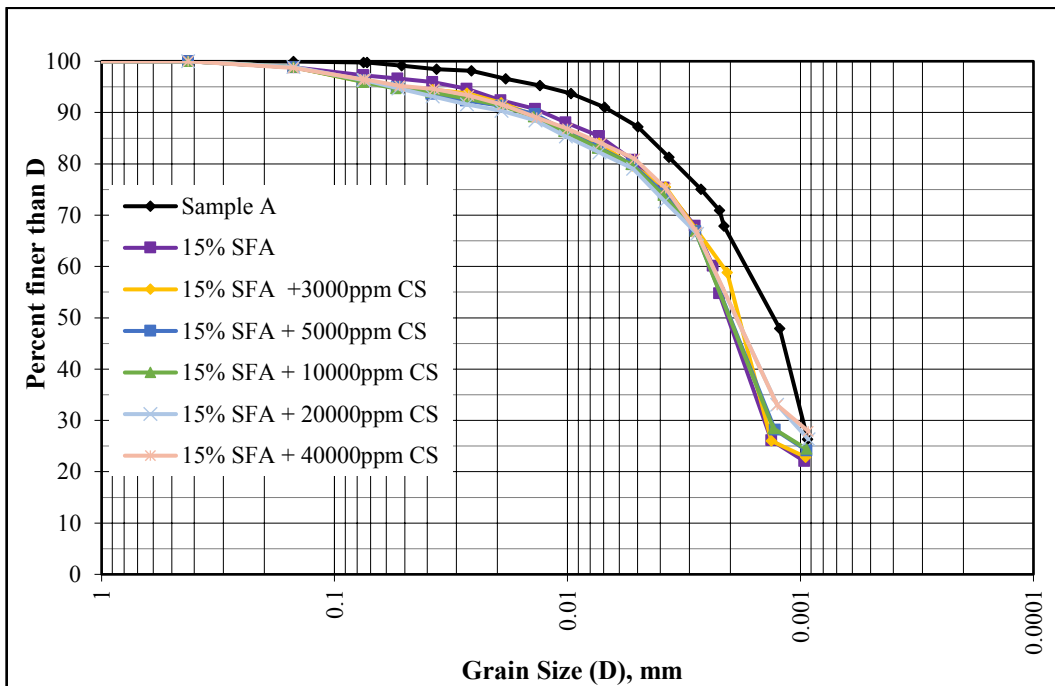


Figure 5.22. Grain size distribution of CS added 15% SFA treated samples

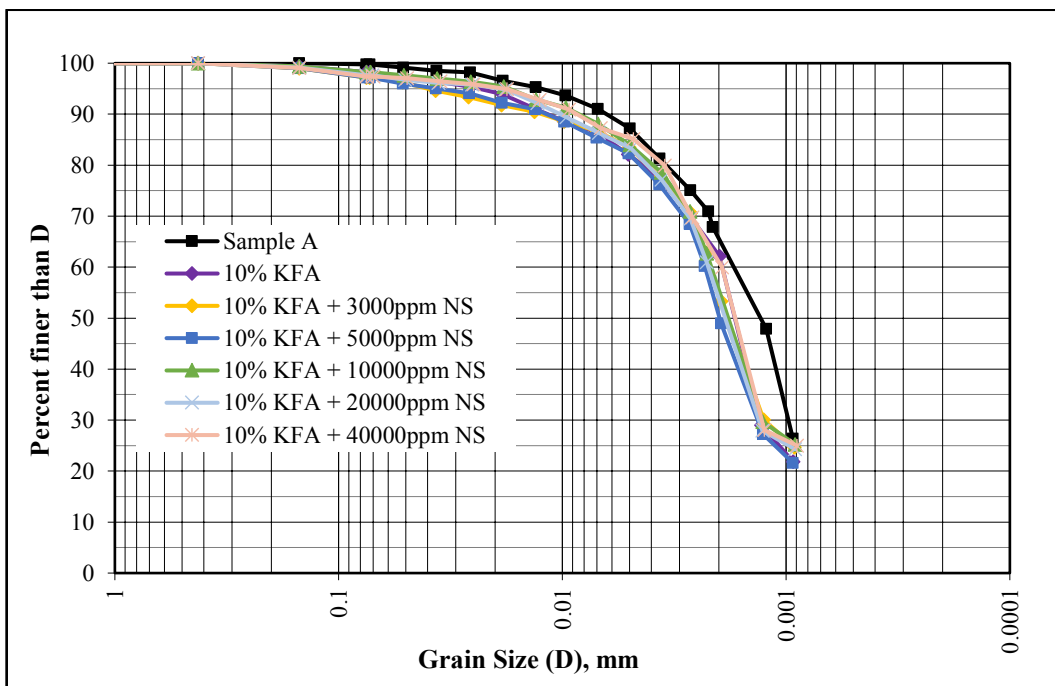


Figure 5.23. Grain size distribution of NS added 10% KFA treated samples

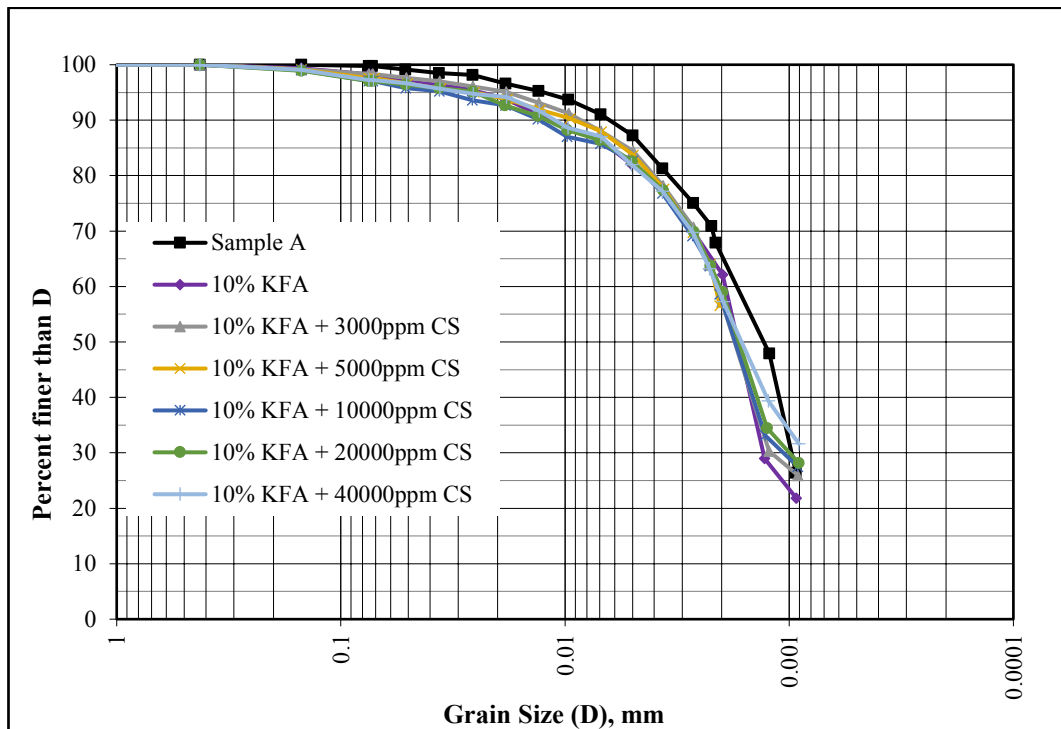


Figure 5.24. Grain size distribution of CS added 10% KFA treated samples

Also, hydrometer tests were tried to be performed on fly ashes. However, as class C fly ashes have self-pozzolanic properties, they started to harden when reacted with water and settle rapidly. Therefore, the obtained results did not present the actual grain size distribution of samples. Fast settling problem was also observed for lime. The hydrometer test photos for KFA is presented in Figure 5.25.



*Figure 5.25.* Hydrometer test for KFA

### **5.2.5. Soil Classification**

The samples were also classified according to the Unified Soil Classification System (USCS) by using the plasticity chart, LL and PI values. The LL and PI of the samples are entered to the plasticity chart. The results are presented in Figure 5.26, 5.27 and 5.28 for 4% L, 15% SFA and 10% KFA treated samples respectively with the values of Sample A.

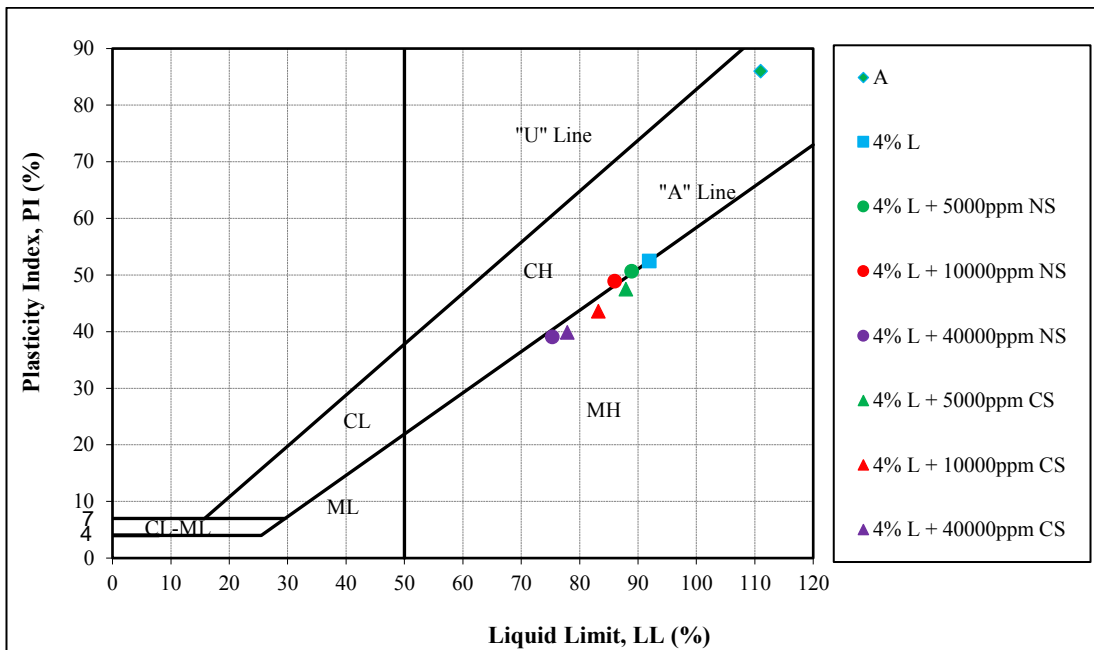


Figure 5.26. Plasticity chart for 4% L treated samples

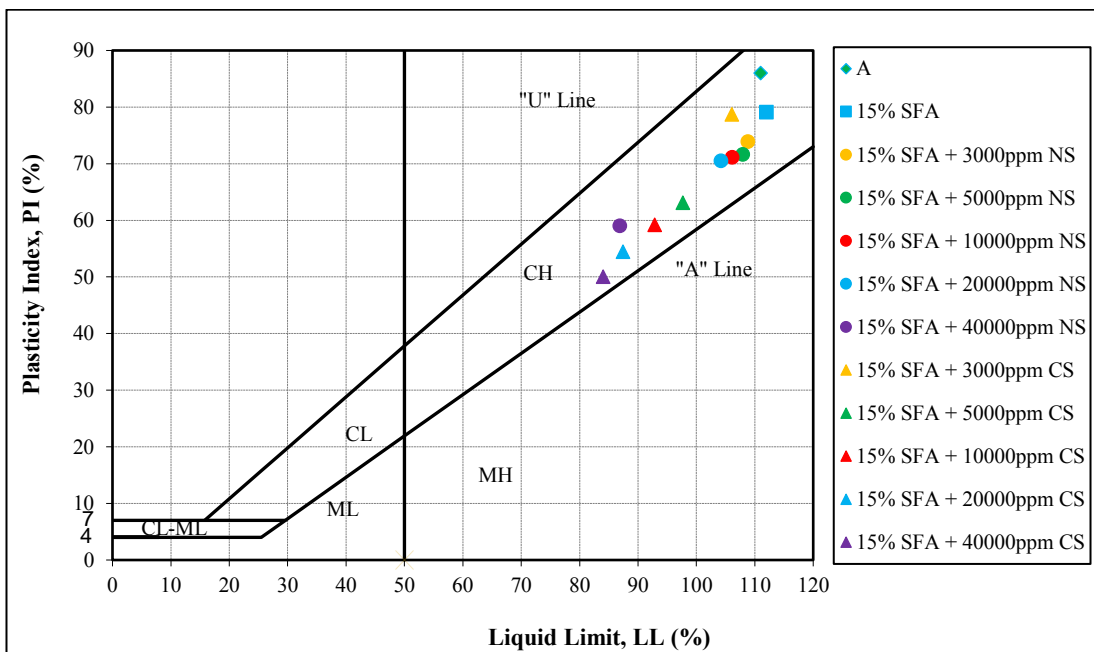


Figure 5.27. Plasticity chart for 15% SFA treated samples

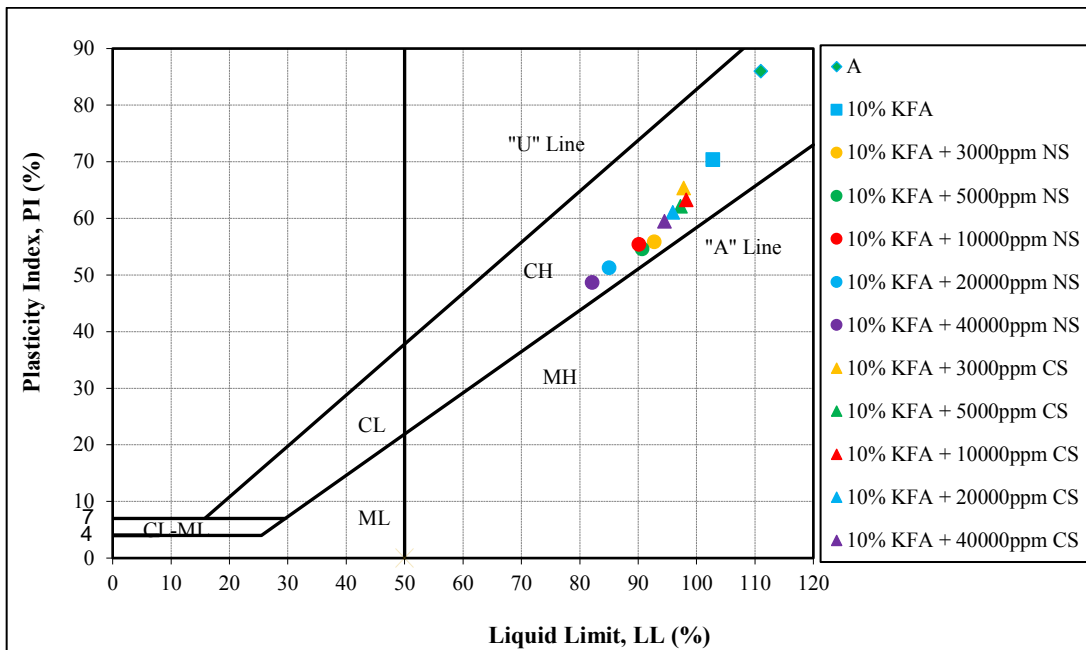


Figure 5.28. Plasticity chart for 10% KFA treated samples

The 4% L treated sample was classified as CH according to USCS and after the addition of 40000ppm NS, 5000ppm CS, 10000ppm CS, and 40000ppm CS, the soil class changed to MH. The soil class remained as CH for the remaining concentrations of NS. Sulfate addition did not affect the soil classification of fly ash treated samples. Although they generally became closer to A-line, they were all classified as CH.

The results are presented in Table 5.1 with clay content, silt content, LL and PI values.

Table 5.1. Classification of samples according to USCS

Sample	Clay (%)	Silt (%)	LL (%)	PI (%)	USCS
A	65.63	34.13	111.0	86.0	CH
4% L	56.77	42.63	91.9	52.5	CH
4% L + 5000ppm NS	57.25	42.12	88.9	50.7	CH
4% L + 10000ppm NS	57.05	42.38	86.0	48.9	CH
4% L + 40000ppm NS	54.89	44.33	75.3	39.1	MH
4% L + 5000ppm CS	60.17	39.14	87.9	47.5	MH
4% L + 10000ppm CS	56.48	42.72	83.2	43.6	MH
4% L + 40000ppm CS	61.05	38.39	77.9	39.9	MH
15% SFA	48.58	48.7	112.0	79.1	CH
15% SFA + 3000ppm NS	48.65	47.42	108.8	73.9	CH
15% SFA + 5000ppm NS	47.32	48.62	107.9	71.6	CH
15% SFA + 10000ppm NS	49.70	45.98	106.1	71.1	CH
15% SFA + 20000ppm NS	47.41	48.46	104.2	70.5	CH
15% SFA + 40000ppm NS	50.30	45.76	86.9	59.0	CH
15% SFA + 3000ppm CS	51.06	44.95	106.1	78.7	CH
15% SFA + 5000ppm CS	49.90	46.34	97.7	63.1	CH
15% SFA + 10000ppm CS	49.65	46.32	92.9	59.2	CH
15% SFA + 20000ppm CS	52.50	43.8	87.5	54.5	CH
15% SFA + 40000ppm CS	52.58	43.88	84.0	50.0	CH
10% KFA	58.30	39.94	102.8	70.4	CH
10% KFA + 3000ppm NS	54.84	42.33	92.8	55.9	CH
10% KFA + 5000ppm NS	50.62	46.59	90.7	54.7	CH
10% KFA + 10000ppm NS	55.56	42.7	90.1	55.4	CH
10% KFA + 20000ppm NS	53.80	43.84	85.0	51.3	CH
10% KFA + 40000ppm NS	61.03	36.34	82.1	48.7	CH
10% KFA + 3000ppm CS	57.37	40.93	97.8	65.4	CH
10% KFA + 5000ppm CS	55.54	42.03	97.3	62.2	CH
10% KFA + 10000ppm CS	57.51	39.56	98.2	63.3	CH
10% KFA + 20000ppm CS	59.35	37.7	95.9	61.1	CH
10% KFA + 40000ppm CS	57.89	39.35	94.5	59.5	CH

### 5.3. Swell Tests

Swelling tests were performed on NS and CS added 15% SFA and 10% KFA treated specimens. Initially tests were performed at 25°C and 3000ppm, 5000ppm, 10000ppm, 20000ppm and 40000ppm sulfate concentrations were used. Then to see the effect of temperature, the swelling tests were performed at 10°C and 40°C. This time only 5000ppm, 10000ppm and 40000ppm sulfate concentrations were used as representative concentrations. To see the curing effect, swelling tests were performed on specimens that were cured at 25°C for 7 and 28 days.

Swelling tests at 25°C were also performed for 5000ppm, 10000ppm, and 40000ppm sulfate added 4% L treated specimens for comparison purposes.

#### 5.3.1. Swell Tests at 25°C

Swelling test results for 4% L, 15% SFA and 10% KFA treated specimens with different NS and CS concentrations are presented in Figure 5.29, 5.30, and 5.31 respectively.

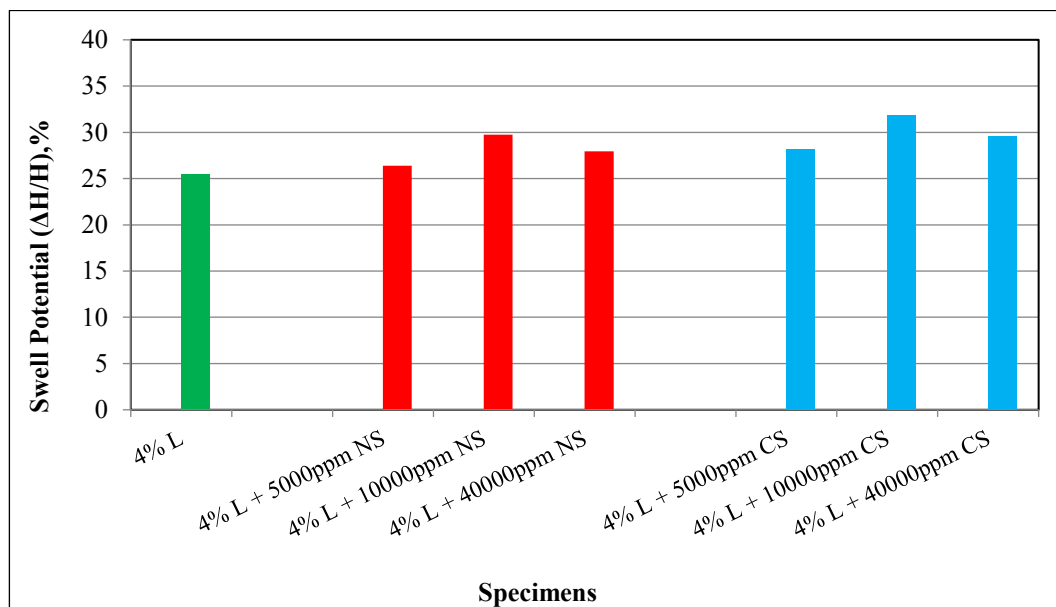


Figure 5.29. Swell percent for sulfate added 4% L treated specimens

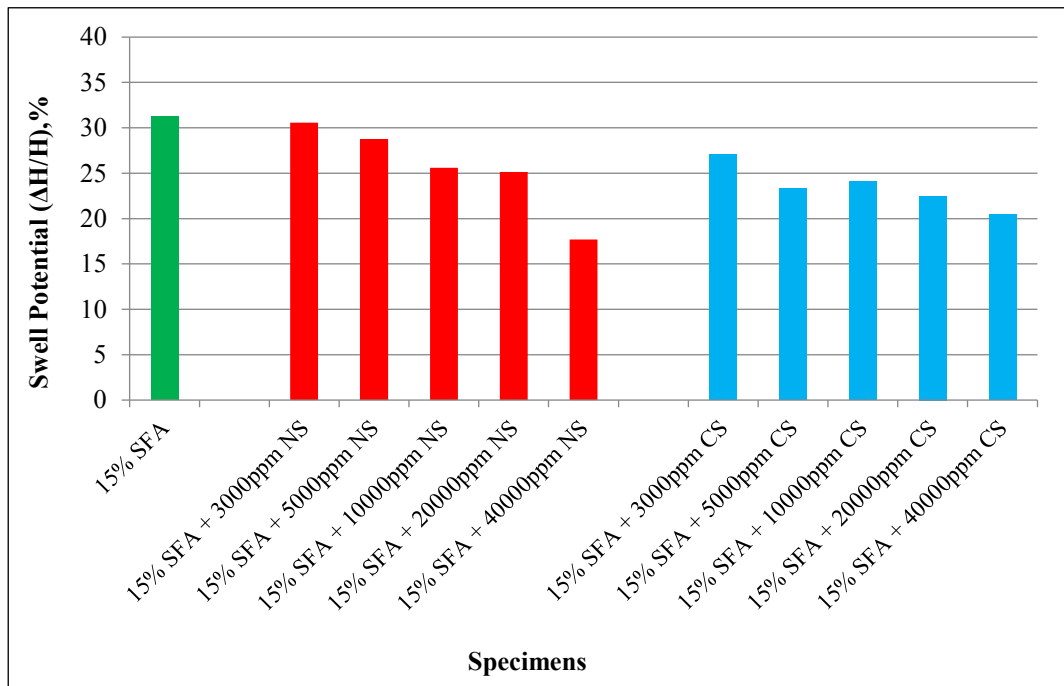


Figure 5.30. Swell percent for sulfate added 15% SFA treated specimens

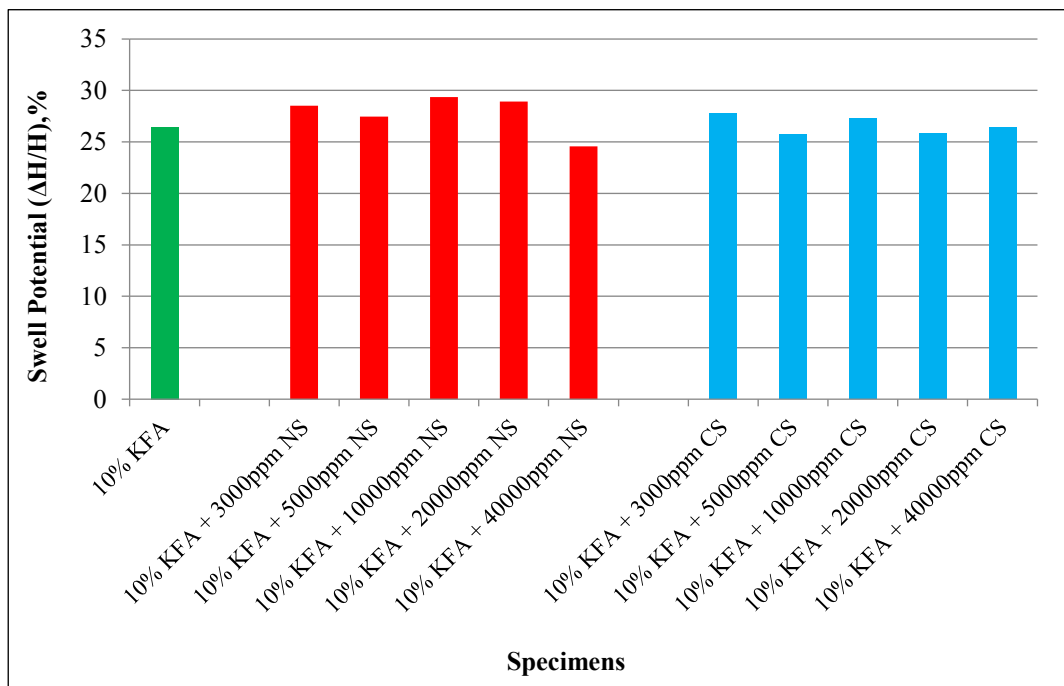


Figure 5.31. Swell percent for sulfate added 10% KFA treated specimens

Readings were taken for 100 days to see the long-term behavior for 40000ppm NS and CS added 15% SFA and 10% KFA added specimens. The swell vs. time graph is presented in Figure 5.32.

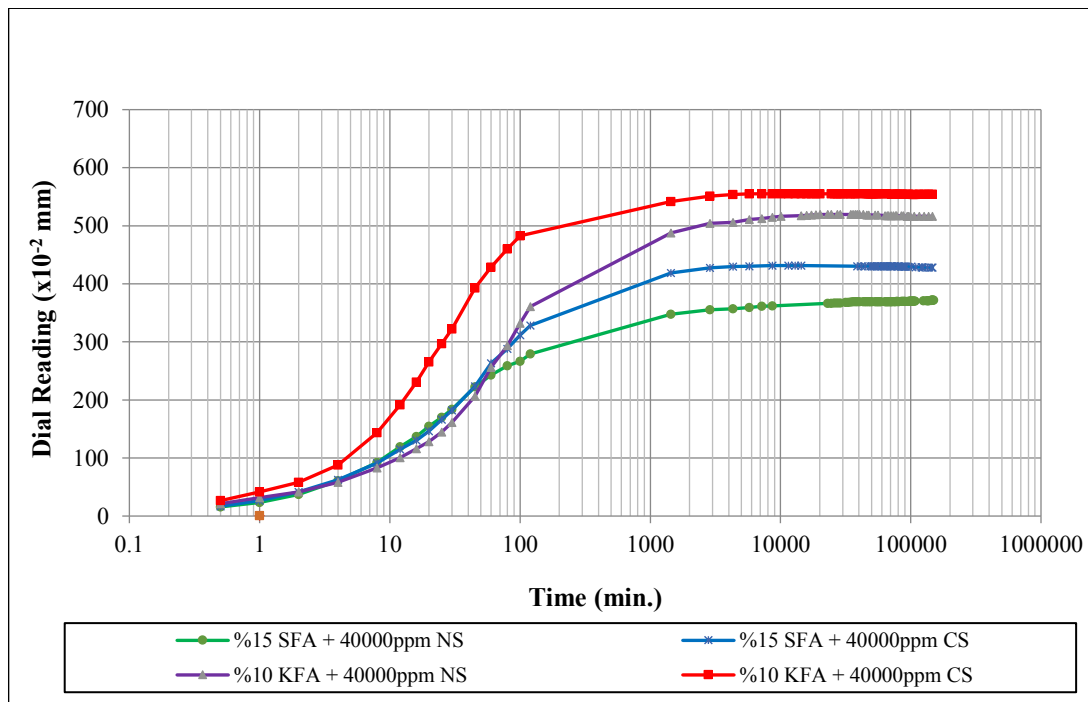


Figure 5.32. Swell vs. time graph for 40000ppm NS and CS added 15% SFA and 10% KFA treated specimens

### 5.3.2. Swell Tests at 10°C and 40°C

Swelling tests were also performed at 10°C and 40°C to see the effect of temperature on swell properties. 5000ppm, 10000ppm and 40000ppm sulfate concentrations were chosen as the representative concentrations and tests were performed on these specimens.

Test results for 10°C, 25°C and 40°C are drawn together to see the effect of temperature on swell potential. Test results for 15% SFA and 10% KFA treated specimens are presented in Figures 5.33- 5.36.

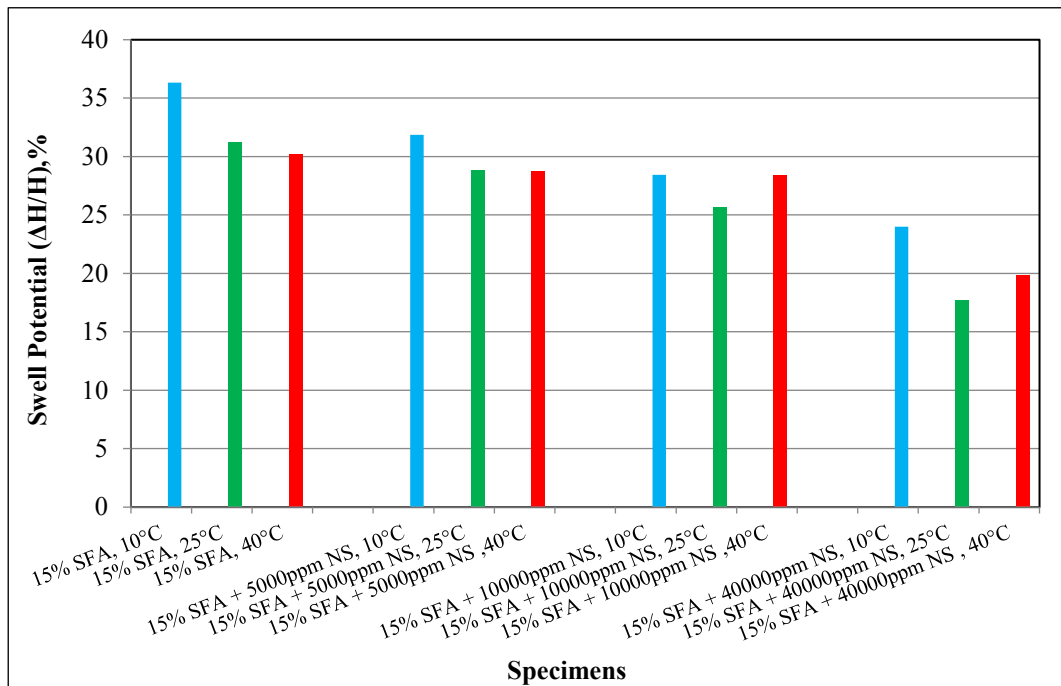


Figure 5.33. Swell percent for NS added 15% SFA treated specimens at 10, 25 and 40°C

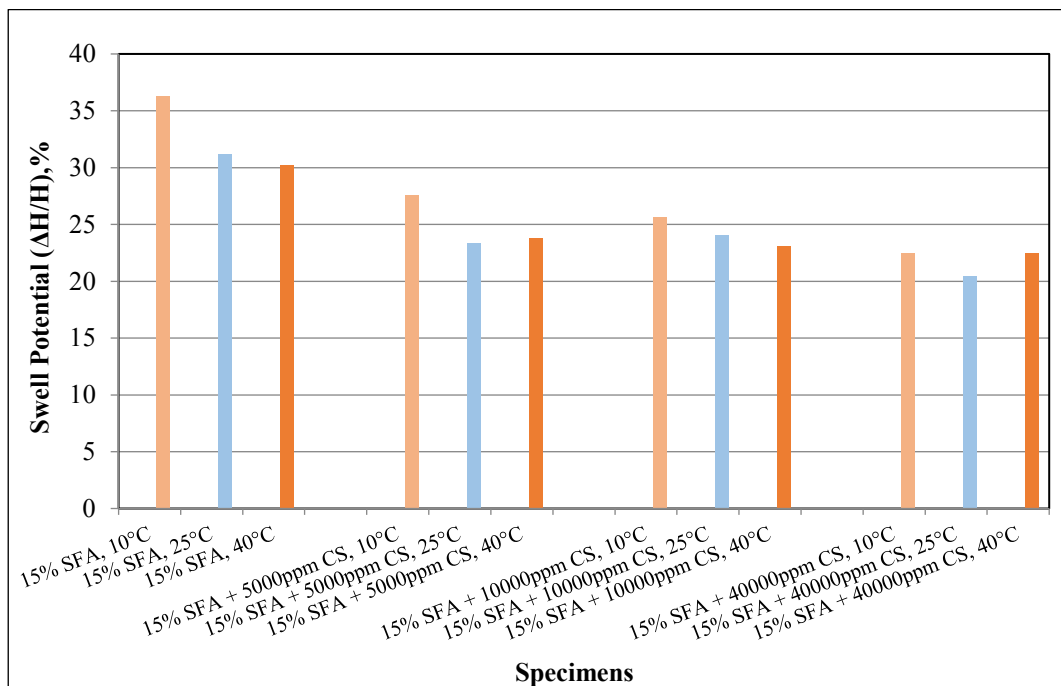


Figure 5.34. Swell percent for CS added 15% SFA treated specimens at 10, 25 and 40°C

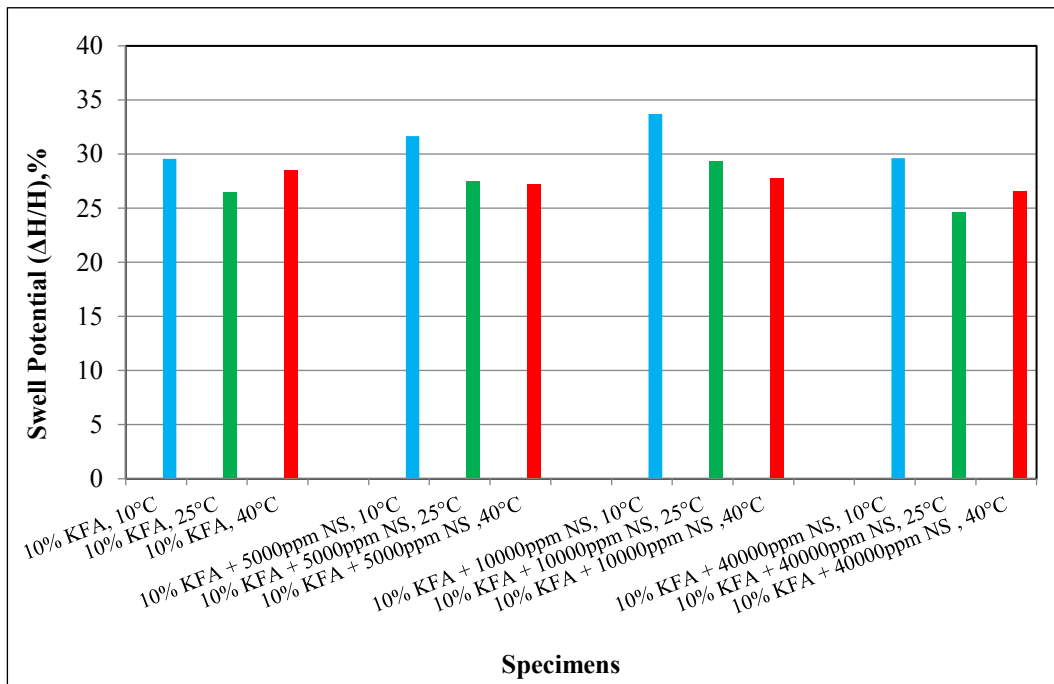


Figure 5.35. Swell percent for NS added 10% KFA treated specimens at 10, 25 and 40°C

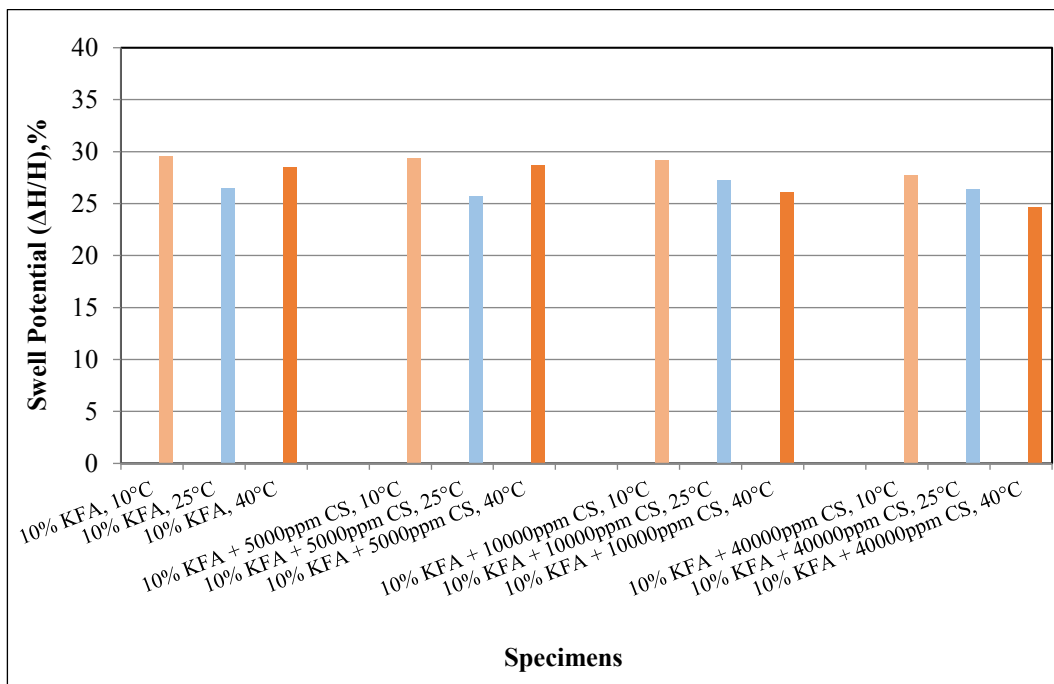


Figure 5.36. Swell percent for CS added 10% KFA treated specimens at 10, 25 and 40°C

### 5.3.3. Swell Tests at 7 days and 28 days Cured Specimens

Swelling tests were also performed at 7 days and 28 days cured specimens to see the effect of curing. Curing temperature was selected as 25°C. 5000ppm, 10000ppm and 40000ppm sulfate concentrations were chosen as the representative concentrations and tests were performed on these specimens.

Test results for uncured, 7 days and 28 days cured specimens are drawn together to see the effect of curing on swell potential. Test results for 15% SFA and 10% KFA treated specimens are presented in Figures 5.37- 5.40.

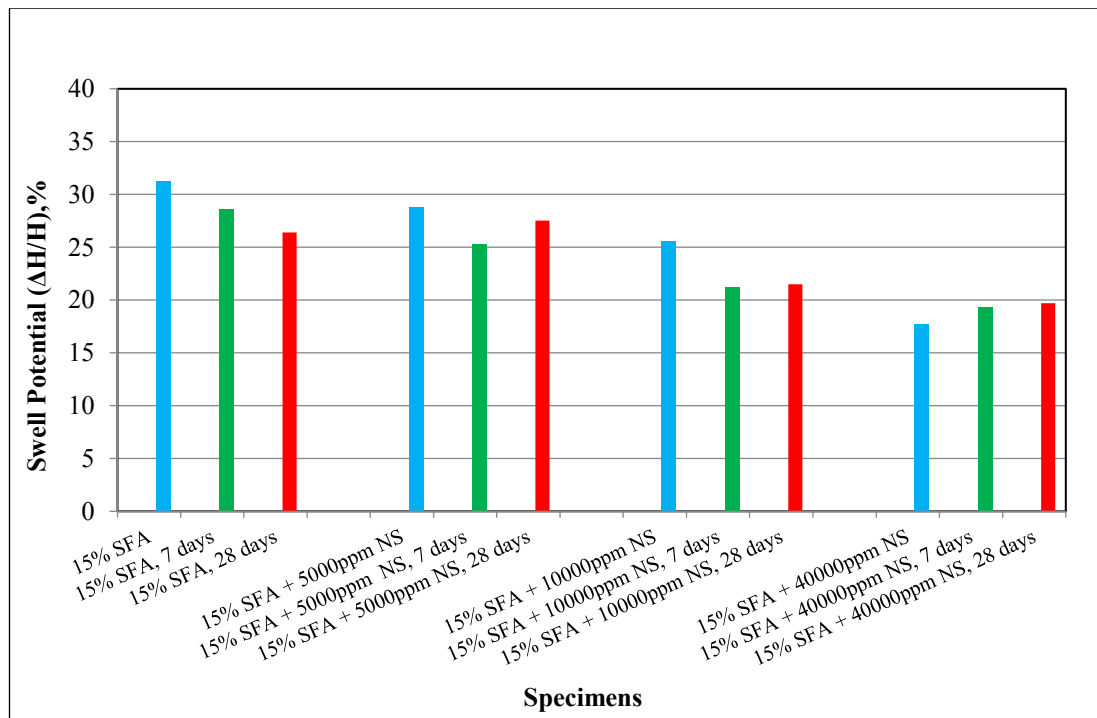


Figure 5.37. Swell percent for NS added 15% SFA treated specimens cured 7 and 28 days at 25°C

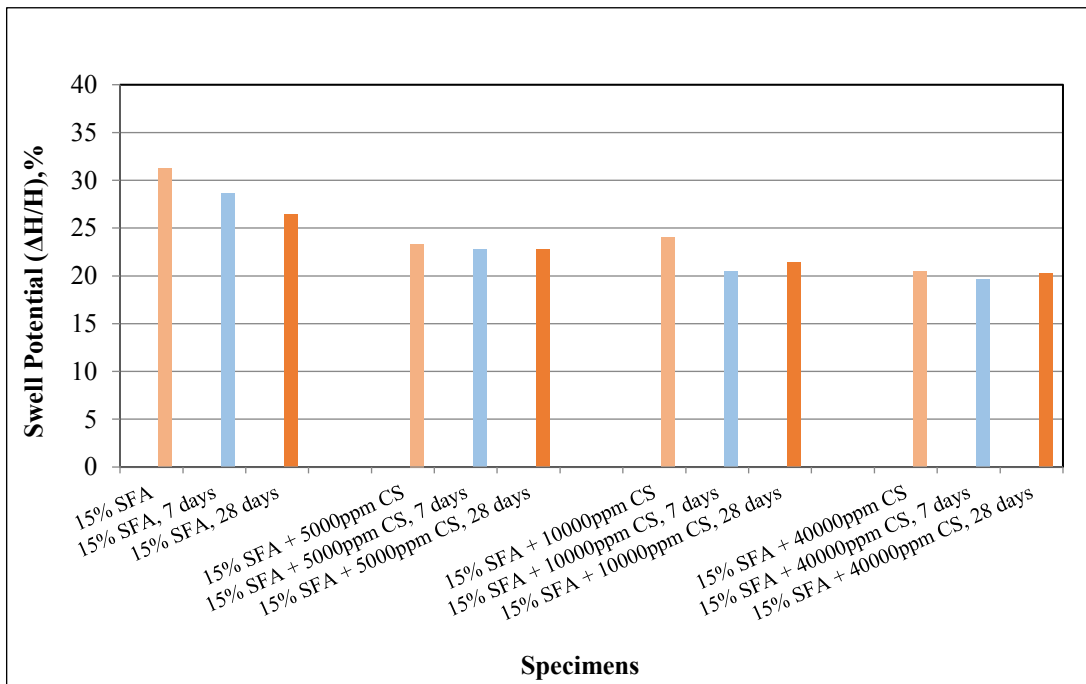


Figure 5.38. Swell percent for CS added 15% SFA treated specimens cured 7 and 28 days at 25°C

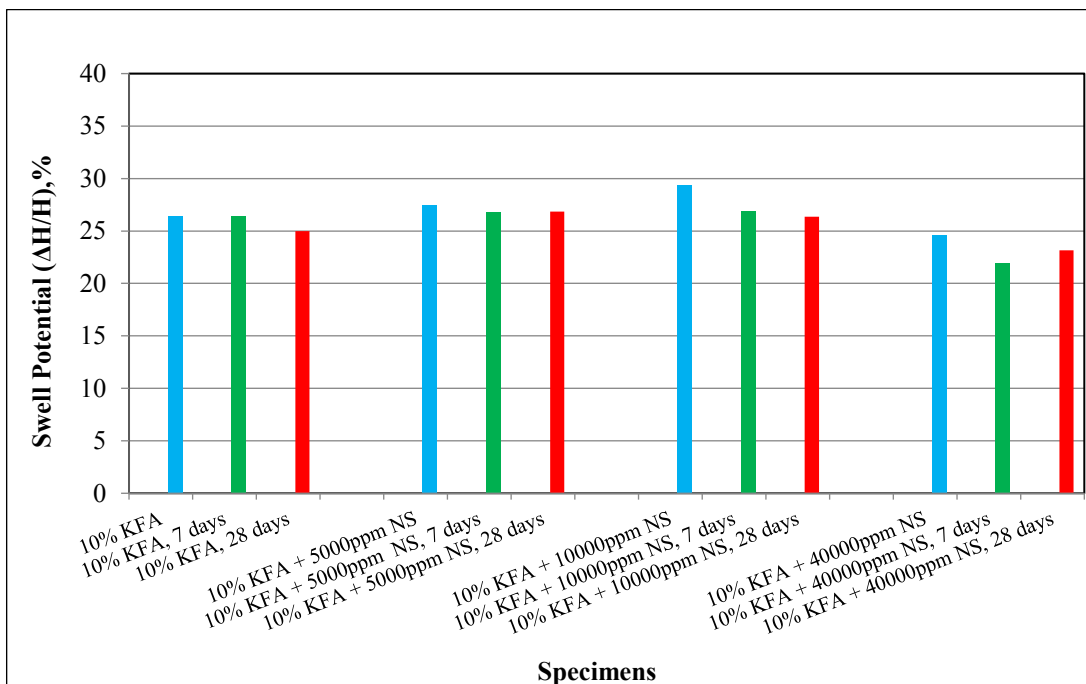


Figure 5.39. Swell percent for NS added 10% KFA treated specimens cured 7 and 28 days at 25°C

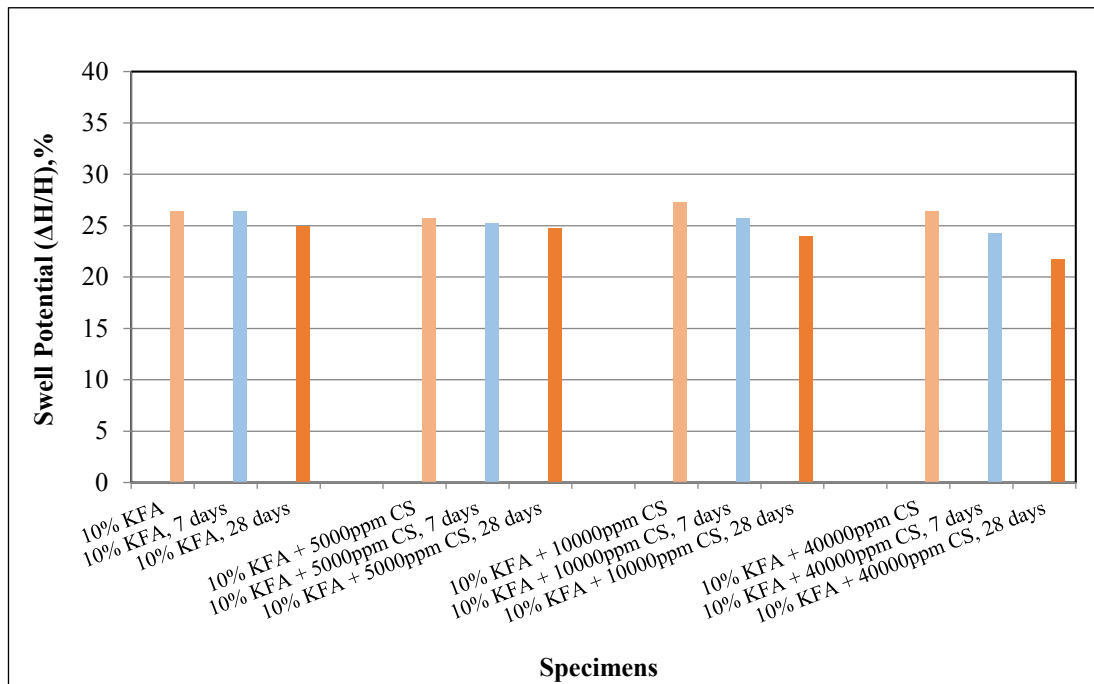


Figure 5.40. Swell percent for CS added 10% KFA treated specimens cured 7 and 28 days at 25°C

Swell vs. time graphs for all specimens are presented in Appendix C.

#### 5.4. UCS Tests

Similar to swelling tests, UCS tests were initially performed at 25°C without curing and 3000ppm, 5000ppm, 10000ppm, 20000ppm and 40000ppm sulfate concentrations were used for both type of sulfates. Then the tests were performed on 7 days and 28 days cured specimens at 10°C, 25°C and 40°C.

UCS tests were also performed on 4% L treated specimens and 5000ppm, 10000ppm and 40000ppm NS and CS added specimens for comparison purposes. These tests were performed on uncured specimens.

##### 5.4.1. UCS Tests at 25°C

UCS test results for 4% L, 15% SFA and 10% KFA treated specimens with different NS and CS concentrations are presented in Figure 5.41, 5.42, and 5.43 respectively.

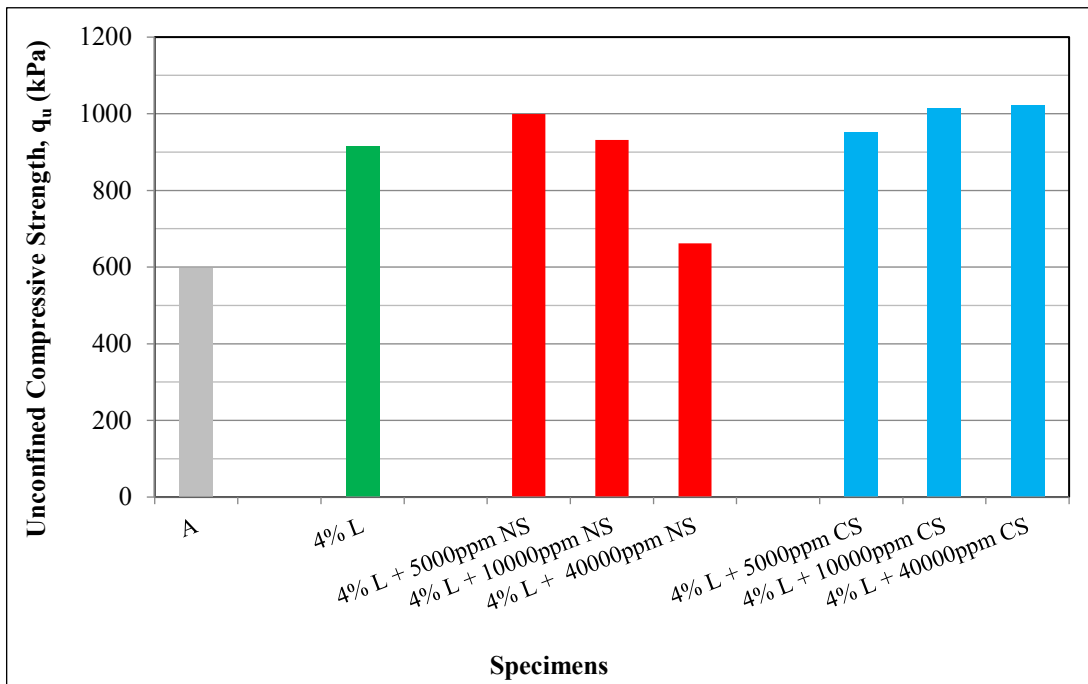


Figure 5.41. UCS of sulfate added 4% L treated specimens

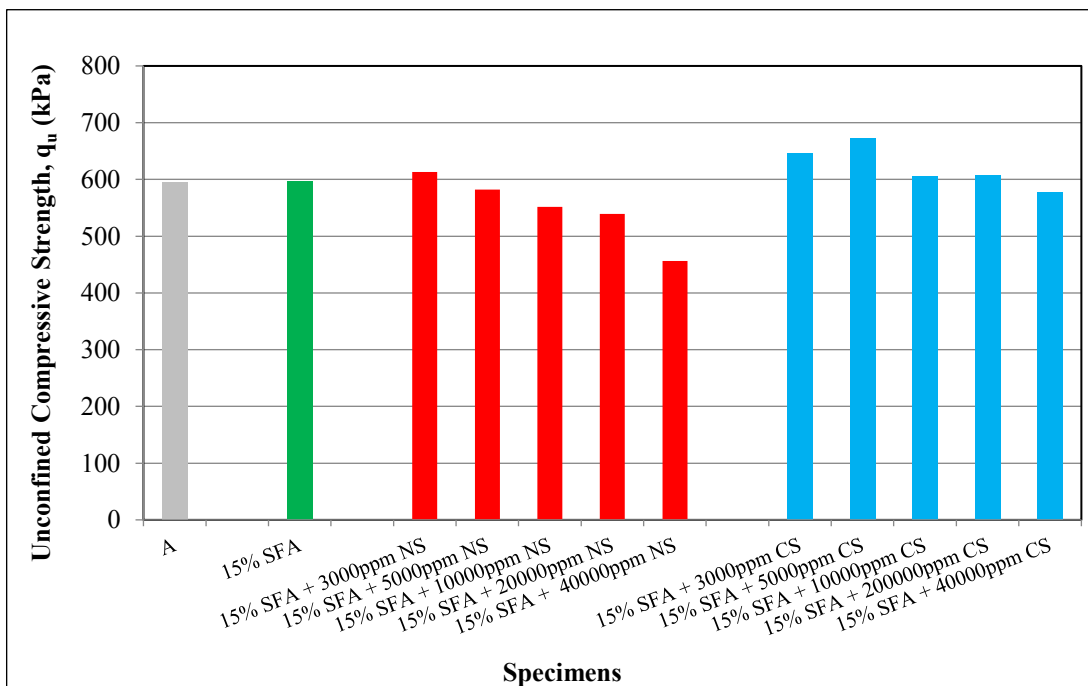


Figure 5.42. UCS of sulfate added 15% SFA treated specimens

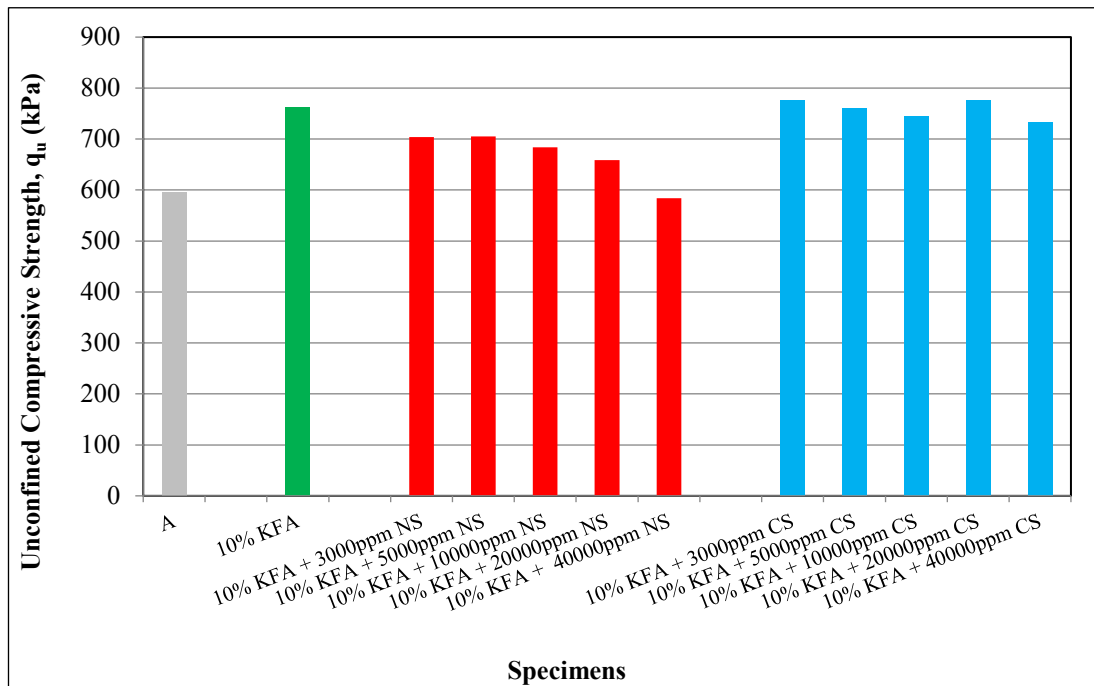


Figure 5.43. UCS of sulfate added 10% KFA treated specimens

#### 5.4.2. UCS Tests for 7 days and 28 days cured specimens at 10, 25 and 40°C

UCS tests were also performed on 7 days and 28 days cured specimens. Specimens were cured at 10°C, 25°C and 40°C to see the effect of temperature besides curing period on UCS. 5000ppm, 10000ppm and 40000ppm sulfate concentrations were chosen as the representative concentrations and tests were performed on these specimens. Test results are presented with the uncured condition to see the effect of curing.

##### 5.4.2.1. 15% SFA treated specimens

UCS test results for 7 days cured NS and CS added 15% SFA treated specimens are presented in Figure 5.44 and 5.45 respectively. Also test results for 28 days cured specimens are presented in Figure 5.46 and 5.47.

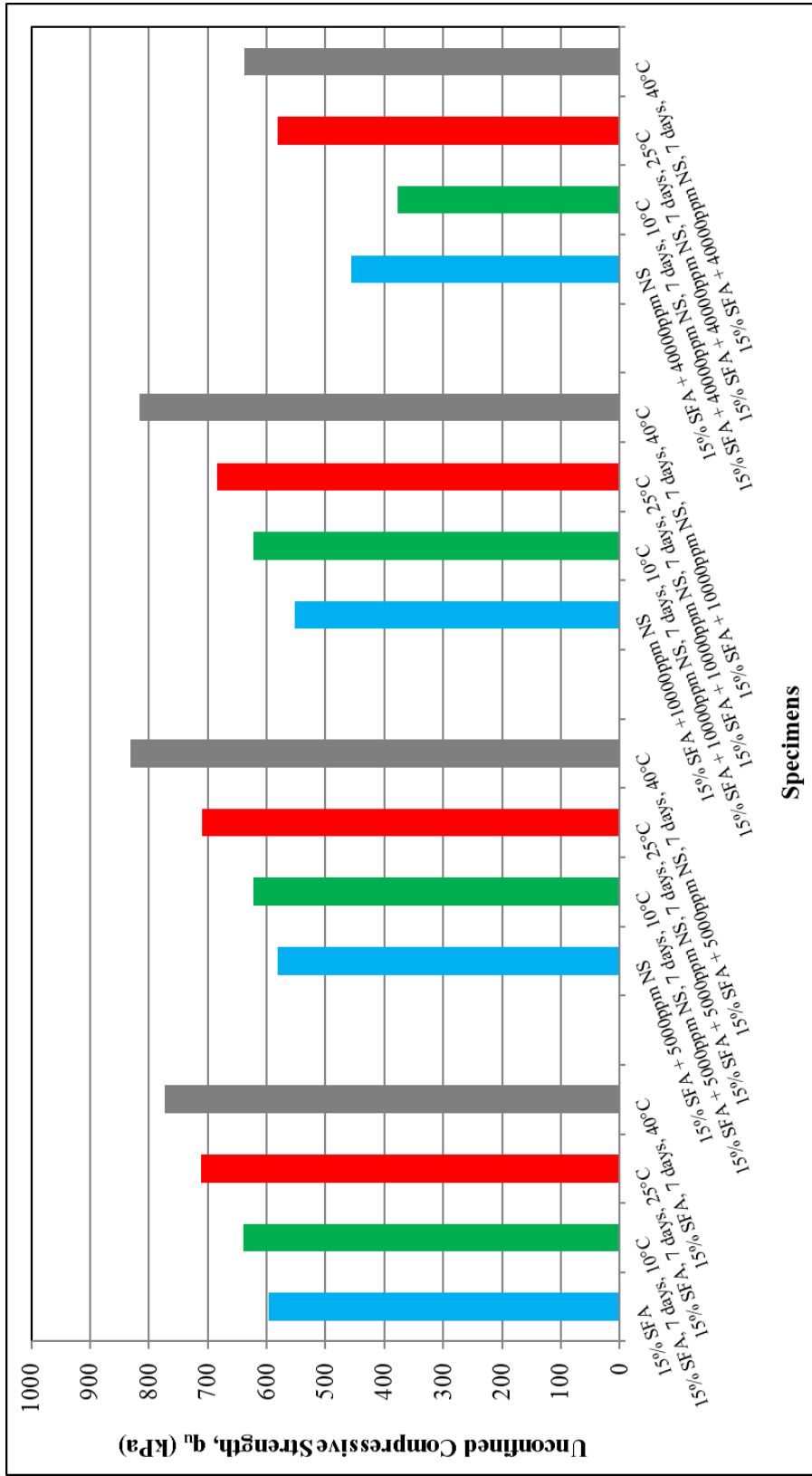


Figure 5.44. Swell percent of NS added 15% SFA treated specimens cured 7 days at 10, 25 and 40°C

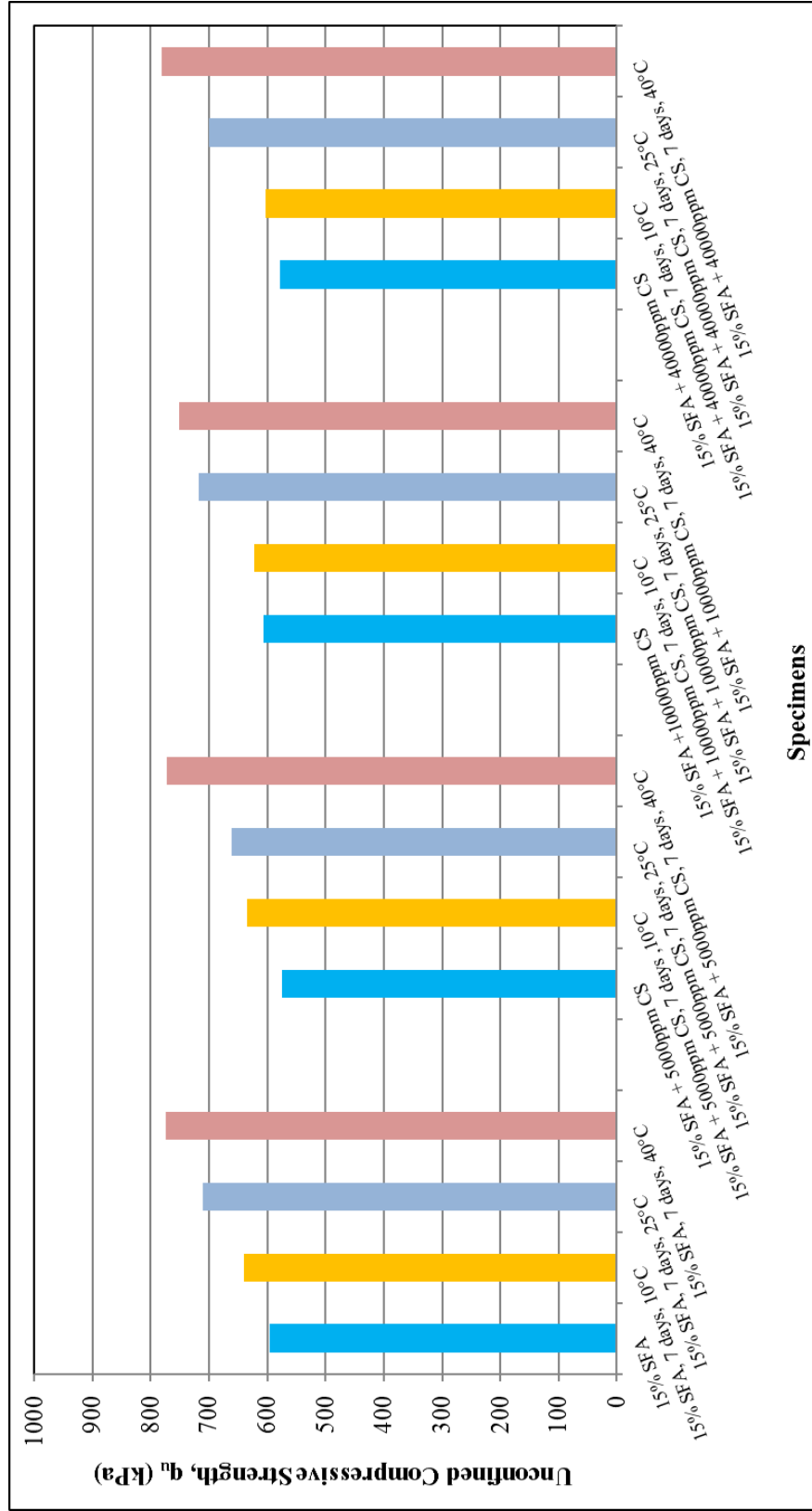


Figure 5.45. Swell percent of CS added 15% SFA treated specimens cured 7 days at 10, 25 and 40°C

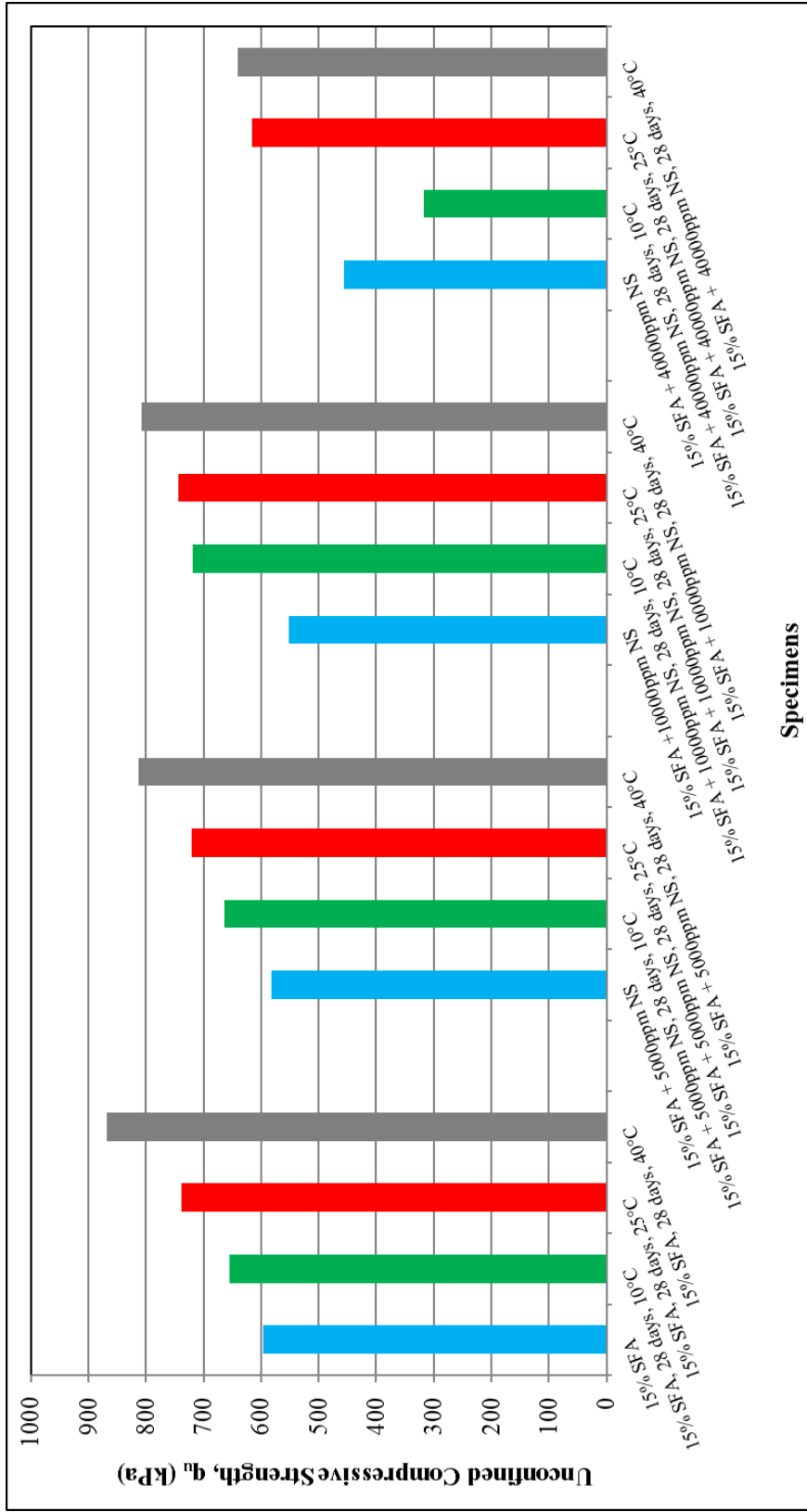


Figure 5.46. Swell percent of NS added 15% SFA treated specimens cured 28 days at 10, 25 and 40°C

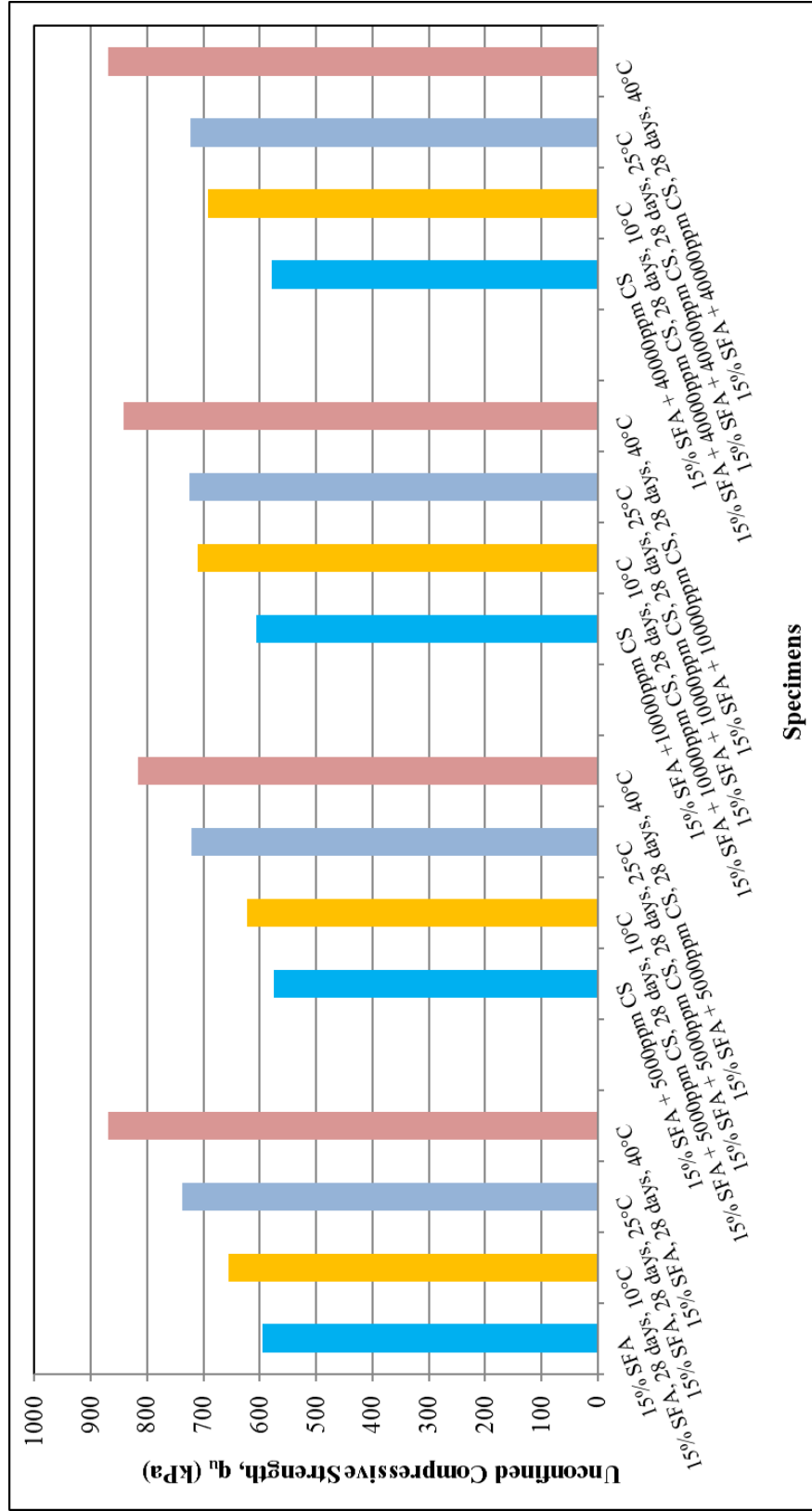


Figure 5.47. Swell percent of CS added 15% SFA treated specimens cured 28 days at 10, 25 and 40°C

#### **5.4.2.2. 10% KFA treated specimens**

UCS test results for 7 days cured NS and CS added 10% KFA treated specimens are presented in Figure 5.48 and 5.49 respectively. Also test results for 28 days cured specimens are presented in Figure 5.50 and 5.51.

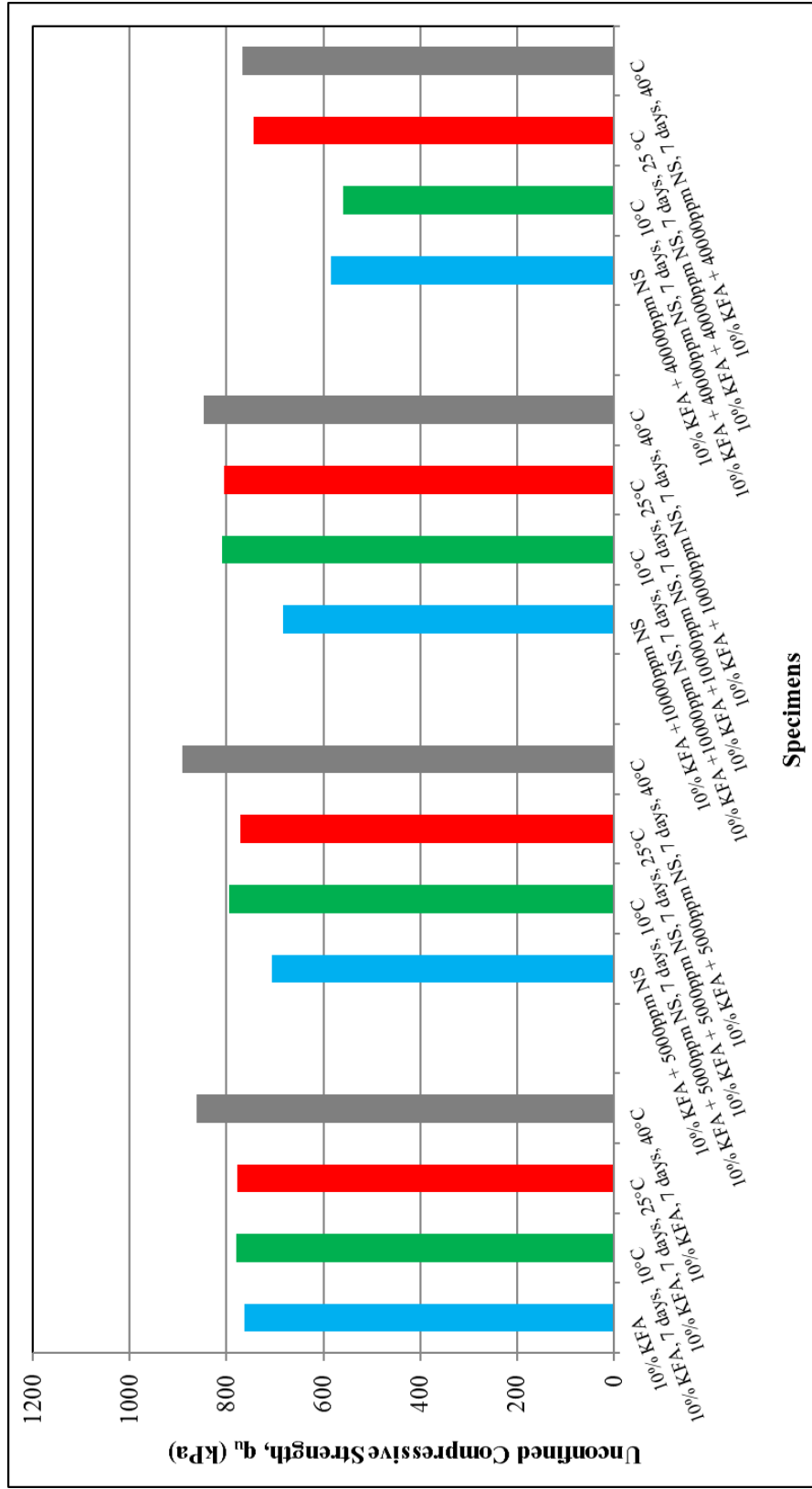


Figure 5.48. Swell percent of NS added 10% KFA treated specimens cured 7 days at 10, 25 and 40°C

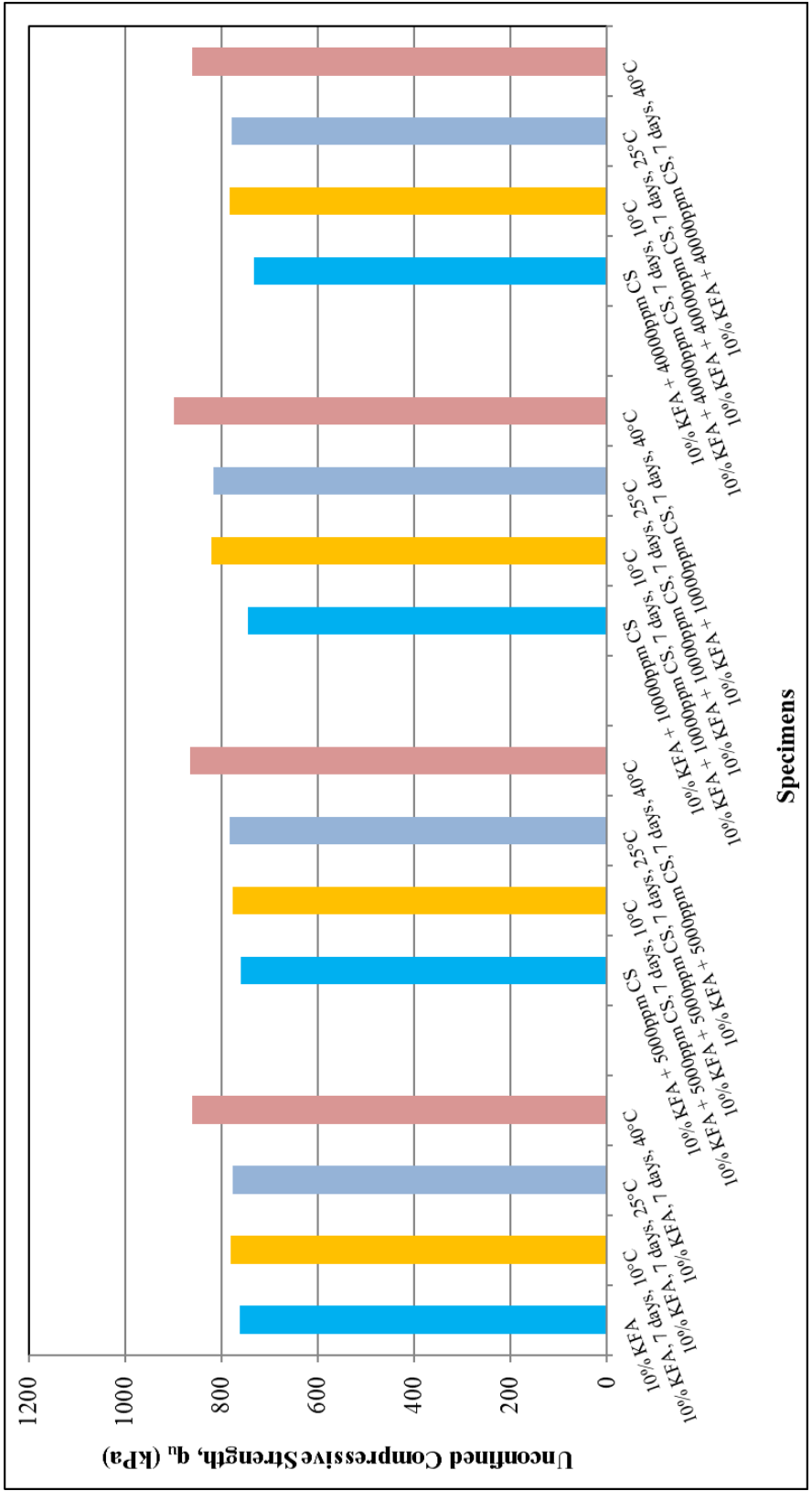


Figure 5.49. Swell percent of CS added 10% KFA treated specimens cured 7 days at 10, 25 and 40°C

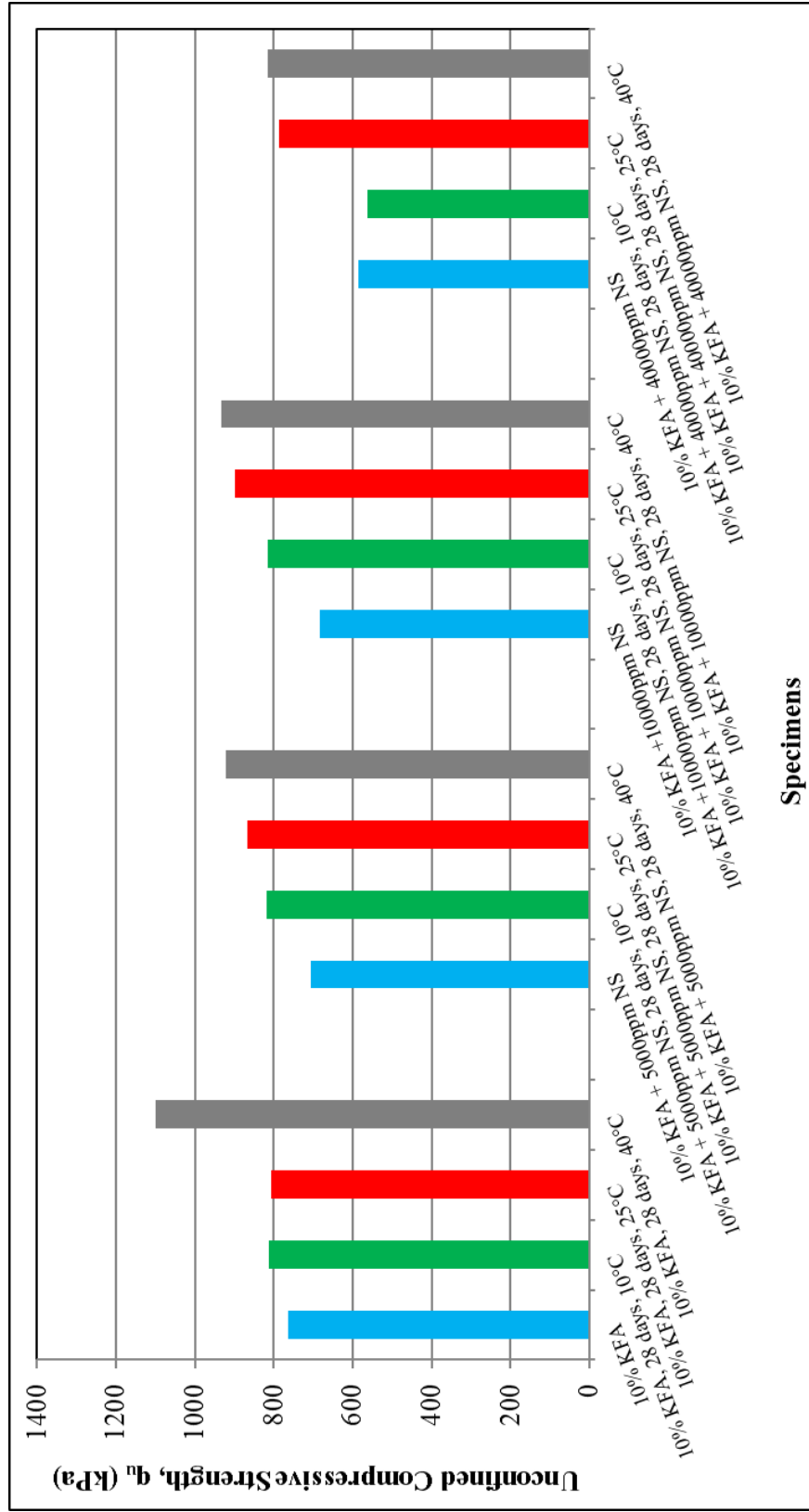


Figure 5.50. Swell percent of NS added 10% KFA treated specimens cured 28 days at 10, 25 and 40°C

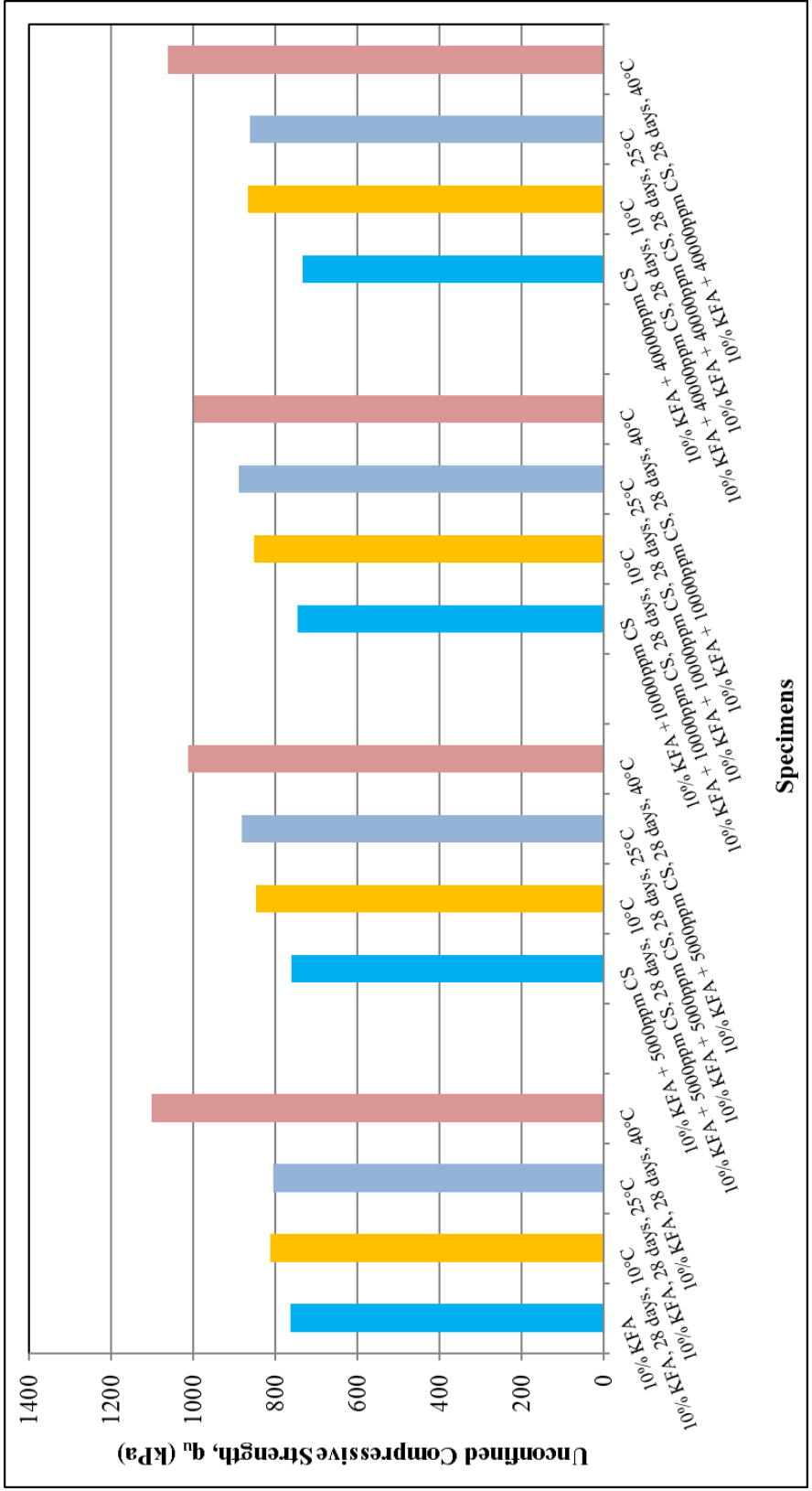


Figure 5.51. Swell percent of CS added 10% KFA treated specimens cured 28 days at 10, 25 and 40°C

### 5.5. Shear Wave Velocity ( $V_s$ ) Tests

$V_s$  tests were performed on Specimen A, 15% SFA, 10% KFA treated and 5000ppm, 10000ppm and 40000ppm NS and CS added fly ash treated specimens by using the James Instruments brand V-meter Mark IV.

The results of the tests are presented in Figure 5.52 and 5.53 for 15% SFA and 10% KFA treated specimens respectively. The  $V_s$  value of Specimen A is also presented in both graphs for comparison purposes.

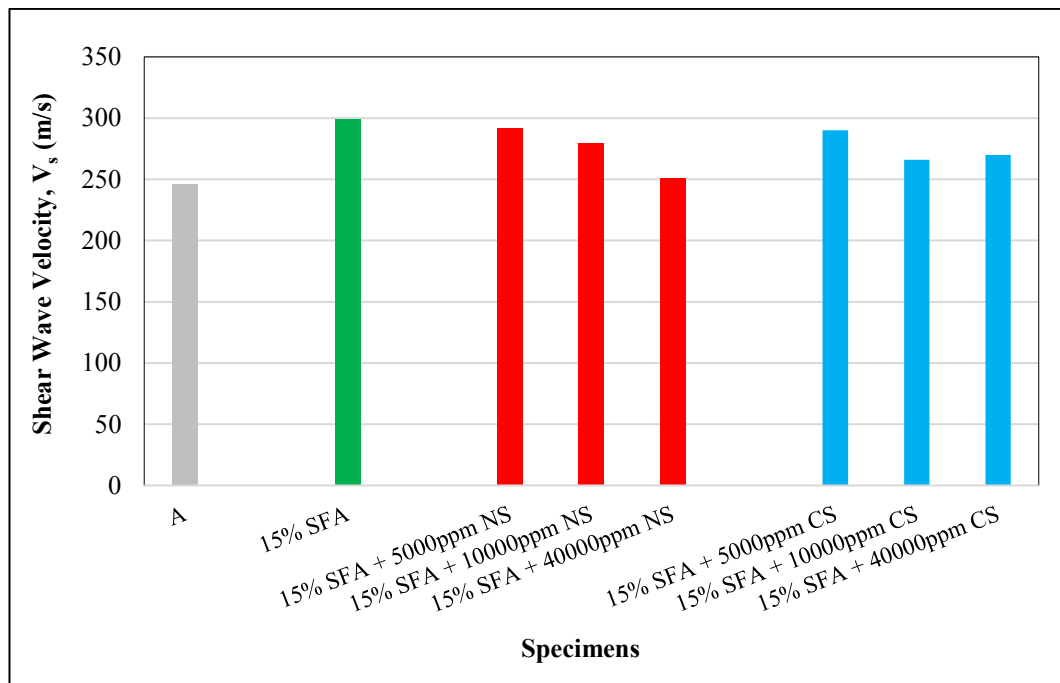


Figure 5.52.  $V_s$  of sulfate added 15% SFA treated specimens

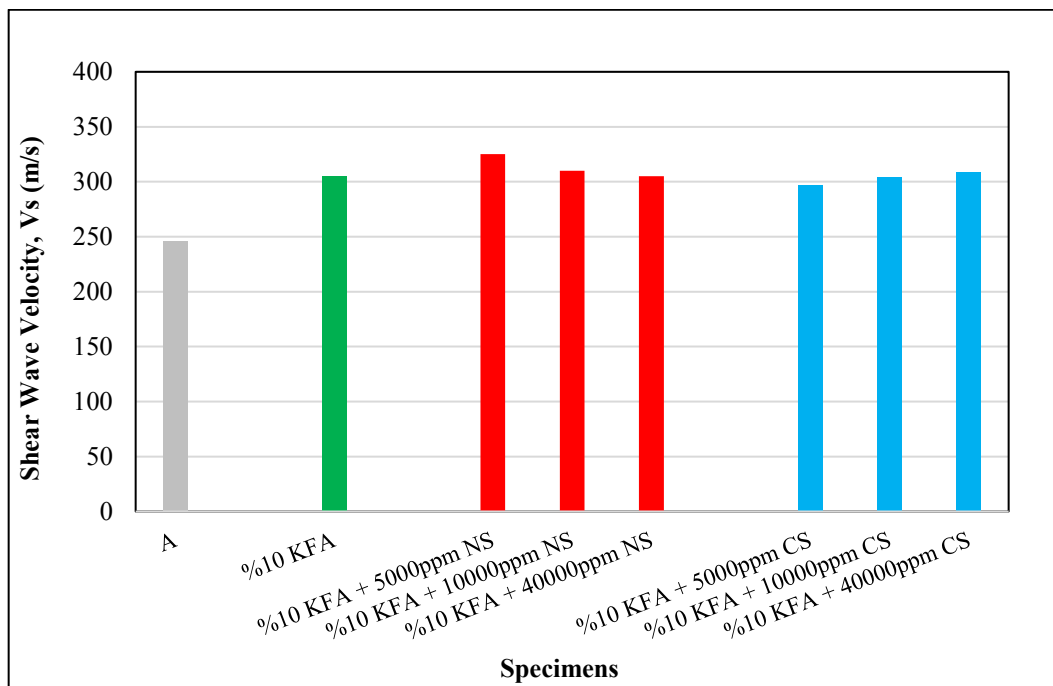


Figure 5.53.  $V_s$  of sulfate added 10% KFA treated specimens

## 5.6. Zeta Potential Tests

Zeta potential is one of the most important factors that affect the swelling potential of soils. Also, if chemical stabilization results cation exchange reaction in soils, electrokinetic properties including zeta potential may change (Arasan and Akbulut, 2010).

Zeta potential tests were performed on Sample A, 15% SFA, 10% KFA treated samples, and 10000ppm and 40000ppm NS and CS added fly ash treated samples to see both the effect of fly ash addition on swelling soil and effect of sulfate addition on fly ash treated samples in terms of cation exchange reactions. pH tests were also performed since zeta potential highly depends on pH values. Zeta potential and pH test results are presented in Figure 5.54 and 5.55 respectively. All the samples have a negative zeta potential values and the absolute values are presented in the graph.

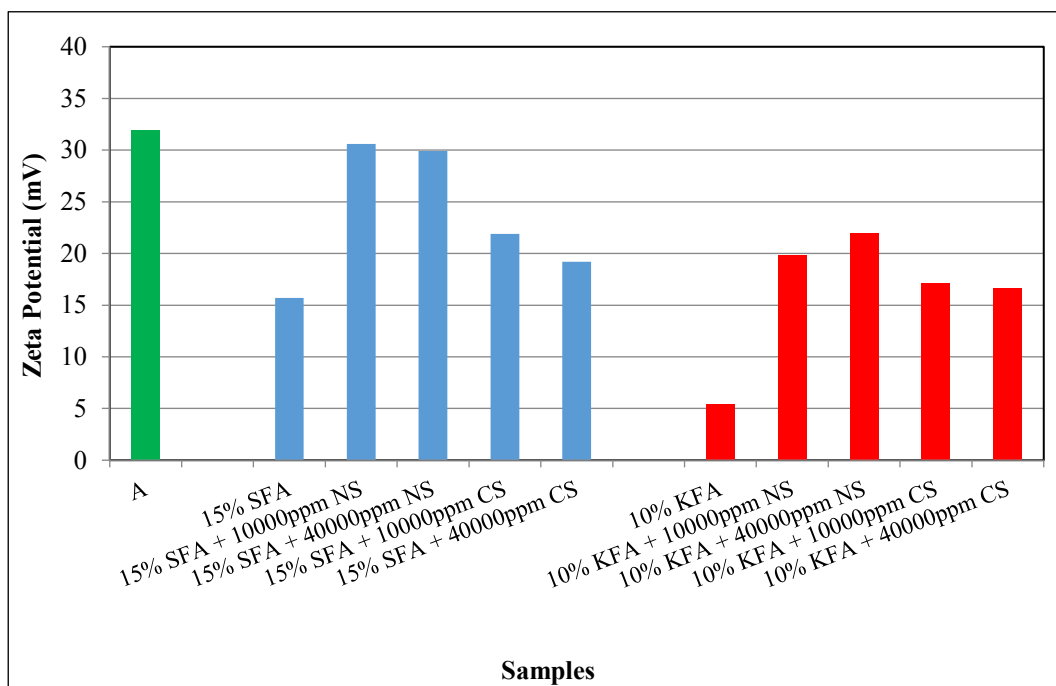


Figure 5.54. Zeta Potential of the samples

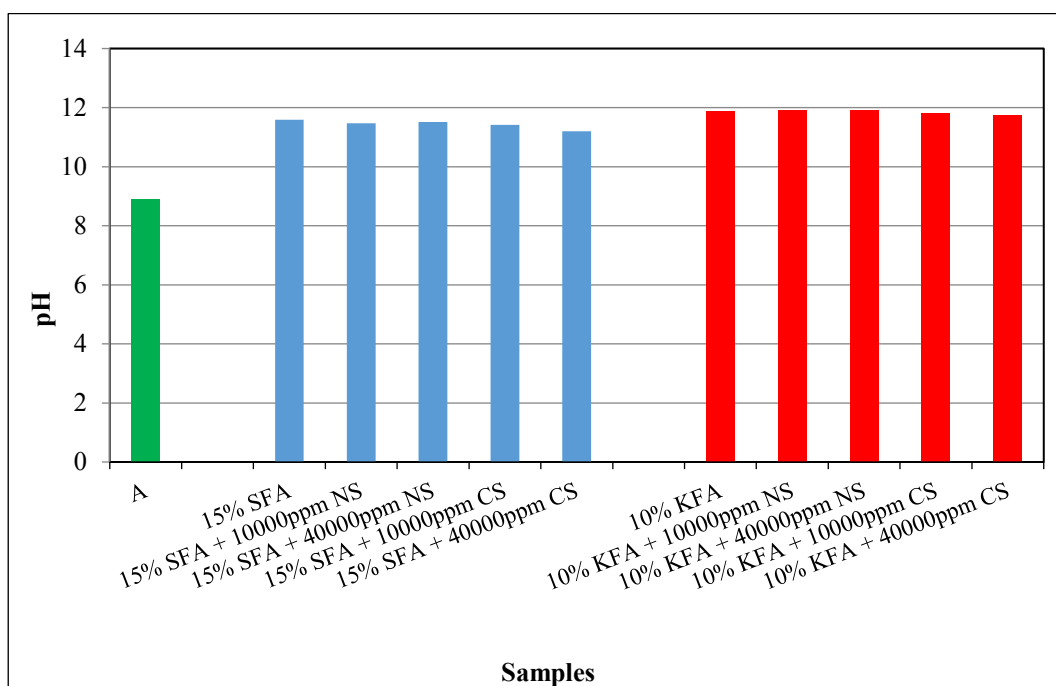


Figure 5.55. pH of the samples

## 5.7. SEM

In this study, SEM analyses were performed at METU Central Laboratory and during analysis, QUANTA 400F Field Emission Scanning Microscope was used. The samples, chosen for SEM analyses were tabulated in Table 5.2. The aim of performing SEM analyses was to determine the probable occurrence of ettringite/thaumasite in the samples.

Table 5.2. *Samples chosen for SEM analyses*

Sample
A
15 % SFA
10 % KFA
15 % SFA + 40000ppm NS
15 % SFA + 40000ppm CS
10 % KFA + 40000ppm NS
15 % SFA + 40000ppm NS cured 28 days at 10 <sup>0</sup> C
15 % SFA + 40000ppm NS cured 28 days at 25 <sup>0</sup> C
10 % KFA + 40000ppm NS cured 28 days at 10 <sup>0</sup> C
10 % KFA + 40000ppm NS cured 28 days at 25 <sup>0</sup> C
15 % SFA + 40000ppm CS cured 28 days at 10 <sup>0</sup> C
10% KFA + 40000ppm CS cured 28 days at 10 <sup>0</sup> C
15% SFA + 40000ppm NS cured 6 months at 10 <sup>0</sup> C

Cracks developed on the 40000ppm NS added 15% SFA treated sample that was cured 28 days at 10<sup>0</sup>C for UCS tests. As the chemical reactions are also time dependent, the curing period increased to 6 months for this sample to better understand the mechanics behind these cracks. After 6 months curing period besides cracks, crystal formation was also observed within the sample.

SEM analysis were also performed on the crystals (Figure 5.56) that was formed within and on the surface of 40000ppm NS added 15% SFA treated sample cured 6 months at 10<sup>0</sup>C besides the samples presented in Table 5.2.



Figure 5.56. Crystal formed within the 40000ppm NS added 15% SFA treated sample cured for 6 months at 10°C

SEM images of the samples are given in Figures 5.57 – 5.65.

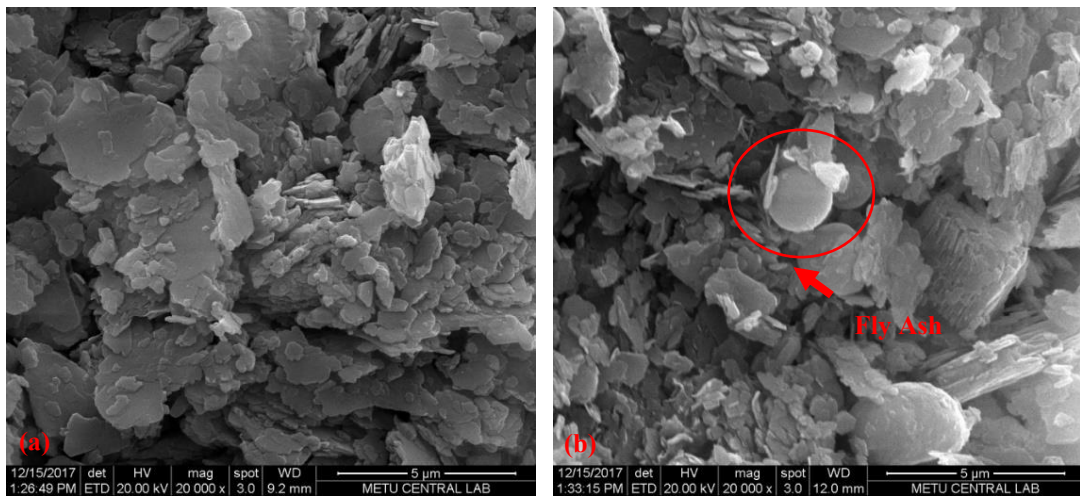


Figure 5.57. SEM images of (a)- Sample A, (b)-15% SFA treated sample (magnification factor=20000)

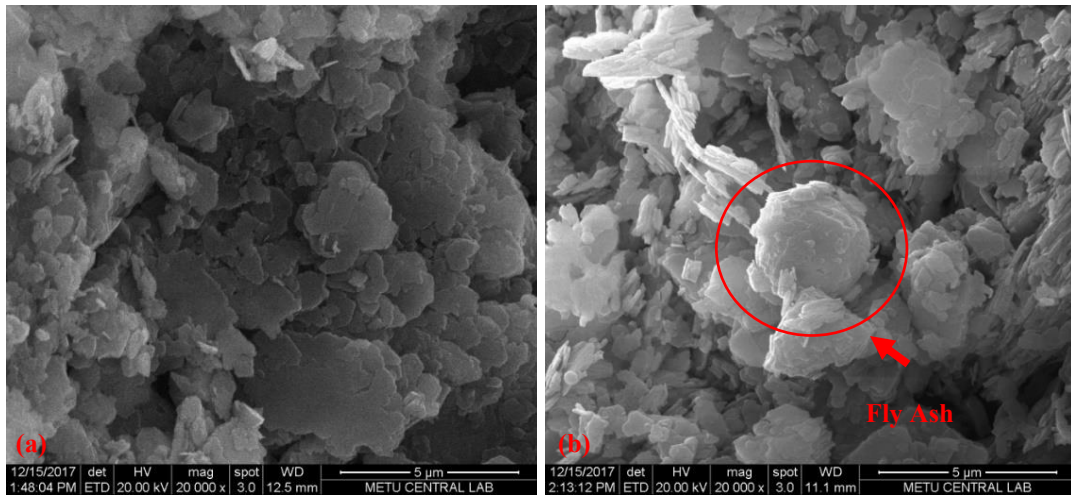


Figure 5.58. SEM images of (a)- 10% KFA treated sample, (b)- 40000ppm NS added 10% KFA treated sample (magnification factor=20000)

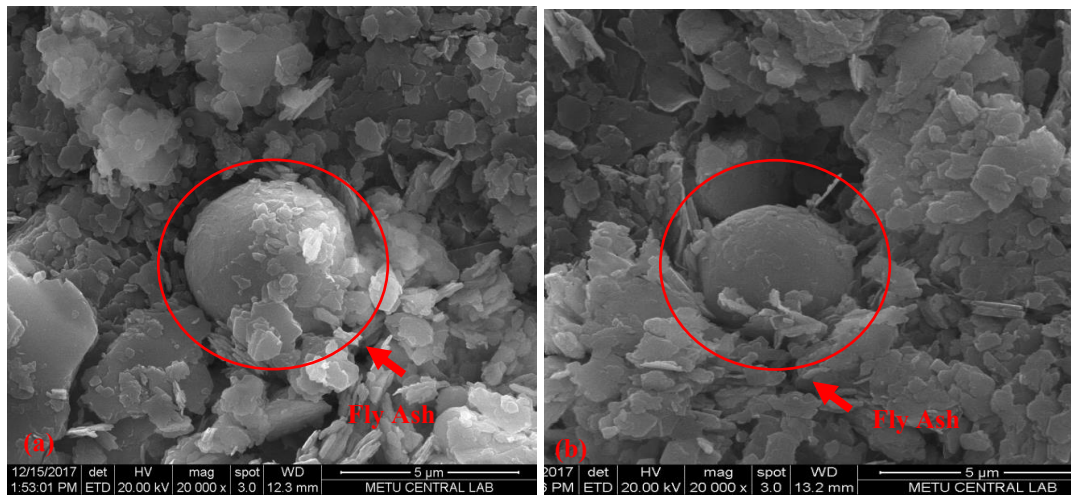


Figure 5.59. SEM images of 15% SFA treated sample with (a)-40000ppm NS (b)- 40000ppm CS (magnification factor=20000)

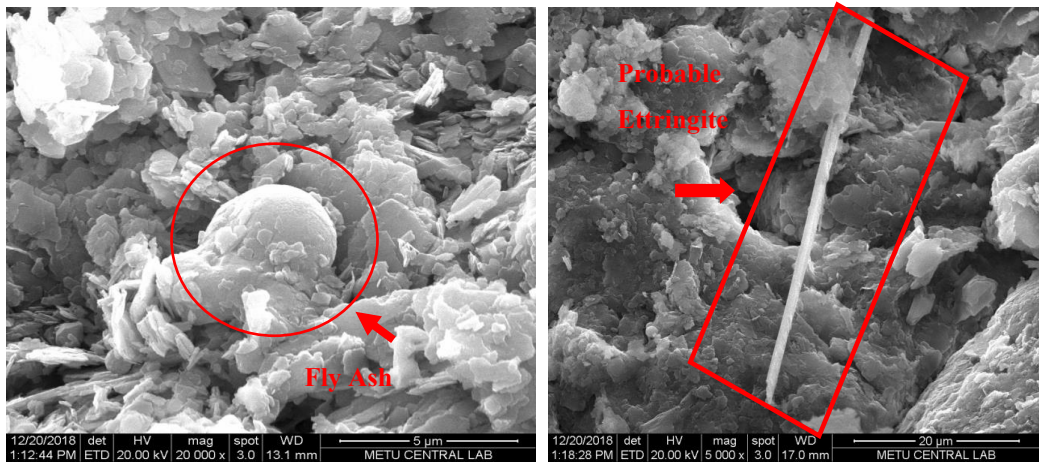


Figure 5.60. SEM images of 28 days cured 40000ppm NS added 15% SFA treated sample at 10°C (magnification factor=20000 and 5000)

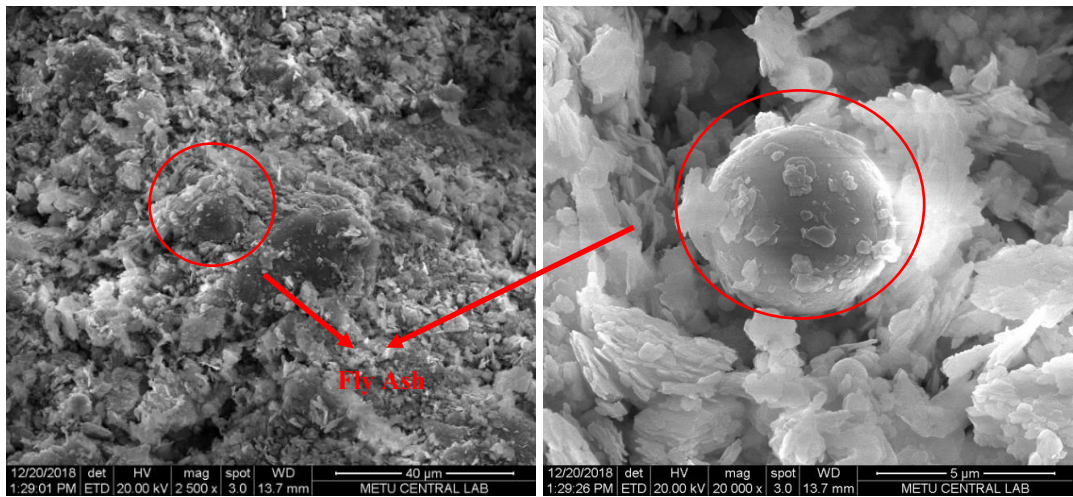


Figure 5.61. SEM images of 28 days cured 40000ppm NS added 15% SFA treated sample at 25°C (magnification factor=2500 and 20000)

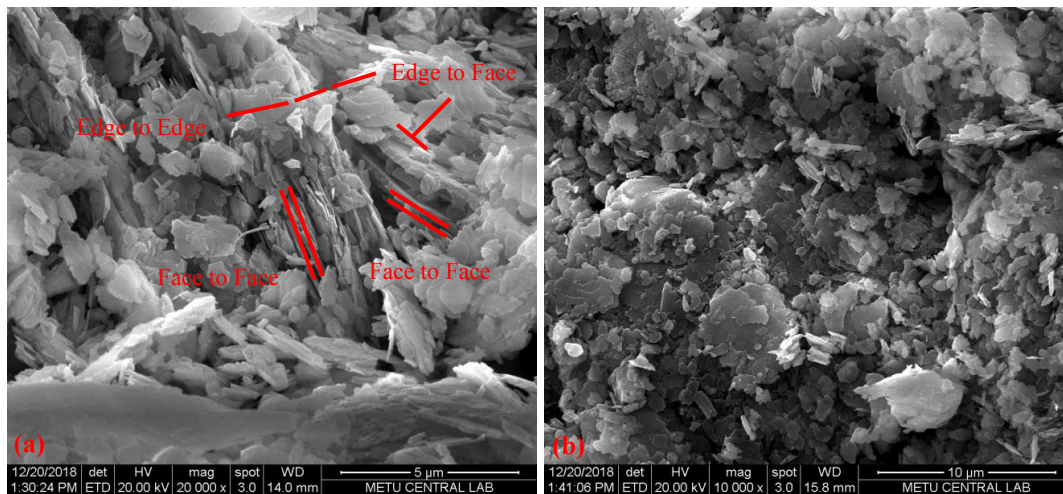


Figure 5.62. SEM images of 28 days cured 40000ppm NS added 10% KFA treated samples (a)-10°C (b)- 25°C (magnification factor=20000 and 10000)

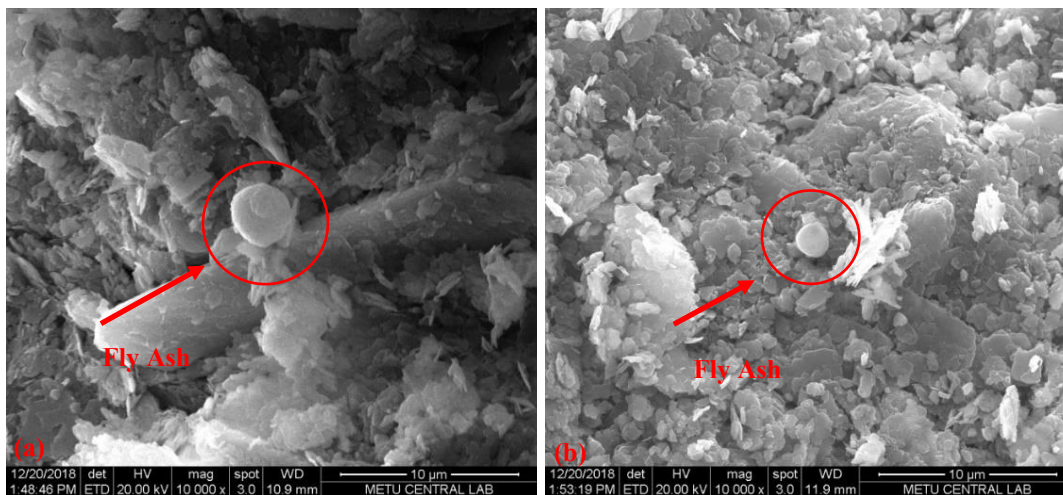


Figure 5.63. SEM images of 28 days cured 40000ppm CS added (a)-15% SFA (b)- 10% KFA treated sample at 10°C (magnification factor= 10000)

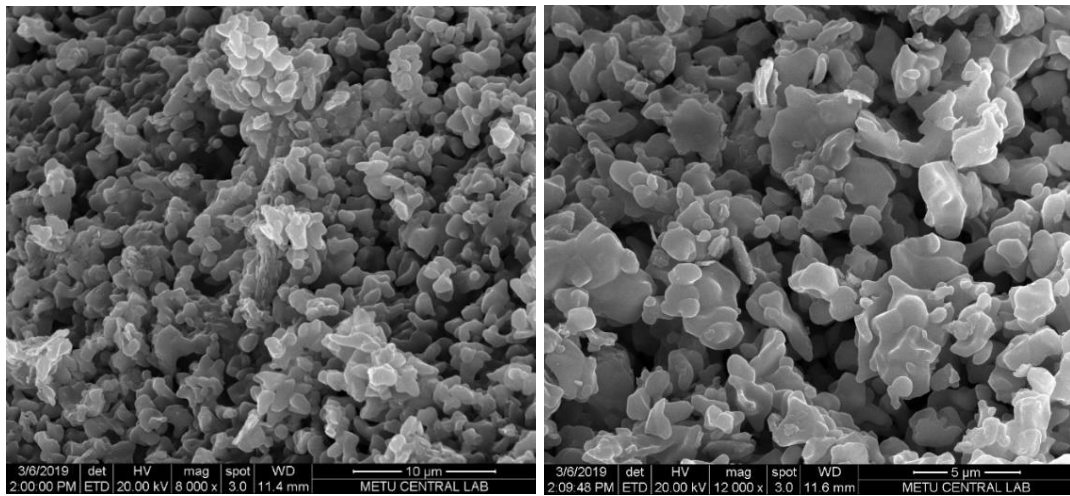


Figure 5.64. SEM images of 6 months cured 40000ppm NS added 15% SFA treated sample at 10°C (magnification factor= 8000 and 12000)

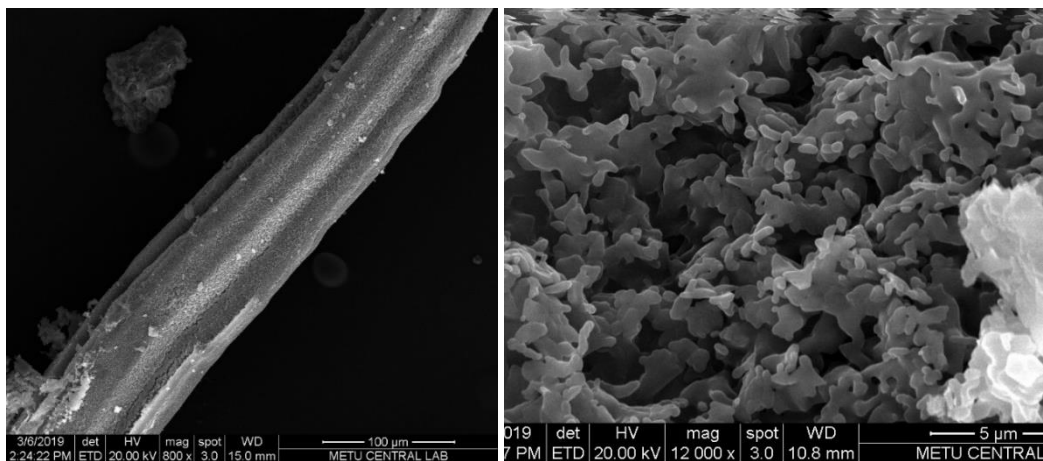
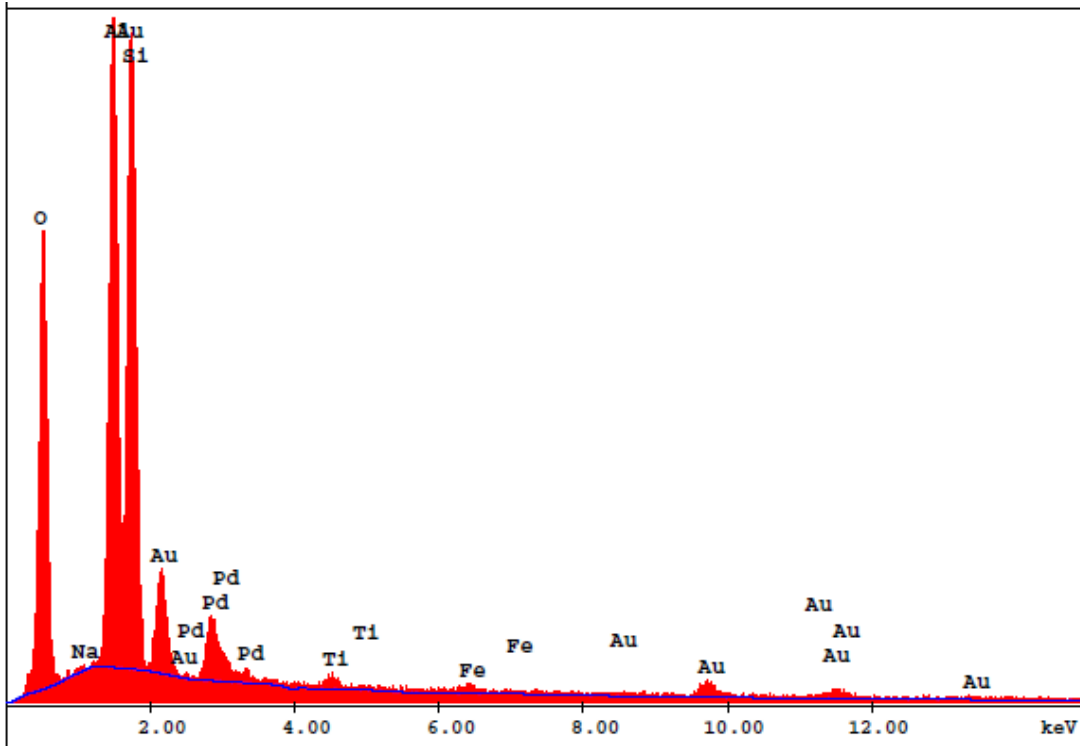


Figure 5.65. SEM images of crystals observed in 6 months cured 40000ppm NS added 15% SFA treated sample at 10°C (magnification factor= 800 and 12000)

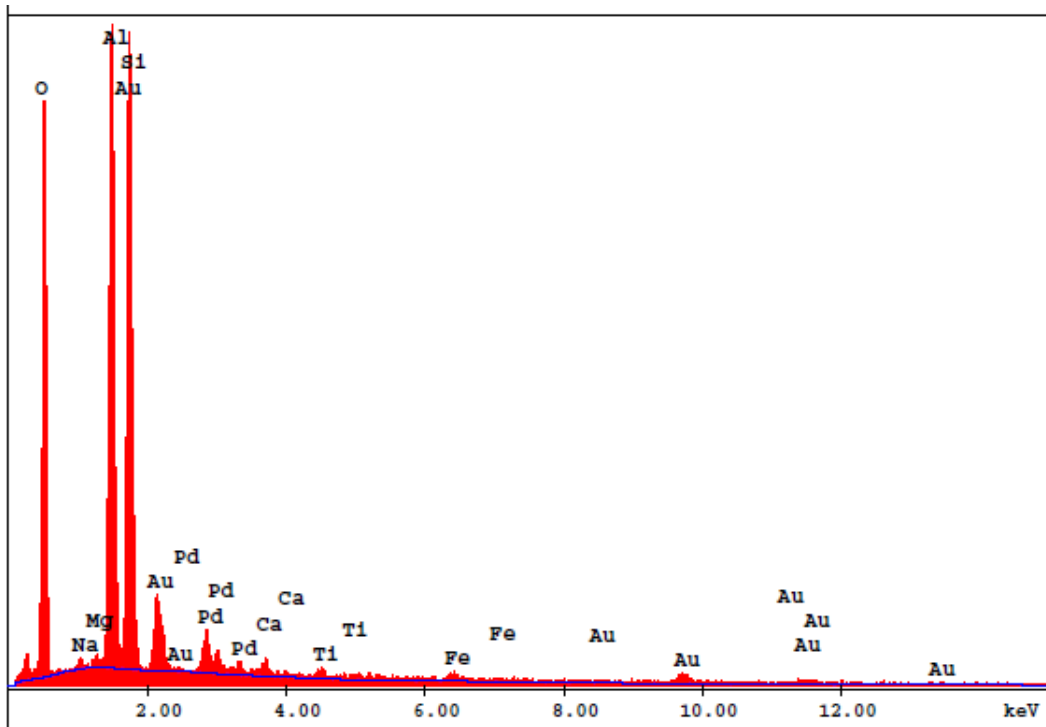
Also, Energy Dispersive X-Ray (EDX) analyses which gives information about the chemical characterization (elements) of a material were performed on the samples. The results are presented in Figures 5.66- 5.70.



EDAX ZAF Quantification (Standardless)  
 Element Normalized  
 SEC Table : Default

Element	Wt %	At %	K-Ratio	Z	A	F
O K	38.12	60.38	0.1067	1.0726	0.2607	1.0004
NaK	0.15	0.16	0.0005	1.0034	0.3661	1.0039
AlK	18.49	17.36	0.1193	0.9980	0.6427	1.0064
SiK	19.80	17.87	0.1211	1.0270	0.5950	1.0008
PdL	6.21	1.48	0.0420	0.8165	0.8268	1.0003
TiK	0.67	0.36	0.0055	0.9154	0.8957	1.0021
FeK	0.82	0.37	0.0073	0.9155	0.9714	1.0090
AuL	15.73	2.02	0.1106	0.6822	1.0302	1.0000
Total	100.00	100.00				

Figure 5.66. EDX diagram of Sample A



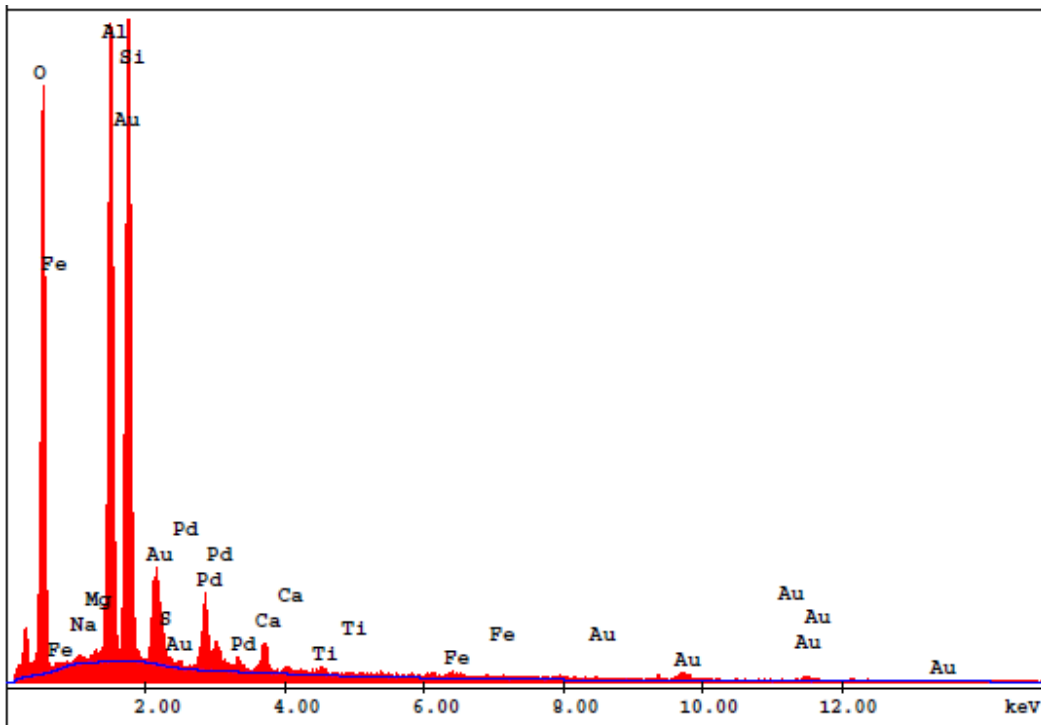
EDAX ZAF Quantification (Standardless)

Element Normalized

SEC Table : Default

Element	Wt %	At %	K-Ratio	Z	A	F
O K	39.32	60.02	0.1132	1.0639	0.2705	1.0004
NaK	0.43	0.46	0.0016	0.9954	0.3788	1.0042
MgK	0.30	0.30	0.0016	1.0202	0.5188	1.0083
AlK	17.97	16.26	0.1174	0.9901	0.6550	1.0071
SiK	21.87	19.02	0.1358	1.0188	0.6089	1.0007
PdL	4.51	1.04	0.0308	0.8087	0.8439	1.0008
CaK	0.85	0.52	0.0070	0.9930	0.8334	1.0009
TiK	0.66	0.34	0.0055	0.9072	0.9077	1.0021
FeK	0.98	0.43	0.0087	0.9064	0.9764	1.0081
AuL	13.10	1.62	0.0909	0.6736	1.0307	1.0000
Total	100.00	100.00				

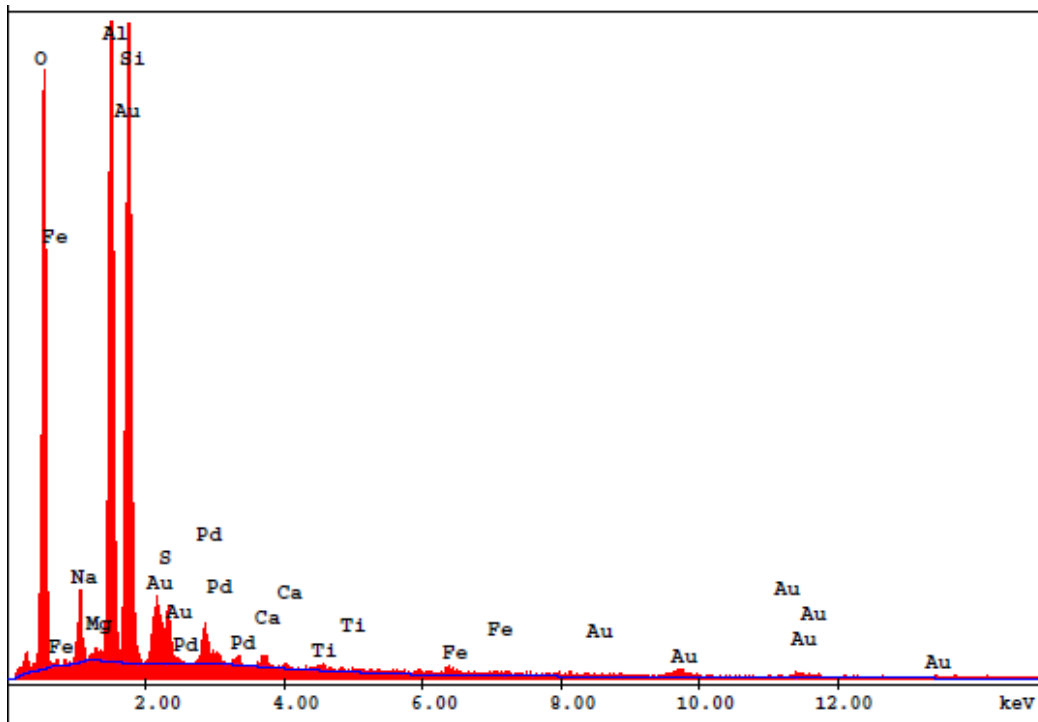
Figure 5.67. EDX diagram of 15% SFA treated sample



EDAX ZAF Quantification (Standardless)  
 Element Normalized  
 SEC Table : Default

Element	Wt %	At %	K-Ratio	Z	A	F
O K	40.21	61.10	0.1117	1.0633	0.2612	1.0004
NaK	0.36	0.38	0.0013	0.9949	0.3714	1.0040
MgK	0.34	0.34	0.0018	1.0197	0.5115	1.0080
AlK	17.23	15.53	0.1113	0.9896	0.6479	1.0070
SiK	20.70	17.92	0.1289	1.0183	0.6105	1.0012
S K	0.40	0.30	0.0025	1.0127	0.6081	1.0029
PdL	7.15	1.63	0.0499	0.8081	0.8630	1.0010
CaK	1.46	0.89	0.0121	0.9923	0.8325	1.0006
TiK	0.46	0.23	0.0038	0.9066	0.9053	1.0016
FeK	0.70	0.30	0.0062	0.9056	0.9757	1.0068
AuL	10.98	1.36	0.0761	0.6726	1.0307	1.0000
Total	100.00	100.00				

Figure 5.68. EDX diagram of 10% KFA treated sample



EDAX ZAF Quantification (Standardless)  
 Element Normalized  
 SEC Table : Default

Element	Wt %	At %	K-Ratio	Z	A	F
O K	39.35	58.39	0.1169	1.0577	0.2807	1.0004
NaK	2.71	2.80	0.0106	0.9897	0.3935	1.0042
MgK	0.29	0.28	0.0015	1.0145	0.5160	1.0084
AlK	17.81	15.67	0.1154	0.9845	0.6538	1.0073
SiK	21.66	18.31	0.1338	1.0131	0.6093	1.0011
S K	2.21	1.63	0.0134	1.0059	0.6047	1.0014
PdL	3.64	0.81	0.0249	0.8032	0.8508	1.0005
CaK	0.50	0.30	0.0042	0.9866	0.8437	1.0006
TiK	0.32	0.16	0.0027	0.9013	0.9160	1.0019
FeK	0.88	0.37	0.0078	0.8997	0.9805	1.0072
AuL	10.64	1.28	0.0733	0.6672	1.0319	1.0000
Total	100.00	100.00				

Figure 5.69. EDX diagram of 40000ppm NS added 15% SFA treated sample

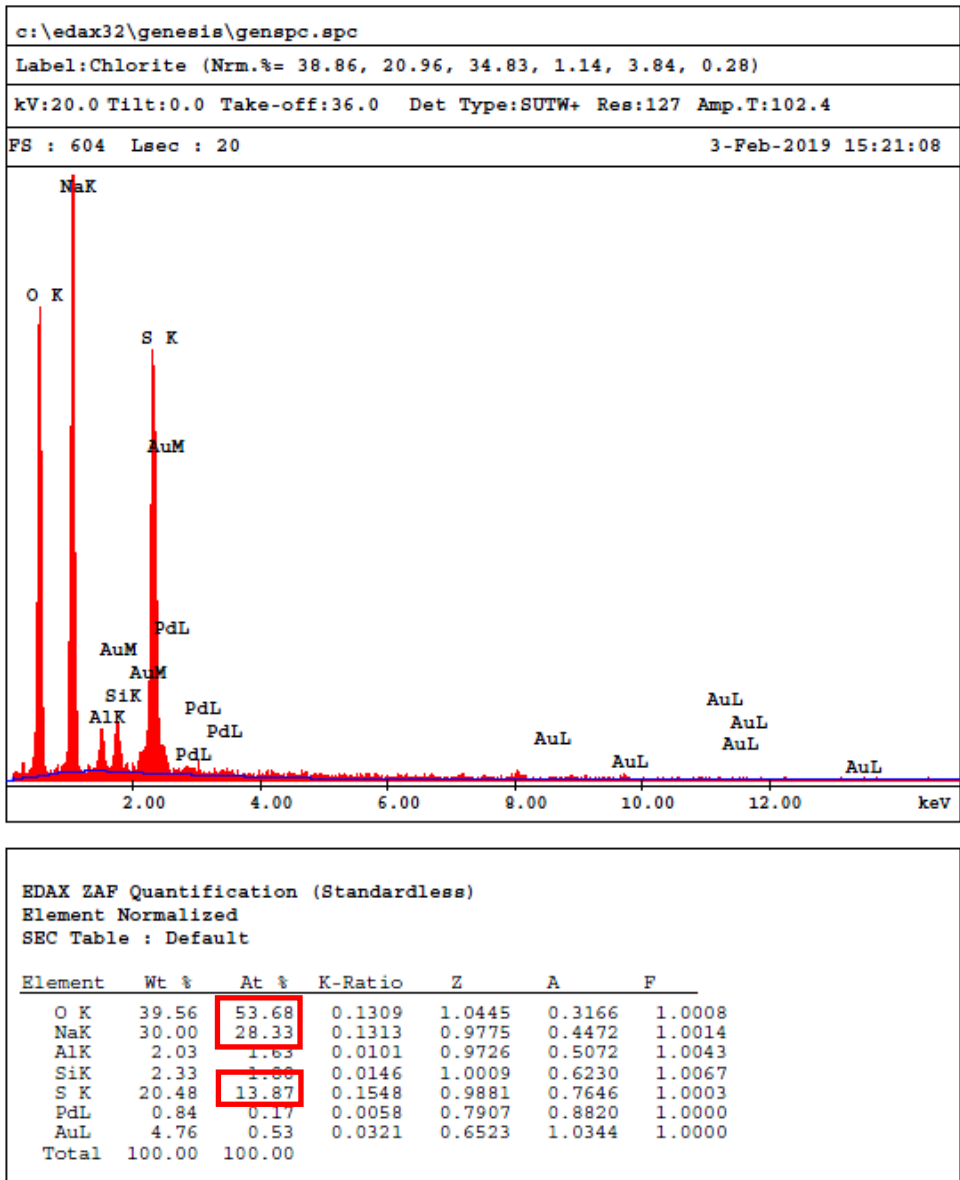


Figure 5.70. EDX diagram of 40000ppm NS added 15% SFA treated sample cured at 10°C for 6 months

Gold (Au) and palladium (Pd) elements observed in the EDX analyses were due to the covering of sample with gold and palladium before the test (Figures 5.66-5.70).

## 5.8. XRD

XRD analyses were performed to determine the reason behind the occurrence of cracks and formation of crystals at 40000ppm NS added 15% SFA treated specimen after curing at 10°C for 28 days and 6 months respectively (Figure 5.71).

The analyses were performed on 40000ppm NS added 15% SFA treated specimens that were cured at 10°C for 28 days and 6 months. Uncured 15% SFA treated and 40000ppm NS added 15% SFA treated specimens cured at 25°C for 28 days were also exposed to analyses for comparison purposes. Analyses were performed in Central Laboratory of METU.

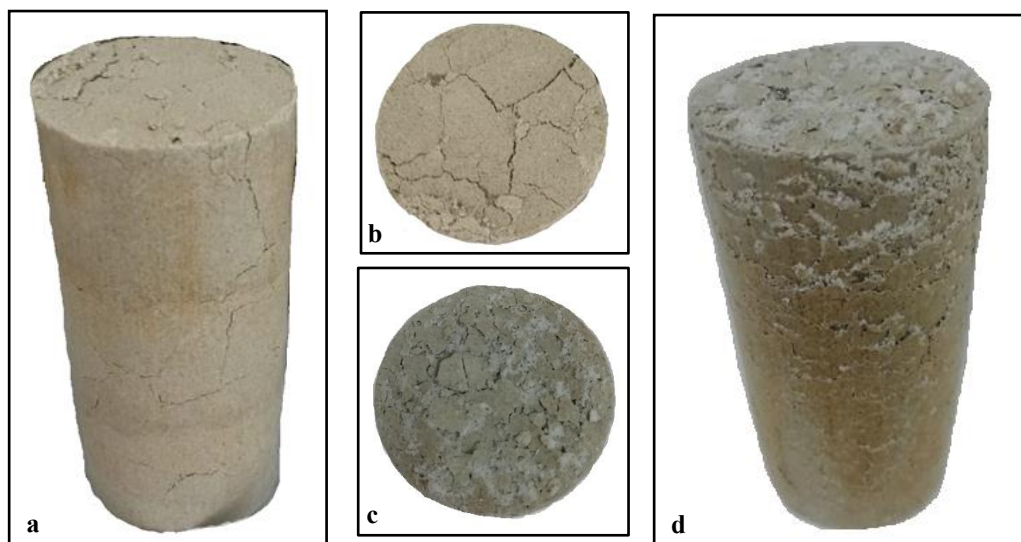


*Figure 5.71.* 40000ppm NS added 15% SFA treated specimens cured at 10°C for a,b -28 days, c,d-6 months

Analyses results are presented in Figures 5.72 –5.74. The results for 28 days cured 40000ppm NS added 15% SFA treated samples at 10°C and 25°C were almost identical, therefore only the result for 10°C is presented. The result for 25°C curing temperature is presented in Appendix B.

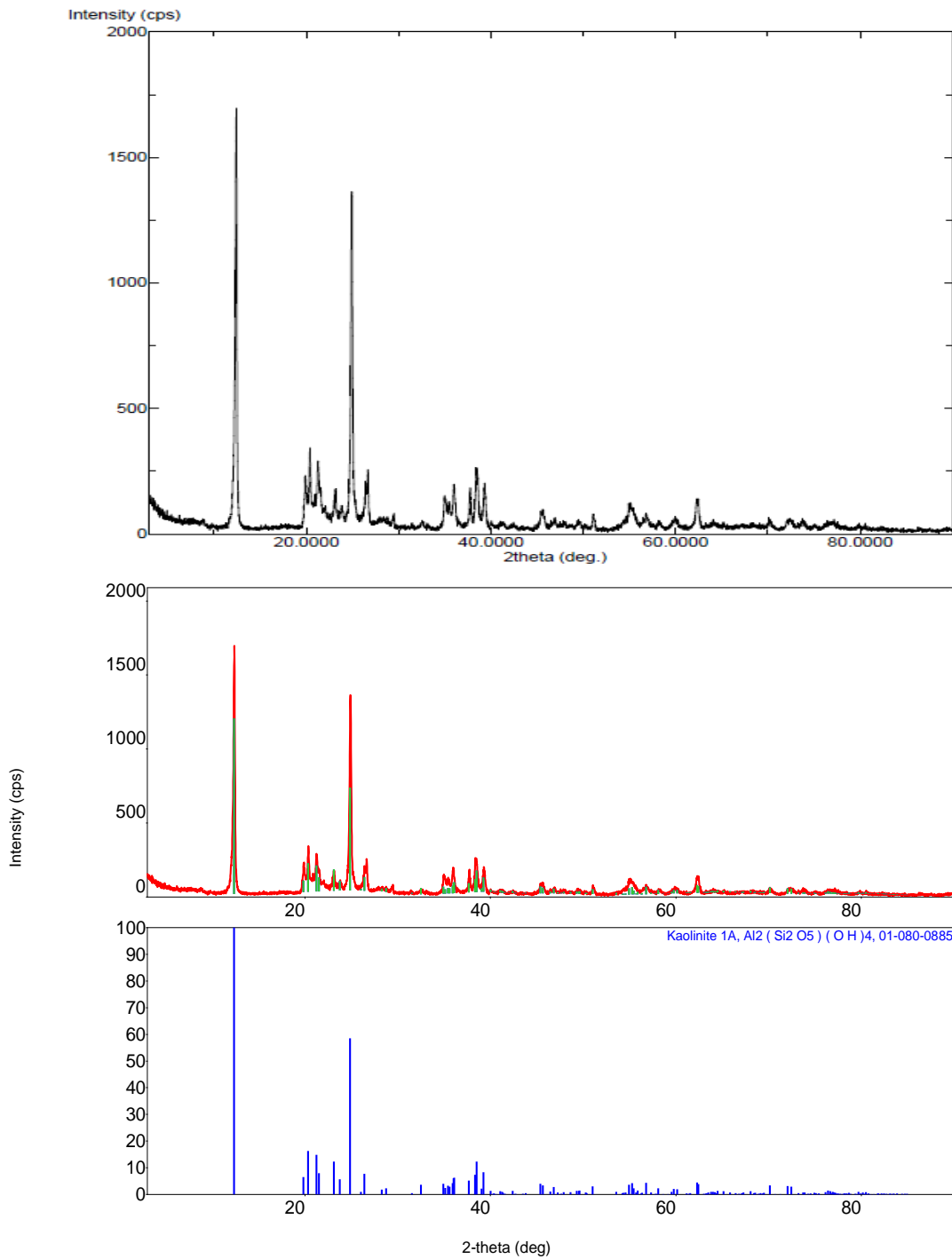


Figure 5.72. XRD of 15% SFA treated sample

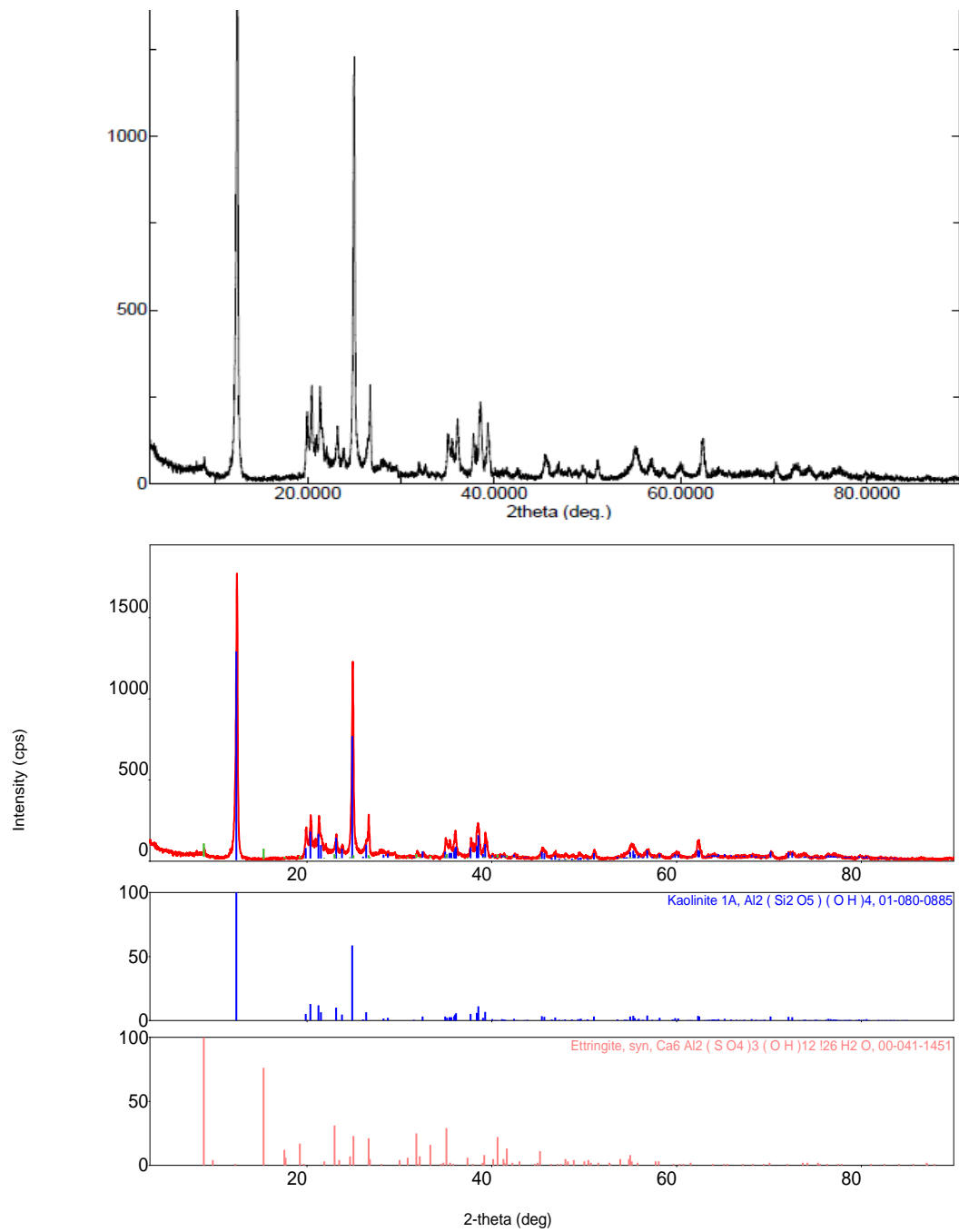


Figure 5.73. XRD of 40000ppm NS added 15% SFA treated sample cured at 10°C for 28 days

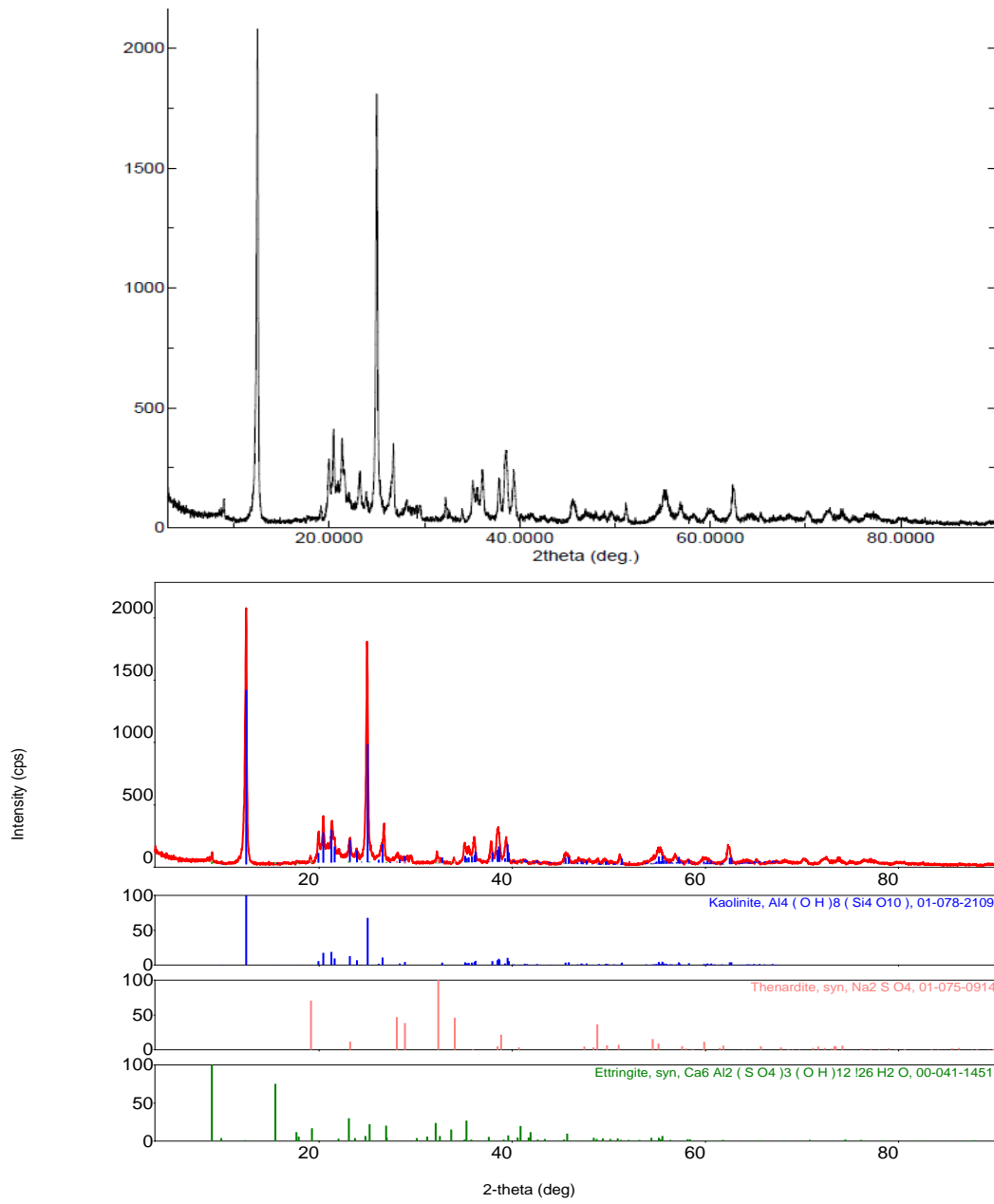


Figure 5.74. XRD of 40000ppm NS added 15% SFA treated sample cured at 10°C for 6 months

## CHAPTER 6

### DISCUSSION ON TEST RESULTS

#### 6.1. Effect of Additives on Specific Gravity ( $G_s$ )

$G_s$  of Sample A, SFA, KFA and L were measured as 2.641, 2.246, 2.579 and 2.500 respectively. The  $G_s$  of Sample A is greater than the additives, therefore, it was expected that the addition of calcium-based stabilizers would cause a reduction in  $G_s$  of the swelling soil. However, the results were different than expected for 10% KFA and 4% L treated samples. The measured and calculated (by mass basis)  $G_s$  values basis are tabulated in Table 6.1.

Table 6.1. *Measured and calculated  $G_s$  values for chemically stabilized soil*

Sample	$G_s$		
	Measured	Calculated	Difference
4% L	2.714	2.636*	0.078
15% SFA	2.579	2.589	-0.010
10% KFA	2.699	2.635	0.064

\*(mass of sample A\* $G_s$  of sample A + mass of additive\* $G_s$  of additive) / total mass  
= (1\*2.641+0.04\*2.500)/1.04=2.636

The calculated and measured values for 15% SFA treated sample is as expected. There is only a 0.01 difference. The acceptable range of two results for CH type soils is presented as 0.03 for the repeated tests by a single operator in ASTM D854. Therefore, the difference is in tolerable limits. However, the measured values are 0.064 and 0.078 unit higher than the calculated ones for 10% KFA and 4% L treated samples respectively. The CaO content of SFA, KFA and L are 11.6%, 29.5%, and 83.7%

respectively. The increase in  $G_s$  for 10% KFA and 4% L treated samples could be due to the pozzolanic reactions occurred as a result of the high calcium content of these additives. As the calcium content of SFA is considerably lower, an increase in  $G_s$  was not observed for this additive.

Same trend was also observed in the studies conducted by Yesilbas (2004), Baytar (2005), and As (2012) for the fly ash and lime treated soils. Lime, fly ash with a CaO content of 13.25%, and fly ash with a CaO content of 31.45% were used as additives respectively in the studies. The results of the tests and the specific gravity values calculated by mass basis are tabulated in Table 6.2.

Table 6.2.  $G_s$  values obtained in Yesilbas (2004), Baytar (2005), and As (2012) studies

Reference	Sample	$G_s$		
		Measured	Calculated	Difference
Yesilbas (2004)	Expansive Soil	2.64	-	-
	Lime	2.76	-	-
	1% Lime	2.66	2.64	0.02
	3% Lime	2.67	2.64	0.03
	5% Lime	2.69	2.65	0.04
	7% Lime	2.70	2.65	0.05
	9% Lime	2.72	2.65	0.07
Baytar (2005)	Expansive Soil	2.76	-	-
	Fly Ash	2.13	-	-
	5% Fly Ash	2.74	2.73	0.01
	10% Fly Ash	2.72	2.70	0.02
	15% Fly Ash	2.69	2.67	0.02
	20% Fly Ash	2.66	2.63	0.03
	25% Fly Ash	2.60	2.60	0
As (2012)	Expansive Soil	2.64	-	-
	Fly Ash	2.56	-	-
	5% Fly Ash	2.65	2.64	0.01
	10% Fly Ash	2.66	2.63	0.03
	15% Fly Ash	2.68	2.63	0.05
	20% Fly Ash	2.68	2.62	0.06

The  $G_s$  of NS and CS are given as 2.7 and 2.32 by the manufacturer. The effect of the addition of different concentrations of NS and CS to  $G_s$  values of 4% L, 15% SFA, and 10% KFA treated samples could be seen in Table 6.3, 6.4 and 6.5 respectively. The measured results are presented with the calculated (by mass basis) ones for all samples.

Table 6.3. *The measured and calculated (by mass basis)  $G_s$  values for sulfate added 4% L treated sample*

Sample	$G_s$			Increase / Decrease in $G_s$ after sulfate addition	Increase / Decrease in $G_s$ after sulfate addition (%)
	Measured	Calculated	Difference		
4% L	2.714	-	-	-	-
4% L + 5000ppm NS	2.702	2.713	-0.011	-0.012	-0.4
4% L + 10000ppm NS	2.717	2.714	0.003	0.003	0.1
4% L + 40000ppm NS	2.808	2.713	0.095	0.094	3.5
4% L + 5000ppm CS	2.699	2.696	0.003	-0.015	-0.6
4% L + 10000ppm CS	2.701	2.71	-0.009	-0.013	-0.5
4% L + 40000ppm CS	2.724	2.699	0.025	0.01	0.4

Sulfate addition did not affect the  $G_s$  of the 4% L treated sample considerably except for 40000ppm NS. This concentration of NS resulted considerable increase (3.5%) in  $G_s$  of 4% lime treated sample.

Table 6.4. The measured and calculated (by mass basis)  $G_s$  values for sulfate added 15% SFA treated sample

Sample	$G_s$			Increase / Decrease in $G_s$ after sulfate addition	Increase / Decrease in $G_s$ after sulfate addition (%)
	Measured	Calculated	Difference		
15% SFA	2.579	-	-	-	-
15% SFA + 3000ppm NS	2.611	2.579	0.032	0.032	1.2
15% SFA + 5000ppm NS	2.646	2.580	0.066	0.067	2.6
15% SFA + 10000ppm NS	2.654	2.580	0.074	0.075	2.9
15% SFA + 20000ppm NS	2.623	2.581	0.042	0.044	1.7
15% SFA + 40000ppm NS	2.695	2.583	0.112	0.116	4.5
15% SFA + 3000ppm CS	2.621	2.578	0.043	0.042	1.6
15% SFA + 5000ppm CS	2.610	2.578	0.032	0.031	1.2
15% SFA + 10000ppm CS	2.580	2.577	0.003	0.001	0.0
15% SFA + 20000ppm CS	2.620	2.575	0.045	0.041	1.6
15% SFA + 40000ppm CS	2.595	2.570	0.025	0.016	0.6

As can be seen in Table 6.4, the addition of NS resulted an increase in  $G_s$  of 15% SFA treated sample. The increment generally increased with increasing sulfate concentration. The maximum increase was obtained for 40000ppm concentration. The increase was probably due to the pozzolanic reactions that occurred as a result of the NS addition.

Gadouri et al. (2017) studied on the effect of NS on the shear strength of clayey soil stabilized with lime and natural pozzolans. The results of the study showed that the addition of NS up to 2% resulted an increase in strength parameters of the stabilized soil. The reason for this increase was explained by the attribution of early pozzolanic reactions due to the sodium hydroxide that occurred as a result of the NS addition.

The addition of CS generally resulted an increase in the  $G_s$  value of the fly ash treated sample, however the effect is not as much as the NS.

Table 6.5. The measured and calculated (by mass basis)  $G_s$  values for sulfate added 10% KFA treated sample

Sample	G <sub>s</sub>			Increase / Decrease in G <sub>s</sub> after sulfate addition	Increase / Decrease in G <sub>s</sub> after sulfate addition (%)
	Measured	Calculated	Difference		
10% KFA	2.699	-	-	-	-
10% KFA + 3000ppm NS	2.711	2.699	0.012	0.012	0.4
10% KFA + 5000ppm NS	2.683	2.699	-0.016	-0.016	-0.6
10% KFA + 10000ppm NS	2.724	2.699	0.025	0.025	0.9
10% KFA + 20000ppm NS	2.718	2.699	0.019	0.019	0.7
10% KFA + 40000ppm NS	2.781	2.699	0.082	0.082	3.0
10% KFA + 3000ppm CS	2.709	2.698	0.011	0.01	0.4
10% KFA + 5000ppm CS	2.697	2.683	0.014	-0.002	-0.1
10% KFA + 10000ppm CS	2.687	2.696	-0.009	-0.012	-0.4
10% KFA + 20000ppm CS	2.711	2.692	0.019	0.012	0.4
10% KFA + 40000ppm CS	2.670	2.686	-0.016	-0.029	-1.1

The addition of sulfate did not generally alter the  $G_s$  of 10% KFA treated samples except for 40000ppm NS added sample. Similar to 15% SFA and 4% L treated samples, 40000ppm NS resulted in a considerable increase in  $G_s$ . The reason for this could be the high CaO content of this fly ash. The pozzolanic reactions may proceed faster as a result of high lime content and lower concentrations of NS may not affect the reaction rates much.

In conclusion, 10% KFA and 4% L treatment caused an increase in  $G_s$  of Sample A, whereas a reduction was observed with the addition of 15% SFA. The addition of sulfate did not alter the  $G_s$  of 10% KFA and 4% L treated samples except for 40000ppm NS. This type and concentration of sulfate resulted 0.094 and 0.082 increase in  $G_s$  of the 10% KFA and 4% L treated samples respectively. Addition of different concentrations of NS and CS generally caused an increase in  $G_s$  of the 15% SFA treated sample. The effect of CS was not as much as the NS, and it was nearly

ignorable. The effect of NS on  $G_s$  of the 15% SFA treated sample generally increased with the rise in sulfate concentration.

## 6.2. Effect of Additives on LL, PL and PI

LL, PL, PI of sample A, fly ash and lime treated samples are presented in Table 6.6 with the percent variation in properties of Sample A after stabilization with additives.

Table 6.6. LL, PL, PI of Sample A, 15% SFA, 10% KFA and 4% L treated samples

Sample	LL (%)	PL (%)	PI (%)	Increase / Decrease after chemical treatment (%)		
				LL	PL	PI
A	111.0	25.0	86.0			
4% L	91.9	39.4	52.5	-17.2	57.6	-39.0
15% SFA	112.0	32.9	79.1	0.9	31.6	-8.0
10% KFA	102.8	32.4	70.4	-7.4	29.6	-18.1

LL of Sample A remained nearly same after SFA addition however, KFA and L treatment caused 7.4 and 17.2% decrease respectively.

Zeta potential of Sample A increased from -31.9mV to -15.7mV and -5.4mV with the addition of 15% SFA and 10% KFA. An increase in zeta potential value (or decrease when absolute value considered) is a sign of cation exchange reactions and a more flocculated structure as will be discussed in Section 6.8. Therefore, considering the more flocculated structure and substitution of some amount of plastic clayey soil with fly ash that consists of non-plastic silt size particles, a decrease in LL was expected after fly ash addition.

Chemical treatment with calcium-based stabilizers affects LL of soils differently according to previous studies.

Nalbantoğlu (2004) studied on the effect of class C fly ash on the stabilization of expansive soils. Two different calcareous soils with different mineral compositions

and SFA with a CaO content of 14.80% were used in the study. The soils were classified as CH and CL according to USCS. LL of the CH type soil decreased however, an increase was observed for CL type soil after fly ash treatment.

An increase in LL of the soils after class C fly ash treatment was also observed in the studies performed by Degirmenci et al. (2007) and Ozdemir (2011). However, opposite behavior was observed at the investigations performed by Cokca (2001), Al-Dahlaki (2007) and Zha et al. (2008), LL of soils decreased after fly ash treatment in their studies.

Bell (1996) studied on the effect of lime treatment on three different soils that originated from montmorillonite, kaolinite, and quartz respectively. Lime resulted an increase in LL of kaolinite and quartz whereas a decrease was observed for montmorillonite.

Croft (1964) explained the increase in LL for lime treated soils by the modification of the interest of clay surface to water due to the alteration originated from the hydroxyl ions. The same phenomenon could be responsible for the increase in LL of the expansive soil after 15% SFA treatment.

Reduction in thickness of the double layer of the clay due to the cation exchange reaction leads an increase in attraction forces and particle flocculation that results in a decrease in liquid limit of the clayey soil after treatment with calcium-based stabilizers (Nalbantoglu and Gucbilmez, 2001). The main reason behind the decrease in LL of Sample A with the addition of 4% L and 10% KFA is probably this phenomenon.

An increase in PL of Sample A was observed after treatment with all types of additives. 15% SFA and 10% KFA treatment made nearly the same effect and approximately 30% increase was observed after fly ash treatment. Maximum increase (57.6%) was observed for 4% L treated sample. Chemical treatment resulted in a decrease in PI of Sample A. 15% SFA, 10% KFA and 4% L treatment caused 8.0%, 18.1% and 39.0 reductions in the PI of Sample A. The decrease in PI increased with

the increase in the CaO content of the additive since both cation exchange and pozzolanic reactions highly depends on the lime content of the additive.

LL, PL, and PI of the sulfate added 4% L, 15% SFA and 10% KFA added samples are presented in Table 6.7, 6.8 and 6.9 respectively with the percent increase/decrease in LL, PL and PI of the chemically treated samples after addition of different sulfate concentrations and types.

Table 6.7. LL, PL, PI of the 4% L and sulfate added samples

Sample	LL (%)	PL (%)	PI (%)	Increase / Decrease after sulfate addition (%)		
				LL	PL	PI
4% L	91.9	39.4	52.5			
4% L + 5000ppm NS	88.9	38.2	50.7	-3.3	-3.0	-3.4
4% L + 10000ppm NS	86	37.1	48.9	-6.4	-5.8	-6.9
4% L + 40000ppm NS	75.3	36.2	39.1	-18.1	-8.1	-25.5
4% L + 5000ppm CS	87.9	40.4	47.5	-4.4	2.5	-9.5
4% L + 10000ppm CS	83.2	39.6	43.6	-9.5	0.5	-17.0
4% L + 40000ppm CS	77.9	38	39.9	-15.2	-3.6	-24.0

Addition of both types of sulfates affected the LL of the 4% L treated sample in a similar way. LL decreased with the addition of sulfate and the decrease rose with the increase in sulfate concentration. LL of the sample decreased by 18.1% and 15.2% with the addition of 40000ppm NS and CS respectively.

PL of the lime treated sample decreased (3% - 8.1%) with NS addition whereas CS addition did not alter the PL value considerably. A decrease in PI value was observed after sulfate addition. The decrease was increased with the rise in sulfate content for both types of sulfates. 40000ppm NS and CS addition made nearly the same effect, 25.5% and 24% decrease were observed respectively. CS was more effective for lower concentrations in reducing the PI and the decrease for 5000ppm and 10000ppm concentrations was higher than that of NS.

Table 6.8. LL, PL, PI of the 15% SFA and sulfate added samples

Sample	LL (%)	PL (%)	PI (%)	Increase / Decrease after sulfate addition (%)		
				LL	PL	PI
15% SFA	112	32.9	79.1			
15% SFA + 3000ppm NS	108.8	34.9	73.9	-2.9	6.1	-6.6
15% SFA + 5000ppm NS	107.9	36.3	71.6	-3.7	10.3	-9.5
15% SFA + 10000ppm NS	106.1	35.0	71.1	-5.3	6.4	-10.1
15% SFA + 20000ppm NS	104.2	33.7	70.5	-7.0	2.4	-10.9
15% SFA + 40000ppm NS	86.9	27.9	59.0	-22.4	-15.2	-25.4
15% SFA + 3000ppm CS	106.1	27.4	78.7	-5.3	-16.7	-0.5
15% SFA + 5000ppm CS	97.7	34.6	63.1	-12.8	5.2	-20.2
15% SFA + 10000ppm CS	92.9	33.7	59.2	-17.1	2.4	-25.2
15% SFA + 20000ppm CS	87.5	33.0	54.5	-21.9	0.3	-31.1
15% SFA + 40000ppm CS	84.0	34.0	50.0	-25.0	3.3	-36.8

LL of 15% SFA treated sample decreased with the addition of both types of sulfate. Addition of 3000ppm, 5000ppm, 10000ppm and 20000ppm NS made nearly the same effect although extra slight decrease was observed with an increase of sulfate concentration. Among NS added samples, decrease made a peak for 40000ppm concentration. The increase of sulfate concentration to 40000ppm resulted in 22.4% decrease in LL of 15% SFA treated sample. The decrease rose with the increase in sulfate concentration for CS added samples. Although the addition of 40000ppm concentration nearly made the same effect for both types of sulfates, the effect of CS was higher for other concentrations. PL of 15% SFA treated sample increased with the addition of 3000ppm, 5000ppm, 10000ppm and 20000ppm NS, however, increase of sulfate concentration to 40000ppm resulted a decrease. PL of the sample decreased 16.7% with the addition of 3000ppm CS whereas the other concentrations of CS did not affect the PL considerably. Similar to LL, PI of the sample decreased with the addition of sulfate except for 3000ppm CS. This concentration did not alter the PI of the sample. 25.4% decrease in PI was obtained for 40000ppm NS and 6.6-10.9% decrease was observed for other NS concentrations. Although the addition of 3000ppm CS did not alter the PI, other concentrations resulted considerable decrease.

The decrease increased with the rise in CS content and 40000ppm sulfate concentration caused a 36.7% decrease.

Table 6.9. *LL, PL, PI of the 10% KFA and sulfate added samples*

Sample	LL (%)	PL (%)	PI (%)	Increase / Decrease after sulfate addition (%)		
				LL	PL	PI
10% KFA	102.8	32.4	70.4			
10% KFA + 3000ppm NS	92.8	36.9	55.9	-9.7	13.9	-20.6
10% KFA + 5000ppm NS	90.7	36.0	54.7	-11.8	11.1	-22.3
10% KFA + 10000ppm NS	90.1	34.7	55.4	-12.4	7.1	-21.3
10% KFA + 20000ppm NS	85.0	33.7	51.3	-17.3	4.0	-27.1
10% KFA + 40000ppm NS	82.1	33.4	48.7	-20.1	3.1	-30.8
10% KFA + 3000ppm CS	97.8	32.4	65.4	-4.9	0.0	-7.1
10% KFA + 5000ppm CS	97.3	35.1	62.2	-5.4	8.3	-11.6
10% KFA + 10000ppm CS	98.2	34.9	63.3	-4.5	7.7	-10.1
10% KFA + 20000ppm CS	95.9	34.8	61.1	-6.7	7.4	-13.2
10% KFA + 40000ppm CS	94.5	35.0	59.5	-8.1	8.0	-15.5

LL of 10% KFA treated sample decreased with the addition of both types of sulfates. The decrease rose with the increase in sulfate concentration for NS whereas the LL of the sample was not affected much from the increase in sulfate concentration for CS only slight fluctuations were observed. LL of 10% KFA treated sample decreased by approximately 10% after the addition of 3000ppm NS and the decrease reached up to 20% with the increase in sulfate concentration to 40000ppm.

A reverse effect in PL was observed with the addition of sulfate when compared with LL. PL of samples generally increased with sulfate addition. 3000ppm caused the maximum increase among all concentrations for NS and the increase was decreased with the rise of sulfate concentration. Although 3000ppm CS did not alter the PL of the sample, other concentrations caused an approximately 8% increase. The increase of sulfate concentration to a higher value than the 5000ppm affected the PL in a similar way as the 5000ppm did for CS added samples.

The PI of the 10% KFA treated sample decreased after addition of both type of sulfates. The decrease generally increased with the rise in sulfate concentration and maximum reduction was observed for 40000ppm sulfate concentration. The effect of addition of NS was higher than that of CS and even addition of 3000ppm NS resulted more decrease (20.6%) than 40000ppm CS (15.5%).

Studies on the effect of sulfate addition on consistency limits of soils treated with calcium-based stabilizers are very limited in the literature.

Kinuthia et al. (1999) studied on the effect of different sulfates on the consistency limits of lime treated soil. Kaolinite with a LL of 61% and PI of 29% was selected as the main source of clay. 6% lime was selected as optimum lime content and different concentrations of CS, NS,  $K_2SO_4$ ,  $MgSO_4$  were added to the lime treated samples. The results of the tests are presented in Figure 6.1.

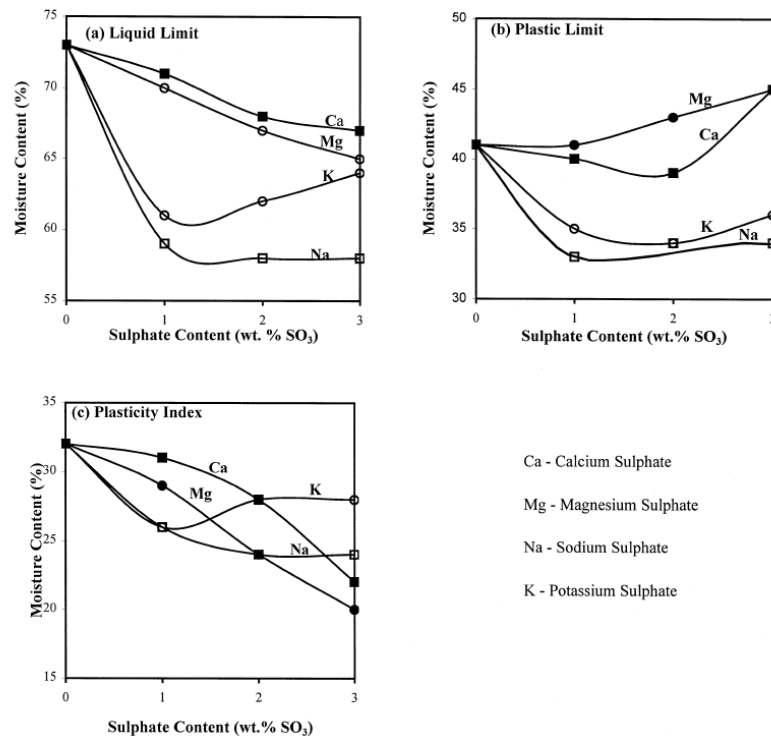


Figure 6.1. Atterberg limits vs. sulfate content for 6% lime treated soil with different metal sulfate addition (Kinuthia et al., 1999)

The addition of sulfate caused a reduction in LL of lime treated soil. The variation in LL was related to the sulfate cations and the monovalent cations (N, K) caused more decrease than the divalent cations (Ca, Mg) did. An increase in PL was observed after the addition of divalent cations while monovalent cations caused a reduction. PI of the lime treated samples decreased after the addition of different concentrations of sulfates. At lower sulfate concentrations monovalent cations resulted in more reduction and with the increase of sulfate level, the effect of divalent cations increased (Kinuthia et al., 1999). The authors also explained the variation in consistency limits for lime treated clay with different sulfate addition by the interactions of the clay particles that are affected by the process of cation exchange.

Yılmaz and Civelekoglu (2009) studied on the effect of gypsum on the stabilization of swelling clay soils. Na bentonite was used as a swelling soil in the study and different quantities of gypsum; 2.5%, 5%, 7.5% and 10% by mass were added to bentonite.

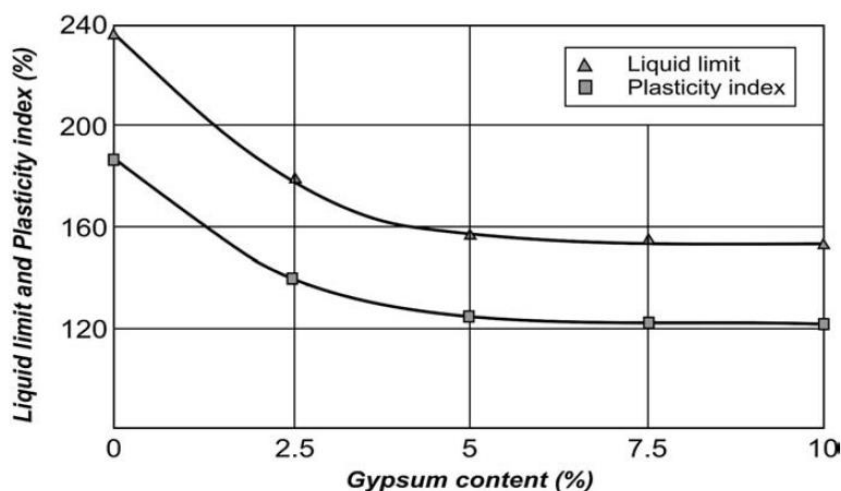


Figure 6.2. Variation of LL and PI with gypsum content (Yılmaz and Civelekoglu, 2009)

A decrease in LL and PI of the samples were observed after addition of gypsum (Figure 6.2). The decrease in LL and PI was explained by the substitution of monovalent sodium by calcium ions that led to a considerable reduction in diffuse double layer thickness by the authors.

Zeta potential of 15% SFA and 10% KFA treated samples increased (in absolute value) after the addition of NS and CS with 10000ppm and 40000ppm concentrations (Figure 5.54) which is a sign of the deterioration of the flocculated structure. Therefore, the consistency limits were probably affected by the pozzolanic reactions besides cation exchange reactions and the effect of pozzolanic reactions were more dominant since an overall reduction in PI was observed.

The increase in zeta potential was less for CS added samples compared to NS added samples for SFA treated soil which may have a contribution to the higher decrease in PI of the CS added samples in contrast to NS added samples with the same concentration.

Wang et al. (1963) explained the decrease in the plasticity of the lime treated soils by the formation of cementitious products which are occurred as a result of the pozzolanic reactions. The study performed by Gadouri et al. (2017) showed the beneficiary effect of the addition of NS (up to some level) on the shear strength of clayey soil stabilized with lime and natural pozzolans as a result of the early pozzolanic reactions.

To sum up, LL of Sample A remained nearly the same after 15% SFA addition, however 10% KFA and 4% L treatment caused a decrease. An increase in PL of Sample A was observed after treatment with all types of additives. Chemical treatment resulted a reduction in PI of Sample A for all additives. LL and PI of the lime and fly ash treated samples decreased with the addition of both type of sulfates. PL of the 4% L treated sample decreased with NS addition whereas CS addition did not alter the PL value considerably. PL of 15% SFA treated sample generally increased with the addition of NS however, it was not affected by CS addition considerably except for

3000ppm concentration. An increase in PL of 10% KFA treated sample was observed after sulfate addition.

### **6.3. Effect of Additives on Shrinkage Limit (SL)**

SL of Sample A, 4% L, 15% SFA, and 10% KFA treated samples were found as 29.5%, 42.5%, 30.1%, and 36.3% respectively.

Considerable increase in SL had been observed for Sample A after 4% L addition, SL of Sample A increased by 44% with lime addition. SL of Sample A remained nearly the same after 15% SFA addition, however, 23% increase was obtained after 10% KFA treatment.

Some basic soil-lime reactions are presented in Section 2.5.1.1.2 (Mallela et. al., 2004). According to these reactions, calcium is one of the main factors that affect the pozzolanic reactions.

Water and temperature are the other leading factors that affect pozzolanic reactions. Water is needed for hydration and the occurrence of pozzolanic reaction and temperature affects the rate of reactions. Higher temperatures (greater than 25-30°C.) cause an increase in the rate of reaction whereas the lower temperature results in the slow proceeding of reactions (Robinson and Thagesen, 2004).

Water, temperature and CaO content are the three important factors affecting the reactions for chemically stabilized soils. Samples were prepared at a water content greater than LL and dried at 105°C. A combination of these three factors for 10% KFA treated samples resulted in the rapid settling of the sample which caused less volume change. However, considerably low CaO content of the SFA was probably not sufficient in increasing the rate of reactions.

Considerable increase in SL of Sample A after lime addition also supports the importance of CaO content in pozzolanic reactions.

SL of sulfate added 4% L, 15% SFA and 10% KFA treated samples are presented in Table 6.10, 6.11, and 6.12 respectively with the percent increase/decrease in the shrinkage limit of stabilized samples after the addition of sulfate.

Table 6.10. *SL of sulfate added 4% L treated samples*

Sample	SL (%)	Increase / Decrease in SL after sulfate addition (%)
4% L	42.5	
4% L + 5000ppm NS	41.6	-2.1
4% L + 10000ppm NS	40.1	-5.6
4% L + 40000ppm NS	37.5	-11.8
4% L + 5000ppm CS	42.9	0.9
4% L + 10000ppm CS	42.9	0.9
4% L + 40000ppm CS	41.9	-1.4

CS addition had not altered the shrinkage limit of 4% L treated sample. Although 5000ppm and 10000ppm NS slightly affected the SL of 4% lime treated soil, an increase of sulfate concentration to 40000ppm resulted in a decrease of 12% in SL of lime treated soil which could be due to the probable ettringite formation.

Table 6.11. *SL of sulfate added 15% SFA treated samples*

Sample	SL (%)	Increase / Decrease in SL after sulfate addition (%)
15% SFA	30.1	
15% SFA + 3000ppm NS	30.4	1.0
15% SFA + 5000ppm NS	30.6	1.7
15% SFA + 10000ppm NS	32.6	8.3
15% SFA + 20000ppm NS	31.5	4.7
15% SFA + 40000ppm NS	31.6	5.0
15% SFA + 3000ppm CS	31.1	3.3
15% SFA + 5000ppm CS	31.2	3.7
15% SFA + 10000ppm CS	32.1	6.6
15% SFA + 20000ppm CS	31.6	5.0
15% SFA + 40000ppm CS	32.8	9.0

SL limit of 15% SFA treated sample slightly changed after the addition of different concentrations of NS and CS. Maximum variation was observed for 40000ppm CS added sample, this sulfate type and concentration resulted 9% increase in SL of 15% SFA treated sample.

Table 6.12. *SL of sulfate added 10% KFA treated samples*

Sample	SL (%)	Increase / Decrease in SL after sulfate addition (%)
10% KFA	36.3	
10% KFA + 3000ppm NS	34.7	-4.4
10% KFA + 5000ppm NS	35	-3.6
10% KFA + 10000ppm NS	37.1	2.2
10% KFA + 20000ppm NS	36.6	0.8
10% KFA + 40000ppm NS	36.4	0.3
10% KFA + 3000ppm CS	36.9	1.7
10% KFA + 5000ppm CS	36.4	0.3
10% KFA + 10000ppm CS	38.3	5.5
10% KFA + 20000ppm CS	37.8	4.1
10% KFA + 40000ppm CS	38.9	7.2

Similar to 15% SFA ash treated sample, SL of 10% KFA treated sample slightly changed after the addition of different concentrations of NS and CS. Maximum variation was observed for 40000ppm CS added sample, this sulfate type and concentration resulted 7.2% increase in SL of 10% KFA treated sample.

In conclusion, SL of Sample A remained nearly the same after 15% SFA addition, however considerable increase was observed after 10% KFA and 4% L treatment. SL of 15% SFA and 10% KFA treated sample slightly changed after the addition of different concentrations of NS and CS. CS addition had not altered the SL of 4% L treated sample. Although 5000ppm and 10000ppm NS slightly affected the SL of 4% L treated sample, an increase of sulfate concentration to 40000ppm resulted in a decrease in SL.

#### 6.4. Effect of Additives on Grain Size Distribution

Hydrometer tests were performed according to ASTM D422 method but with a slight modification as previously described in Section 4.5.6. Silt, clay and total fine content of the sulfate added 4% L, 15% SFA and 10% KFA treated samples are presented in Table 6.13, 6.14, and 6.15 respectively. The values for Sample A are also presented in each table for comparison purposes.

Table 6.13. Grain size distribution for Sample A, 4% L treated, and sulfate added samples

Sample	Fine Content (%)	Silt Content (%)	Clay Content (%)
A	99.76	34.13	65.63
4% L	99.40	42.63	56.77
4% L + 5000ppm NS	99.37	42.12	57.25
4% L + 10000ppm NS	99.43	42.38	57.05
4% L + 40000ppm NS	99.22	44.33	54.89
4% L + 5000ppm CS	99.31	39.14	60.17
4% L + 10000ppm CS	99.2	42.72	56.48
4% L + 40000ppm CS	99.44	38.39	61.05

The addition of lime made the same effect with class C fly ashes on the grain size distribution of Sample A. Decrease in clay content and increase in silt content was observed which resulted in the shifting of grain size distribution curve of Sample A to coarser side. This could be due to the flocculation of clay particles after addition of calcium-based stabilizer. Sulfate addition did not affect the grain size distribution of 4% lime treated sample considerably.

There is an anomaly in the grain size distribution curve of 40000ppm CS added sample compared to other concentrations (Figure 5.20). This is due to the fact that 40000ppm CS added sample hardened and expand. The hydrometer test photo for 40000ppm CS added 4% lime treated is presented in Figure 6.3.



Figure 6.3. Hydrometer view of 40000ppm CS added 4% L treated sample

Table 6.14. Grain size distribution for Sample A, 15% SFA treated and sulfate added samples

Sample	Fine Content (%)	Silt Content (%)	Clay Content (%)
A	99.76	34.13	65.63
15% SFA	97.28	48.70	48.58
15% SFA + 3000ppm NS	96.07	47.42	48.65
15% SFA + 5000ppm NS	95.94	48.62	47.32
15% SFA + 10000ppm NS	95.68	45.98	49.70
15% SFA + 20000ppm NS	95.87	48.46	47.41
15% SFA + 40000ppm NS	96.06	45.76	50.3
15% SFA + 3000ppm CS	96.01	44.95	51.06
15% SFA + 5000ppm CS	96.24	46.34	49.9
15% SFA + 10000ppm CS	95.97	46.32	49.65
15% SFA + 20000ppm CS	96.30	43.8	52.50
15% SFA + 40000ppm CS	96.46	43.88	52.58

The grain size distribution of Sample A shifted to the coarser side after addition of 15% SFA. This is an expected result since fly ashes mostly consist of silt size particles. The addition of calcium-based stabilizers causes flocculation of the clay particles. This could be the secondary effect in decreasing clay content and increasing the silt content of Sample A after fly ash addition. The addition of different concentrations of NS and CS did not affect the grain size distribution of 15% SFA treated sample considerably, only slight fluctuations observed in silt and clay content.

Table 6.15. Grain size distribution for Sample A, 10% KFA treated and sulfate added samples

Sample	Fine Content (%)	Silt Content (%)	Clay Content (%)
A	99.76	34.13	65.63
10% KFA	98.24	39.94	58.30
10% KFA + 3000ppm NS	97.17	42.33	54.84
10% KFA + 5000ppm NS	97.21	46.59	50.62
10% KFA + 10000ppm NS	98.26	42.70	55.56
10% KFA + 20000ppm NS	97.64	43.84	53.8
10% KFA + 40000ppm NS	97.37	36.34	61.03
10% KFA + 3000ppm CS	98.3	40.93	57.37
10% KFA + 5000ppm CS	97.57	42.03	55.54
10% KFA + 10000ppm CS	97.07	39.56	57.51
10% KFA + 20000ppm CS	97.05	37.70	59.35
10% KFA + 40000ppm CS	97.24	39.35	57.89

The grain size distribution of Sample A shifted to the coarser side after addition of 10% KFA similar to 15% SFA treated sample. Although total fine content did not alter much, a slight fluctuation in silt and clay content of the sample was observed after sulfate addition. However, the changes are ignorable. An anomaly was observed in the grain size distribution curve of 40000ppm CS added sample compared to other concentrations similar to 40000ppm CS added 4% L treated sample (Figure 5.24).

In conclusion, the grain size distribution of Sample A shifted to the coarser side after addition of 15% SFA, 10% KFA and 4% L. The addition of different concentrations of NS and CS did not affect the grain size distribution of fly ash and lime treated samples considerably, only slight fluctuations observed in silt and clay content. Anomalies were observed at the grain size distribution curves of 40000ppm CS added 10% KFA and 4% L treated samples. This was thought to be due to the low solubility of gypsum 2.5 g/L. Although water used in compaction procedure of specimens (24.5%) is not enough for all CS to dissolve, high amount of water used in hydrometer analyses allowed to dissolve all CS and caused ettringite related reactions.

## **6.5. Effect of Additives on Swell Percentage**

### **6.5.1. Effect of Additives on Swell Percentage of Specimen A**

The effect of addition of different concentrations of two different fly ashes (5%, 10%, 15%, and 20%) and lime (2%, 3%, 4%, and 5%) was investigated during the study. The swell potential of the specimens with different type and concentration of additives are presented in Table 6.16 with the percent variation in swell potential of specimen A. The additives are non-plastic materials, therefore some of the reduction in swell potential was due to the replacement of swelling soil with non-swelling material. This reduction was calculated by the percent mass of the additive in the total mixture as a rough estimation. The remaining swell decrease considered to be due to the chemical reactions. The share of each effect on total decrease was also presented in Table 6.16.

Table 6.16. Swell percent for fly ash and lime treated expansive soil

Specimen	Swell Percent, $\Delta H/H$ (%)	Increase / Decrease in Swell Potential after fly ash and lime addition (%)		
		total	due to replacement of non-swelling material	due to chemical reactions
A	112.9	-	-	-
2% L	38.5	-65.9	-2.0	-63.9
3% L	24.8	-78.0	-2.9	-75.1
4% L	25.5	-77.4	-3.8	-73.6
5% L	26.2	-76.8	-4.8	-72.0
5% SFA	55.3	-51.0	-4.8	-46.2
10% SFA	36.3	-67.8	-9.1	-58.7
15% SFA	31.2	-72.4	-13.0	-59.4
20% SFA	28.0	-75.2	-16.7	-58.5
5% KFA	24.5	-78.3	-4.8	-73.5
10% KFA	26.5	-76.5	-9.1	-67.4
15% KFA	33.2	-70.6	-13.0	-57.6
20% KFA	34.5	-69.4	-16.7	-52.7

The swell potential of Specimen A decreased with lime addition. 2% L decreased swell potential by 65.9%, increasing the lime content to 3% caused further reduction in swell percent. Swell percent of 3%, 4% and 5% L treated samples were very close to each other, this could be due to the carbonation reactions. Although 3% L was the optimum lime content, 4% L was chosen as optimum lime content to make the CaO content higher and to be able to see the ettringite effect better.

Addition of SFA to the Specimen A decreased the swell potential considerably, the decrease of swell potential increased with the increase in fly ash content. However, further increase of fly ash content from 10% did not affect the swell potential when the net decreases that are considered to occur due to chemical reactions, are taken into account. 10%, 15% and 20% fly ash content made nearly the same effect in terms of net decreases. Therefore, it can be stated that optimum fly ash content for SFA is 10%.

The calcium content of the additive is an important factor for sulfate bearing soils, therefore 15% was chosen as optimum SFA content for this study with the aim of increasing calcium content in the mixture.

Similar effect with SFA was observed after the addition of KFA to the Specimen A. Swell potential considerably decreased with the addition of fly ash. Maximum reduction was observed for 5% fly ash content and a further increase in fly ash amount increased the swell potential. This could be the result of the high SO<sub>3</sub> content of the KFA. In terms of the total decrease in swell potential 5% and 10% fly ash addition nearly made the same effect although a slight increase was observed when the concentration increased from 5% to 10%. As in SFA, to make the calcium content in the mixture high, 10% fly ash was chosen as the optimum value.

Although all additives resulted in a decrease in the swell potential of expansive soil, it can be stated that the beneficiary effect of KFA and lime was higher than that of SFA according to the percent decreases in swell potential for 5% concentrations. It was due to the relatively low calcium content of SFA compared to other additives since both short term and long-term chemical reactions are dependent on the calcium content. As the calcium content of lime (83.7%) is higher than KFA (29.5%), it was expected that lime would result in more decrease in swell potential than the KFA for the same concentration. However, the results were not as expected, their effects were nearly same, addition of 5% L and 5% KFA caused 76.8% and 78.3% decrease in swell potential of Specimen A. This was probably due to the carbonation reactions that occur when the excessive amount of calcium exists at the environment as previously discussed for 5% L and self- pozzolanic properties of class C fly ashes.

#### **6.5.2. Effect of Sulfate on Swell Potential of Chemically Treated Soils**

Primary tests were performed on 5000ppm, 10000ppm and 40000ppm NS and CS added 4% L treated specimens to see the effect of sulfate on swelling soil treated with calcium-based stabilizers. Then main tests were performed on NS and CS added 15% SFA and 10% KFA treated specimens. 3000ppm, 5000ppm, 10000ppm,

20000ppm and 40000ppm sulfate concentrations were used. Since temperature is one of the main factors affecting the ettringite formations, tests were performed at a constant temperature of 25°C.

Test results are tabulated in Table 6.17, 6.18 and 6.19 with the percent decrease/increases in the swell percentage of chemically treated specimens after the addition of different sulfate concentrations for 4% L, 15% SFA and 10% KFA treated specimens respectively.

Table 6.17. Swell percent for sulfate added 4% L treated specimens

Specimen	Swell Percent, $\Delta H/H$ (%)	Decrease / Increase in Swell Potential after sulfate addition (%)
4% L	25.5	
4% L + 5000ppm NS	26.4	3.5
4% L + 10000ppm NS	29.8	16.9
4% L + 40000ppm NS	27.9	9.4
4% L + 5000ppm CS	28.1	10.2
4% L + 10000ppm CS	31.8	24.7
4% L + 40000ppm CS	29.5	15.7

Swell percentage of 4% L treated specimen generally increased after addition of different concentrations of sulfate except for 5000ppm NS concentration, for this concentration it remained nearly same only a 3.5% increase had been observed. Addition of 10000ppm and 40000ppm NS resulted in 16.9 and 9.4% increase in swell potential respectively.

The addition of CS affected swell potential more than that of NS. 10.2%, 24.7%, and 15.7% increase in the swell potential of 4% lime treated specimen had been observed after the addition of 5000ppm, 10000ppm and 40000ppm sulfate concentrations.

For both sulfate type, 10000ppm sulfate concentration affected the swell potential more considerably.

Table 6.18. Swell percent for sulfate added 15% SFA treated specimens

Specimen	Swell Percent, $\Delta H/H$ (%)	Decrease in Swell Potential after sulfate addition (%)
15% SFA	31.2	
15% SFA + 3000ppm NS	30.6	-1.9
15% SFA + 5000ppm NS	28.8	-7.7
15% SFA + 10000ppm NS	25.6	-17.9
15% SFA + 20000ppm NS	25.1	-19.6
15% SFA + 40000ppm NS	17.7	-43.3
15% SFA + 3000ppm CS	27.0	-13.5
15% SFA + 5000ppm CS	23.3	-25.3
15% SFA + 10000ppm CS	24.1	-22.8
15% SFA + 20000ppm CS	22.5	-27.9
15% SFA + 40000ppm CS	20.4	-34.6

Swell potential of 15% SFA treated specimen decreased with the addition of both types of sulfate except for 3000ppm NS. The swelling potential of the specimen nearly remained same for this concentration of NS however, further increase in sulfate concentration resulted a decrease in swell potential. 5000ppm NS caused 7.7% reduction and a decrease in the swell potential increased with the increase in NS concentration.

5000ppm, 10000ppm and 20000ppm CS addition made nearly the same effect, however, increase of sulfate concentration to 40000ppm further decreased the swell potential.

The beneficiary effect of sulfate addition in decreasing the swell potential was higher for CS than that of NS up to 20000ppm sulfate concentration. When the sulfate concentration was increased to 40000ppm, the maximum reduction was observed for NS added specimen. Swell percent of 15% SFA treated specimen decreased by 43.3% and 34.6% with the addition of 40000ppm NS and CS respectively.

Table 6.19. Swell percent for sulfate added 10% KFA treated specimens

Specimen	Swell Percent, $\Delta H/H$ (%)	Decrease/ Increase in Swell Potential after sulfate addition (%)
10% KFA	26.5	
10% KFA + 3000ppm NS	28.5	7.5
10% KFA + 5000ppm NS	27.5	3.8
10% KFA + 10000ppm NS	29.4	10.9
10% KFA + 20000ppm NS	28.9	9.1
10% KFA + 40000ppm NS	24.6	-7.2
10% KFA + 3000ppm CS	27.8	4.9
10% KFA + 5000ppm CS	25.7	-3.0
10% KFA + 10000ppm CS	27.3	3.0
10% KFA + 20000ppm CS	25.8	-2.6
10% KFA + 40000ppm CS	26.4	-0.4

The swell potential of 10% KFA treated specimen slightly increased up to 20000ppm sulfate concentration with the addition of NS. 3000ppm, 5000ppm, 10000ppm and 20000ppm caused 7.5%, 3.8%, 10.9% and 9.1% increase in swell potential respectively however 40000ppm sulfate addition caused 7.2% reduction in swell potential of fly ash treated specimen.

The swell potential of the specimen remained nearly the same or slightly change with the addition of CS. The swell potential of 10% KFA changed by 2.6-4.9% with the addition of 3000ppm to 20000ppm concentrations and remained the same for 40000ppm concentration of CS.

Sulfate addition affected the fly ash and lime treated specimens differently. Although a general increase was observed in the swell potential of 4% L treated specimen, the swell potential of 15% SFA treated specimen decreased considerably with the addition of both types of sulfates. Swell potential of 10% KFA treated specimen was not affected much from the sulfate addition especially for CS. The variation in the effect of sulfate was probably due to the CaO content of the additives, as ettringite formation highly depends on calcium exists in the environment. The rate and amount of ettringite

formation generally increase with the increase in calcium content. Also, the high sulfate content of KFA had probably adverse effect on swell properties.

40000ppm CS and NS added fly ash treated specimens that were exposed to 100 days testing period showed that any significant change had not been observed in swell potential in long term (Figure 5.32).

### **6.5.3. Swell Tests at 10°C and 40°C**

Swelling tests were also performed at 10°C and 40°C to see the effect of temperature on swell properties. 5000ppm, 10000ppm and 40000ppm sulfate concentrations were chosen as the representative concentrations and tests were performed on these specimens.

Test results are tabulated in Table 6.20 and 6.21 for 15% SFA and 10% KFA treated specimens respectively with the percent decrease/increases in the swell percentage of fly ash treated specimen and sulfate added fly ash treated specimens at 10°C and 40°C compared to 25°C.

Table 6.20. Swell percent for sulfate added 15% SFA treated specimens at 10°C, 25°C and 40°C

Specimen	Temperature	Swell Percent, $\Delta H/H$ (%)	Percent Increase / Decrease in swell percent with respect to 25°C
15% SFA	10°C	36.3	16.3
	25°C	31.2	
	40°C	30.2	-3.2
15% SFA + 5000ppm NS	10°C	31.9	10.8
	25°C	28.8	
	40°C	28.7	-0.3
15% SFA + 10000ppm NS	10°C	28.4	10.9
	25°C	25.6	
	40°C	28.4	10.9
15% SFA + 40000ppm NS	10°C	24	35.6
	25°C	17.7	
	40°C	19.8	11.9
15% SFA + 5000ppm CS	10°C	27.6	18.5
	25°C	23.3	
	40°C	23.8	2.1
15% SFA + 10000ppm CS	10°C	25.7	6.6
	25°C	24.1	
	40°C	23.1	-4.1
15% SFA + 40000ppm CS	10°C	22.5	10.3
	25°C	20.4	
	40°C	22.5	10.3

Swell potential of 15% SFA treated specimen and the sulfate added specimens increased with the decrease of temperature from 25°C to 10°C. 16.3% increase was observed for 15% SFA treated specimen. The highest increase (35.6%) had been observed for 40000ppm NS added specimen within the sulfate added specimens that provided the maximum beneficiary effect in reducing the swell potential of fly ash treated specimen at 25°C. Decreasing the temperature made nearly the same effect in remaining sulfate added specimens, an average increase of approximately 10% had been observed in the swell potential of the aforementioned specimens.

Swell potential of 15% SFA treated specimen changed slightly with the increase of temperature from 25°C to 40°C. 3.2% decrease in swell potential had been observed for this specimen which was ignorable. The increase of temperature from 25°C to 40°C also caused a slight fluctuation (0.3-4.1%) in swell potential of 5000ppm NS, 5000ppm CS and 10000ppm CS added specimens. Rise in temperature also caused an approximately 10% increase in the swell potential of 10000ppm NS, 40000ppm NS and 40000ppm CS added specimens. It could be stated that the increase of temperature from 25°C to 40°C did not cause a dramatic change in the swell potential of the specimens, only a slight increase/decrease had been observed. These could be the result of the fact that 25°C is sufficient for most of the chemical reactions to occur and further increase of temperature does not affect the result much also small increases (10%) in swell potential of 10000ppm NS, 40000ppm NS, and 40000ppm CS could be a sign of ettringite formation.

Cation exchange, flocculation, pozzolanic reactions, and carbonation are the leading mechanisms that result improvement of engineering properties of soils when clayey soils are mixed with lime in an aqueous medium (Little, 1995; West and Carder, 1997; Al-Rawas, 2005). One of the main factors affecting the rate of reactions is temperature. The rate of reactions increases with the rise in temperature (Robinson and Thagesen, 2004).

The study on the effect of curing time and temperature on the  $q_u$  of lime and fly ash treated soil that was performed by Beeghly (2003) showed the importance of temperature on the rate of chemical reactions. The results of the study were summarized in Table 6.21.

Table 6.21. Change in  $q_u$  according to curing conditions (Beeghly, 2003)

Specimen	Curing Conditions		$q_u$ (kPa)
	Time	Temperature	
4% L + 8% FA	3 day	50°C	1517
	7 day	40°C	1241
	28 day	22°C	1172
	56 day	22°C	1379

Both rise in curing time and temperature caused an increase in the strength. Soil that had no sulfate concentration was used during the study of Beeghly (2003).

Temperature is also the major cause of swelling in kaolinite or montmorillonite mixtures under sulfate environments, and the rate of ettringite formation and swelling would be greater during summer (Rajasekaran, 2005).

Therefore, the increase in swell potential at 10°C could be explained by the decrease in the rate of beneficial chemical reactions at lower temperatures that results in higher swelling percentages.

Table 6.22. Swell percent for sulfate added 10% KFA treated specimens at 10°C, 25°C and 40°C

Specimen	Temperature	Swell Percent, $\Delta H/H$ (%)	Percent Increase / Decrease in swell percent with respect to 25°C
10% KFA	10°C	29.6	11.7
	25°C	26.5	
	40°C	28.5	7.5
10% KFA + 5000ppm NS	10°C	31.7	15.3
	25°C	27.5	
	40°C	27.2	-1.1
10% KFA + 10000ppm NS	10°C	33.7	14.6
	25°C	29.4	
	40°C	27.8	-5.8
10% KFA + 40000ppm NS	10°C	29.6	20.3
	25°C	24.6	
	40°C	26.6	8.1
10% KFA + 5000ppm CS	10°C	29.3	14.0
	25°C	25.7	
	40°C	28.7	11.7
10% KFA + 10000ppm CS	10°C	29.2	7.0
	25°C	27.3	
	40°C	26.1	-4.4
10% KFA + 40000ppm CS	10°C	27.7	4.9
	25°C	26.4	
	40°C	24.7	-6.4

A similar trend with 15% SFA treated specimens had been observed with 10% KFA treated specimens. Swell potential of specimen increased with the decrease of temperature from 25°C to 10°C. 11.7% increase in swell potential was observed for 10% KFA treated specimen. The swell potential of NS added specimens were affected more than the CS added ones from the temperature decrease. Swell potential of 5000ppm, 10000ppm and 40000ppm NS added specimens increased by 15.3%, 14.6% and 20.3% respectively. However, swell potential of 5000ppm, 10000ppm and 40000ppm CS added specimens increased by 14.0%, 7.0% and 4.9% respectively.

Swell potential of 10% KFA treated specimen increased by 7.5% with the increase of temperature from 25°C to 40°C. This could be due to the high sulfate content of this fly ash. A slight decrease in swell potential had been observed for 5000ppm NS, 10000ppm NS, 10000ppm CS, and 40000ppm CS added specimens. Swell percentage of these specimen decreased by 1.1% - 6.4% with temperature increase. However, the swell potential of 40000ppm NS and 5000ppm CS added specimens increased by 8.1% and 11.7% respectively.

All specimens affected more from the temperature decrease than the increase.

#### **6.5.4. Swell Tests for 7 days and 28 days Cured Specimens**

Swelling tests were also performed at 7 days and 28 days cured specimens to see the effect of curing. The curing temperature was chosen as 25°C. 5000ppm, 10000ppm and 40000ppm sulfate concentrations were chosen as the representative concentrations and tests were performed on these specimens.

Test results are tabulated in Table 6.23 and 6.24 for 15% SFA and 10% KFA treated specimens respectively with the percent decrease/increases in the swell percentage of fly ash treated specimen and sulfate added fly ash treated specimens after curing. Percent decrease/increases in swell percentage are also tabulated for the increase of curing period from 7 days to 28 days.

Table 6.23. Swell percent for sulfate added 15% SFA treated specimens cured at 25°C for 7 and 28 days

Specimen	Curing Period	Swell Percent, $\Delta H/H$ (%)	Percent Increase / Decrease in Swell Percent after curing (%)	Percent Increase / Decrease in Swell Percent after increase in curing period from 7 days to 28 days (%)
15% SFA	0	31.2		
	7	28.7	-8.0	
	28	26.4	-15.4	-8.0
15% SFA + 5000ppm NS	0	28.8		
	7	25.3	-12.2	
	28	27.5	-4.5	8.7
15% SFA + 10000ppm NS	0	25.6		
	7	21.2	-17.2	
	28	21.5	-16.0	1.4
15% SFA + 40000ppm NS	0	17.7		
	7	19.3	9.0	
	28	19.7	11.3	2.1
15% SFA + 5000ppm CS	0	23.3		
	7	22.8	-2.1	
	28	22.8	-2.1	0.0
15% SFA + 10000ppm CS	0	24.1		
	7	20.4	-15.4	
	28	21.4	-11.2	4.9
15% SFA + 40000ppm CS	0	20.4		
	7	19.6	-3.9	
	28	20.2	-1.0	3.1

As can be seen in Table 6.23, the swell potential of the 15% SFA treated specimen decreased by 8% after curing 7 days at 25°C. The increase of curing time from 7 days to 28 days resulted in a further decrease in swell potential. Swell potential of 15% SFA treated specimen decreased by 15.4% after 28 days curing period.

Swell potential of sulfate added specimens except for 5000ppm CS, 40000ppm CS and 40000ppm NS added specimens decreased after curing 7 days at 25°C. However,

swell potential of 40000ppm NS added specimen increased by 9% after 7 days curing period and that of 5000ppm CS and 40000ppm CS specimens nearly remained the same.

A similar trend was observed for 28 days curing period for all sulfate added specimens with the 7 days one. Increase of curing period from 7 days to 28 days did not affect the swell potential of sulfate added specimens considerably, therefore it could be stated that 7 days curing period was sufficient for completion of most of the reactions for sulfate added specimens.

The decrease of the swell potential with curing could be explained by the pozzolanic reactions which are time and temperature-dependent chemical reactions.

The beneficiary effect of curing had been observed by many researchers such as Cokca (2001), Nalbantoglu and Gucbilmez (2001), Ansary et al., (2003), on reducing the swell potential for fly ash treated specimens. Cokca (2001) attributed the decrease in swelling potential due to curing to the time-dependent pozzolanic and self-hardening properties (formation of cementitious compounds) of fly ashes.

An increase in the swell potential of the 40000ppm NS added specimens could be due to the probable ettringite formation.

Table 6.24. Swell percent for sulfate added 10% KFA treated specimens cured at 25°C for 7 and 28 days

Specimen	Curing Period	Swell Percent, $\Delta H/H$ (%)	Percent Increase / Decrease in Swell Percent after curing (%)	Percent Increase / Decrease in Swell Percent after an increase in curing period from 7 days to 28 days (%)
10% KFA	0	26.5		
	7	26.4	-0.4	
	28	25.0	-5.7	-5.3
10% KFA + 5000ppm NS	0	27.5		
	7	26.8	-2.5	
	28	26.9	-2.2	0.4
10% KFA + 10000ppm NS	0	29.4		
	7	26.9	-8.5	
	28	26.4	-10.2	-1.9
10% KFA + 40000ppm NS	0	24.6		
	7	21.9	-11.0	
	28	23.2	-5.7	5.9
10% KFA + 5000ppm CS	0	25.7		
	7	25.3	-1.6	
	28	24.7	-3.9	-2.4
10% KFA + 10000ppm CS	0	27.3		
	7	25.7	-5.9	
	28	24.0	-12.1	-6.6
10% KFA + 40000ppm CS	0	26.4		
	7	24.3	-8.0	
	28	21.8	-17.4	-10.3

Swell potential of 10% KFA treated specimen remained nearly the same after 7 days curing period, this could be the result of the high sulfate content of the KFA. However, a 5.7% reduction in swell potential had been observed for this specimen after 28 days curing period.

The swell potential of all the sulfate added specimens decreased after 7 and 28 days curing periods however, the decrease was ignorable for 5000ppm sulfate

concentrations. Swell potential of 10000ppm NS added specimen remained nearly the same when the curing time increased from 7 days to 28 days, however, a slight increase in swell potential had been observed for 28 days cured 40000ppm NS added sample compared to 7 days curing condition.

The swell potential of 10000ppm and 40000ppm CS added specimens decreased by 5.9% and 8% respectively after 7 days curing period. An increase in curing time to 28 days resulted in a further decrease in the swell potential of these specimens and the total decrease in swell potential reached up to 12.1% and 17.4% respectively.

The results of the swelling tests could be summarized as presented below;

- 4% L, 15% SFA and 10% KFA addition resulted the decrease of swelling potential of Sample A approximately to one fourth of its initial value.
- Sulfate addition affected the swell potential of the fly ash and lime treated specimens differently. Although not dramatic, a general increase was observed in the swell potential of 4% L treated specimen after sulfate addition. The swell potential of 15% SFA treated specimen decreased considerably with the addition of both types of sulfates. Swell potential of 10% KFA treated specimen was not affected much from the sulfate addition, especially for CS.
- The reduction of temperature from 25°C to 10°C caused an increase in the swell potential of fly ash treated and sulfate added fly ash treated specimens. The highest increase had been observed for 40000ppm NS added specimen within the sulfate added specimens for both 15% SFA and 10% KFA treated specimens.
- The increase of temperature from 25°C to 40°C did not generally affect the swell potential of 15% SFA treated specimen and the specimens with low concentrations of sulfate (5000ppm NS, 5000ppm CS, and 10000ppm CS). The rise in temperature caused an approximately 10% increase in the swell potential of 10000ppm NS, 40000ppm NS, and 40000ppm CS added specimens.

- A slight increase in swell potential of 10% KFA treated specimen was observed with the increase of temperature from 25°C to 40°C. The sulfate added 10% KFA treated specimens were not affected much from the temperature increase except for 40000ppm NS and 5000ppm CS. Average increase of 10% was observed in the swell potential of these two specimens.
- Swelling potential of all specimens affected more from the temperature decrease than the increase.
- Curing had a beneficiary effect in reducing the swell potential of 15% SFA treated specimen. The swell potential of sulfate added specimens remained nearly the same or slightly decreased after 7 days curing period except for 40000ppm NS. A slight increase in swell percent was observed for this concentration of NS. Although the rise in curing period affected the 15% SFA treated specimen positively, sulfate added specimens were not generally affected by the increase in the curing period.
- Swell potential of 10% KFA treated specimen was not affected considerably from the curing, however swell potential of sulfate added specimens generally decreased after 7 days curing period. An increase in curing period did not affect the sulfate added specimens except for 10000ppm and 40000ppm CS. Further reduction in swell potential was provided for these two specimens with the rise of the curing period from 7 days to 28 days.

## **6.6. Effect of Additives on Strength**

### **6.6.1. Effect of Additives on Strength of Specimen A**

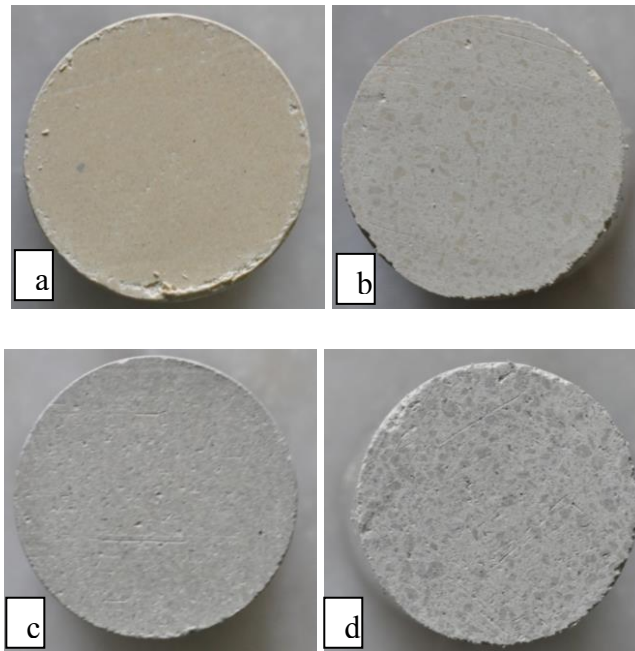
The effect of addition of 4% L, 15% SFA and 10% KFA were investigated during the study. The  $q_u$  of the specimens with different types and concentrations of additives are presented in Table 6.25 with the percent variation in  $q_u$  of specimen A.

Table 6.25.  $q_u$  for Specimen A, fly ash and lime treated soils

Specimen	$q_u$ (kPa)	Increase / Decrease in $q_u$ after fly ash and lime addition (%)
A	595.3	
4% L	914.6	53.6
15% SFA	595.9	0.1
10% KFA	762.4	28.1

$q_u$  of Specimen A remained nearly the same after 15% SFA treatment. However, addition of 10% KFA and 4% L resulted 28.1% and 53.6% increase in  $q_u$  of Specimen A. Lime resulted the maximum increase in  $q_u$  with its highest CaO content and SFA that had considerably low calcium content did not affect the  $q_u$  of the specimen A since the chemical reactions causing the strength increase in soils that are treated with calcium-based stabilizers are directly related to the calcium content. Besides chemical reactions, the sample preparation method has also effect on  $q_u$  of the specimens. Therefore, to be able to see the effect, two methodologies were used in soil + water mixing. The first method was named as Sieved and in this method, all the samples were sieved through #30 and #16 sieves. This was the selected procedure used during the study. The second method was called as Non-Sieved, in this method materials were mixed with water, and the mixture was slightly crushed but not sieved, it was only mixed thoroughly. In both methods, samples were waited at least one hour at the desiccator after mixing with water before compaction. Dry sample preparation and compaction procedures were the same for both methods. The tests were performed on Specimen A, 15% SFA and 10% KFA treated specimens.

The photos of Specimen A and 10% KFA treated specimens prepared by Sieved and Non-Sieved Method are presented in Figure 6.4



*Figure 6.4.* Photos of specimens a- Specimen A (sieved), b- Specimen A (non-sieved), c- 10% KFA treated soil (sieved), d-10% KFA treated soil (non-sieved)

As can be seen from the figure, non-sieved specimens showed a more heterogeneous structure. The darker parts of the specimens were due to the higher water content of the particles at these parts.

Results of the  $q_u$  tests were presented in Figure 6.5, 6.6 and 6.7 for Specimen A, 15% SFA and 10% KFA ash treated specimens accordingly.

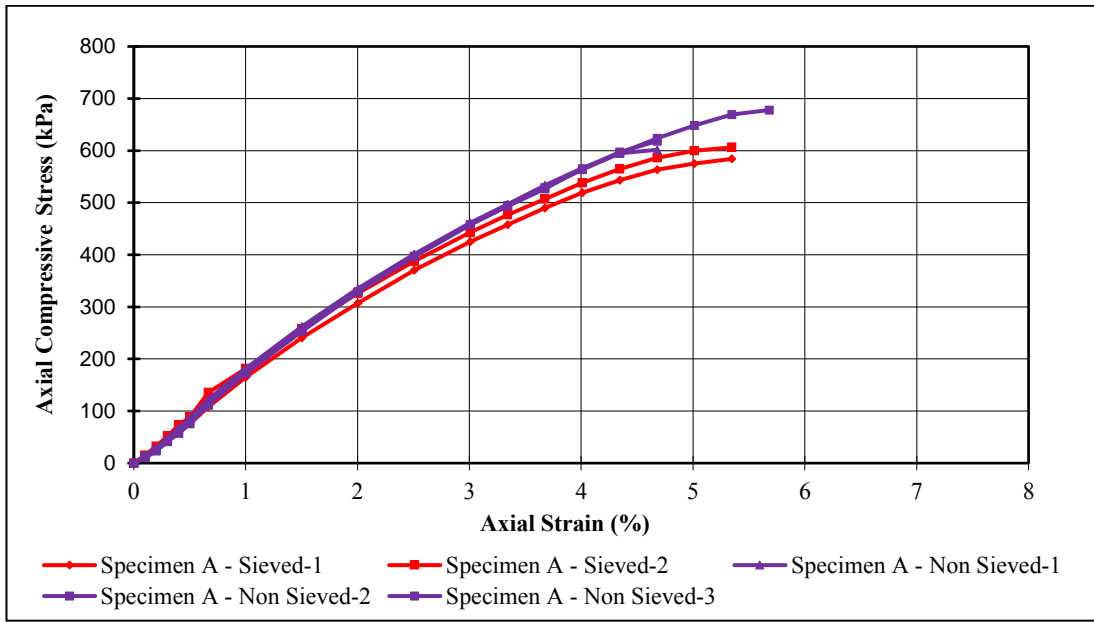


Figure 6.5.  $q_u$  test results for Specimen A

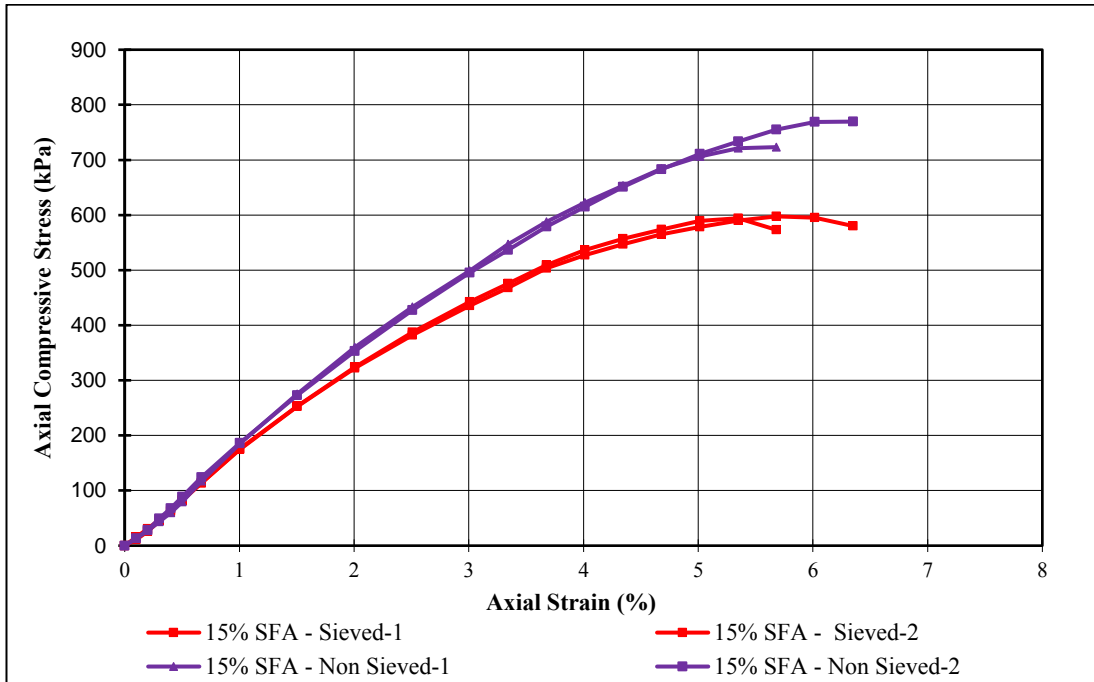


Figure 6.6.  $q_u$  test results for 15% SFA treated specimen

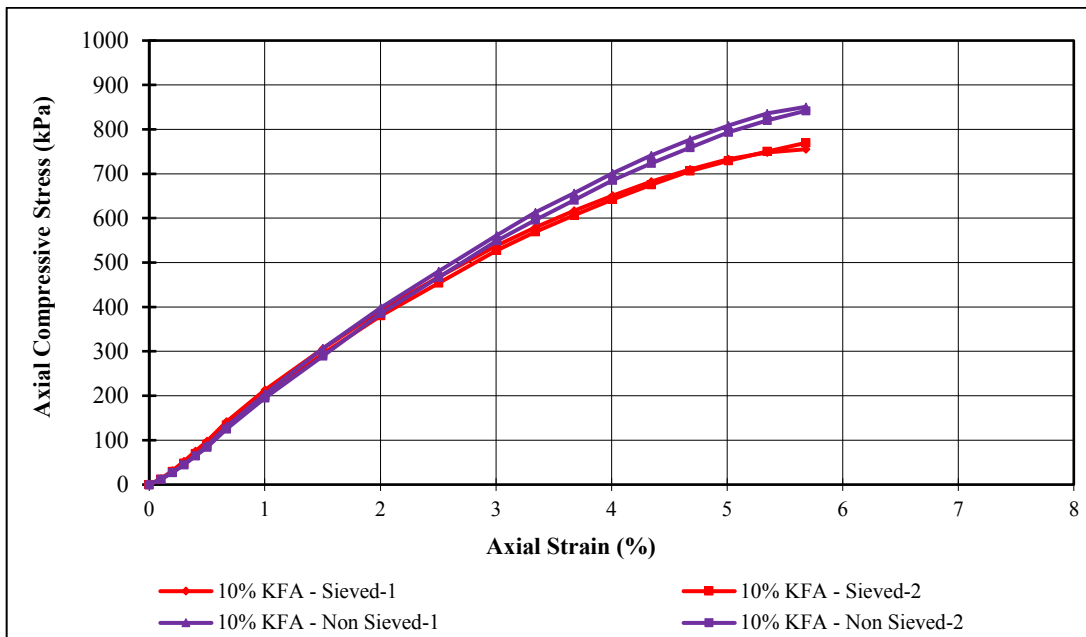


Figure 6.7.  $q_u$  test results for 10% KFA treated specimen

Results of the  $q_u$  tests for the specimens prepared by two different methods are summarized in Table 6.26.

Table 6.26.  $q_u$  for sieved and non-sieved specimens

Specimen	Average $q_u$ (kPa)	
	Sieved	Non-Sieved
A	595.3	633.0
15% SFA	595.9	746.5
10% KFA	762.4	846.4

Specimens that were prepared by non-sieved method had higher strengths than sieved ones. This could be results of the fact that in the sieved method, the mixture was crushed and sieved through #30 sieve and this could affect the flocculation of the particles and could cause a more dispersed structure for fly ash treated specimens.

Chemical stabilization consists of pulverization of soil, spreading additive, water addition, mixing and compaction steps (National Lime Association, 2004). The soil-additive mixture is not sieved at field application, however sieved method was chosen in this study to be able to obtain more homogenous specimens.

#### **6.6.2. Effect of Sulfate on Strength of Chemically Treated Soils**

Primary tests were performed on 5000ppm, 10000ppm and 40000ppm NS and CS added 4% L treated specimens to see the effect of sulfate on soil treated with calcium-based stabilizers. Then main tests were performed on NS and CS added 15% SFA and 10% KFA treated specimens. 3000ppm, 5000ppm, 10000ppm, 20000ppm and 40000ppm sulfate concentrations were used. Since temperature is one of the main factors affecting the ettringite formations, specimen preparations and tests were performed at a constant temperature of approximately 25°C.

Test results are tabulated in Table 6.27, 6.28 and 6.29 with the percent decrease/increases in  $q_u$  of chemically treated specimens after the addition of different sulfate concentrations for 4% L, 15% SFA and 10% KFA treated specimens respectively.

Table 6.27.  $q_u$  for sulfate added 4% L treated specimens

Specimen	$q_u$ (kPa)	Increase / Decrease in $q_u$ after sulfate addition (%)
4% L	914.6	
4% L + 5000ppm NS	999.1	9.2
4% L + 10000ppm NS	931.6	1.9
4% L + 40000ppm NS	661.9	-27.6
4% L + 5000ppm CS	951.3	4.0
4% L + 10000ppm CS	1014.1	10.9
4% L + 40000ppm CS	1021.1	11.6

Strength values of 4% L treated specimen generally slightly increased or remained nearly the same after addition of both types of sulfates at different concentrations except for 40000ppm NS. 27.6% decrease in  $q_u$  observed for this sulfate concentration which was thought to be a probable cause of ettringite formation. 10000ppm NS and 5000ppm CS did not affect the strength values considerably and addition of 5000ppm NS, 10000ppm CS and 40000ppm CS resulted an average increase of 10% in  $q_u$  of 4% L treated soil.

Table 6.28.  $q_u$  for sulfate added 15% SFA treated specimens

Specimen	$q_u$ (kPa)	Increase / Decrease in $q_u$ after sulfate addition (%)
15% SFA	595.9	
15% SFA + 3000ppm NS	613	2.9
15% SFA + 5000ppm NS	582	-2.3
15% SFA + 10000ppm NS	551.7	-7.4
15% SFA + 20000ppm NS	539.1	-9.5
15% SFA + 40000ppm NS	456.1	-23.5
15% SFA + 3000ppm CS	646	8.4
15% SFA + 5000ppm CS	671.5	12.7
15% SFA + 10000ppm CS	605.9	1.7
15% SFA + 20000ppm CS	606.4	1.8
15% SFA + 40000ppm CS	578	-3.0

$q_u$  of 15% SFA treated specimen remained nearly the same after addition of 3000ppm and 5000ppm NS. However further increase in sulfate content resulted in a decrease in  $q_u$  values. The reduction increased with the increase in sulfate content,  $q_u$  values of 15% SFA treated specimen decreased by 7.4%, 9.5% and 23.5% respectively with the addition of 10000ppm, 20000ppm and 40000ppm NS respectively.

Although the addition of 3000ppm and 5000ppm CS slightly increased (8.4% and 12.7%) the  $q_u$  of 15% SFA treated specimen, it remained nearly the same for 10000ppm, 20000ppm and 40000ppm sulfate concentrations. Therefore, it could be stated that  $q_u$  of 15% SFA treated specimen did not alter much with the addition of CS generally.

Table 6.29.  $q_u$  for sulfate added 10% KFA treated specimens

Specimen	$q_u$ (kPa)	Decrease/ Increase in Swell Potential after sulfate addition (%)
10% KFA	762.4	
10% KFA + 3000ppm NS	703.8	-7.7
10% KFA + 5000ppm NS	705.4	-7.5
10% KFA + 10000ppm NS	683.9	-10.3
10% KFA + 20000ppm NS	658.4	-13.6
10% KFA + 40000ppm NS	583.9	-23.4
10% KFA + 3000ppm CS	775.4	1.7
10% KFA + 5000ppm CS	759.8	-0.3
10% KFA + 10000ppm CS	744.9	-2.3
10% KFA + 20000ppm CS	776.2	1.8
10% KFA + 40000ppm CS	733.4	-3.8

A similar trend with 15% SFA treated specimen had been observed for 10% KFA treated specimen after sulfate addition.  $q_u$  values decreased with the addition of NS. An increase in sulfate content affected the strength values negatively and the  $q_u$  values generally decreased further with the increase in sulfate content. The  $q_u$  values of the specimen decreased by 7.7%, 7.5%, 10.3%, 13.6% and 23.4% after addition of

3000ppm, 5000ppm, 10000ppm, 20000ppm and 40000ppm NS respectively. However, CS addition did not affect the strength of the specimen considerably. Variation was only between 0.3-3.8% after addition of 3000ppm to 40000ppm sulfate concentration. Therefore, it could be stated that  $q_u$  of 10% KFA treated specimen was not generally affected much from the addition of CS.

### **6.6.3. Effect of Curing Time and Temperature on Strength of Sulfate Added Fly Ash Treated Specimens**

$q_u$  tests were also performed on 7 days and 28 days cured specimens. The specimens were cured at 10°C, 25°C and 40°C to see the effect of temperature besides curing period on strength. 5000ppm, 10000ppm and 40000ppm sulfate concentrations were chosen as the representative concentrations and tests were performed on these specimens.

#### **6.6.3.1. Sulfate Added 15% SFA Treated Specimens**

UCS test results for NS and CS added 15% SFA treated specimens after curing at 10°C, 25°C and 40°C for 7 days and 28 days are presented in Table 6.30 and 6.31. Test results are presented with the uncured condition to see the effect of curing. Percent decrease/increases in strength values are also presented in the table which is calculated based on 3 different reference points namely;

1.  $q_u$  of each uncured specimen is taken as reference point
2.  $q_u$  of 15% SFA treated specimen is taken as reference point
3.  $q_u$  of 15% SFA treated specimen cured 7 or 28 days at 10°C, 25°C and 40°C are taken as reference for the sulfate added specimens that are cured at the same temperature.

Table 6.30. Average  $q_u$  for sulfate added 15% SFA treated specimens after 7 days curing at 10, 25 and 40°C

Specimen	Curing Period (days)	Temperature	$q_u$ (kPa)	% Increase / Decrease in $q_u$ after curing for each specimen	% Increase / Decrease in $q_u$ of 15% SFA treated specimen	% Increase / Decrease in $q_u$ of 7 days cured 15% SFA treated specimens after sulfate addition in different temperatures
15% SFA	0	25°C	595.9			
	7	10°C	640.1	7.4	7.4	
		25°C	711.2	19.3	19.3	
		40°C	773.4	29.8	29.8	
15% SFA + 5000ppm NS	0	25°C	582		-2.3	
	7	10°C	622.9	7.0	4.5	-2.7
		25°C	709.7	21.9	19.1	-0.2
		40°C	831.3	42.8	39.5	7.5
15% SFA + 10000ppm NS	0	25°C	551.7		-7.4	
	7	10°C	622.9	12.9	4.5	-2.7
		25°C	684.9	24.1	14.9	-3.7
		40°C	816.3	48.0	37.0	5.5
15% SFA + 40000ppm NS	0	25°C	456.1		-23.5	
	7	10°C	378.2	-17.1	-36.5	-40.9
		25°C	580.6	27.3	-2.6	-18.4
		40°C	638.5	40.0	7.1	-17.4
15% SFA + 5000ppm CS	0	25°C	575.2		-3.5	
	7	10°C	634	10.2	6.4	-1.0
		25°C	661.7	15.0	11.0	-7.0
		40°C	772.2	34.2	29.6	-0.2
15% SFA + 10000ppm CS	0	25°C	605.9		1.7	
	7	10°C	623	2.8	4.5	-2.7
		25°C	717	18.3	20.3	0.8
		40°C	750.6	23.9	26.0	-2.9
15% SFA + 40000ppm CS	0	25°C	578		-3.0	
	7	10°C	602.9	4.3	1.2	-5.8
		25°C	699.4	21.0	17.4	-1.7
		40°C	781.4	35.2	31.1	1.0

When the  $q_u$  of each specimen in uncured condition is taken as reference point, following results are obtained;

The  $q_u$  of 15% SFA treated specimen increased with the curing for all temperatures. An increase in strength increased with the rise in temperature. 10°C, 25°C and 40°C curing temperatures resulted in 7.4%, 19.3% and 29.8% increase respectively in the strength of 15% SFA treated specimens.

The  $q_u$  of all sulfate added specimens except for 40000ppm NS added specimen increased (2.8-12.9%) after curing at 10°C. However, 17.1% reduction was observed in the strength of 40000ppm NS added specimen after curing 7 days at 10°C.

$q_u$  of all sulfate added specimens increased when the curing temperature increased to 25°C. The percent increase was higher than that of 10°C. The  $q_u$  of the 5000ppm, 10000ppm and 40000ppm NS added specimens increased by 21.9%, 24.1% and 27.3% respectively after curing at 25°C. An increase of 15.0%, 18.3% and 21.0% in  $q_u$  was observed for 5000ppm, 10000ppm and 40000ppm CS added specimens. The percent increase in  $q_u$  values increased with the rise in sulfate concentrations for both sulfate types.

40°C curing temperature affected the strengths of the specimens in a similar way with 25°C, the strength values of all sulfate added specimen increased after 7 days curing at that temperature. The percent increases were higher than that of 25°C. The percent increases of NS treated specimens were very close to each other, strength values increased by approximately 40%. The  $q_u$  values of the CS added specimens increased by 34.2%, 23.9% and 35.2% respectively for 5000ppm, 10000ppm and 40000ppm sulfate concentrations.

When the  $q_u$  of 15% SFA treated specimen in uncured condition is taken as a reference point, the following results are obtained;

The  $q_u$  of 15% SFA treated specimen increased after addition of sulfate and exposed to curing except for 40000ppm NS added specimens and increase of curing temperature resulted in further increase in strength. The  $q_u$  of 15% SFA treated specimen increased by 1.2-6.4% after the addition of sulfates and cured 7 days at 10°C. The increase in strength reaches to 11.0-20.3% when the curing temperature increased to 25°C and 22.5-39.5% for 40°C curing temperature. The beneficiary effect of 5000ppm and 10000ppm NS was higher than CS added specimens for 40°C.

However, a 36.5% decrease in  $q_u$  was observed for the specimen after 40000ppm NS addition and curing at 10°C. When the curing temperature increased to 25°C, the decrease in  $q_u$  value reduced only to 2.6% which was ignorable. Further increasing of curing temperature to 40°C resulted 7.1% increase in strength value. Therefore, it could be stated that for the temperatures around 10°C, addition of 40000ppm NS caused a decrease in strength values and when the temperatures increased above 25°C, although the strength values did not decrease, beneficiary effect of curing was lost and the strength values of the specimen remained nearly the same.

When the  $q_u$  of 15% SFA treated specimen cured 7 days at different temperatures are taken as the reference point for the sulfate added specimens cured at the same temperature, following results are obtained;

The addition of sulfate did not affect the  $q_u$  values of cured specimens of 15% SFA except for 40000ppm NS considerably. As can be seen from Table 6.30, the absolute variation in strength values varied between 0.2 and 7.5%. The decrease in  $q_u$  of 7 days cured specimens at 10, 25 and 40°C after 40000ppm NS addition was 40.9%, 18.4%, and 17.4% respectively.

Table 6.31. Average  $q_u$  for sulfate added 15% SFA treated specimens after 28 days curing at 10, 25 and 40°C

Specimen	Curing Period (days)	Temperature	$q_u$ (kPa)	% Increase / Decrease in $q_u$ after curing for each specimen	% Increase / Decrease in $q_u$ of 15% SFA treated specimen	% Increase / Decrease in $q_u$ of 28 days cured 15% SFA treated specimens after sulfate addition in different temperatures
15% SFA	0	25°C	595.9			
	28	10°C	655.5	10.0	10.0	
		25°C	737.7	23.8	23.8	
		40°C	868.5	45.7	45.7	
15% SFA + 5000ppm NS	0	25°C	582		-2.3	
	28	10°C	664	14.1	11.4	1.3
		25°C	720.1	23.7	20.8	-2.4
		40°C	813.4	39.8	36.5	-6.3
15% SFA + 10000ppm NS	0	25°C	551.7		-7.4	
	28	10°C	718.6	30.3	20.6	9.6
		25°C	743.8	34.8	24.8	0.8
		40°C	807.3	46.3	35.5	-7.0
15% SFA + 40000ppm NS	0	25°C	456.1		-23.5	
	28	10°C	317	-30.5	-46.8	-51.6
		25°C	616.1	35.1	3.4	-16.5
		40°C	641.3	40.6	7.6	-26.2
15% SFA + 5000ppm CS	0	25°C	575.2		-3.5	
	28	10°C	621.7	8.1	4.3	-5.2
		25°C	720.4	25.2	20.9	-2.3
		40°C	816.4	41.9	37.0	-6.0
15% SFA + 10000ppm CS	0	25°C	605.9		1.7	
	28	10°C	709.5	17.1	19.1	8.2
		25°C	724.1	19.5	21.5	-1.8
		40°C	840.9	38.8	41.1	-3.2
15% SFA + 40000ppm CS	0	25°C	578		-3.0	
	28	10°C	692.4	19.8	16.2	5.6
		25°C	722.3	25.0	21.2	-2.1
		40°C	868.8	50.3	45.8	0.0

When the  $q_u$  of each specimen in uncured condition is taken as a reference point, the following results are obtained;

The  $q_u$  of 15% SFA increased after curing for 28 days. The increase in strength value rose with an increase in temperature. The percent increase values were 10.0%, 23.8% and 45.7% for 10°C, 25°C and 40°C respectively.

A similar trend with 15% SFA treated specimen was obtained for sulfate added specimens except for 40000ppm NS concentration cured at 10°C. The  $q_u$  of the 5000ppm and 10000ppm NS added specimen increased by 14.1% and 30.3% after curing 28 days at 10°C and the  $q_u$  values increased by 23.7% and 34.8% for 25°C and 39.8% and 46.3% for 40°C.

The increase in  $q_u$  for 5000ppm, 10000ppm and 40000ppm CS added specimens were 8.1%, 17.1%, 19.8% for 10°C, 25.2%, 19.5% and 25% for 25°C and 41.9%, 38.8% and 50.3% for 40°C respectively.

Curing at 10°C for 28 days resulted a 30.5% decrease in  $q_u$  of 40000ppm NS added 15% SFA treated specimen. The decrease in this specimen was due to cracks that were formed after the curing period. Although the  $q_u$  of the specimen decreased for curing temperature of 10°C, a similar trend with other sulfate concentrations had been observed for this specimen when the curing temperature increased to 25°C and 40°C, the  $q_u$  of this specimen increased by 35.1% and 40.6% respectively for the aforementioned temperatures.

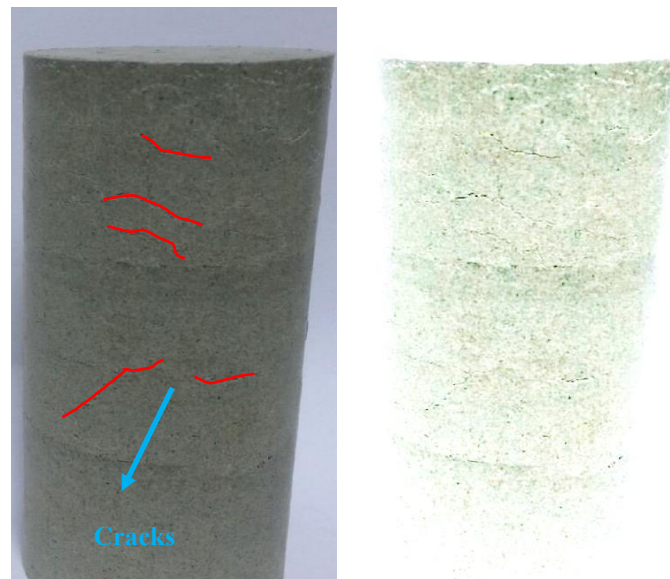


Figure 6.8. 40000ppm NS added 15% SFA treated specimen after 28 days curing at 10°C

When the  $q_u$  of 15% SFA treated specimen in the uncured condition is taken as a reference point, the following results are obtained;

The  $q_u$  of 15% SFA treated specimen increased after addition of sulfate and exposed to curing except for 40000ppm NS added specimens, increase of curing temperature results further increase in strength.

The  $q_u$  of 15% SFA treated specimen increased by 4.3-20.6% after the addition of sulfates and cured 28 days at 10°C. The increase in strength reaches to 20.8-24.8% when the curing temperature increased to 25°C and 35.5-45.8% for 40°C curing temperature.

However, a 46.8% decrease in  $q_u$  is observed for the specimen after 40000ppm NS addition and curing at 10°C. When the curing temperature increased to 25°C, the decrease in  $q_u$  value reduced to 3.4% which was ignorable. Further increasing of curing temperature to 40°C resulted 7.6% increase in strength. Therefore, similar to 7 days curing condition, it could be stated that for the temperatures around 10°C, addition of 40000ppm NS caused a decrease in strength values and when the temperatures increased above 25°C, although the strength values did not decrease, beneficiary effect of curing was lost and the strength values of the specimen remained nearly the same.

When the  $q_u$  of 15% SFA treated specimen cured 28 days at different temperatures are taken as the reference point for the sulfate added specimens cured at the same temperature, following results are obtained;

The addition of sulfate did not affect the  $q_u$  values of cured specimens of 15% SFA except for 40000ppm NS considerably. As can be seen from Table 6.31, the absolute variation in strength values varies between 0.0 and 9.6%. The decrease in 28 days cured specimen of 15% SFA at 10, 25 and 40°C after 40000ppm NS addition is 51.6%, 16.5% and 26.2% respectively.

Test results for 7 days and 28 days cured specimens are presented in Table 6.32 with the percent decrease/increase in strength of 15% SFA treated specimen and sulfate added fly ash treated specimens with the rise of curing period from 7 days to 28 days.

Table 6.32. Average  $q_u$  for sulfate added 15% SFA treated specimens after 7 and 28 days curing at 10, 25 and 40°C

Specimen	Temperature	$q_u$ , (kPa)		Percent Increase / Decrease in $q_u$ after increase in curing period (%)
		7 days curing	28 days curing	
15% SFA	10°C	640.1	655.5	2.4
	25°C	711.2	737.7	3.7
	40°C	773.4	868.5	12.3
15% SFA + 5000ppm NS	10°C	622.9	664	6.6
	25°C	709.7	720.1	1.5
	40°C	831.3	813.4	-2.2
15% SFA + 10000ppm NS	10°C	622.9	718.6	15.4
	25°C	684.9	743.8	8.6
	40°C	816.3	807.3	-1.1
15% SFA + 40000ppm NS	10°C	378.2	317	-16.2
	25°C	580.6	616.1	6.1
	40°C	638.5	641.3	0.4
15% SFA + 5000ppm CS	10°C	634	621.7	-1.9
	25°C	661.7	720.4	8.9
	40°C	772.2	816.4	5.7
15% SFA + 10000ppm CS	10°C	623	709.5	13.9
	25°C	717	724.1	1.0
	40°C	750.6	840.9	12.0
15% SFA + 40000ppm CS	10°C	602.9	692.4	14.8
	25°C	699.4	722.3	3.3
	40°C	781.4	868.8	11.2

For 15% SFA treated specimen the increase of curing time from 7 days to 28 days, did not affect the strength values considerably for 10°C and 25°C, the variation was 2.4% and 3.7%. However, when the curing temperature increased to 40°C, the obtained  $q_u$  values were 12.3% higher for 28 days cured specimen that of 7 days cured one.

The  $q_u$  value of 40000ppm NS added specimen cured 28 days at 10°C decreased by 16.2% compared to the 7 days cured one, however for 25°C the strength value increased by 6.1% when the curing time increased from 7 days to 28 days and the strength values were nearly same for 7 days and 28 days cured specimens at 40°C. The further decrease of the strength value for the specimen cured at 10°C with the rise in curing time was the result of the increase in the deterioration of the structure due to chemical reactions.

For 5000ppm and 10000ppm NS added specimens, a similar trend with 40000ppm concentration was observed for curing temperatures of 25°C and 40°C, strength values remained nearly the same or slightly increased when the curing time increased from 7 days to 28 days. These could be the result of the fact that most of the pozzolanic reactions are completed within 7 days. Also, for 10°C curing temperature the strength value of 5000ppm NS added specimen increased by 6.6% with the increase of curing time from 7 days to 28 days and 15.4% increase was observed for 10000ppm NS added specimen.

The strength values for 5000ppm CS added specimen was not affected much from the increase of curing time from 7 days to 28 days. Although 8.9% increase was obtained for 25°C, strength values were not altered for 10°C and 40°C.

A similar behavior was observed for 10000ppm and 40000ppm CS added specimen. The strength values remained nearly the same for 25°C and it increased by 13.9% and 14.8% for 10°C and 12.0% and 19.0% for 40°C respectively with the increase of curing time from 7 days to 28 days.

#### **6.6.3.2. Sulfate Added 10% KFA Treated Specimens**

UCS test results for NS and CS added 10% KFA treated specimens after curing at 10°C, 25°C and 40°C for 7 days and 28 days are presented in Table 6.33 and 6.34. Test results are presented with the uncured condition to see the effect of curing. Percent decrease/increases in strength values are also presented in the table which are calculated based on 3 different reference points namely;

1.  $q_u$  of each uncured specimen is taken as the reference point
2.  $q_u$  of 10% KFA treated specimen is taken as the reference point
3.  $q_u$  of 10% KFA treated specimen cured 7 or 28 days at 10, 25 and 40°C are taken as reference for the sulfate added specimens that are cured at the same temperature.

Table 6.33. Average  $q_u$  for sulfate added 10% KFA treated specimens after 7 days curing at 10, 25 and 40°C

Specimen	Curing Period (days)	Temperature	$q_u$ (kPa)	% Increase / Decrease in $q_u$ after curing for each specimen	% Increase / Decrease in $q_u$ of 10% KFA treated specimen	% Increase / Decrease in $q_u$ of 7 days cured 10% KFA treated specimens after sulfate addition in different temperatures
10% KFA	0	25°C	762.4			
	7	10°C	780.7	2.4	2.4	
		25°C	776.9	1.9	1.9	
		40°C	861.1	12.9	12.9	
10% KFA + 5000ppm NS	0	25°C	705.4		-7.5	
	7	10°C	793.9	12.5	4.1	1.7
		25°C	771.4	9.4	1.2	-0.7
		40°C	892.3	26.5	17.0	3.6
10% KFA + 10000ppm NS	0	25°C	683.9		-10.3	
	7	10°C	809.1	18.3	6.1	3.6
		25°C	804.4	17.6	5.5	3.5
		40°C	847.8	24.0	11.2	-1.5
10% KFA + 40000ppm NS	0	25°C	583.9		-23.4	
	7	10°C	560	-4.1	-26.5	-28.3
		25°C	744	27.4	-2.4	-4.2
		40°C	766.6	31.3	0.6	-11.0
10% KFA + 5000ppm CS	0	25°C	759.8		-0.3	
	7	10°C	776.2	2.2	1.8	-0.6
		25°C	782.2	2.9	2.6	0.7
		40°C	864.4	13.8	13.4	0.4
10% KFA + 10000ppm CS	0	25°C	744.9		-2.3	
	7	10°C	819.9	10.1	7.5	5.0
		25°C	816.7	9.6	7.1	5.1
		40°C	898.7	20.6	17.9	4.4
10% KFA + 40000ppm CS	0	25°C	733.4		-3.8	
	7	10°C	783.6	6.8	2.8	0.4
		25°C	778.3	6.1	2.1	0.2
		40°C	860.4	17.3	12.9	-0.1

When the  $q_u$  of each specimen in the uncured condition is taken as a reference point, the following results are obtained;

The  $q_u$  of the 10% KFA treated soil remained nearly the same after curing for 7 days at 10°C and 25 °C, however increasing the curing temperature to 40°C caused a 12.9% increase in the strength of the specimen.

For 5000ppm and 10000ppm NS added specimen, the curing at 10°C and 25°C made nearly the same effect and an average increase of 11% and 18% compared to the uncured condition was obtained for 5000ppm and 10000ppm respectively. Further increase of temperature to 40°C increased the beneficiary effect and the strength values of the specimens with 5000ppm and 10000ppm sulfate concentrations increased by 26.5% and 24.0%.

Curing at 10°C resulted in a slight decrease in  $q_u$  of 40000ppm NS added specimen compared to non-cured conditions. This was a similar behavior as observed for 15% SFA treated specimen however, the effect was not that much. The increase of the curing temperature to 25°C and 40°C, turned the behavior similar to the other concentrations and 27.4% and 31.3% increase in strength was observed respectively.

Curing at 10°C and 25°C made the same effect for CS added specimens, an average increase of approximately 2.5%, 10% and 6.5% in strength was observed for 5000ppm, 10000ppm and 40000ppm sulfate concentrations respectively. However, rising of curing temperature to 40°C resulted in a further increase in strength of these specimens and 13.8%, 20.6% and 17.3% increase in strength values were observed for these specimens accordingly.

When the  $q_u$  of 10% KFA treated specimen in the uncured condition is taken reference point, the following results are obtained;

The  $q_u$  of 10% KFA treated specimen remained nearly the same for 5000ppm and 10000ppm NS concentrations after being cured 7 days at 10°C and 25°C. However,

increasing the curing temperature to 40°C resulted in 17.0% and 11.2% increase respectively in  $q_u$  of uncured 10% KFA treated specimen.

Addition of 40000ppm NS to 10% KFA treated specimen resulted a decrease of 26.5% in  $q_u$  after curing 7 days at 10°C, however when the curing temperature increased to 25°C the decrease in  $q_u$  reduced to 2.4% which was ignorable. The  $q_u$  of the fly ash treated specimen did not alter after the addition of 40000ppm NS and cured 7 days at 40°C.

The  $q_u$  of the 10% KFA treated specimens remained nearly the same after the addition of 5000ppm, 10000ppm and 40000ppm CS and cured 7 days at 10°C and 25°C, percent increase in strength varying between 1.8-7.5% had been observed. However, increasing curing temperature to 40°C resulted in 13.4%, 17.9% and 12.9% increase in strength value of the 10% KFA treated specimen respectively for 5000ppm, 10000ppm and 40000ppm concentrations.

When the  $q_u$  of 10% KFA treated specimen cured 7 days at different temperatures are taken as the reference point for the sulfate added specimens cured at the same temperature, following results are obtained;

The addition of sulfate did not affect the  $q_u$  values of cured specimens of 10% KFA except for 40000ppm NS that was cured at 10°C and 40°C. As can be seen from Table 6.33, the absolute variation in strength values varies between 0.1 and 5.1%. The decrease in 7 days cured specimens at 10°C and 40°C after 40000ppm NS addition is 28.3% and 11.0% respectively.

Table 6.34. Average  $q_u$  for sulfate added 10% KFA treated specimens after 28 days curing at 10, 25 and 40°C

Specimen	Curing Period (days)	Temperature	$q_u$ (kPa)	% Increase / Decrease in $q_u$ after curing for each specimen	% Increase / Decrease in $q_u$ of 10% KFA treated specimen	% Increase / Decrease in $q_u$ of 28 days cured 10% KFA treated specimens after sulfate addition in different temperatures
10% KFA	0	25°C	762.4			
	28	10°C	813.5	6.7	6.7	
		25°C	805.1	5.6	5.6	
		40°C	1100.6	44.4	44.4	
10% KFA + 5000ppm NS	0	25°C	705.4		-7.5	
	28	10°C	818.4	16.0	7.3	0.6
		25°C	866.9	22.9	13.7	7.7
		40°C	921.6	30.6	20.9	-16.3
10% KFA + 10000ppm NS	0	25°C	683.9		-10.3	
	28	10°C	815.4	19.2	7.0	0.2
		25°C	898.3	31.3	17.8	11.6
		40°C	933.8	36.5	22.5	-15.2
10% KFA + 40000ppm NS	0	25°C	583.9		-23.4	
	28	10°C	562.1	-3.7	-26.3	-30.9
		25°C	785.1	34.5	3.0	-2.5
		40°C	815.8	39.7	7.0	-25.9
10% KFA + 5000ppm CS	0	25°C	759.8		-0.3	
	28	10°C	847.8	11.6	11.2	4.2
		25°C	882.2	16.1	15.7	9.6
		40°C	1013.5	33.4	32.9	-7.9
10% KFA + 10000ppm CS	0	25°C	744.9		-2.3	
	28	10°C	851	14.2	11.6	4.6
		25°C	888.3	19.3	16.5	10.3
		40°C	997.5	33.9	30.8	-9.4
10% KFA + 40000ppm CS	0	25°C	733.4		-3.8	
	28	10°C	867	18.2	13.7	6.6
		25°C	861.3	17.4	13.0	7.0
		40°C	1061.6	44.8	39.2	-3.5

When the  $q_u$  of each specimen in the uncured condition is taken as a reference point, the following results are obtained;

The  $q_u$  of the 10% KFA treated soil remained nearly the same after curing 28 days at 10°C and 25°C, however, the rise of the curing temperature to 40°C caused a 44.4% increase in  $q_u$  of the specimen.

Strength values increased after curing for 5000ppm and 10000ppm NS added specimens and the increase in strength increased with the rise in curing temperature. The strength value of the 5000ppm NS added specimen increased by 16.0%, 22.9%, and 30.6% respectively for 10°C, 25°C and 40°C curing temperatures. The increase was 19.2%, 31.3% and 36.5% for the same curing temperatures for 10000ppm NS added specimen.

Curing at 10°C resulted in a slight decrease in  $q_u$  of 40000ppm NS added specimen compared to non-cured conditions. This resulted from the little cracks that were formed due to chemical reactions (Figure 6.9). When the curing temperature increased to 25°C and 40°C, the trend turned similar to other concentrations and the strength value increased with curing. The increase is 34.5% and 39.7% for 25°C and 40°C respectively.

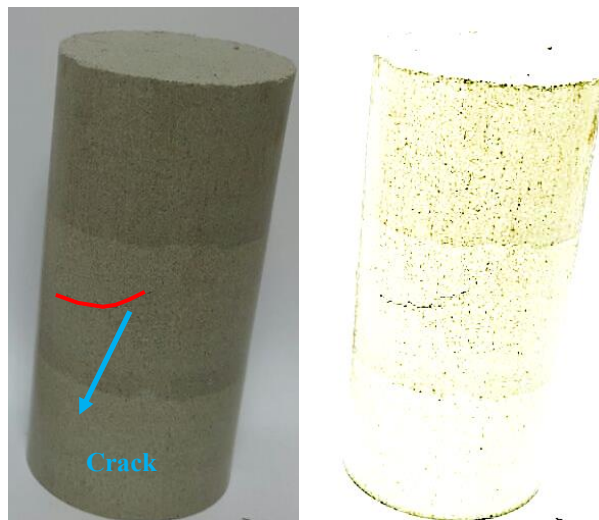


*Figure 6.9.* 40000ppm NS added 10% KFA treated specimen after 28 days curing at 10°C

The strength values of CS added specimens increased with curing and the increase in strength values generally increased with the rise in both sulfate concentration and temperature.

When the  $q_u$  of 10% KFA treated specimen in the uncured condition is taken as a reference point, the following results are obtained;

Addition of 5000ppm and 10000ppm NS made the same effect on 10% KFA treated specimen after cured for 28 days at different temperatures. 5000ppm and 10000ppm sulfate addition resulted in an increase of 7.3 and 7.0% for 10°C, 13.7 and 17.8% for 25°C and 20.9 and 22.5 % for 40°C curing temperatures respectively.

Addition of 40000ppm NS to 10% KFA treated specimen resulted in a decrease of 26.3% in  $q_u$  after curing 28 days at 10°C however, 3% and 7% increase in strength was observed when the curing temperature increased to 25°C and 40°C.

Addition of 5000ppm, 10000ppm and 40000ppm CS made the same effect on 10% KFA treated specimen after cured for 28 days at different temperatures. Average increase of 12%, 15% and 34% in strength was observed for 10°C, 25°C and 40°C curing temperatures respectively after addition of different concentrations of CS.

When the  $q_u$  of 10% KFA treated specimen cured 28 days at different temperatures are taken as the reference point for the sulfate added specimens cured at the same temperature, following results are obtained;

Addition of 5000ppm and 10000ppm NS did not alter the strength of the 10% KFA, however, a 30.9% decrease in strength was observed after the addition of 40000ppm NS for curing temperature of 10°C. Addition of 5000ppm, 10000ppm and 40000ppm CS resulted in an increase of 4.2%, 4.6%, and 6.6% respectively on the strength of 10% KFA treated specimen that was cured 28 days at 10°C.

The addition of both sulfate type in different concentrations resulted in a slight increase on the  $q_u$  of 10% KFA treated specimen that was cured 28 days at 25°C except for 40000ppm NS concentrations, an increase of 7-11.6% in strength was observed after addition of sulfate for that specimens. 40000ppm NS did not affect the strength of the fly ash treated specimen considerably for the curing temperature of 25°C.

The addition of both sulfate type in different concentrations resulted in a decrease in the  $q_u$  of 10% KFA treated specimen that was cured 28 days at 40°C. The effect of NS addition was higher than that of CS. Addition of 5000ppm, 10000ppm and 40000ppm NS resulted a decrease of 16.3%, 15.2%, and 25.9%, and same concentrations of CS resulted in a decrease of 7.9 %, 9.4%, and 3.5% respectively on the strength of the fly ash treated specimen that was cured 28 days at 40°C.

Test results for 7 days and 28 days cured specimens are presented in Table 6.35 with the percent decrease/increase in strength of 10% KFA treated specimen and sulfate added fly ash treated specimens with the rise of curing period from 7 days to 28 days.

Table 6.35. Average  $q_u$  for sulfate added 10% KFA treated specimens after 7 and 28 days curing at 10, 25 and 40°C

Specimen	Temperature	$q_u$ , (kPa)		Percent Increase / Decrease in $q_u$ after increase in curing period (%)
		7 days curing	28 days curing	
10% KFA	10°C	780.7	813.5	4.2
	25°C	776.9	805.1	3.6
	40°C	861.1	1100.6	27.8
10% KFA + 5000ppm NS	10°C	793.9	818.4	3.1
	25°C	771.4	866.9	12.4
	40°C	892.3	921.6	3.3
10% KFA + 10000ppm NS	10°C	809.1	815.4	0.8
	25°C	804.4	898.3	11.7
	40°C	847.8	933.8	10.1
10% KFA + 40000ppm NS	10°C	560	562.1	0.4
	25°C	744	785.1	5.5
	40°C	766.6	815.8	6.4
10% KFA + 5000ppm CS	10°C	776.2	847.8	9.2
	25°C	782.2	882.2	12.8
	40°C	864.4	1013.5	17.2
10% KFA + 10000ppm CS	10°C	819.9	851	3.8
	25°C	816.7	888.3	8.8
	40°C	898.7	997.5	11.0
10% KFA + 40000ppm CS	10°C	783.6	867	10.6
	25°C	778.3	861.3	10.7
	40°C	860.4	1061.6	23.4

Increase of curing period did not affect the  $q_u$  of the 10% KFA treated specimen considerably for curing temperatures of 10°C and 25°C, an average increase of only 4% increase was observed. However, the effect of curing time increased with the increase in temperature to 40°C. The strength of 7 days cured specimen increased by 27.8% when the curing period was increased to 28 days.

The strength values of CS added specimens generally increased further with the rise of curing period for all curing temperatures however the effect of curing period was higher for 40°C.

Increasing the curing period from 7 days to 28 days for curing temperature of 10°C did not alter the strength values of the NS added specimens considerably. However, for 25°C curing temperature, the strength values increased by 12.4%, 11.7%, and 5.5% for the 5000ppm, 10000ppm and 40000ppm sulfate concentrations respectively with the increase of curing period from 7 days to 28 days. A similar trend had been observed when the curing temperature increased to 40°C. The strength values increased by 3.3%, 10.1% and 6.4% for these concentrations when the curing period increased from 7 to 28 days.

The cracks of 40000ppm NS added specimen became visible when the curing period increased from 7 days to 28 days for 10°C. Therefore, to determine the reason behind the cracks and strength decrease, the curing period of specimens were increased for 40000ppm NS added 15% SFA and 10% KFA treated specimens. 40000ppm NS added 4% L was also exposed to curing for comparison purposes.

Views of the specimens with different curing times are presented in Figure 6.10, 6.11 and 6.12 for 15% SFA, 10% KFA and 4% L treated specimens respectively.

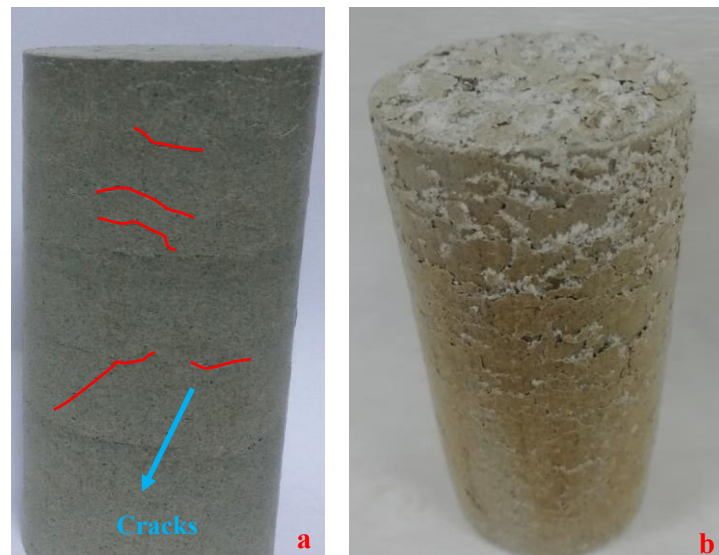


Figure 6.10. 40000ppm NS added 15% SFA treated specimen cured at 10°C for a- 28 days, b- 6 months



Figure 6.11. 40000ppm NS added 10% KFA treated specimen cured at 10°C for a- 28 days, b- 3 months, c- 9 months



*Figure 6.12.* 40000ppm NS added 4% L treated specimen cured at 10°C for a- 4 months, b- 9 months

As can be seen in Figure 6.10, 6.11 and 6.12, with the increase in curing periods the cracks increased and also crystals formed within and at the surface of the specimens.

The same specimens were also cured at 40°C for 6 months, however, any cracks did not occur on the surface of the specimens as can be seen in Figure 6.13.

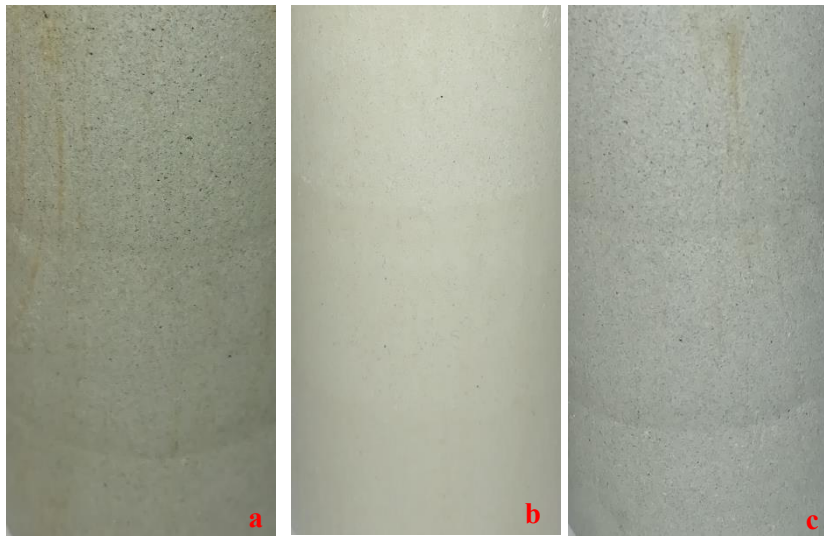


*Figure 6.13.* 40000ppm NS added a-10% KFA, b-4% L, c-15% SFA treated specimen cured at 40°C for 6 months

Soil that contains high amount of water-soluble sulfates shows an expansive event similar to that of frost heave and expansive clays. These soils expand due to the drop in daytime temperatures at night. The daytime temperature which is approximately 32.2°C decreases under 4.4°C at night. This expansion resulted in damages in lightweight structures, roads, etc. This phenomenon called salt heave in the literature and cause vertical expansion independent of the shrinking and swelling characteristics of clayey soils. The swelling of some soils that are located at the surface in arid- areas mainly occurs as a result of the properties of NS and probably different water-soluble salts. Only soils that contain NS show expansive characteristics, not all soils. Soils with 5000ppm NS concentration may swell more than the ones with up to or higher than 100000ppm concentration. Some soils that contain high amount of NS exhibit very low expansion (Blaser and Scharer, 1969).

Two main characteristics of soils that contain NS are listed as follows by Blaser and Scharer (1969);

- The salt is deposited on the ground surface as a result of the evaporation of the moisture in the soil that contains NS in hot weather.

- The moisture in the soil that contains NS results occurrence of crystals, an increase in soil volume and expansion when the ambient temperatures decrease to the low levels.

Two characteristics of NS that induce soil expansion is presented below (Blaser and Scharer,1969);

- The NS in solution shows a tendency to link H<sub>2</sub>O when the temperature falls below 32°C. The NS forms the solid phase that is known as mirabilite (Na<sub>2</sub>SO<sub>4</sub> 10H<sub>2</sub>O) by binding 10H<sub>2</sub>O molecules. The solid phase of NS dissolves in its own water when the temperatures increase during high humidity seasons and reach the surface with the help of capillary action.
- A high amount of NS exists in the moisture of the soil when the temperature exceeds 32°C. The temperature decrease causes a reduction in solubility of NS and an increase in hydration. The expansion of soil crystals against the structure of the soil is observed during this process.

Morphology of the NS crystals varies according to the humidity of the environment and pore size of the material. Pore size also affects the size and growth of the crystals. Crystal morphology of NS is presented in Figure 6.14 (Xusheng, et al., 2017).

Although mirabilite generally has a needle-like structure (Figure 6.14a), anhydrous NS (thenardite) which is formed by the transformation from mirabilite with the reaching of temperature to 32.4°C, still exhibits needle-like branches (Figure 6.14b). Anhydrous NS turns into a form that likes powder when the soil containing NS exposed to wetting-drying cycles (Figure 6.14c). The shapes of the salt crystals in solution and in the soil are different than each other. The crystals that exist in soils are generally too small to be seen by naked eyes and SEM is used for their observation. The shape of salt crystals, including some forms of mirabilite, that take part in NS solutions can be visible by naked eyes due to their larger size (Figure 6.14f).

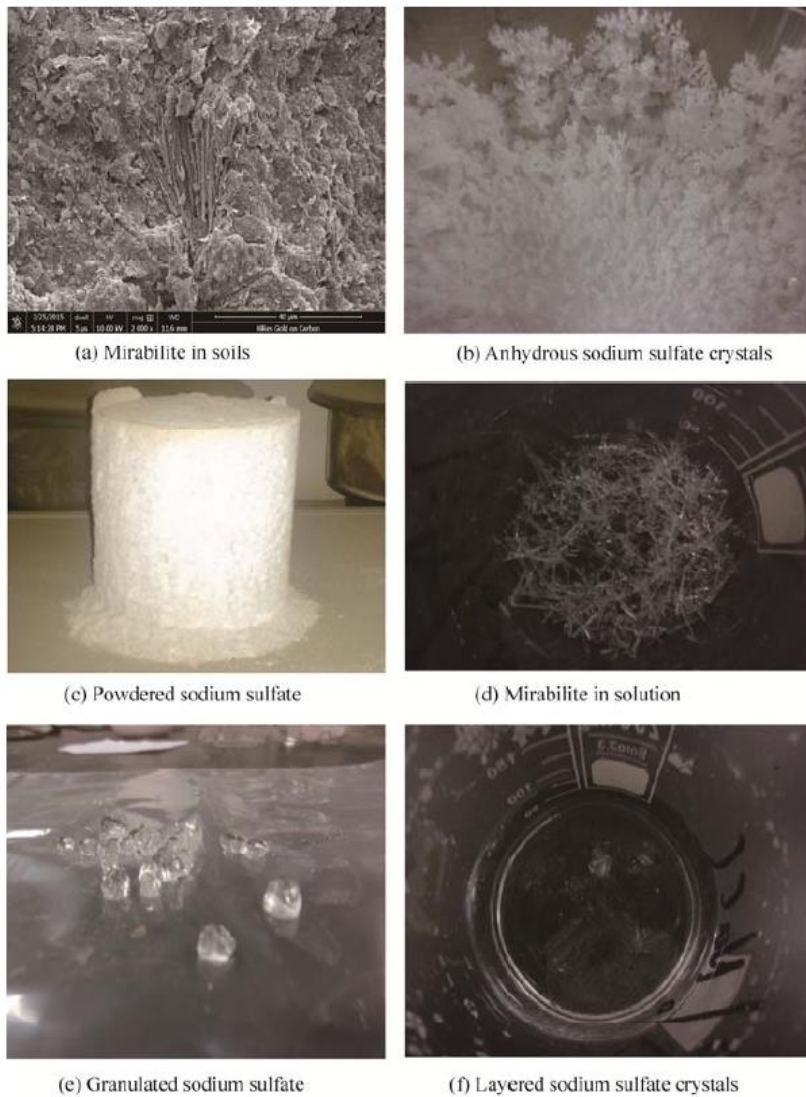


Figure 6.14. Crystal morphology of sodium sulfate (Xusheng et al., 2017)

Powder like form of NS that is observed in soils that are exposed to cycling wetting-drying was also observed on the 40000ppm NS added 10% KFA treated specimen that was cured at 40°C for 28 days. This specimen was waited at room temperature after exposing to  $q_u$  tests. Since the specimens were prepared by mixing water, drying these specimens made the same effect with cyclic wetting-drying cycles (Figure 6.15).



Figure 6.15. Views form powdered of NS, a- study of Xusheng et al., 2017, b- this study (dry form of 40000ppm NS Added 10% KFA treated specimen cured at 40°C for 28 days.)

The crystals formed at 40000ppm NS added specimens that were cured at 10°C were determined as thenardite from the SEM and XRD analyses performed on 40000ppm NS added 15% SFA treated specimen that was cured 10°C for 6 months. Also, ettringite was also observed within this specimen. The detailed evaluations of SEM and XRD results are presented in Section 6.9 and 6.10 respectively. Ettringite was also observed in 40000ppm NS added 15% SFA treated specimen that was cured 10°C for 28 days but with a lower intensity. Therefore, it could be stated that the combined effect of ettringite formation and salt expansion resulted in the decrease in strength and cracks, however, major contribution belongs to salt expansion which considered to be occurred by the formation of thenardite at lower temperatures.

Curing temperature and period have an important effect on the rate of pozzolanic reactions. The rate of reactions increases with the increase in temperature and time (Ruff, 1965 and Wild et al., 1986). Wild et. al. (1986) studied on the effect of curing time and temperature on the strength of lime treated soils. They used red-marl and different lime compositions in their studies and performed UCS tests on specimens cured at 3 different temperatures namely; 25 °C, 50°C and 75°C up to 24 weeks.

At the end of their study, they found a marked increase in the rate of strength development with increasing curing time and temperatures. The results of the tests for 25°C and 75°C are presented in Figure 6.16 and 6.17 accordingly.

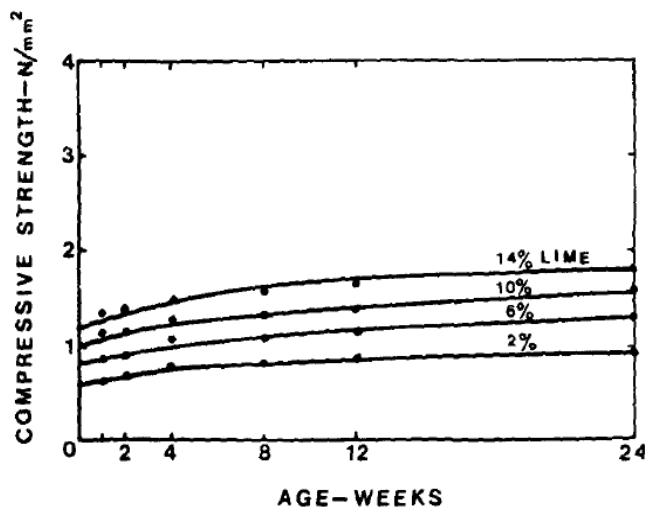


Figure 6.16. UCS against curing time for soil-lime cylinders of various compositions cured in a moist environment at 25°C (Wild et al., 1986)

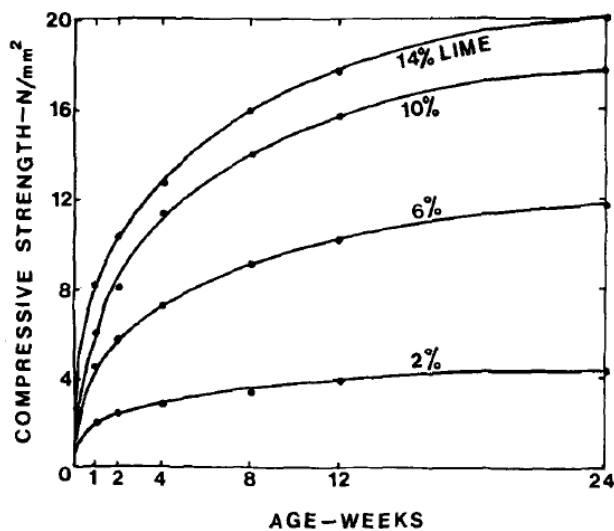


Figure 6.17. UCS against curing time for soil-lime cylinders of various compositions cured in a moist environment at 75°C (Wild et al., 1986)

In our study maximum strength values were obtained for the specimens that were cured at 40°C. This is probably due to the increase in the rate of pozzolanic reactions with increasing temperature which are the dominant chemical reactions that satisfy the strength increase in chemically stabilized soils by means of production of cementing products.

Also, the beneficiary effect of CS (gypsum) was also observed in the previous studies performed on both untreated soils and soils treated with calcium-based stabilizers.

Wild (1998) studied the effect of curing on gypsum added lime and GBFS (granulated blast furnace slag) treated specimens. Industrial kaolinite was used as a source of kaolinite with LL=61%, and PI=29%. Lime and GBFS were used as additives.

The specimens prepared for  $q_u$  tests were cured for 7 and 28 days at 30°C and 100% relative humidity.

Different lime (L), slag (S) and gypsum (G) contents were used. Control soil was prepared with the addition of 6% lime to kaolinite. The level of gypsum used was 2, 4 and 6% by weight which was approximately equivalent to approximately 1, 2 and 3% by mass of  $SO_3$ .

The results of the tests are presented in Figure 6.18.

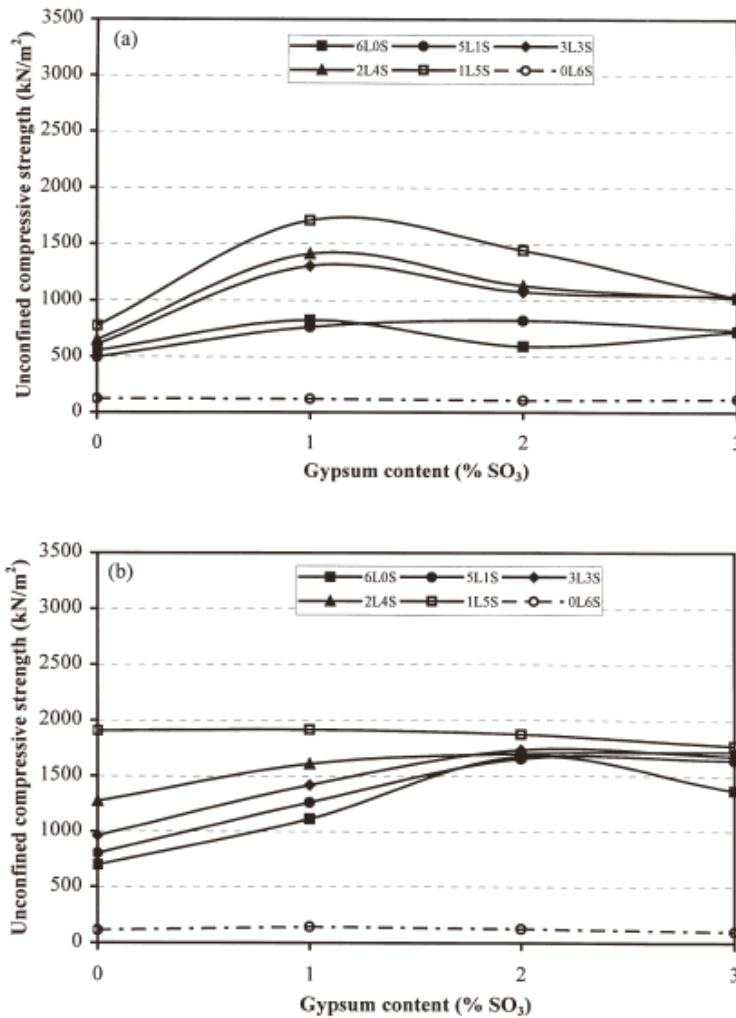


Figure 6.18.  $q_u$  vs. gypsum content for kaolinite- lime- GBFS mixtures moist cured at  $30^\circ\text{C}$  and 100% relative humidity at a- 7 days, b- 28 days (Wild, 1998)

The author summarizes the results as below;

The strength generally increased for gypsum added specimen after a curing period of 7 days. The strength increase rose with the increase in replacement of lime with GBFS. The addition of gypsum increased not only the rate of pozzolanic reactions between lime and kaolinite but also hydration of slag accelerated more effectively. An increase in the curing period generally resulted further increase in strength of gypsum added

specimens, but this time strength increase was greater for low replacement levels and the improvement decreased when the lime was substituted with slag.

The accelerating effect of the addition of gypsum on the GBFS hydration was not observed for 28 days since the strength of the specimen with 1:5 lime to GBFS ratio was not affected by sulfate addition. However, a considerable increase in strength was observed for the 28 days cured specimen with 6:0 lime to GBFS ratio after the addition of sulfate. If the specimen consisted only GBFS, strength increase was not observed after the addition of sulfate which was a sign that gypsum could accelerate the hydration of slag if lime activated the GBFS. The authors stated that the optimum sulfite content for 7 days cured specimens were 1% and the strength increase was mainly due to the increase in the rate of hydration reactions of GBFS. Sulfate had no considerable effect of the specimen that was prepared by using only lime and cured for 7 days. However, the strength of 28 days cured lime treated specimen increased considerably with the increase of sulfite level from 0% SO<sub>3</sub> to 2% SO<sub>3</sub>. This increase was explained by the contribution of reaction products of gypsum-clay-lime reactions to strength at later periods.

Yilmaz and Civelekoglu (2009) studied on the effect of gypsum on the stabilization of swelling clay soils. Bentonite was used as a swelling soil in the study and different quantities of gypsum; 2.5%, 5%, 7.5% and 10% by mass were added to bentonite. Besides Atterberg limits and free swell tests,  $q_u$  tests were performed on treated and untreated specimens, after a curing period of 7 days.  $q_u$  test results are presented in Figure 6.19.

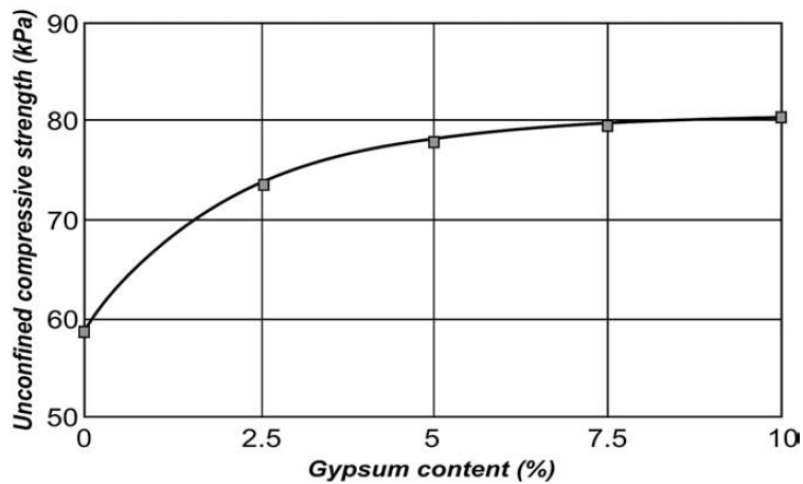


Figure 6.19. Variation of UCS with gypsum content (Yılmaz and Civelekoglu, 2009)

Researchers did not directly explain the reason for the increase in strength with the addition of gypsum. But they explained the stabilization with gypsum by the modification of cation exchange capacity of the bentonite after the addition of gypsum, and the substitution of replaceable monovalent ions of bentonite by the calcium ion.

The study performed by Gadouri et al. (2017) showed the beneficiary effect of the addition of NS (up to some level) on the shear strength of clayey soil stabilized with lime and natural pozzolans as a result of the early pozzolanic reactions.

The results of the unconfined compressive strength tests could be summarized as presented below;

- Addition of 10% KFA and 4% L resulted an increase in the strength of Specimen A and it remained nearly the same after 15% SFA treatment.
- The strength of uncured fly ash and lime treated specimens was generally affected negatively from NS addition and the maximum reduction was observed for 40000ppm concentration. CS addition had no significant effect on the strength properties of specimens treated with calcium-based stabilizers.

- The strength of 15% SFA treated specimen and sulfate added specimens increased after curing except for 40000ppm NS. The rise increased with the increase in temperature and maximum increase was obtained for 40°C. Strength reduction was observed for 40000ppm NS added specimen that was cured at 10°C, however the strength of the specimen increased with the rise of curing temperature to 25°C and 40°C similar to other concentrations. The strength of the uncured 15% SFA treated specimen increased after the addition of sulfates and exposed to curing except for 40000ppm NS added specimens. The strength of 40000ppm NS added specimen decreased after curing at 10°C and remained nearly the same for the curing temperatures of 25°C and 40°C which means that the beneficiary effect of curing was lost after addition of 40000ppm NS. The strength of sulfate added specimens generally increased or remained nearly the same after the rise of curing period from 7 days to 28 days except for 40000ppm NS added specimen cured at 10°C. The strength of this specimen further decreased with the increase of curing period.
- The strength of 10% KFA treated specimen remained the same for the curing temperatures of 10°C and 25°C and an increase was observed with the rise of curing temperature to 40°C. The increase of curing period did not affect the  $q_u$  of the 10% KFA treated specimen for the curing temperatures of 10°C and 25°C, however beneficial effect increased with the rise of curing period for 40°C. The strength of the sulfate added specimens increased except for 40000ppm NS added specimen after curing. The strength increase was approximately the same for curing temperatures of 10°C and 25°C and an additional increase was observed with the rise of temperature to 40°C. Similar to 15% SFA treated specimen, strength reduction was observed for 40000ppm NS added specimen that was cured at 10°C, however the strength of specimen increased with the rise of curing temperature to 25°C and 40°C. The strength of the uncured 10% KFA treated specimen remained same after addition of sulfates and exposed to 7 days curing at 10°C and 25°C except for 40000ppm NS, however an increase in strength was observed with the rising of curing

temperature to 40°C. The strength of 40000ppm NS added specimen decreased after curing at 10°C and remained nearly the same for the curing temperatures of 25°C and 40°C. The strength values of CS added 10% KFA treated specimens generally increased further with the rise of curing period for all curing temperatures however, the effect of curing period was higher for 40°C. The strength values of the NS added specimens were not affected by the increase of curing period for 10°C, however a slight increase was observed for the curing temperatures of 25°C and 40°C.

### 6.7. Effect of Additives on Shear Wave Velocity

$V_s$  is a valuable parameter that could be used for the estimation of the many other geotechnical parameters with the help of the correlations suggested in the literature by different researchers.

Shear wave velocity tests were performed on Specimen A, 15% SFA, 10% KFA treated specimens and 5000ppm, 10000ppm and 40000ppm NS and CS added fly ash treated specimens to see both the effect of fly ash addition on swelling soil and effect of sulfate addition on fly ash treated specimens.

Also, the correlations between the undrained shear strength ( $c_u$ ) and  $V_s$  given in the literature are used to calculate the  $V_s$  values for comparison purposes. The used correlations are given in Table 6.36.

Table 6.36. Correlations between  $c_u$  and  $V_s$

Reference	Correlation
Dickenson (1994)	$V_s=23.c_u^{0.475}$
Yun et al. (2006)	$V_s=19.4.c_u^{0.36}$
Levesques et al. (2007)	$V_s= c_u^{(1/1.59)}. 7.93$
Likitlersuang and Kyaw, 2010)	$V_s=(c_u/P_a)^{0.372}. 187$

$P_a$ = Atmospheric Pressure

$c_u$  values could be estimated from the  $q_u$  test results as follows;

$$c_u \approx q_u/2 \quad (6.1)$$

$V_s$  values that are calculated using the correlations given in Table 6.36 and  $c_u$  values are presented in Table 6.37 with the  $V_s$  of the specimens that are directly determined from the laboratory tests.

The graphical representation of the results is also presented in Figures 6.20 and 6.21 for 15% SFA and 10% KFA treated specimens respectively.

Table 6.37. Measured and calculated  $V_s$  values

Specimen	Unconfined Compressive Strength ( $q_u$ ), kPa	Undrained Shear Strength, $c_u = q_u/2$ (kPa)	Shear Wave Velocity, $V_s$ , (m/s)					
			Laboratory	Literature				
				Dickenson (1994)	Yun et al. (1994)	Likitlersuang and Kyaw (2010)	Average Value	
A	595.3	297.7	246	344	151	285	281	265
15% SFA	595.9	298.0	299	344	151	285	281	265
15% SFA + 5000ppm NS	582	291.0	292	340	150	281	278	262
15% SFA + 10000ppm NS	551.7	275.9	280	332	147	272	273	256
15% SFA + 40000ppm NS	456.1	228.1	251	303	137	241	254	234
15% SFA + 5000ppm CS	671.5	335.8	290	364	157	308	293	281
15% SFA + 10000ppm CS	605.9	303.0	266	347	152	288	282	267
15% SFA + 40000ppm CS	578	289.0	270	339	149	280	278	261
10% KFA	762.4	381.2	305	387	165	333	308	298
10% KFA + 5000ppm NS	705.4	352.7	325	373	160	317	299	287
10% KFA + 10000ppm NS	683.9	342.0	310	368	158	311	295	283
10% KFA + 40000ppm NS	583.9	292.0	305	341	150	282	279	263
10% KFA + 5000ppm CS	759.8	379.9	297	386	165	332	307	298
10% KFA + 10000ppm CS	744.9	372.5	304	383	163	328	305	295
10% KFA + 40000ppm CS	733.4	366.7	309	380	163	325	303	293

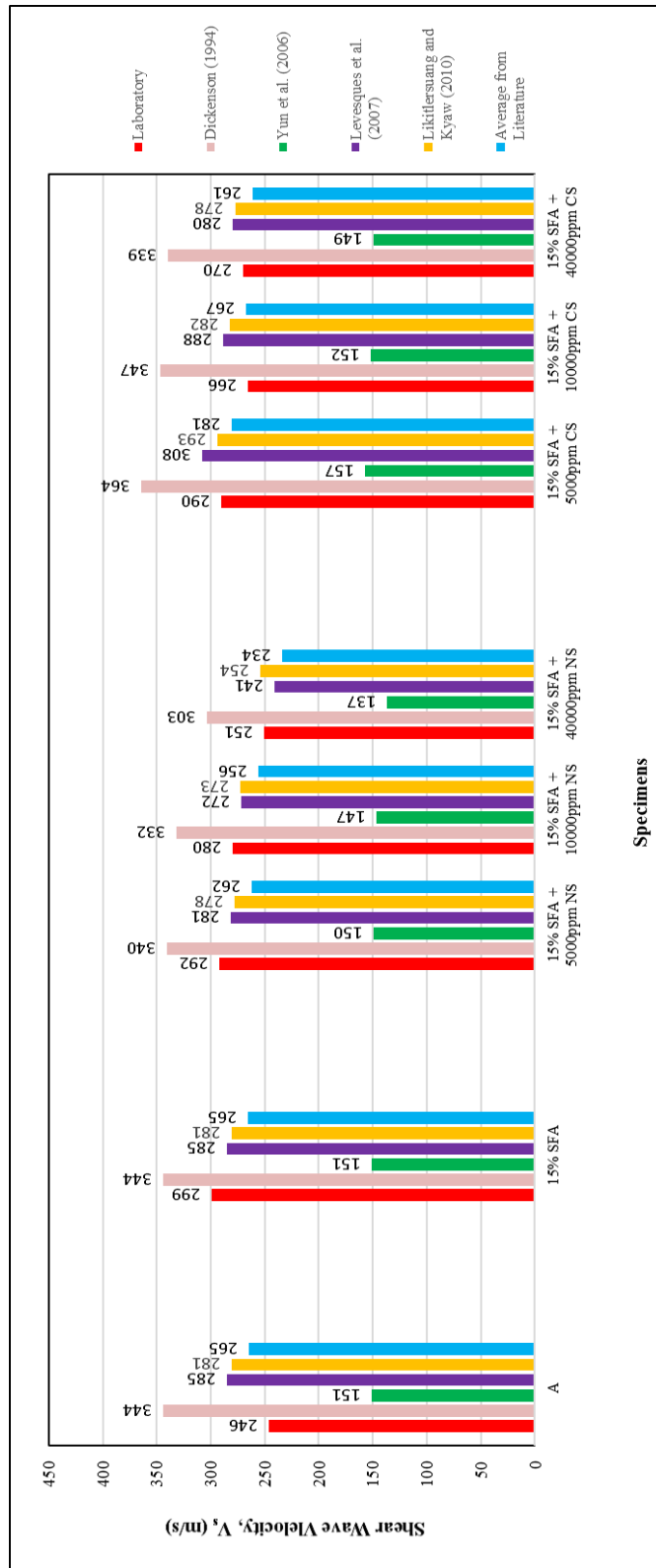


Figure 6.20. Measured and calculated  $V_s$  values for sulfate added 15% SFA treated specimens

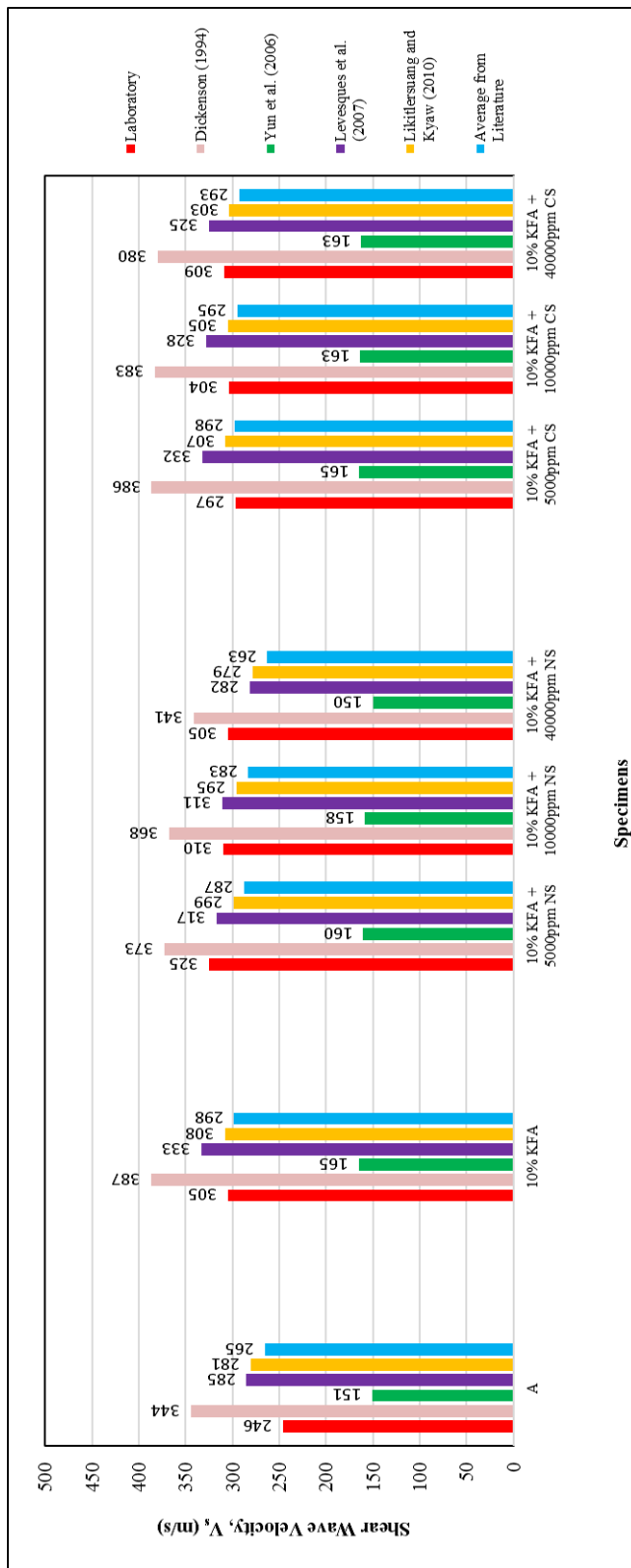


Figure 6.21. Measured and calculated  $V_s$  values for sulfate added 10% KFA treated specimens

The  $V_s$  of 15% SFA treated specimen decreased with NS addition and the decrease increased with increasing sulfate concentration. This is similar behavior that was also observed in  $q_u$  tests. Although the strength of the 15% SFA treated specimen remained nearly the same after the addition of different concentrations of CS, decrease in  $V_s$  of 15% SFA treated specimen was observed with CS addition.

$V_s$  of 10% KFA treated specimen was not affected from the sulfate addition considerably, similar behavior was also observed in strength tests after CS addition, whereas strength of the specimen decreased with NS addition.

The equations recommended by Levesques et al. (2007) and Likitlersuang and Kyaw (2010) generally give closer results to laboratory measurements whereas the equations proposed by Dickenson (1994) and Yun et al. (2006) gives higher and lower  $V_s$  values respectively.  $c_u$  is equal to  $q_u/2$  for fully saturated clays and as the specimens are not fully saturated, this may also affect the values found by using the correlations.

#### **6.8. Effect of Additives on Zeta Potential**

Zeta potential is one of the most important factors that affect the swelling potential of soils. Also, if chemical stabilization results cation exchange reaction in soils, electrokinetic properties including zeta potential may change (Arasan and Akbulut, 2010). Clays have generally negative zeta potential value (Kaya and Yukselen, 2005).

Zeta potential tests were performed on Sample A, 15% SFA, 10% KFA treated samples and 10000ppm and 40000ppm NS and CS added fly ash treated samples to see both the effect of fly ash addition on swelling soil and effect of sulfate addition on fly ash treated samples in terms of cation exchange reactions. pH tests were also performed since zeta potential highly depends on pH values.

Zeta potential and pH values of Sample A and fly ash treated samples are presented in Table 6.38 with the variation in the values of Sample A after fly ash addition.

Table 6.38. Results of pH and zeta potential tests for Sample A and fly ash treated samples

Sample	pH	Zeta Potential (mV)	Increase / Decrease after fly ash addition in	
			pH	Zeta Potential (mV)
A	8.88	-31.9		
15% SFA	11.59	-15.7	2.71	16.2
10% KFA	11.88	-5.4	3.00	26.5

The results for sulfate added fly ash treated samples are presented in Table 6.39.

Table 6.39. Results of pH and zeta potential tests for sulfate added fly ash treated samples

Sample	pH	Zeta Potential (mV)	Percent Increase / Decrease after sulfate addition in	
			pH	Zeta Potential (mV)
15% SFA	11.59	-15.7		
15% SFA + 10000ppm NS	11.47	-30.6	-0.12	-14.9
15% SFA + 40000ppm NS	11.51	-29.9	-0.08	-14.2
15% SFA + 10000ppm CS	11.41	-21.9	-0.18	-6.2
15% SFA + 40000ppm CS	11.20	-19.2	-0.39	-3.5
10% KFA	11.88	-5.4		
10% KFA + 10000ppmNS	11.91	-19.8	0.03	-14.4
10% KFA + 40000ppm NS	11.90	-22	0.02	-16.6
10% KFA + 10000ppm CS	11.81	-17.1	-0.07	-11.7
10% KFA + 40000ppm CS	11.72	-16.6	-0.16	-11.2

The zeta potential values of the samples are entered to the Figure 6.22 that shows the variation in aggregation/dispersion level depending on the average zeta potential value prepared by Yong et al. (2012) to see the effect of fly ash and sulfates.

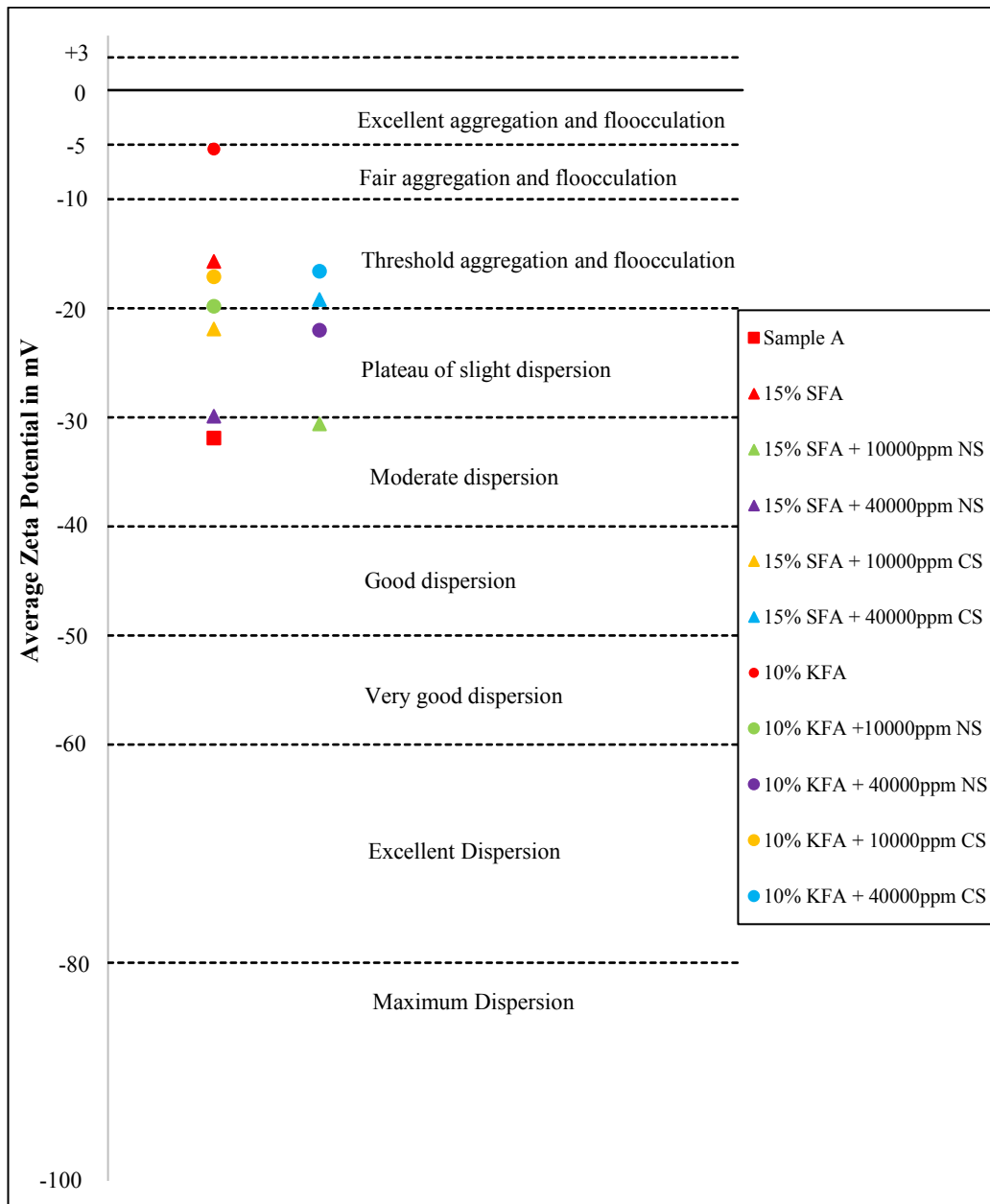


Figure 6.22. The variation in aggregation/ dispersion level of the samples according to zeta potential values (Yong et al., 2012)

Cation exchange, flocculation, pozzolanic reactions, and carbonation are the leading mechanisms that result improvement of engineering properties of soils when clayey soils are mixed with lime in an aqueous medium (Little, 1995; West and Carder, 1997;

Al-Rawas, 2005). Cation exchange and flocculation are the rapid reactions that occur immediately with the mixing of soil and lime (Mallela et. al., 2004).  $\text{Ca}^{2+}$  ions, released from lime replace with  $\text{Na}^+$ ,  $\text{K}^+$  and  $\text{H}^+$  ions that exist in the soil. Replacement of univalent ions with calcium ions results in an increase in the attraction between soil particles (Mallela et al., 2004). Floccs are formed when the soil particles come closer to each other as a result of the attraction and cation exchange.

As can be seen in Table 6.38, Zeta potential of Sample A increased with the addition of fly ashes. Although the concentration of SFA used higher than that of KFA, 10% KFA treatment caused more increase than 15% SFA. This was an expected result since the cation exchange reactions are depended on  $\text{Ca}^{2+}$  content, the CaO content of KFA (29.5%) is higher than that of SFA (11.6%). Fly ash addition caused a more flocculated structure as can be seen in Figure 6.22.

As the zeta potential of Sample A increased after the addition of fly ashes, it could be stated that besides pozzolanic reactions, cation exchange reactions are also effective on the stabilization mechanism. An increase in pH value of swelling soil was also observed after adding both types of fly ash.

The decrease in zeta potential was observed for 15% SFA and 10% KFA treated samples after the addition of both types of sulfate (Table 6.39). The effect of NS was higher than that of CS and NS resulted in more reduction in zeta potential values. This could be probably due to the cations of sulfate, Na is monovalent and Ca is divalent cation which directly affects the cation exchange reactions.

The addition of NS caused approximately the same amount of decrease in zeta potential values of both fly ash treated samples however percent decrease was much higher for 10% KFA treated sample.

It could be stated that the addition of sulfates adversely affected the fly ash treated samples since comparatively more dispersed structure was obtained. This could be due to the probable ettringite formation since CS addition with divalent Ca cation also resulted a decrease in zeta potential.

In conclusion, an absolute reduction in the zeta potential of Sample A was observed after 15% SFA and 10% KFA treatment. The effect of 10% KFA was higher. Zeta potential of 15% SFA and 10% KFA treated samples increased (in absolute value) after the addition of NS and CS with 10000ppm and 40000ppm concentrations.

## **6.9. SEM**

It could be seen from Figure 5.57a that Sample A has a plate-like microstructure which means that the dominant clay mineral that forms the sample is kaolinite. This is a foregone conclusion as Sample A is formed artificially as containing 85% kaolinite and 15% bentonite.

For the 15% SFA treated sample, fly ash particles could be observed in the sample (Figure 5.57b), however, fly ash particles could not be observed in 10% KFA treated sample this could be result of the fact that the fly ash ratio in 10% KFA is less and soil and the hydration products may coat the surface of fly ash (Figure 5.58a).

For 15% SFA treated samples with 40000ppm NS and 40000ppm CS concentrations and 10% KFA treated sample with 40000ppm NS concentration, fly ash could be easily observed within the sample (Figure 5.58b and 5.59). However, any ettringite formations had not been observed within the uncured sulfate added samples.

Ettringite has a needle-like structure. Typical SEM view of ettringite is presented in Figure 6.23.

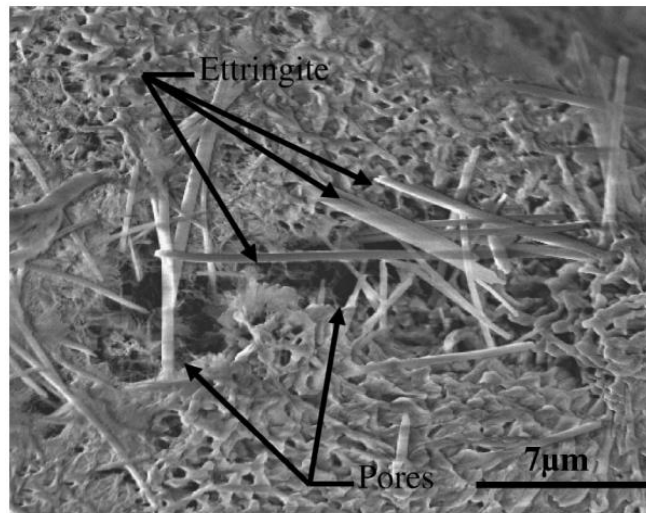


*Figure 6.23.* SEM micrograph of ettringite needles demonstrating porous volume (Cardenas et al., 2011)

A probable ettringite/thaumasite formation was only observed for the 40000ppm NS added 15% SFA treated sample cured for 28 days cured at 10<sup>0</sup>C (Figure 5.60).

Although ettringite formation was determined by the XRD method for 40000ppm NS added 15% SFA treated sample cured at 25<sup>0</sup>C for 28 days, any sign of ettringite formation was not observed from SEM analyses for the same sample (Figure 5.61). This could be due to the fact that only the surface of the samples could be investigated by the help of the SEM. So, this method gives better results for perfectly homogenous materials. However, our samples are not perfectly homogenous and ettringite/thaumasite crystals were probably not occurred in every part of the sample. Therefore, the determination of ettringite /thaumasite crystals will be a little bit chance by this method.

Buttress et al. (2015) studied on the effect of sulfate on two different lime stabilized clayey soils. The clay content of both soils was the same (60%), however, the clay minerals were different. One of the soils contained kaolinite whereas the other contained montmorillonite. At the end of the study, it was found out that ettringite crystals that were formed in the soil containing kaolinite were very small and it was

very difficult to detect with XRD and SEM analyses whereas ettringite crystals that were formed within the soil containing montmorillonite were relatively very large and easily detectable by the analyses. Since Sample A comprised mostly kaolinite this phenomenon may result in not observing ettringite crystals in the sulfate added samples.

Thenardite mineral (NS) that was observed in SEM images of 40000ppm NS added 15% SFA treated sample cured for 6 months at 10<sup>0</sup>C was not observed on the same sample that was cured at the same temperature but with a duration of 28 days. So, it could be stated that the occurrence of this mineral is time-dependent. The analysis results are coherent with XRD in terms of detecting thenardite formation. Thenardite was also observed on the 6 months cured sample on XRD analyses whereas it was not observed for 28 days cured sample.

SEM views of the thenardite were presented in Figure 6.24 with the ones that were observed in the study performed by Rodriquez-Navarro et al. (2000).

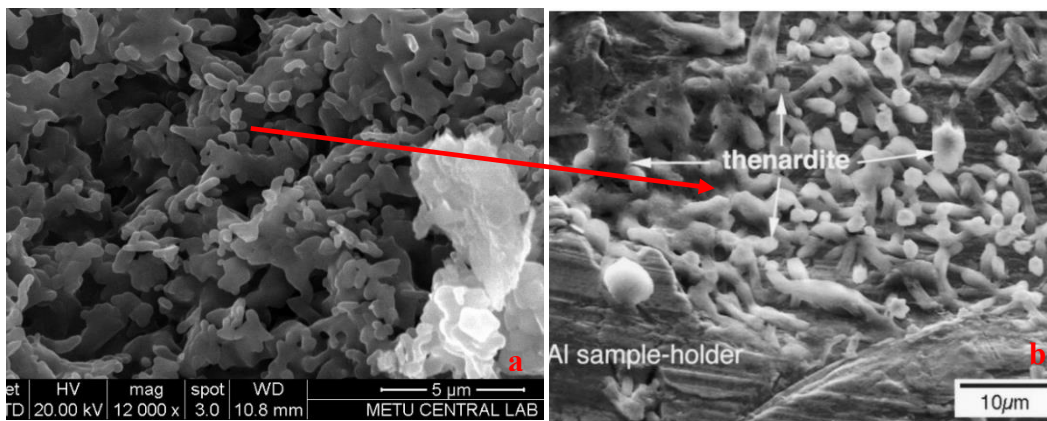
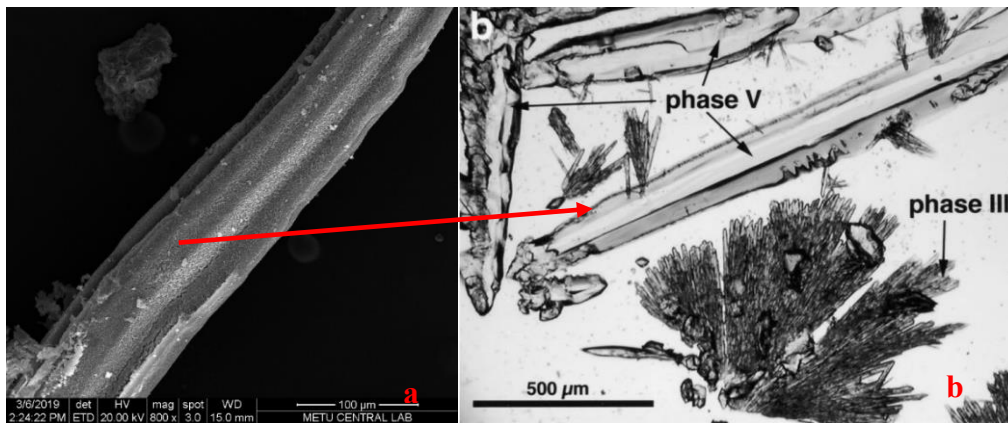


Figure 6.24. SEM views of thenardite a- this study, b- study performed by Rodriques- Navarro et al. (2000)

Gold ( $A_u$ ) and palladium ( $P_d$ ) elements observed in the EDX analyses were due to the covering of sample with gold and palladium before the test (Figures 5.66-5.70). S (Sulfur) had been observed not only in NS and CS added samples but also in 10% KFA treated sample (Figure 5.68). This is due to the fact that this fly ash contains high amount of  $SO_3$  (14.6%).

Thenardite with a chemical formula of NS was also detected in EDX analyses on the 40000ppm NS added 15% SFA treated sample cured for 6 months at  $10^{\circ}C$  as considering the atomic percentages existing in Figure 5.70. The probable ettringite

formation that was observed in SEM analyses of 40000ppm NS added 15% SFA treated sample cured for 28 days at 10<sup>0</sup>C could not be supported by the EDX since the device could not be able to directly focus on the formed structure.

In conclusion, ettringite/thaumasite formation could not be directly observed in SEM analyses. This might be due to the fact that our samples are not perfectly homogenous, ettringite/thaumasite crystals were probably not occurred in every part of the sample and only the surface of the sample could be detected by SEM. Thenardite mineral was observed in SEM images of 40000ppm NS added 15% SFA treated sample cured for 6 months at 10<sup>0</sup>C and the existence of thenardite was also supported by EDX.

#### **6.10. XRD**

The analyses were performed on 40000ppm NS added 15% SFA treated samples that were cured at 10<sup>0</sup>C for 28 days and 6 months. Uncured 15% SFA treated sample and 40000ppm NS added 15% SFA treated sample cured at 25<sup>0</sup>C for 28 days were also exposed to analyses for comparison purposes.

The METU Central laboratory uses a program that includes a library of probable 2 $\theta$  (deg) and d (A) for several materials to interpret the XRD patterns.

The main material within the uncured 15% SFA treated sample was found as kaolinite and sign of ettringite formation was not observed. The results for 28 days cured 40000ppm NS added 15% SFA treated samples at 10<sup>0</sup>C and 25<sup>0</sup>C were nearly identical and the sign of ettringite formation was observed for both samples. When the curing period increased from 28 days to 6 months for the sample cured at 10<sup>0</sup>C, thenardite formation was observed besides ettringite which are the crystals that were seen clearly by naked eyes on the samples.

XRD pattern of different phases of the thenardite is presented in Figure 6.25 (Rodriquez-Navarro et al., 2000).

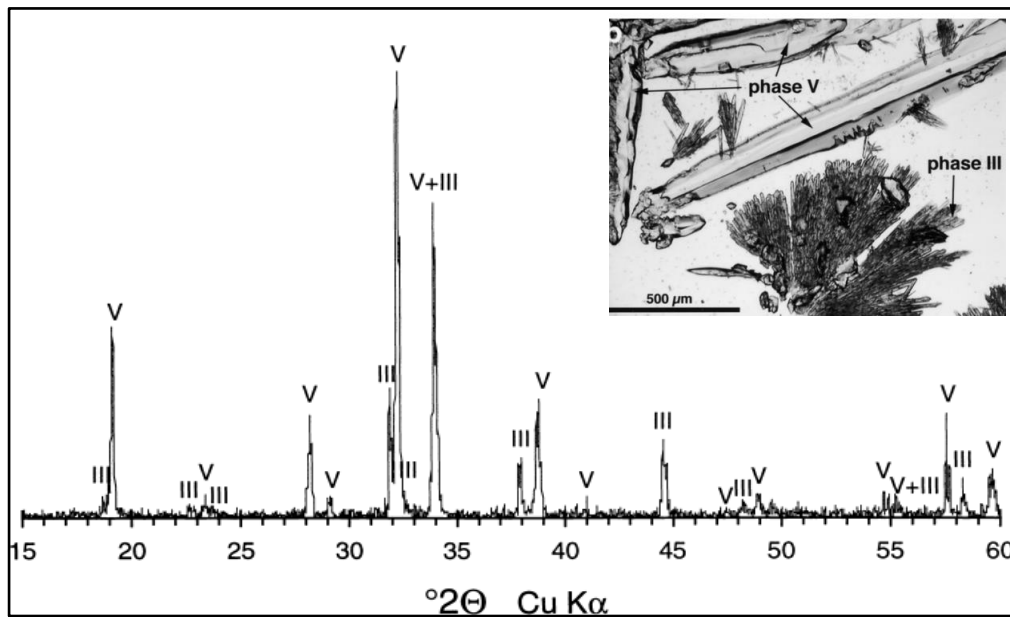


Figure 6.25. XRD pattern of different phases of thenardite (phases III and V) (Rodriquez- Navarro et al., 2000)

Hunter (1988) presents the chemical formula of ettringite and thaumasite as follows;



Once ettringite has nucleated, it continues to grow and when the temperature decreases below  $15^\circ\text{C}$ , ettringite is transformed into thaumasite.



Formation of thaumasite was expected instead of ettringite for the samples that were cured at  $10^\circ\text{C}$  as the ettringite turns into thaumasite when the temperature falls below  $15^\circ\text{C}$ .

XRD patterns of ettringite and thaumasite are very similar especially for the low angle-high intensity lines due to the similarity between the crystallographic structure of these two minerals (Colleparidi, 1999). As the thaumasite or ettringite existed in small amounts in the sample, it was very difficult to determine them in XRD analyses due to the resolution of the X-ray equipment. This may result in small shifts of  $2\theta$  (deg)

values compared to the ones given in the literature also thaumasite may form instead of ettringite for the sample cured at 10°C.

Analyses results for 40000ppm NS added 15% SFA treated samples that were cured at 10°C for 28 days and 6 months are presented in Figures 6.26 and 6.27 respectively.

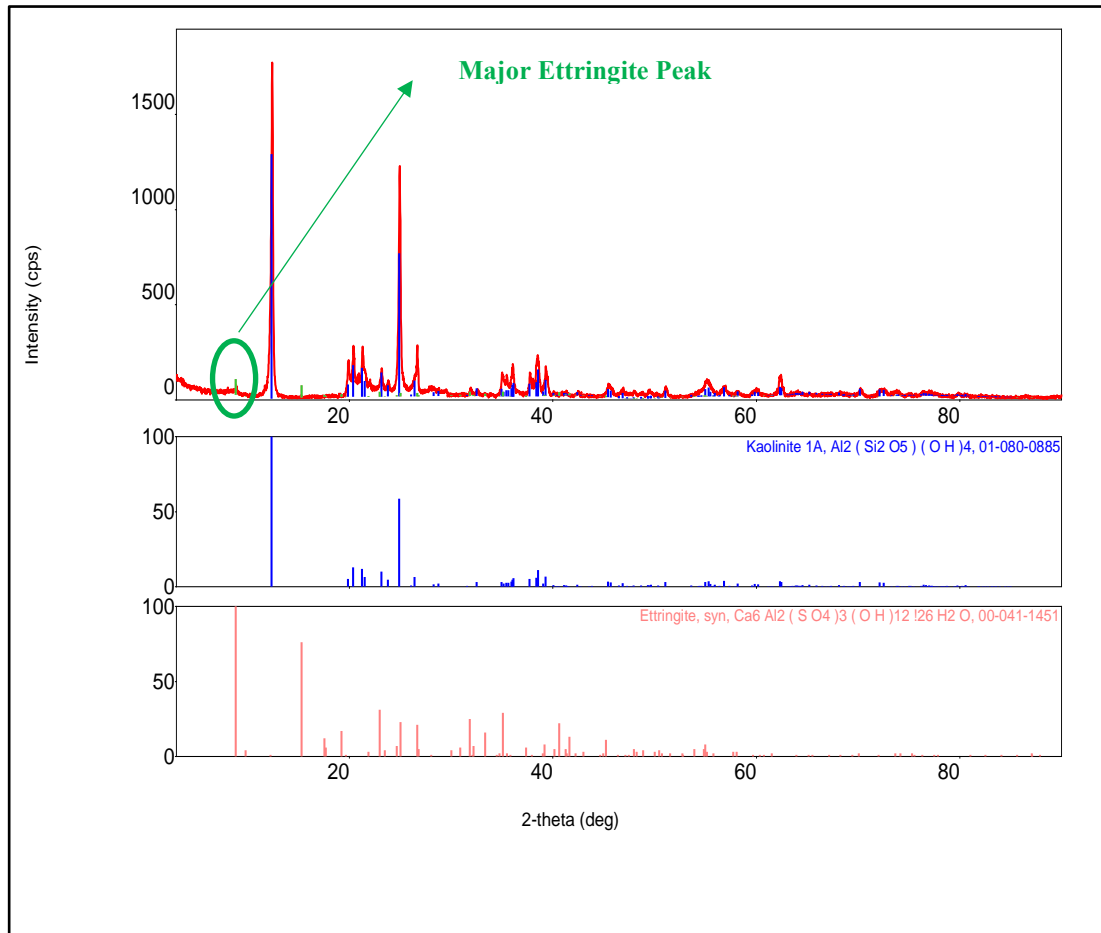


Figure 6.26. XRD analyses of 40000ppm NS added 15% SFA treated sample after 28 days curing at 10°C

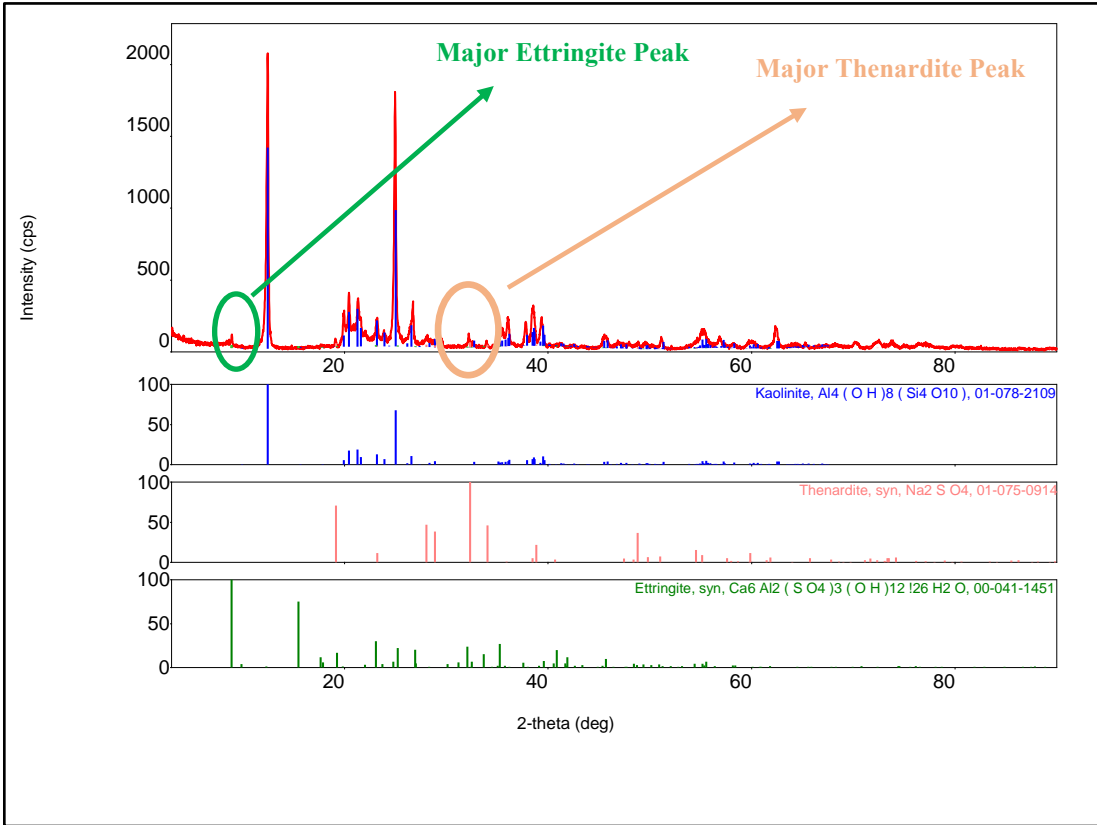


Figure 6.27. XRD analyses of 40000ppm NS added 15% SFA treated sample after 6 months curing at 10°C

Analyses results are drawn together and presented in Figure 6.28 to see difference in the amount of ettringite formed.

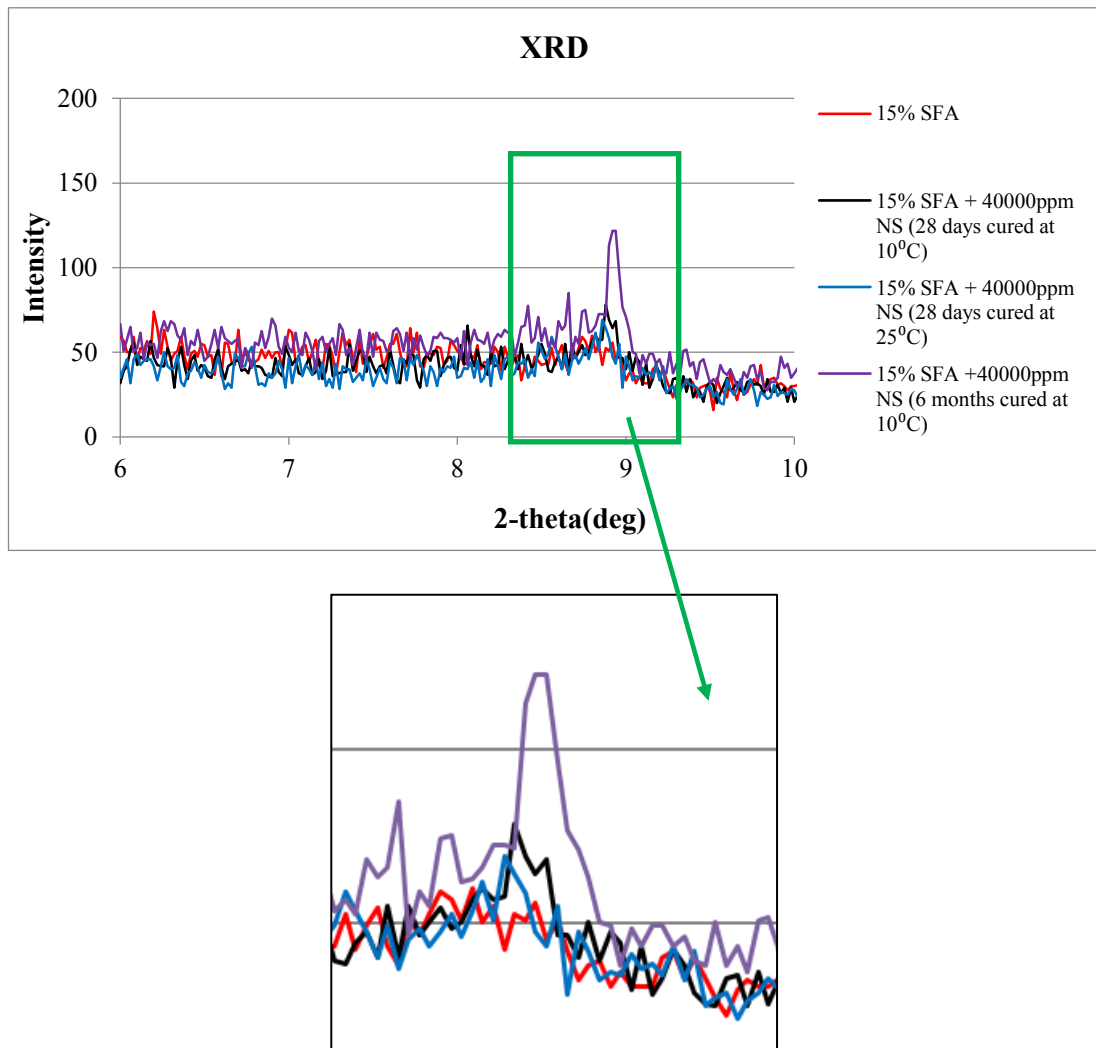


Figure 6.28. XRD analyses of uncured 15% SFA treated sample and 40000ppm NS added 15% SFA treated samples cured at 10°C for 28 days and 6 months and cured at 25°C for 28 days

As can be seen from Figure 6.28, intensity of the major ettringite peak increased with the increase of curing day from 28 days to 6 months for 10°C which is a sign of the rise in the ettringite formation. Also, a slight increase was observed when the temperature decreased from 25°C to 10°C.

Strength reduction of the 40000ppm NS added samples that were cured at 10°C was probably due to the combined effect of thaumasite/ettringite and thenardite formations.

In conclusion, sign of ettringite formation was observed for 40000ppm NS added 15% SFA treated specimens in XRD analyses. The intensity of the peaks increased with the decrease of curing temperature and an increase in curing period. Thenardite was also observed besides ettringite within the 40000ppm NS added 15% SFA treated specimen that was cured at 10°C for 6 months.

## CHAPTER 7

### CONCLUSIONS

This study aims to investigate the behavior of class C fly ashes beside lime that is used with sulfate bearing soils, attract attention to ettringite induced heave problems in Turkey and investigate the suitability of usage of high sulfate class C fly ashes in clayey soil stabilization. Lime was used for comparison purposes during the study.

In this study, when the index properties are considered it was seen that sulfate addition had a beneficiary effect in reducing the plasticity of fly ash and lime treated soils. Sulfate addition affected the swell potential of each treated specimen differently. Swell potential of 15% SFA treated specimen was affected positively from sulfate addition and a reduction was observed. Although not dramatic, a general increase was observed in the swell potential of 4% L treated specimen after sulfate addition. Swell potential of 10% KFA treated specimen was not affected much from the sulfate addition, especially for CS. The strength of uncured fly ash and lime treated specimens was generally affected negatively from NS addition and the maximum reduction was observed for 40000ppm concentration. CS addition had no significant effect on the strength properties of specimens treated with calcium-based stabilizers. The temperature had an important effect on both swell and strength properties of sulfate added specimens. The rate of beneficial chemical reactions generally slowed down with the decrease of temperature from 25°C to 10°C and an opposite behavior was observed with the increase of temperature to 40°C. Curing had an important effect on increasing the strength of specimens.

One of the most important aim of this study is to investigate the behavior of class C fly ashes beside lime that is used with sulfate bearing soils. Although similar effect was observed in terms of physical and mechanical properties, the effect of sulfate

differed in terms of swelling properties. The swelling potential of 4% L treated specimen affected adversely from sulfate addition, however beneficiary effect was observed for SFA treated specimen with a low calcium and sulfate content. Therefore, it could be stated that class C fly ashes with low calcium and sulfate content could be chosen instead of lime in stabilization of sulfate-bearing soils.

The most important finding of this study was the dramatic decrease in strength of 40000ppm NS added fly ash treated specimens that were cured at 10°C as a result of the salination and ettringite formation. This concentration of NS also caused the reduction of the beneficiary effect of curing in higher temperatures. Although the strength values of the specimens treated with different calcium-based stabilizers generally reacted similarly, the swelling properties showed completely different behavior. Therefore, stating certain risk levels of sulfate for sulfate-bearing soils treated with calcium-based stabilizers will not be meaningful as the behavior affected by many factors besides sulfate level such as calcium content of additives, temperature of the environment, water content, chemical and physical properties of soils, type of sulfate etc.

The other aim of this study is to investigate the suitability of usage of high sulfate class C fly ashes in clayey soil stabilization. In this study, the beneficiary effect of 10% KFA was higher than the 15% SFA in terms of physical, swelling and strength properties. Although KFA has higher sulfate content, which prevents the usage of it in concrete production according to ASTM C-618, it was more satisfactory in improving the soil properties and no adverse effect was observed although a higher concentration than the required one was used. The usage of this type of fly ashes will be beneficial in reducing the environmental problems related to the deposition of fly ashes. Therefore, it could be stated that high sulfate class C fly ashes could be used in clayey soil stabilization according to test results.

Also, it was found out from this study that both class C fly ash and lime were not sufficient in preventing the salt heave problem.

The swelling associated problems could be solved by taking drainage precautions. However, strength reduction in 40000ppm NS added specimens cured at 10<sup>0</sup>C occurred with it's own mixing and compaction water not by taking extra water from environment and drainage will not be helpful for the prevention of the strength reduction problems.

It should not be forgotten that these findings are valid for this specific soil, calcium-based stabilizers and applied conditions and it could also be seen from the previous studies that each soil reacted differently to the addition of calcium-based stabilizers and sulfates. However, the findings of this study could be used as a guideline for the soils with similar chemical and physical properties with Sample A.

Required laboratory tests should be applied according to project criteria before application of the chemical treatment in sulfate-bearing soils by also considering the environmental factors such as temperature variation. Firstly, the sulfate level of the soil should be determined. All the tests should be performed by using the water that will be used in real site application not by using distilled water. As water is a probable sulfate source, the sulfate content of the water should also be determined. The properties of the additive are important factors in soil stabilization, therefore the laboratory tests should also be performed on the selected additive. Great attention should be paid especially in case of using class C fly ash as the properties of fly ashes depend on many factors such as coal source, boiler and emission control, etc., and even the properties of the fly ash produced in the same power plant may vary. The seasonal variation of soil temperature with depth should be measured if possible. Otherwise, previous studies should be used if available. The laboratory tests should be performed at different temperatures as reflecting the real site conditions. In case of observing adverse effect in any of the physical, mechanical, and swelling properties, different methods like mellowing, double application, using GBFS, class F fly ash, etc. should be selected by considering the project criteria like economy and duration.

### **Recommendations for Future Researches**

In this investigation, the studies were mainly focused on the effect of sulfates on an expansive soil treated with two different class C fly ashes. Therefore, to better estimate the behavior of the sulfate bearing soils treated with class C fly ashes, the tests could be performed on different soils that have different physical and chemical properties treated with the same fly ashes since physical and chemical properties of the soil have also a major influence in ettringite related problems. Cyclic swell-shrink tests could also be performed on samples to determine the long-term behavior by reflecting the moisture content variation in the soils occurs at the site as a result of the seasonal temperature variation, rainfalls, etc.

Also, studies could be focused on the methods for preventing salination problems since this topic did not attract much attention and in this study, it was found out that chemical stabilization was not effective in preventing these problems. Also, for all soil mechanics tests, the effect of temperatures especially the lower ones on the soil properties should be investigated carefully, since generally the tests are performed at room temperature that will not be satisfactory at reflecting the real site conditions.

## REFERENCES

- Abdi, M. R. and Wild, S. 1993. Sulphate expansion of lime-stabilized kaolinite: I. physical characteristics. *Clay Minerals*, 28, 555–567.
- Akbulut, S. and Arasan, S. 2010. The variations of cation exchange capacity, pH, and zeta potential in expansive soils treated by additives. *International Journal of Civil and Structural Engineering*, 1(2), 139–154.
- Al-Ani T. and Sarapaa O. 2008. *Clay and Clay Mineralogy, Physical - chemical properties and Industrial Uses*. Geological Survey of Finland, 94 pages.
- Al-Dahlaki, M. H. 2007. Effect of fly ash on the engineering properties of swelling soils. *Journal of Engineering and Development*, 11(3), ISSN 1813-7822.
- Al-Mhaidib, A. I. and Al-Shamrani, M. A. 1996. Swelling characteristics of lime treated expansive soils. *Geotechnical Engineering, Journal of Southeast Asian Geotechnical Society*, 27 (2), 37–53.
- Al-Rawas, A. A., Hago, A. W. and Al-Sarmi, H. 2005. Effect of lime, cement and Sarooj (artificial pozzolan) on the swelling potential of an expansive soil from Oman. *Building and Environment*, 40(5), 681–687.
- American Coal Ash Association, 2003. *Fly Ash Facts for Highway Engineers*. Report No. FHWA-IF-03-019, U.S. Department of Transportation Federal Highway Administration.
- Ansary, M.A., Siddique A. and Hasan K.A. 2003. A Study of lime stabilization on soil of a selected reclaimed site of Dhaka City. *Proceedings of 12<sup>th</sup> Asian Regional Conference on Soil Mechanics and Geotechnical Engineering*. 1: 439-442, World Scientific Publishing Co. Pte. Ltd., Singapore
- Ardani, A. 1992. *Expansive Soil Treatment Methods in Colorado*. Report No. CDOT-DTD-R-92-2, Federal Highway Administration.
- As, M. 2012. Effect of cyclic swell- shrink on swell percentage of an expansive clay stabilized by class C fly ash. M.S. Thesis, METU, Turkey, 115 pages.
- Ashford, S. A., Jakrapiyanum, W. and Lukkanaprasit, P. 1997. Amplification of earthquake ground motion in Bangkok. Report No. Cu\CE\EVR\1997.002, Chulalongkorn University, Bangkok, Thailand.
- ASTM. 1970. *Special Procedures for Testing Soil and Rock for Engineering Purposes*. 5<sup>th</sup> edition, ASTM Special Publication 479, Easton.
- ASTM Standard D427. 2004. *Standard Test Method for Shrinkage Factors of Soils by the Mercury Method*. ASTM International, West Conshohocken, PA.

ASTM Standard D422. 2007. Standard Test Method for Particle-Size Analysis of Soils. ASTM International, West Conshohocken, PA.

ASTM Standard D5102. 2009. Standard Test Methods for Unconfined Compressive Strength of Compacted Soil-Lime Mixtures. ASTM International, West Conshohocken, PA.

ASTM Standard D5239. 2012. Standard Practice for Characterizing Fly Ash for Use in Soil Stabilization. ASTM International, West Conshohocken, PA.

ASTM Standard D4546. 2014. Standard Test Methods for One- Dimensional Swell or Collapse of Soils. ASTM International, West Conshohocken, PA.

ASTM Standard D854. 2014. Standard Test Methods for Specific Gravity of Soil Solids by Water Pycnometer. ASTM International, West Conshohocken, PA.

ASTM Standard C618. 2015. Standard Specification of Coal Fly Ash and Raw or Calcined Natural Pozzolan for Use in Concrete. ASTM International, West Conshohocken, PA.

ASTM Standard D2166. 2016. Standard Test Method for Unconfined Compressive Strength of Cohesive Soil. ASTM International, West Conshohocken, PA.

ASTM Standard D4318. 2017. Standard Test Method for Liquid Limit, Plastic Limit and Plasticity Index of Soils. ASTM International, West Conshohocken, PA.

ASTM Standard D6276. 2019. Standard Test Method for Using pH to Estimate the Soil- Lime Proportion Requirement for Soil Stabilization. ASTM International, West Conshohocken, PA.

Aydin, M., Sisman, A., Gultekin, A. and Dehghan, B. 2015. An experimental performance comparison between different shallow ground heat exchangers. Proceedings World Geothermal Congress, 19-25 April 2005, Melbourne, Australia.

Baglari, D. and Dash, S. K. 2013. Improvement of expansive soil by lime and reinforcement. Proceedings of Indian Geotechnical Conference (December 22 -24), Roorkee.

Barton, C. D. and Karathanasis, A. D. 2002. Clay minerals. In: Lal, R. (Ed.), Encyclopedia of Soil Science. Marcel Dekker, New York, USA, pp. 187–192.

Baytar, A. O. 2005. Effects of fly ash and desulphogypsum on the geotechnical properties of Cayırhan Soil. M.S. Thesis, METU, Turkey, 82 pages.

Beeghly, J. H. 2003. Recent Experiences with lime-fly ash stabilization of pavement subgrade soils, base and recycles asphalt. Proceeding of International Ash Utilization Symposium, Lexington, pp. 435-452.

- Belchior, I. M. R. M., Casagrande, M. D. T. and Zornberg, J. G. 2017. Swelling behavior evaluation of a lime-treated expansive soil through centrifuge test. *Journal of Materials in Civil Engineering*, 29(12), 04017240-1–04017240-12.
- Bell, F. 1996. Lime stabilization of clay minerals and soils. *Engineering Geology*, 42(4), 223-237.
- Bhuvaneshwari, S., Robinson, R. G. and Gandhi, S. R. 2014. Behavior of lime treated cured expansive soil composites. *Indian Geotechnical Journal*, 44(3), 278–293.
- Blaser, H. D, and Scherer, O. J. 1969. Expansion of soils containing sodium sulfate caused by drop in ambient temperatures. Highway Research Board, Special Report 103, pp. 150–160.
- British Standard BS 1377-3. 1990. Methods of Test for Soils for Civil Engineering Purposes- Part 3: Chemical and electro-chemical tests. British Standard Institution, London.
- Britpave. 2005. Technical Guidelines: Stabilization of Sulfate- Bearing Soils. The British In-situ Concrete Paving Association, Ref. BP/16.
- Britpave. 2007. Technical Guidelines: HBM and Stabilization 1- The design and specification of Parking areas and Hardstandings. The British In-situ Concrete Paving Association, Ref. BP/26.
- Bunaciu, A. A., Udristoiu, E. G. and Aboul-Enein, H. Y. 2015. X-ray diffraction: instrumentation and applications. *Critical Reviews in Analytical Chemistry*, 45(4), 289–299.
- Buttress, A. J., Grenfell, J. A. and Airey, G. D. 2015. Accelerated swell testing of artificial sulfate bearing lime stabilized cohesive soils. *Materials and Structures*, 48(11), 3635–3655.
- Cardenas, H., Kupwade-Patil, K. and Eklund, S. 2011. Recovery from sulfate attack in concrete via electrokinetic nanoparticle treatment. *Journal of Materials in Civil Engineering*, 23(7), 1103–1112.
- Celik, A. O. 2014. Evaluation of hydrated lime stabilization of sulfate bearing expansive soils. Ph.D. Thesis, Eastern Mediterranean University, North Cyprus, 114 pages.
- Cherian, C. and Arnepalli, D. N. 2015. A critical appraisal of the role of clay mineralogy in lime stabilization. *International Journal of Geosynthetics and Ground Engineering*, 1(1), 1–20.
- Chindris, L., Stefanescu, D. P., Radermacher, L., Radeanu, C. and Popa, C. 2017. Expansive soil stabilization - General considerations. 17<sup>th</sup> International Multidisciplinary Scientific GeoConference Surveying Geology and Mining Ecology Management, SGEM, 17(32), 247–256.

- Choudhary, O. P. and Choudhary, P. 2017. Scanning electron microscope: Advantages and disadvantages in imaging components. *International Journal of Current Microbiology and Applied Sciences*, 6(5), 1877–1882.
- Cokca, E. 2001. Use of class C fly ashes for the stabilization of expansive soil. *Journal of Geotechnical and Geoenvironmental Engineering*, 127(7), 568-573.
- Colorado Geological Survey. n.d. Heaving in bedrocks. Available at: <http://coloradogeologicalsurvey.org/geologic-hazards/heaving-bedrock/> (last visited on 31.10.2019)
- Colleparidi, M. 1999. Thaumasite formation and deterioration in historic buildings. *Cement and Concrete Composites*, 21(2), 147–154.
- Croft, J. 1964. The pozzolanic reactivities of some New South Wales fly ashes and their application to soil stabilization. *Proceeding of 2<sup>nd</sup> Australian Road Research Board (ARRB) Conference, Melbourne.*
- Das, B. M. (2008). *Advanced Soil Mechanics*. 3<sup>rd</sup> edition, Taylor and Francis Group, London and Newyork.
- Deb, T. and Pal, S. K. 2014. Effect of fly ash on geotechnical properties of local soil-fly ash mixed samples. *International Journal of Research in Engineering and Technology*, 3(5), 507-516.
- Degirmenci, N., Okucu, A. and Turabi, A. 2007. Application of phosphogypsum in soil stabilization. *Building and Environment*, 42(9), 3393–3398.
- Dempsey, B.J. and Thompson, M.R. 1968. Durability properties of lime-soil mixtures. *Highway Research Record No. 235*, National Research Council, Washington D.C.
- Dickenson, S. E. 1994. Dynamic response of soft and deep cohesive soils during the Loma Prieta earthquake of October 17, 1989. Ph.D. Thesis, University of California, Berkeley, CA, 331 pages.
- Dwivedi, A. and Jain, M. K. 2014. Fly ash – waste management and overview: A Review, *Recent Research in Science and Technology*, 6(1), 30–35.
- Eades, J. L. and Grim, R. E. 1960. A quick test to determine lime requirements for lime stabilization. *The 45<sup>th</sup> Annual Meeting of the committee on Lime and Lime-Fly Ash Stabilization*, 61–72.
- Fang, H. 1991. *Foundation Engineering Handbook*, 2<sup>nd</sup> edition, Van Nostrand Reinhold, America.
- Firoozi, A. A., Olgun, C.G., Firoozi, A.A. and Baghini, M.S. 2017. Fundamentals of soil stabilization. *International Journal of Geo-Engineering*, 8:26, 1-16.

- Florides, G. and Kalogirou, S. 2005. "Annual ground temperature measurements at various depths. Proceedings of CLIMA-2005 Conference, 9-12 October, Lousanne, Switzerland.
- Foster, M. D. 1954. The Relation between composition and swelling in clays\*. *Clays and Clay Minerals*, 3(1), 205–220.
- Fredlund, D.G., Rahardjo, M.D. and Fredlund, M.D. 2012. *Unsaturated Soil Mechanics in Practice*. 1<sup>st</sup> edition, John Wiley & Sons. Inc, New Jersey.
- Gadouri, H., Harichane, K. and Ghrici, M. 2017. Effect of sodium sulphate on the shear strength of clayey soils stabilized with additives. *Arabian Journal of Geosciences*, 10:218, 1-17.
- Gaily, A.H.M. 2012. Engineering behavior of lime treated high sulfate soils. M.S. Thesis, The University of Texas, Arlington, 111 pages.
- General Directorate of Highways. 2013. *Technical Specification for Highways 2013*, Turkey.
- General Directorate of Mineral Research and Exploration. 2010. *Mine and Energy Resources of Ankara, Turkey*, 8 pages.
- Grim, R. E. 1942. Modern concepts of clay materials. *The Journal of Geology*, 50(3), 225–275.
- Guney, Y., Sari, D., Cetin, M. and Tuncan, M. 2007. Impact of cyclic wetting-drying on swelling behavior of lime-stabilized soil. *Building and Environment*, 42(2), 681–688.
- Harris, P., Harvey, O., Jackson, L., DePugh, M. and Puppala, A. 2014. Killing the ettringite reaction in sulfate-bearing soils. *Transportation Research Record: Journal of the Transportation Research Board*, No. 2462, 109–116.
- Harris, P., Holdt, J. V., Sebesta, S. and Scullion, T. 2006. Recommendations for stabilization of high-sulfate soils in Texas, Report No. FHWA/TX-06/4240-3, Texas Department of Transportation
- Hartuti, S., Kambara, S., Takeyama, A., Hanum, F. F. and Desfitri, E. R. 2018. Chemical stabilization of coal fly ash for simultaneous suppressing of As, B, and Se leaching. In: *Coal Fly Ash Beneficiation - Treatment of Acid Mine Drainage with Coal Fly Ash* (eds. Akinyemi, S., and Gitari, M.), Intech, Croatia, 29-51.
- Higgins, D. 2005. Soil stabilization with ground granulated blast furnace slag. UK Cementitious Slag Makers Association (CSMA), 1–15. Available at: [http://www.ukcsma.co.uk/files/csma\\_report\\_on\\_soil\\_stabilisation.pdf](http://www.ukcsma.co.uk/files/csma_report_on_soil_stabilisation.pdf).
- Higgins, D. D., Phipps, S. and Coates, A. 2013. A Comparison of 3 Swell / Stability Tests on Clay Soils Treated with Lime, Cement And GGBS. BRITPAVE Soil Stabilization Task Group: Project Report, 12 pages.

- Hunter, D.B. 1988. Lime-induced heave in sulfate-bearing clay soils. *Journal of Geotechnical Engineering*, 114 (2), 150-167.
- Ige, J. A. and Ajamu, S. O. 2015. Unconfined compressive strength test of a fly ash stabilized sandy soil. *International Journal of Latest Research in Engineering and Technology*, 1(3), 1–11.
- Jackson, M.L., 2005. *Soil Chemical Analysis: advance course: a manual of methods useful for instruction and research in soil chemistry of soils, soil fertility, and soil genesis*. Revised 2<sup>nd</sup> edition, Parallel Press, Madison, Wisconsin.
- Jawad, I.T., Taha, M.R., Majeed, Z.H. and Khan, T.A. 2014. Soil stabilization using lime: Advantages, disadvantages and proposing a potential alternative. *Research Journal of Applied Sciences, Engineering and Technology*, 8(4), 510-520.
- Jayalath, C. P. G., Gallage, C. and Miguntanna, N.S. 2016. Factors affecting the swelling pressure measured by the oedemeter method., *International Journal of Geomate*, 11(24), 2397–2402.
- Ji-ru, Z. and Xi, C. 2002. Stabilization of expansive soil by lime and fly ash. *Journal of Wuhan University of Technology- Material Science Edition*, 17(4), 73-77.
- Kalantari, B. 2012. Engineering significant of swelling soils. *Research Journal of Applied Sciences, Engineering and Technology*, 4(17), 2874–2878.
- Kavak, A., Gungor, A.G., Avsar, C., Atbas, B. and Akyarlı, A. 2008. A lime stabilization application on a divided road project. 12<sup>nd</sup> Conference of Soil Mechanics and Foundation Engineering, Selcuk University, Konya.
- Kaya, A. and Yukselen, Y. 2005. Zeta potential of clay minerals and quartz contaminated by heavy metals. *Canadian Geotechnical Journal*, 42(5), 1280–1289.
- Kinuthia, J. M., Wild, S. and Jones, G. I. 1999. Effects of monovalent and divalent metal sulphates on consistency and compaction of lime-stabilized kaolinite. *Applied Clay Science*, 14(1–3), 27–45.
- Knappett, J. A. and Craig, R. F. 2012. *Craig's Soil Mechanics*. 8<sup>th</sup> Edition, Spon Press, London and Newyork.
- Kolias, S., Kasselouri-Rigopoulou, V. and Karahalios, A. 2005. Stabilization of clayey soils with high calcium fly ash and cement. *Cement and Concrete Composites*, 27(2), 301–313.
- Kumar, N. and Kumbhat, S. 2016. *Essentials in Nanoscience and Nanotechnology*. 1<sup>st</sup> edition, John Wiley & Sons. Inc., New Jersey.
- Levesques, C.L, Locat, J. and Leroueil, S. 2007. Characterization of postglacial sediments of the Saguenay Fjord, Quebec. *Characterization and Engineering Properties of Natural Soils*, Vol. 4, Taylor & Francis Group, London, 2645-2677.

- Likitlersuang, S., and Kyaw, K. (2010). A study of shear wave velocity correlations of Bangkok subsoil. *Obras y proyectos*, 7, 27–33.
- Little, D. N. 1995. Handbook for stabilization of pavement subgrades and base courses with lime. National Lime Association, 219 pages.
- Little, D. N. and Graves, R. 1995. Guidelines for Use of Lime in Sulfate-bearing Soils. Chemical Lime Company, Fort Worth, Texas.
- Little, D. N. and Nair, S. 2009. Recommended Practice for Stabilization of Sulfate Rich Subgrade Soils. National Cooperative Highway Research Program Transportation Research Board of the National Academies, Report No. Web-only document 145, 54 pages.
- Little, D. N., Nair, S. and Herbert, B. 2010. Addressing sulfate-induced heave in lime treated soils. *Journal of Geotechnical and Geoenvironmental Engineering*, 136(1), 110–118.
- Little, N. D., Herbert, B. and Kunagalli, S. N. 2002. Ettringite formation in lime-treated soils: establishing thermodynamic foundations for engineering practice. Transportation Research Board for Presentation and Publication at the 2005 annual meeting in Washington, D.C, paper no. 05-2239.
- Mackiewicz, S. M. and Ferguson, E. G. 2005. Stabilization of Soil with Self-Cementing Coal Ashes. 2005 World of Coal Ash (WOCA), April 11-15, Lexington, Kentucky, USA, 1–7.
- Mallela, J., Von Quintus, H., Smith, K. L. and Eres Consultants. 2004. Consideration of Lime-stabilized Layers in Mechanistic-empirical Pavement Design. The National Lime Association, Arlington, Virginia, USA.
- Malvern Instruments Limited. 2015. Zeta potential- an introduction in 30 minutes. Technical note, 15 pages.
- McCarthy, M. J., Csetenyi, L. J., Sachdeva, A. and Dhir, R. K. 2012a. Identifying the role of fly ash properties for minimizing sulfate-heave in lime-stabilized soils. *Fuel*. Elsevier Ltd, 92(1), 27–36.
- McCarthy, M. J., Csetenyi, L. J., Sachdeva, A. and Dhir, R. K. 2012b. Fly ash influences on sulfate-heave in lime-stabilized soils. *Proceedings of the Institution of Civil Engineers- Ground Improvement*, 165(3), 147–158.
- McCarthy, M. J., Csetenyi, L. J., Sachdeva, A. and Jones, M. R. 2009. Role of fly ash in the mitigation of swelling in lime stabilized sulfate-bearing soils. 2009 World of Coal Ash (WOCA) Conference. Lexington, KY, USA.
- Mir, B. A. and Sridharan, A. 2019. Mechanical behavior of fly-ash-treated expansive soil. *Proceedings of the Institution of Civil Engineers- Ground Improvement*, 172(1), 12–24.

- Misra, V. B., Reddy, P. S. R. and Mohapatra, B. K. 2004. Mineral Characterization and Processing. Allied Publishers Private Limited.
- Mitchell, J. K. 1986. Practical problems from surprising soil behavior. *Journal of the Geotechnical Engineering Division, ASCE*, 112(3), 259-289.
- Mittermayr, F., Bauer, C., Klammer, D., Bottcher, M. E., Leis, A., Escher, P. and Dietzel, M. 2012. Concrete under sulphate attack: An isotope study on sulphur sources. *Isotopes in Environmental and Health Studies*, 48(1), 105–117.
- Moayedi, H., Asadi, A., Moayedi, F., Huat, B. B. K. and Kazamien, S. 2011. Using secondary additives to enhance the physicochemical properties of kaolinite. *International Journal of Physical Sciences*, 6(8), 2004–2015.
- Mohammed, A. and Vipulanandan, C. 2015. Testing and modeling the short-term behavior of lime and fly ash treated sulfate contaminated CL soil. *Geotechnical and Geological Engineering*, 33(4), 1099–1114.
- Mohn, D. 2015. Impact of Gypsum Bearing Water on Soil Subgrades Stabilized with Lime or Portland Cement. M.S. Thesis, University of Akron, USA, 170 pages.
- Murray, H. H. 2007. Applied clay mineralogy: occurrences, processing and applications of kaolins, bentonites, palygorskite-sepiolite, and common clays. 1<sup>st</sup> edition, Elsevier, Amsterdam; Oxford.
- Murthy, V. N. S. 2002. Geotechnical Engineering: Principles and Practices of Soil Mechanics and Foundation Engineering. Marcel Dekker Inc., New York.
- Nalbantoğlu, Z. 2004. Effectiveness of class C fly ash as an expansive soil stabilizer. *Construction and Building Materials*, 18(6), 377–381.
- Nalbantoğlu, Z. and Gucbilmez, E. 2001. Improvement of calcareous expansive soils in semi-arid environments. *Journal of Arid Environments*, 47(4), 453-463.
- Nath, B. D., Molla, M. K. A. and Sarkar, G. 2017. Study on strength behavior of organic soil stabilized with fly ash. *International Scholarly Research Notices*. Hindawi, 1–6.
- National Lime Association, 2000. Guidelines for Stabilization of Soils Containing Sulfates Austin White Lime, Chemical Lime, Texas Lime. Technical Memorandum, 16 pages.
- National Lime Association, 2004. Lime-Treated Soil Construction Manual: Lime Stabilization & Lime Modification. Bulletin 326, (January). Available at: <http://scholar.google.com/scholar?hl=en&btnG=Search&q=intitle:Lime-Treated+Soil+Construction+Manual+Lime+Stabilization+&+Lime+Modification#0>.
- Nelson, J.D. and Miller, D.J. 1992. Expansive Soils, Problems and Practice in Foundation and Pavement Engineering, 1<sup>st</sup> edition, John Wiley and Sons Inc., United States.

- Oweis, I. S., Khera, R. P. 1998. *Geotechnology of Waste Management*, 2<sup>nd</sup> Edition, PWS Publishing Company, Boston.
- Ozdemir, M. A. 2011. Improvement of Bearing Capacity of a Soft Soil by the Addition of Fly Ash. M.S. Thesis, METU, Turkey, 119 pages.
- Ozmen, E. 2011. Termik santral küllerinin yönetimi. Atık Yönetimi Sempozyumu, Antalya.
- Prusinski, J. R. and Bhattacharja, S. 1999. Effectiveness of Portland cement and lime in stabilizing clay soils. *Transportation Research Record Journal of the Transportation Research Board*, 1652, 215-227.
- Puppala, A. J. and Cerato, A. 2009. Heave distress problems in chemically- treated sulfate-laden materials. *Geo-Strata*, 10(2), 28-32.
- Puppala, A. J., Congress, S. S. C., Talluri, N. and Wattanasanthicharoen, E. 2019. Sulfate-heaving studies on chemically treated sulfate-rich geomaterials. *Journal of Materials in Civil Engineering*, 31(6), 04019076-1–04019076-9.
- Puppala, A. J., Griffin, J. A., Hoyos, L. R. and Chomtid, S. 2004. Studies on sulfate-resistant cement stabilization methods to address sulfate-induced soil heave. *Journal of Geotechnical and Geoenvironmental Engineering*, 130(4), 391–402.
- Puppala, A. J., Intharasombat, N. and Vempati, R. K. 2005. Experimental studies on ettringite-induced heaving in soils, *Journal of Geotechnical and Geoenvironmental Engineering*, 131(3), 325–337.
- Puppala, A. J., Talluri, N., Gaily, A. and Chittoori, C.S. 2013. Heaving mechanism in high sulfate soils. *Proceedings of the 18<sup>th</sup> International Conference on Soil Mechanics and Geotechnical Engineering*, 3125-3128, Paris.
- Puppala, A. J., Wattanasanticharoen, E. and Punthutaecha, K. 2003. Experimental evaluations of stabilization methods for sulphate-rich expansive soils. *Ground Improvement*, 7(1), 25-35.
- Rajasekaran, G. 2005. Sulphate attack and ettringite formation in the lime and cement stabilized marine clays. *Ocean Engineering*, 32(8–9), 1133–1159.
- Rao, S. M. and Shivananda, P. 2005. Impact of sulfate contamination on swelling behavior of lime-stabilized clays, *Journal of ASTM International*, 2(6), 209–218.
- Robinson. R. and Thagesen B. 2004. *Road Engineering for Development*. 1<sup>st</sup> edition, Spoon Press, London.
- Rodriguez-Navarro, C., Doehne, E. and Sebastian, E. 2000. How does sodium sulfate crystallize? Implications for the decay and testing of building materials. *Cement and Concrete Research*, 30(10), 1527–1534.

- Rollings, B. R. S., Burkes, J. P. and Rollings, M. P. 1999. Sulfate attack on cement-stabilized sand. *Journal of Geotechnical and Geoenvironmental Engineering*, 125(5), 364–372.
- Ruff, C. G. 1965. Time-Temperature-Strength-Reaction Product Relationships in Lime-Bentonite-Water Mixtures. Ph.D. Thesis, Iowa State University, Iowa, 60 pages.
- Seco, A., Ramirez, F., Miqueleiz, L. and Garcia, B. 2011. Stabilization of expansive soils for use in construction, *Applied Clay Science*, 51(3), 348–352.
- Sharma, R., Bisen, D. P., Shukla, U. and Sharma, B. G. 2012. X-ray diffraction: a powerful method of characterizing nanomaterials. *Recent Research in Science and Technology*, 4(8), 77–79.
- Sharma, S. S., Verma, D. S., Khan, L. U., Kumar, S. and Khan, S. B. 2018. *Handbook of Materials Characterization*, 1<sup>st</sup> edition, Springer International Publishing AG, Cham, Switzerland.
- Stavridakis, E.I., 2006. Assessment of anisotropic behavior of swelling soils on ground and construction work. In: *Expansive Soils: Recent Advances in Characterization and Treatment* (eds. Al-Rawas, A.A. and Goosen, M.F.A.). Taylor and Francis Group, London, 371-385.
- Texas Department of Transportation, 2005. *Guidelines for Treatment of Sulfate-Rich Soils and Bases in Pavement Structures*. Construction Division Materials & Pavements Section Geotechnical, Soils & Aggregates, Brach. TxDOT 09/2005.
- Tran, T. D., Cui, Y., Tang, A. M., Audiguier, M. and Cojean, R. 2014. Effects of lime treatment on the microstructure and hydraulic conductivity of Héricourt clay. *Journal of Rock Mechanics and Geotechnical Engineering*, 6(5), 399–404.
- Turker, P., Erdogan B., Katnas, F. and Yeginobalı, A. 2009. *Classification and Properties of Fly Ashes in Turkey*, 4<sup>th</sup> edition, Turkish Cement Producers Association.
- Turkish Standard TS EN 196-2. 2013. *Methods of testing cement- Part 2: Chemical analysis of cement*, Turkish Standard Institution, Turkey.
- Turkish Standard TS EN 459-1. 2011. *Building lime- Part 1: Definitions, specifications and conformity criteria*, Turkish Standard Institution, Turkey.
- Turkish Statistical Institute, 2014. *Statistics of used water, generated waste- water and wastes by thermal powerplants*. Turkey.
- U. S. Department of Transportation- Federal Highway Administration. 2008. *User Guidelines for byproduct and Secondary Use Materials in Pavement Construction*. Publication Number: FHWA-RD-97-148.
- Uyanik, S. and Topeli, M. 2012. *Development Fly Ash Utilization in Turkey and Contribution of ISKEN to the Market*. Euro Coal Ash 2012 conference, Thessaloniki, Greece.

- Verruijt, A. 2001. Soil Mechanics. 1<sup>st</sup> edition, Delf University of Technology, Holland.
- Wang, J., Mateos, M. and Davidson, D. 1963. Comparative effects of hydraulic, calcitic and dolomitic limes and cement in soil stabilization. Stabilization of Soil with Lime and Fly Ash. Highway Research Board bulletin, Washington, 29, 42-54.
- Wang, J.X. 2016. Expansive soils and practice in foundation engineering. 2016 Louisiana Transportation Conference, Baton Rouge, Louisiana, 28.02 – 02.03.
- Weir, M., Mandell, A. and Farver, J. 2014. Role of Sulfates on Highway Heave in Lake County, Ohio. Report No. FHWA/OH-2014/4, U.S. Department of Transportation Federal Highway Administration.
- West, G. and Carder, D. R. 1997. Review of lime piles and lime-stabilized soil columns. Report No. TRL Report 305, Transport Research Laboratory.
- Wild, S., Arabi, M. and Leng-Ward, G. 1986. Soil-lime reaction and microstructural development at elevated temperatures. Clay Minerals, 21(3), 279–292.
- Wild, S., Kinuthia, J. M., Jones, G. I. and Higgins, D. D. 1998. Effects of partial substitution of lime with ground granulated blast furnace slag (GGBS) on the strength properties of lime-stabilized sulphate-bearing clay soils. Engineering Geology, 51(1), 37–53.
- X-ray Diffraction Table (n.d). Retrieved from <http://www.webmineral.com/MySQL/xray.php?ed1#.XbwgJZIzaUk> (last visited on 27/09/2019).
- Xusheng, W., Zhemin, Y., Haiyan, W. and Crossley, W. 2017. An experimental study of salt expansion in sodium saline soils under transient conditions. Journal of Arid Land, 9(6), 865-878.
- Yesilbas, G. 2004. Stabilization of Expansive Soils Using Aggregate Waste, Rock Powder and Lime. M.S. Thesis, METU, Turkey, 112 pages.
- Yilmaz, I. and Civelekoglu, B. 2009. Gypsum: As an additive for stabilization of swelling clay soils. Applied Clay Science, 44, 166-172.
- Yong, R. N. AND Warkentin, B.P. 1975. Soil properties and Behavior. 1<sup>st</sup> edition, Elsevier Scientific Publishing Company, Amsterdam.
- Yong, R. N., Nakano, M. and Pusch, R. 2012. Environmental Soil Properties and Behavior. 1<sup>st</sup> edition, CRC Press.
- Yun, T. S., Narsilio, G. A. and Santamarina, J. G. 2006. Physical characterization of core samples recovered from Gulf of Mexico. Marine and Petroleum Geology, 23, 893-900.
- Zha, F., Liu, S., Du, Y. and Cui, K. 2008. Behavior of Expansive Soils Stabilized with Fly Ash. Natural Hazards, 47, 509-523.

Zhou, W., Apkarian, R. P., Wang, Z. L. and Joy, D. 2006. Fundamentals of scanning electron microscopy. In: Scanning Microscopy for Nanotechnology Techniques and Applications (eds. Zhou, W. and Wang, Z. L.), Springer, Newyork, 1-40,

## APPENDICES

### A. CHEMICAL ANALYSES REPORTS

Chemical compositions of Sample A, SFA and KFA were determined by XRF method in Central Laboratory of METU and that of lime was provided from the producer. The results are presented in Figure A.1- A.4. The results for the lime are also presented in Table A.1.

SQX Calculation Result							
Sample : 16544-1B-U				Date analyzed : 2016- 3- 1 16:22			
Application : EZS103XNV		Model : Bulk		Balance :			
				Matching library:			
				File :		16544-1B-U	
No.	Component	Result	Unit	Det.limit	El.line	Intensity	w/o normal
1	SiO2	51.6	wt%	0.07498	Si-KA	48.2300	44.2418
2	Al2O3	41.3	wt%	0.05324	Al-KA	69.6092	35.4046
3	CO2	3.46	wt%	0.77000	C -KA	0.0700	2.9707
4	Fe2O3	1.22	wt%	0.01186	Fe-KA	6.5291	1.0432
5	TiO2	1.09	wt%	0.03243	Ti-KA	0.8536	0.9315
6	CaO	0.505	wt%	0.00875	Ca-KA	1.3934	0.4330
7	K2O	0.504	wt%	0.00804	K -KA	1.6879	0.4328
8	Na2O	0.165	wt%	0.02931	Na-KA	0.0450	0.1417
9	MgO	0.152	wt%	0.04024	Mg-KA	0.1125	0.1307
10	P2O5	0.0604	wt%	0.01057	P -KA	0.1061	0.0518
11	SrO	0.0227	wt%	0.00334	Sr-KA	1.4908	0.0195
12	ZrO2	0.0223	wt%	0.00358	Zr-KA	1.9472	0.0191

Figure A.1. Chemical analyses report of Sample A (Central Laboratory of METU, Report No. 16544)

SQX Calculation Result							
Sample : 16916somaBU		Date analyzed : 2016- 4- 1 14:20					
Application : EZS101XNV		Model : Bulk		Balance :			
				Matching library:			
				File : 16916somaBU			
No.	Component	Result	Unit	Det.limit	El.line	Intensity	w/o normal
1	SiO2	45.8	wt%	0.01577	Si-KA	1042.0072	43.5030
2	Al2O3	26.6	wt%	0.01188	Al-KA	886.9850	25.2810
3	CaO	11.6	wt%	0.00423	Ca-KA	731.7551	11.0016
4	CO2	5.14	wt%	0.15333	C -KA	2.3830	4.8890
5	Fe2O3	4.38	wt%	0.02130	Fe-KB1	68.4441	4.1627
6	SO3	1.79	wt%	0.00306	S -KA	57.6071	1.6985
7	K2O	1.54	wt%	0.00269	K -KA	124.4853	1.4622
8	MgO	1.20	wt%	0.00892	Mg-KA	17.6766	1.1434
9	TiO2	1.02	wt%	0.00849	Ti-KA	12.4405	0.9715
10	Na2O	0.454	wt%	0.00967	Na-KA	2.5791	0.4313
11	P2O5	0.299	wt%	0.00247	P -KA	11.7490	0.2842
12	V2O5	0.0718	wt%	0.00736	V -KA	1.4401	0.0682
13	SrO	0.0594	wt%	0.00094	Sr-KA	50.6071	0.0565
14	MnO	0.0392	wt%	0.00344	Mn-KA	2.1907	0.0373
15	Cr2O3	0.0289	wt%	0.00478	Cr-KA	1.0649	0.0275
16	ZnO	0.0249	wt%	0.00156	Zn-KA	6.1335	0.0237
17	NiO	0.0130	wt%	0.00197	Ni-KA	1.8493	0.0124
18	Rb2O	0.0129	wt%	0.00092	Rb-KA	10.4764	0.0122

**Rigaku**

Figure A.2. Chemical analyses report of SFA (Central Laboratory of METU, Report No. 16916)

SQX Calculation Result							
Sample : 16916sivasBU		Date analyzed : 2016- 4- 1 13:49					
Application : EZS101XNV		Model : Bulk		Balance :			
				Matching library:			
				File : 16916sivasBU			
No.	Component	Result	Unit	Det.limit	El.line	Intensity	w/o normal
1	CaO	29.5	wt%	0.00614	Ca-KA	1914.0793	28.7161
2	SiO2	25.3	wt%	0.01093	Si-KA	648.2719	24.6160
3	SO3	14.6	wt%	0.00625	S -KA	589.8135	14.2341
4	Al2O3	11.9	wt%	0.00826	Al-KA	375.2089	11.6190
5	CO2	7.35	wt%	0.17314	C -KA	3.7825	7.1531
6	Fe2O3	5.87	wt%	0.00485	Fe-KA	359.3413	5.7189
7	MgO	2.77	wt%	0.00849	Mg-KA	38.0517	2.6948
8	K2O	0.966	wt%	0.00242	K -KA	86.4575	0.9408
9	TiO2	0.780	wt%	0.00970	Ti-KA	7.3397	0.7593
10	Na2O	0.306	wt%	0.01103	Na-KA	1.6784	0.2979
11	P2O5	0.287	wt%	0.00237	P -KA	14.4166	0.2797
12	SrO	0.163	wt%	0.00115	Sr-KA	103.2521	0.1583
13	ZnO	0.0595	wt%	0.00185	Zn-KA	11.0876	0.0579
14	Cr2O3	0.0450	wt%	0.00512	Cr-KA	1.2202	0.0438
15	MoO3	0.0424	wt%	0.00136	Mo-KA	31.3914	0.0412
16	NiO	0.0285	wt%	0.00243	Ni-KA	3.0781	0.0277
17	ZrO2	0.0197	wt%	0.00123	Zr-KA	33.6552	0.0192

**Rigaku**

Figure A.3. Chemical analyses report of KFA (Central Laboratory of METU, Report No. 16916)



Table A.1. *Chemical Analyses results for lime (BASTAS Cement Factory)*

<b>Item</b>	<b>Unit</b>	<b>Limit Value (TS EN 459-1)</b>	<b>Analyses Result</b>
CaO + MgO	%	$\geq 70$	86.43
MgO	%	$\leq 5$	2.75
SO <sub>3</sub>	%	$\leq 2$	0.66
CO <sub>2</sub>	%	$\leq 12$	9.23
Active Lime	%	$\geq 55$	76.42
Volume invariance	mm	$\leq 20$	1.00
Part retaining on 90 $\mu\text{m}$ sieve	%	$\leq 7$	6.30
Part retaining on 200 $\mu\text{m}$ sieve	%	$\leq 2$	1.60
Free water	%	$\leq 2$	1.04
Penetration	mm	10- 50	22.00
Amount of air	%	$\leq 12$	1.70

## B. XRD RESULTS

The results for 28 days cured 40000ppm NS added 15% SFA treated samples at 10°C and 25°C were nearly identical, the results are presented in Figure B.1.

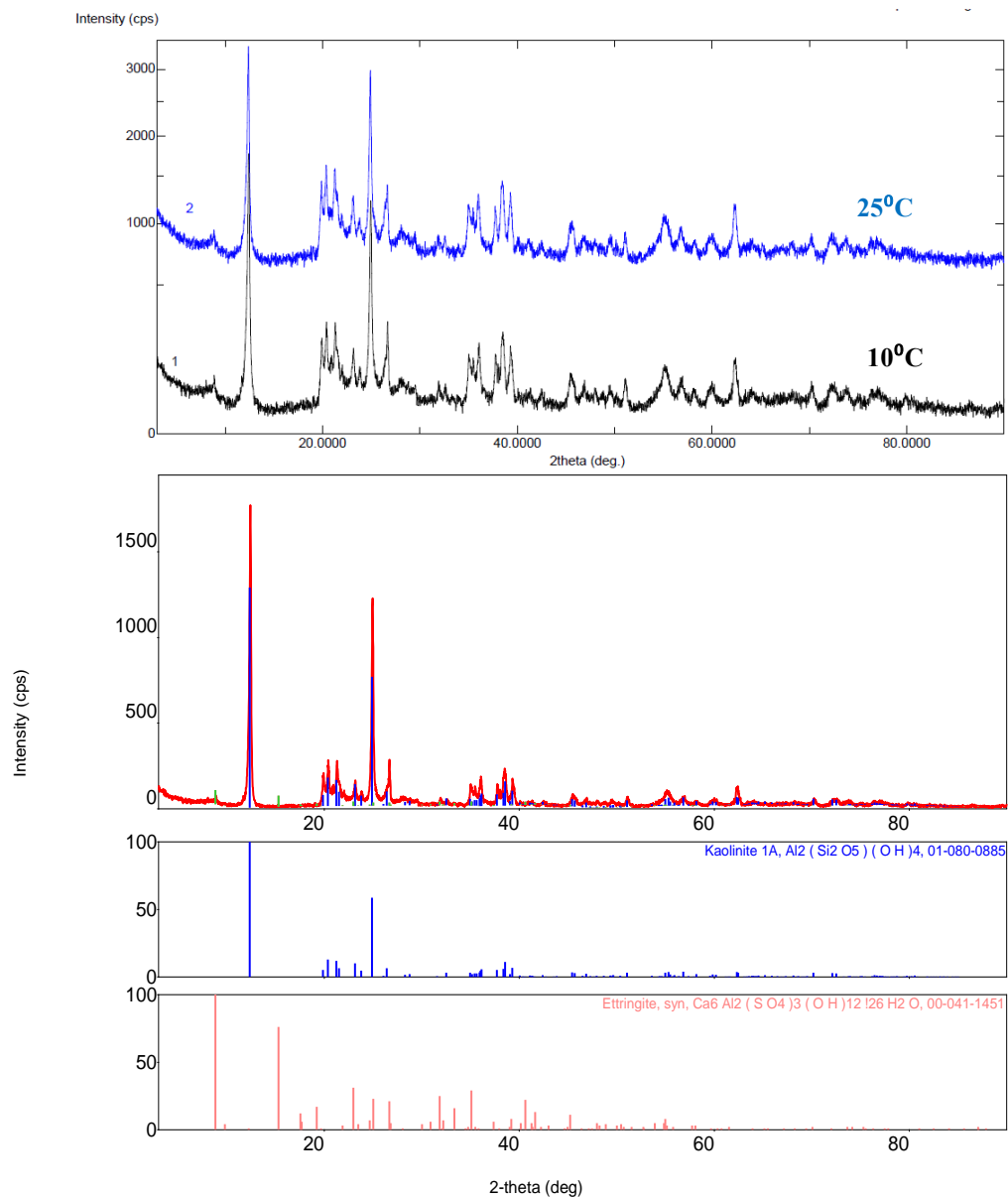


Figure B.1. XRD for 40000ppm NS added 15% SFA cured 28 days at 10°C and 25°C

### C. SWELL VERSUS TIME GRAPHS

Swell vs. time graphs for SFA, KFA, L treated specimens, sulfate added 4% L, 15% SFA and 10% KFA treated specimens, sulfate added 15% SFA and 10% KFA treated specimens at 10°C and 40°C, 7 days and 28 days cured sulfate added 15% SFA and 10% KFA treated specimens are presented in Figures C.1 to C.17.

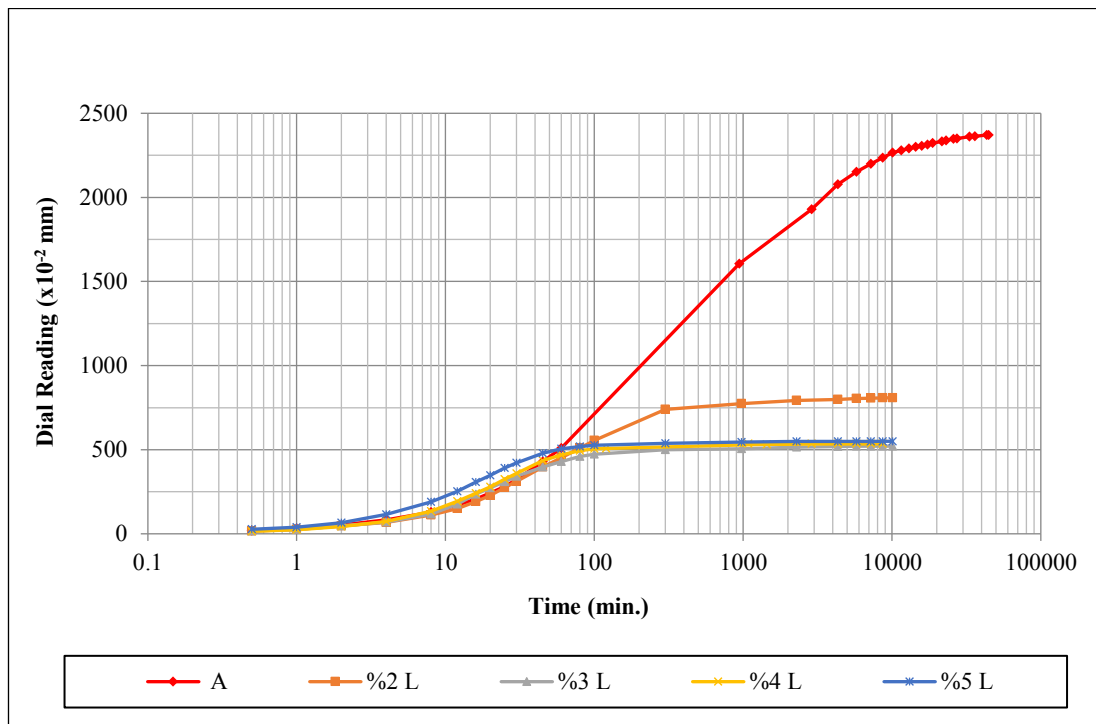


Figure C.1. Swell vs. time graphs for specimen A and lime treated specimens

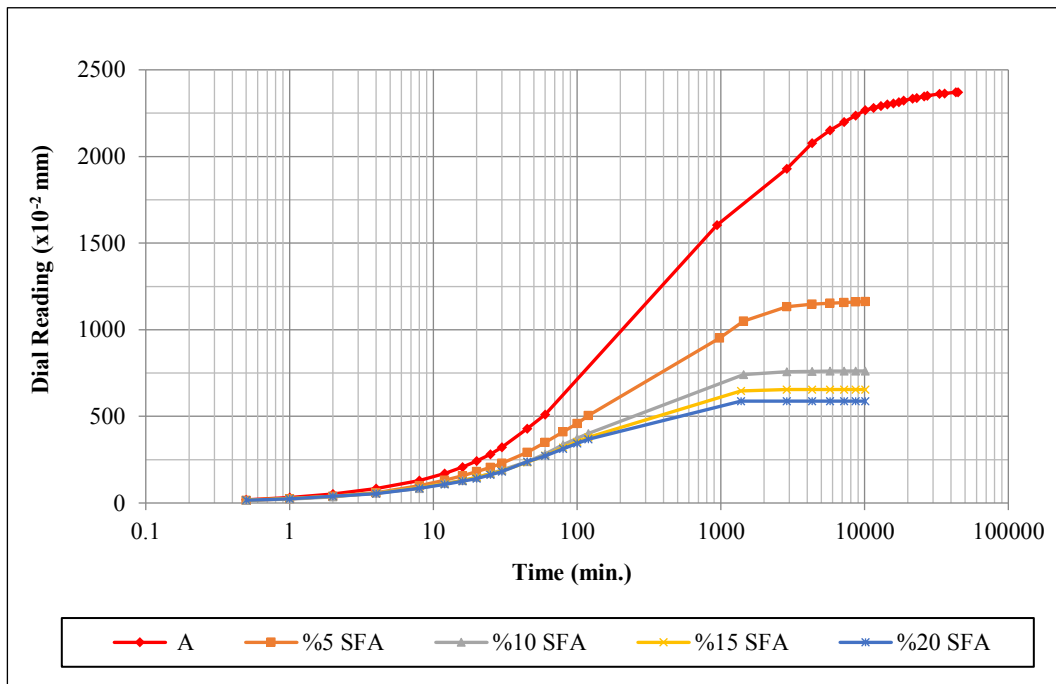


Figure C.2. Swell vs. time graphs for specimen A and SFA treated specimens

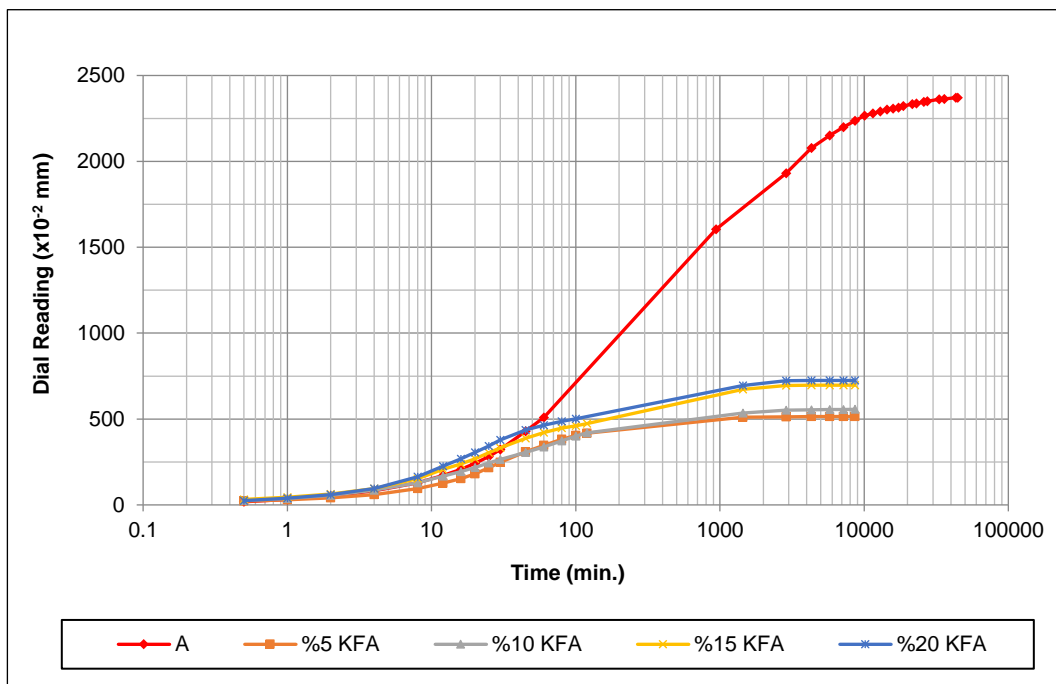


Figure C.3. Swell vs. time graphs for specimen A and KFA treated specimens

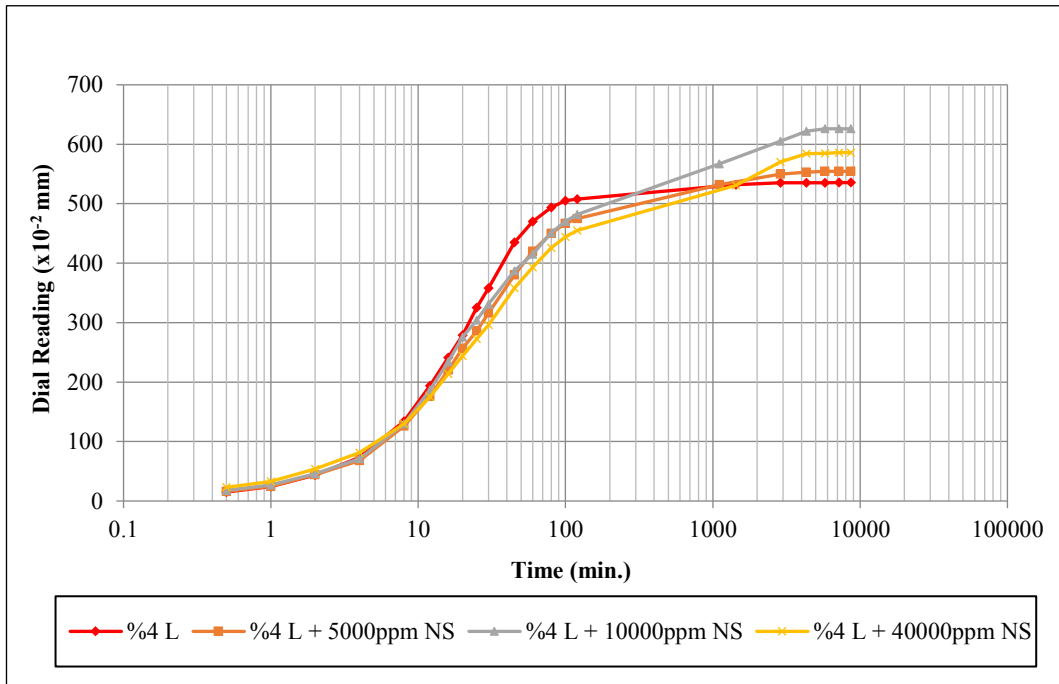


Figure C.4. Swell vs. time graphs for NS added 4% L treated specimens

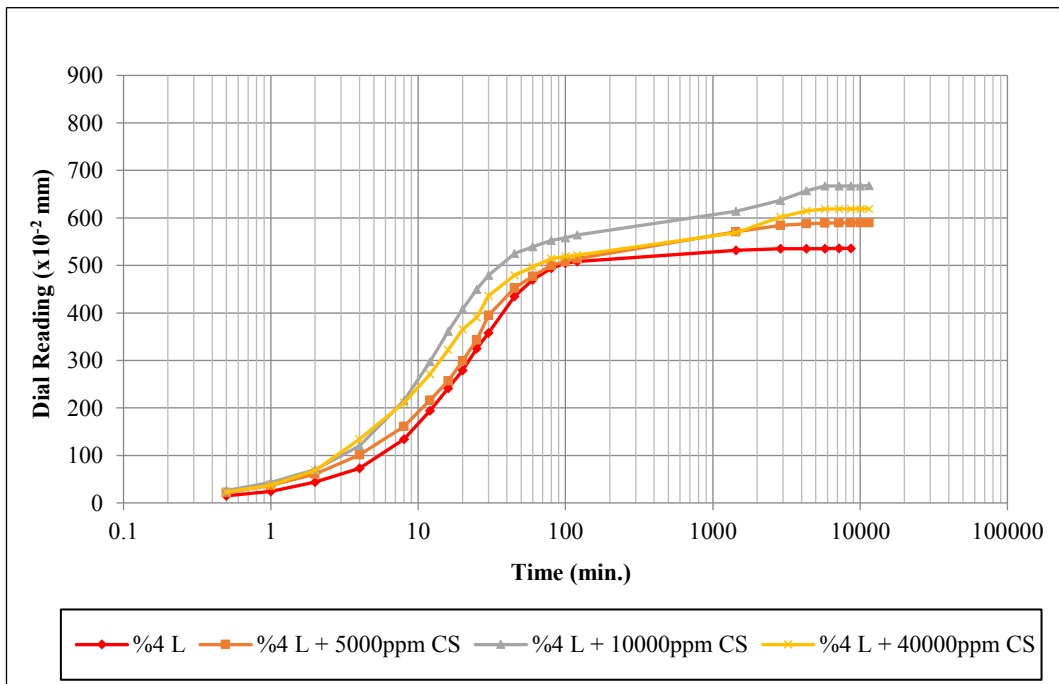


Figure C.5. Swell vs. time graphs for CS added 4% L treated specimens

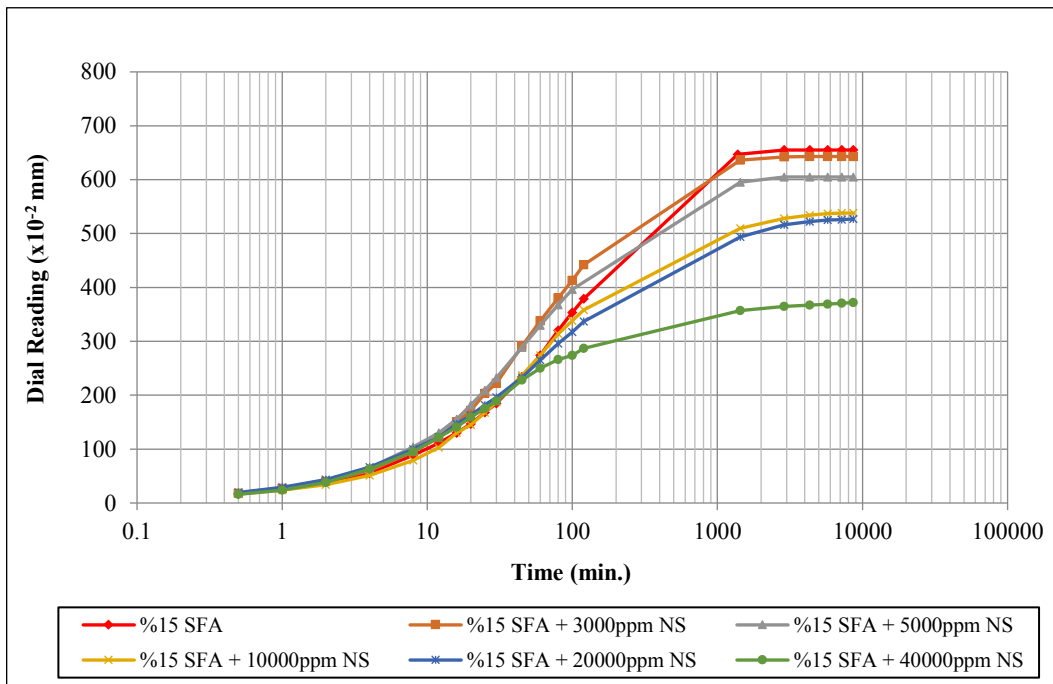


Figure C.6. Swell vs. time graphs for NS added 15% SFA treated specimens

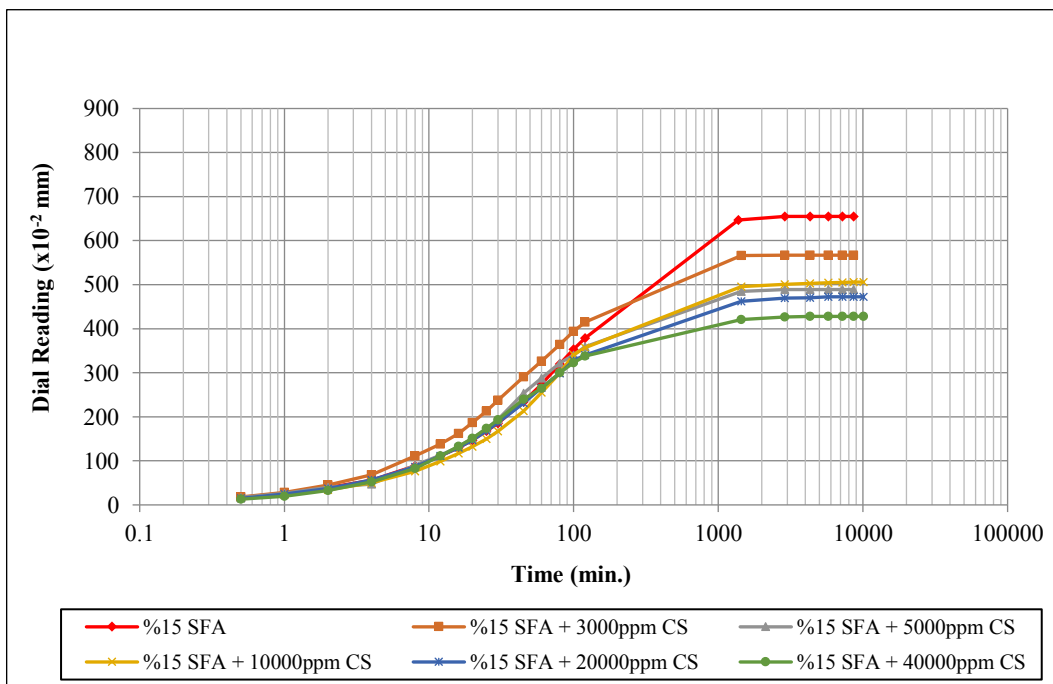


Figure C.7. Swell vs. time graphs for CS added 15% SFA treated specimens

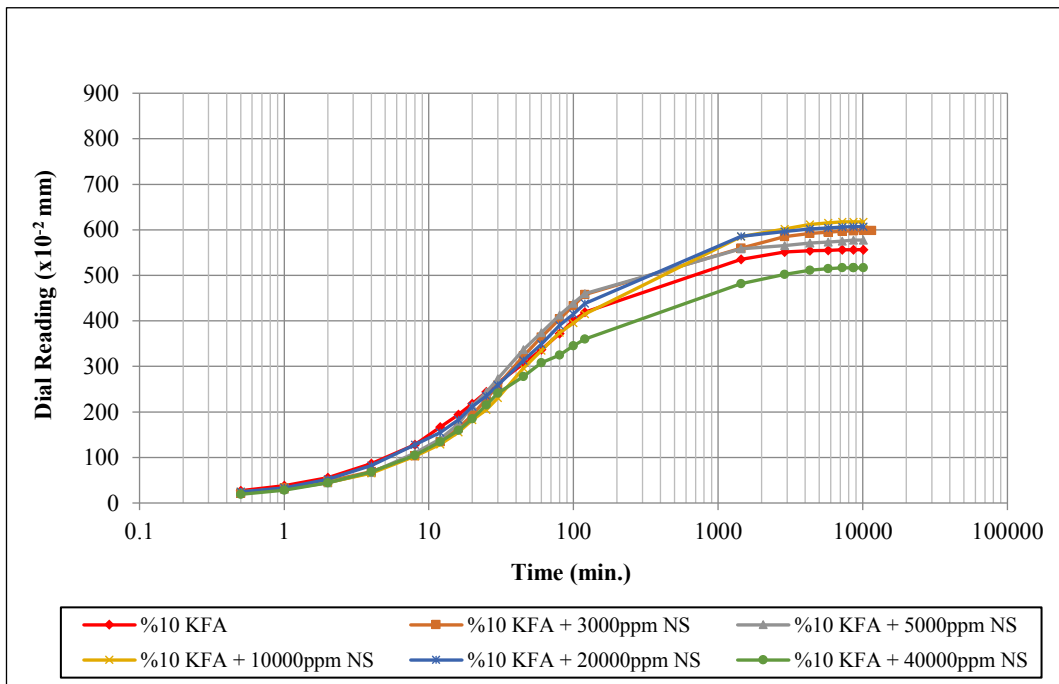


Figure C.8. Swell vs. time graphs for NS added 10% KFA treated specimens

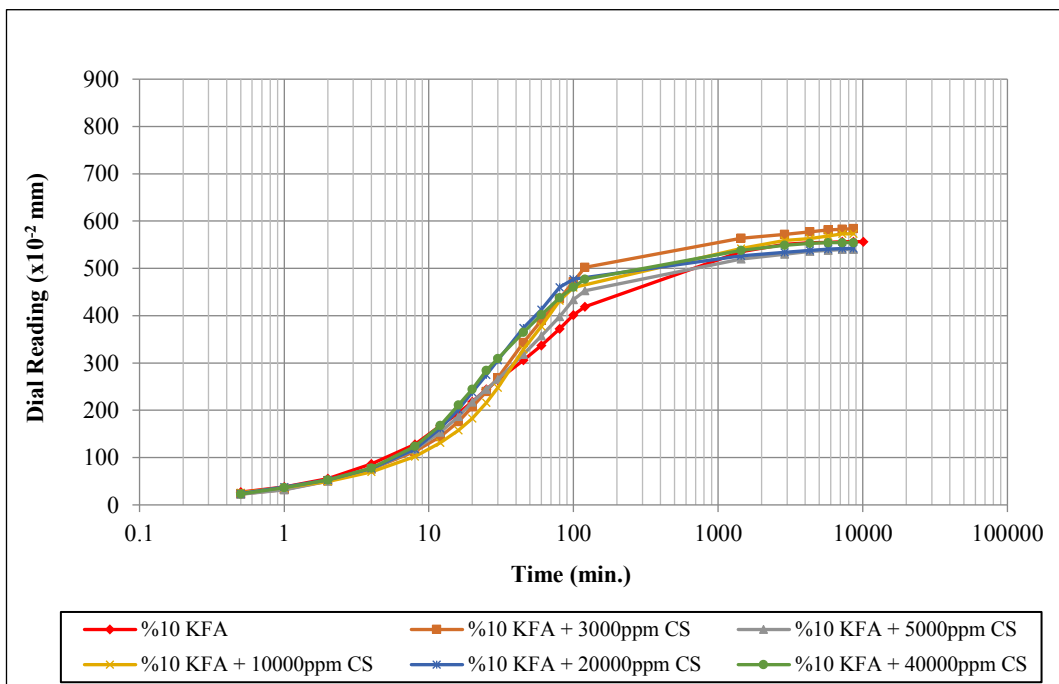


Figure C.9. Swell vs. time graphs for CS added 10% KFA treated specimens

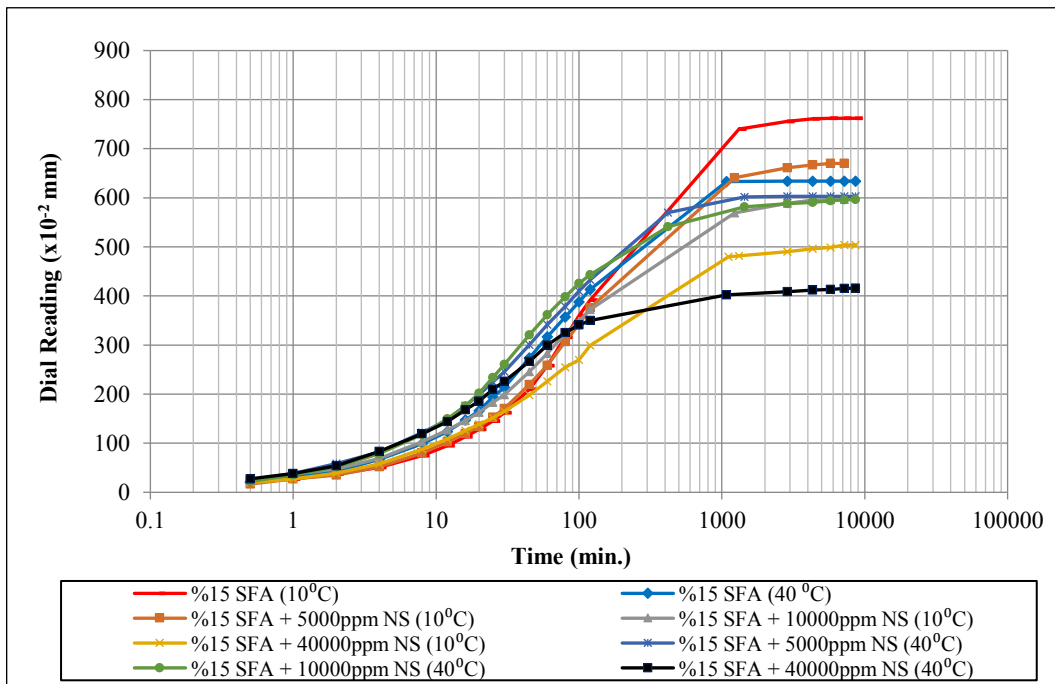


Figure C.10. Swell vs. time graphs for NS added 15% SFA treated specimens at 10°C and 40°C

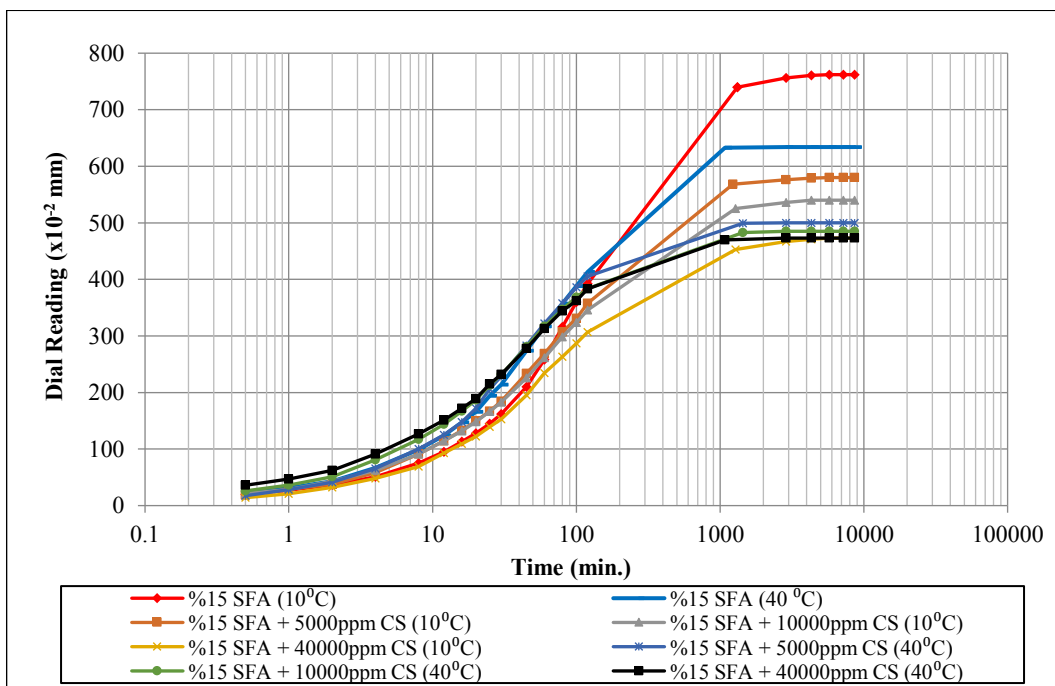


Figure C.11. Swell vs. time graphs for CS added 15% SFA treated specimens at 10°C and 40°C

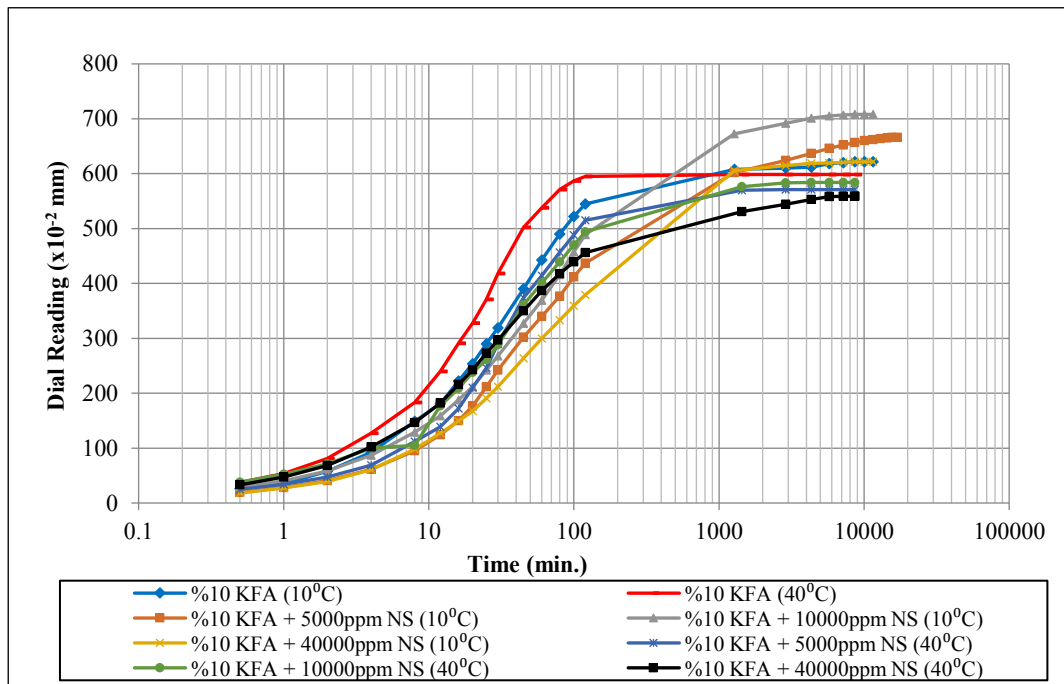


Figure C.12. Swell vs. time graphs for NS added 10% KFA treated specimens at 10°C and 40°C

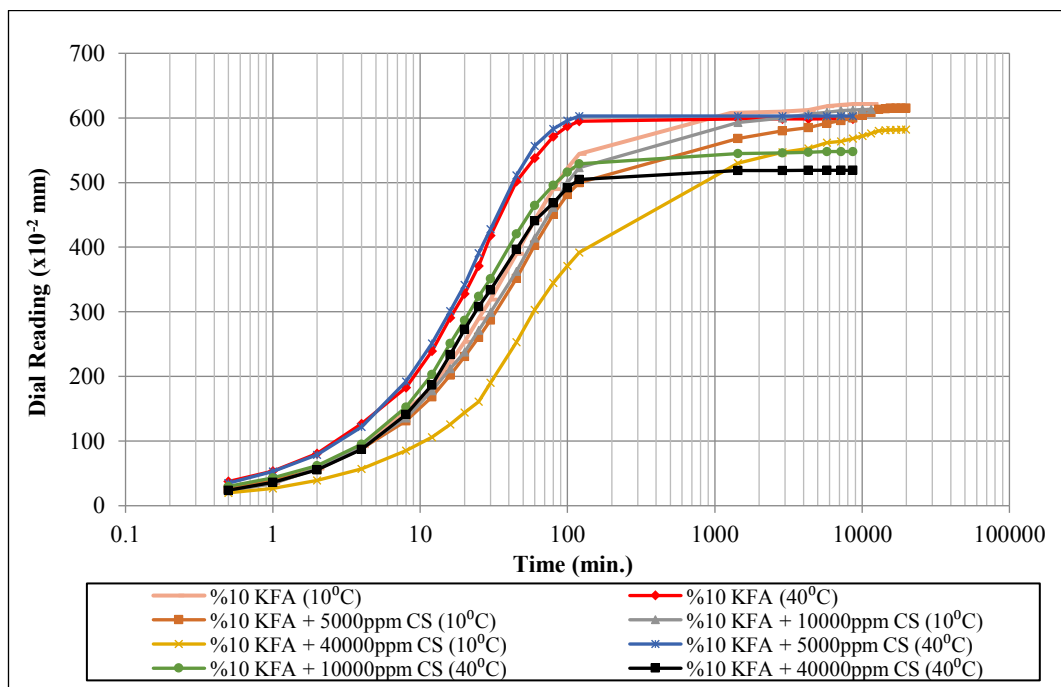


Figure C.13. Swell vs. time graphs for CS added 10% KFA treated specimens at 10°C and 40°C

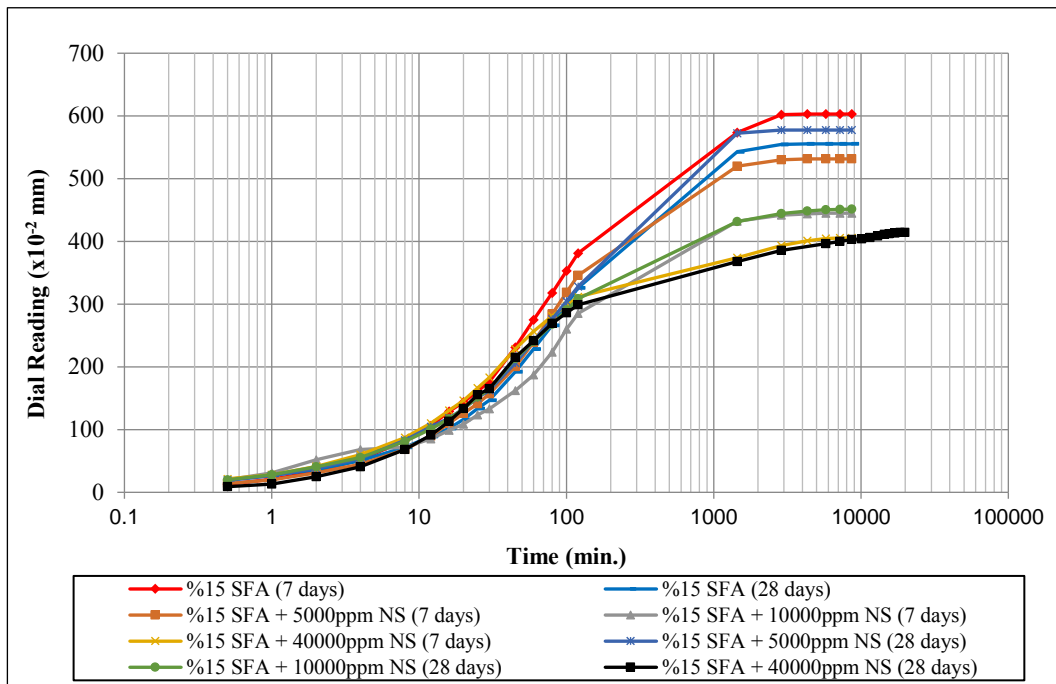


Figure C.14. Swell vs. time graphs for NS added 15% SFA treated specimens cured for 7 and 28 days

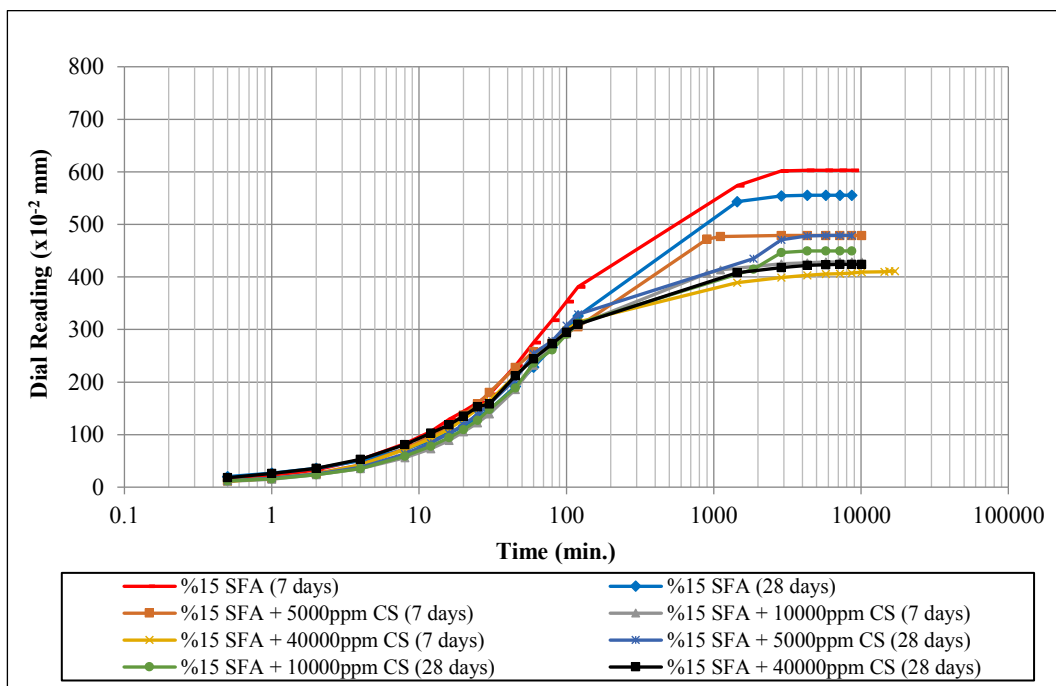


Figure C.15. Swell vs. time graphs for CS added 15% SFA treated specimens cured for 7 and 28 days

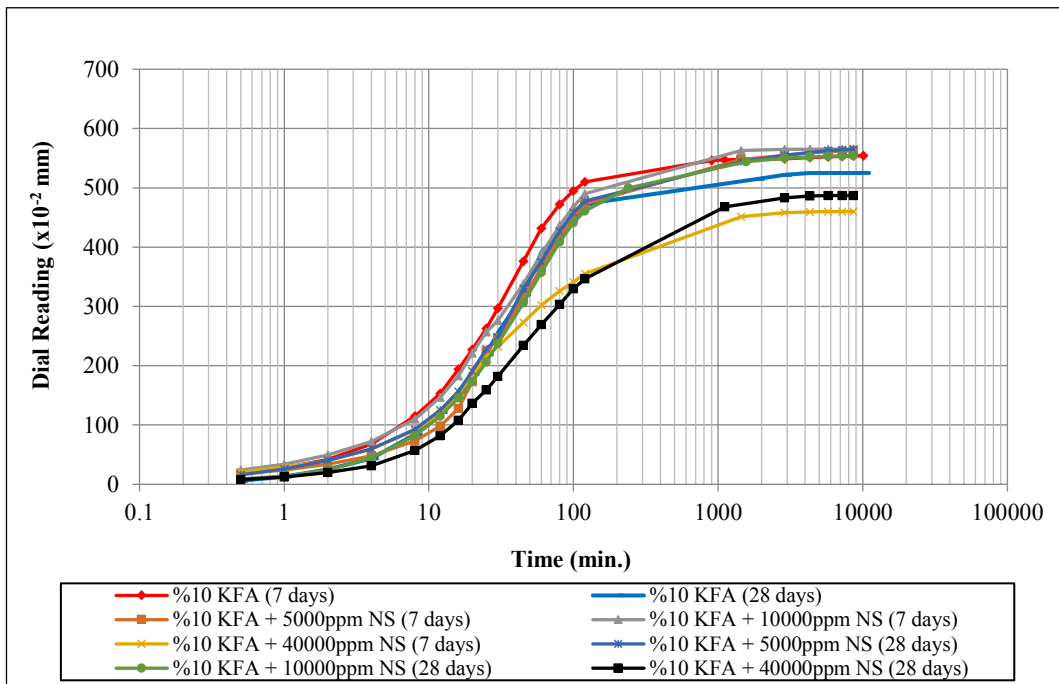


Figure C.16. Swell vs. time graphs for NS added 10% KFA treated specimens cured for 7 and 28 days

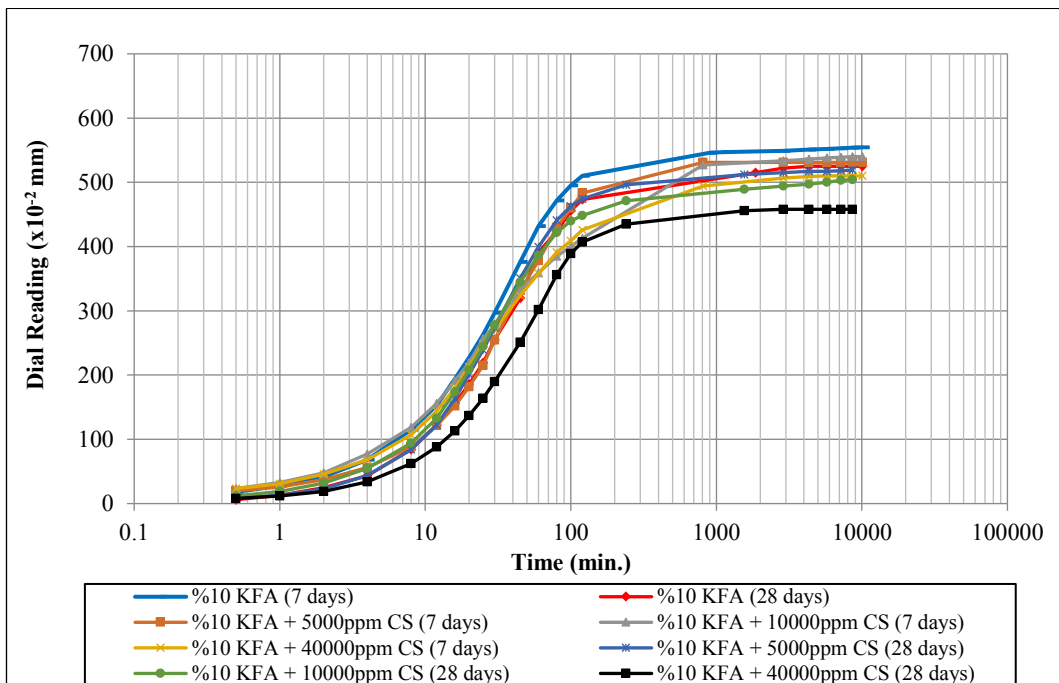


Figure C.17. Swell vs. time graphs for CS added 10% KFA treated specimens cured for 7 and 28 days



## CURRICULUM VITAE

### PERSONAL INFORMATION

Surname, Name : As, Mehmet  
Nationality : Turkish (TC)  
Date and Place of Birth : 9 July 1985, Balıkesir  
Phone : +90 535 436 47 77  
E-mail : Mehmet.as@metu.edu.tr

### EDUCATION

Degree	Institution	Year of Graduation
MS	METU Civil Engineering	2012
BS	Anadolu Univ. Business Administration	2011
BS	METU Civil Engineering	2008
High School	FEKAL Anatolian High School, Balıkesir	2003

### WORK EXPERIENCE

Year	Place	Enrollment
2008-Present	TOKER Drilling and Eng. Conc. Co.	Chief of Design Group

### FOREIGN LANGUAGES

Advanced English, Elementary German and Italian

### PUBLICATIONS

1. As, M. and Cokca, E. 2015. Effect of Cyclic Swell-Shrink on Swell Percentage of an Expansive Clay Stabilized by Class C Fly Ash. 15<sup>th</sup> National Conference of Soil Mechanics and Foundation Engineering, METU, October 16-17, Ankara, Turkey. (in Turkish).
2. Kalpakci, V., Ozturk, S., Yaman, G. and As, M. 2015. A Case History on Slope Instabilities Observed in Soils with Gypsum and Precautions. 6<sup>th</sup> Geotechnical Symposium, Cukurova University, 26-27 November, Adana, Turkey. (in Turkish).

3. As, M. and Cokca, E. 2018. Effect of Sulfate on Class C Fly Ash Stabilized Expansive Soils. 17<sup>th</sup> National Conference of Soil Mechanics and Foundation Engineering, İstanbul University, 26-28 September, İstanbul, Turkey. (in Turkish).

## **HOBBIES**

Swimming, Movies, Documentaries, Bird Feeding, Animals